

**IMPROVING THE FLOW OF PETROLEUM
PRODUCTS IN PIPELINES USING NATURAL
ADDITIVES AND POWDERS**



**MASTER OF ENGINEERING
UNIVERSITI MALAYSIA PAHANG**

DECLARATION OF THESIS AND COPYRIGHT

Author's full name : NITHIYA A/P ARUMUGAM

Date of birth : 13 FEB 1985

Title : IMPROVING THE FLOW OF PETROLEUM PRODUCTS
IN PIPELINES USING NATURAL ADDITIVES AND
POWDERS

Academic Session : 2011/2012

I declare that this thesis is classified as:

- CONFIDENTIAL** (Contains confidential information under the Official Secret Act 1972)
- RESTRICTED** (Contains restricted information as specified by the organization where research was done)
- OPEN ACCESS** I agree that my thesis to be published as online open access (Full text)

I acknowledge that Universiti Malaysia Pahang reserve the right as follows:

1. The thesis is the Property of Universiti Malaysia Pahang
2. The Library of Universiti Malaysia Pahang has the right to make copies for the purpose of research only.
3. The Library has the right to make copies of the thesis for academic exchange

Certified By:

(Student's Signature)

(Signature of Supervisor)

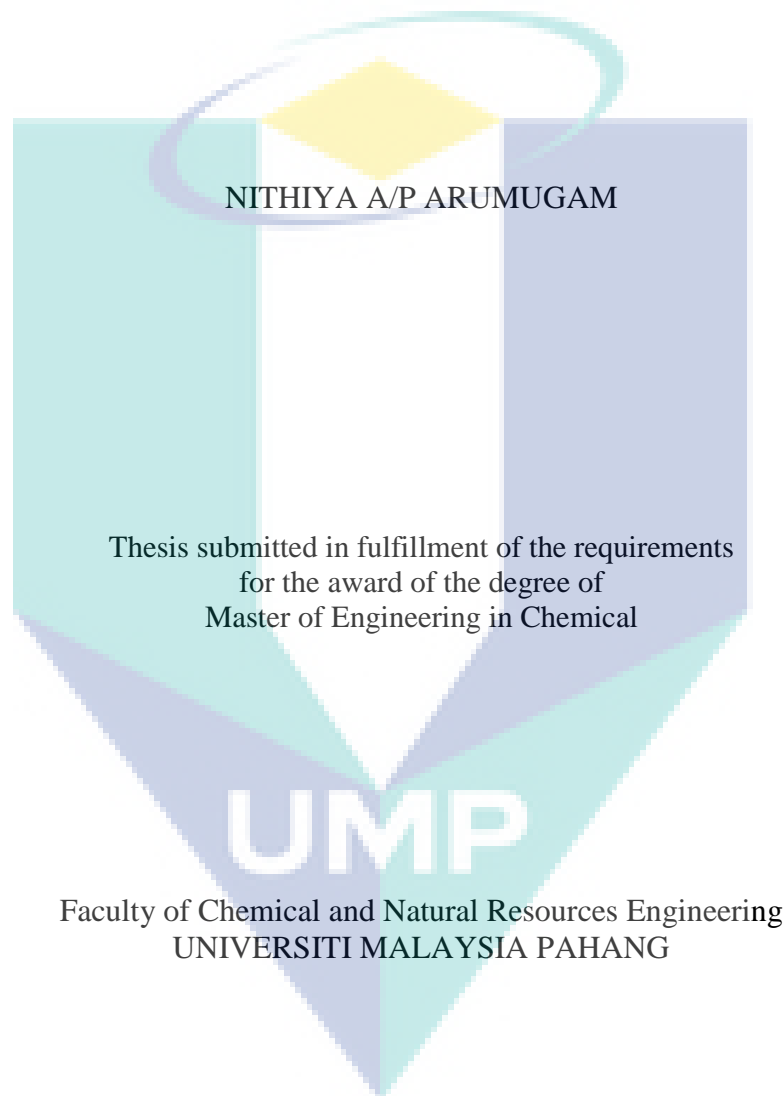
850213-14-5192

ASSOC. PROF. DR. HAYDER A. ABDUL BARI

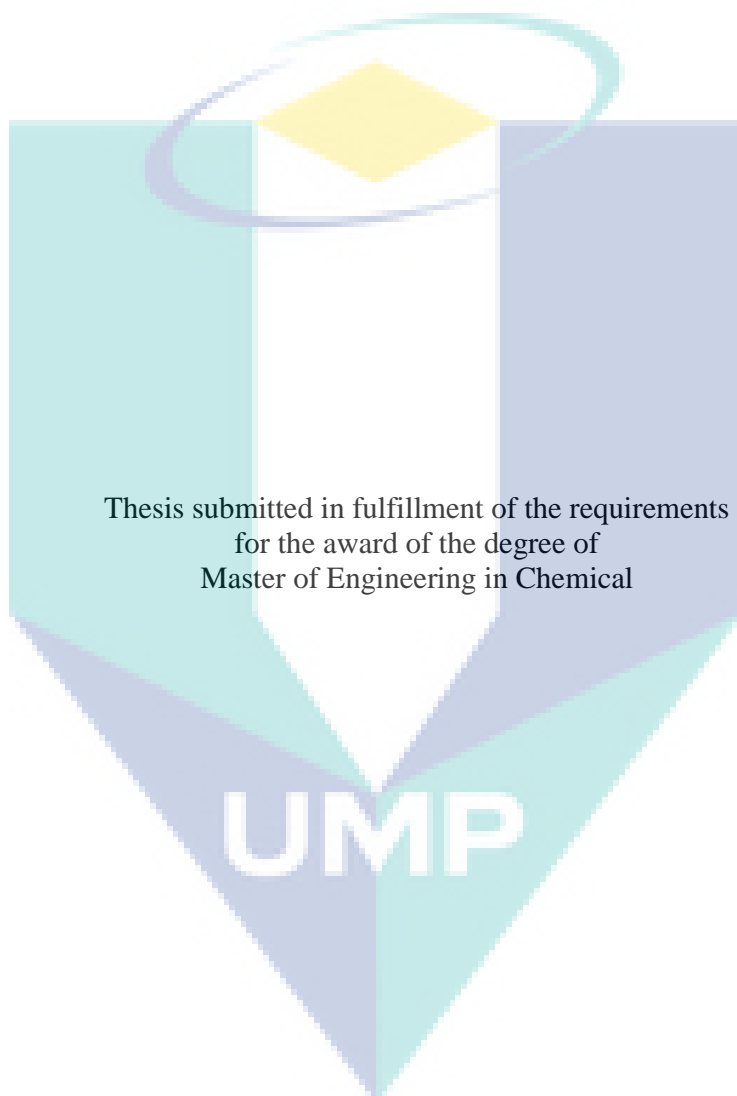
New IC/ Passport Number
Date: 6th JULY 2012

Name of Supervisor
Date: 6th JULY 2012

IMPROVING THE FLOW OF PETROLEUM PRODUCTS IN PIPELINES USING
NATURAL ADDITIVES AND POWDERS



JULY 2012



Thesis submitted in fulfillment of the requirements
for the award of the degree of
Master of Engineering in Chemical

SUPERVISOR'S DECLARATION

We hereby declare that we have checked this thesis and in our opinion, this thesis is adequate in terms of scope and quality for the award of the degree of Master of Engineering in Chemical.

Name of Supervisor: ASSOCIATE PROFESSOR DR.HAYDER A. ABDUL BARI

Position: ASSOCIATE PROFESSOR

Date: 6th JULY 2012

Name of Co-Supervisor: DR. ARUN GUPTA

Position: SENIOR LECTURER

Date: 6th JULY 2012



UMP

STUDENT'S DECLARATION

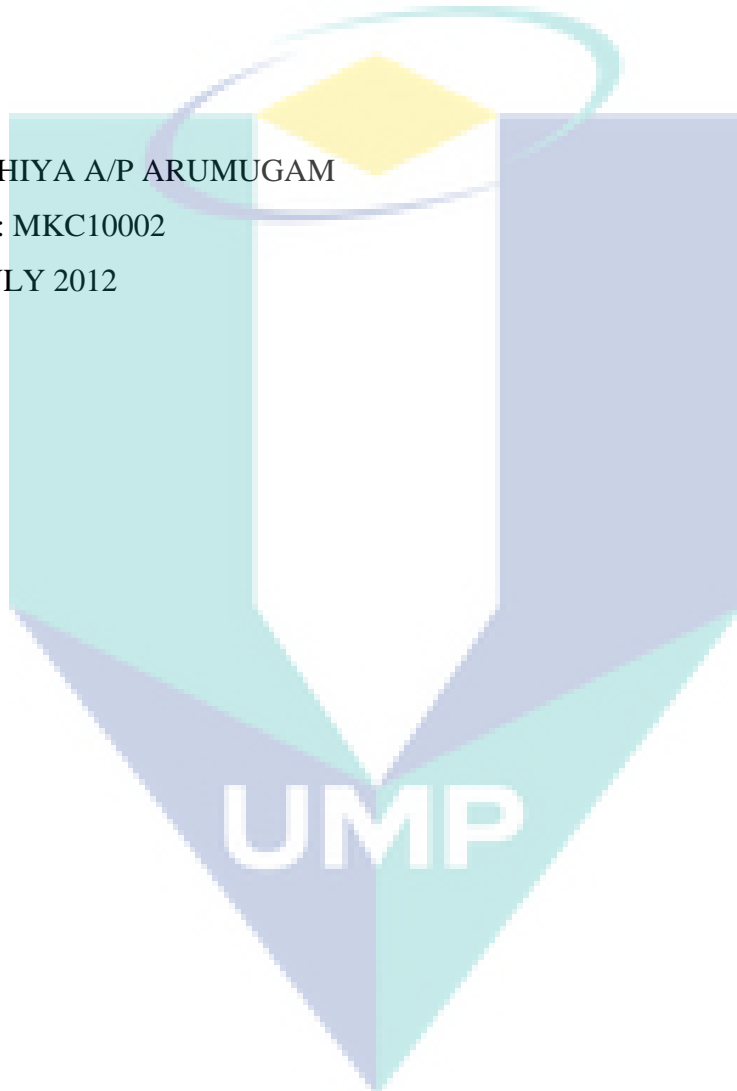
I hereby declare that the work in this thesis is my own except for quotations and summaries which have been duly acknowledged. The thesis has not been accepted for any degree and is not concurrently submitted for award of other degree.

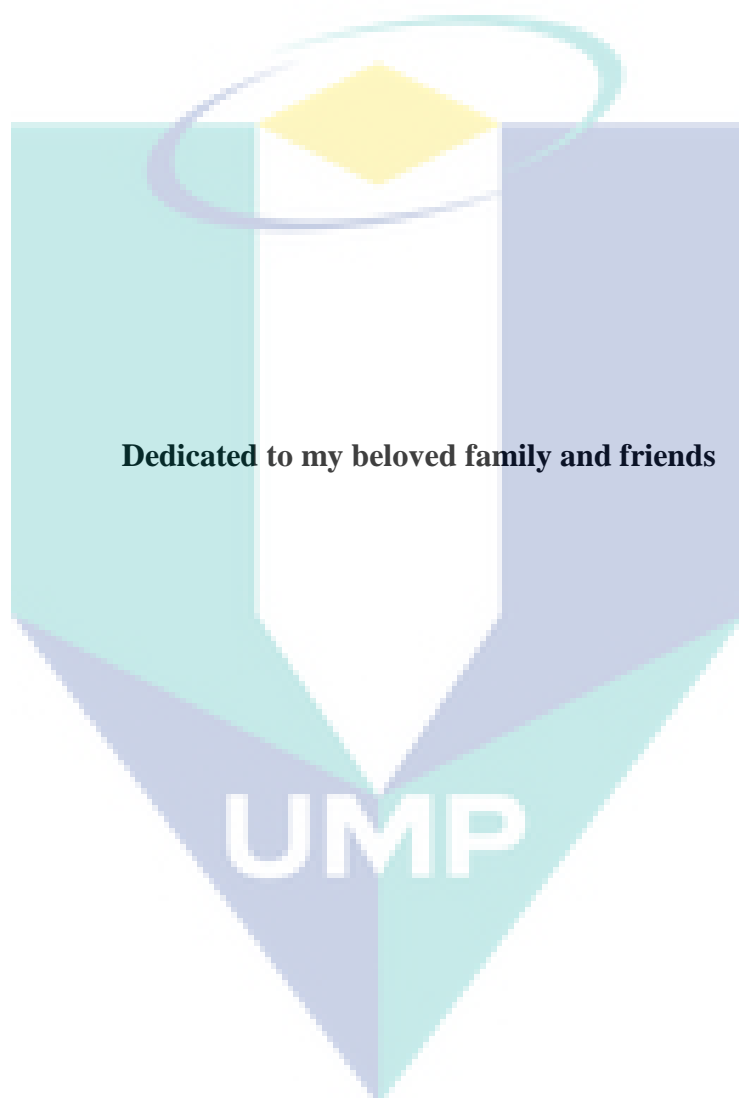
Signature

Name: NITHIYA A/P ARUMUGAM

ID Number: MKC10002

Date: 6th JULY 2012





ACKNOWLEDGEMENTS

I am grateful and would like to express my deepest gratitude to my main supervisor Associate Professor Dr. Hayder A. Abdul Bari for his supervisions, ideas, invaluable guidance, continuous encouragement, constant support and friendships in making this research possible. He taught me a lot especially in conducting research, publishing papers and attending conferences. I could not finish this thesis without his encouragement. He has always impressed me with his outstanding professional conduct, his strong conviction for research that a master program is just the beginning of lifelong learning experience in the research field. I appreciate his consistent support from the first day I applied to graduate program to these concluding moments. I am truly thankful for his progressive vision about my training in engineering, his tolerance of my naïve mistakes, and his commitment to my future career.

I also would like to express very special thanks to my co-supervisor Dr. Arun Gupta for his guidance, suggestions, co-operations and supports especially in completing modeling of drag reduction. He helped me a lot in thought and understanding of using STATISTICA software throughout this study. Without his continuous supports and motivation, this thesis will not complete as it is now.

My sincere thanks go to University Malaysia Pahang (UMP) for providing facilities and fund to support my study and librarian in the UMP for providing relevant literatures. Lecturers, teaching engineers and technical unit of the Faculty of Natural Resources and Chemical Engineering also deserve special thanks for their guidance in preparing the equipments for laboratory works and made my stay at UMP pleasant and unforgettable.

I acknowledge my sincere indebtedness and gratitude to my parents Mr. Arumugam and Mrs. Saraswathy. Gratitude also extended to my brothers Kalidas, Jagathisan and Saravanan for their endless loves, care and moral support throughout my academic years in the UMP. I cannot find the appropriate words that could properly describe my appreciation for the family's devotion, supports and faith in my ability to attain my goals.

ABSTRACT

Liquids transportation through pipelines is considered one of the most power consuming sectors in the industry due to the turbulent mode these liquids are transported within. Skin friction formed by turbulent flow in pipe becomes the main aspect for researchers to explore the field of fluid mechanics. Frictional drag formed in pipelines transporting liquid can be reduced spectacularly by adding minute amounts of drag reducing agents. Drag reduction (DR) is a phenomenon where eddies changes its structure to interact with added material in transporting system for pumping power saving. During the past few decades, artificial additives were used to solve the problem. Most of these additives are not environmentally friendly with high level of toxicity. Therefore, in this present work two novel and environmentally friendly drag reducing agents were introduced. This thesis outlines the performance of natural additives and powders as drag reducing agent in transporting water and diesel via pipelines. The natural additives extracted from the leaves of *Hibiscus rosa-sinensis* (an agricultural waste) and red gypsum (waste from titanium dioxide manufacturing industry) are the two new drag reducers introduced. The extracted water soluble mucilage then converted to be oil soluble through adapted phase solubility inversion method. The objectives of this research is to analyze the effect of selected investigated materials based on solution concentration, fluid's Reynolds number, pipe diameter and length of testing section. In order to achieve the objectives of this study, an experimental rig consists of three galvanized pipes of different diameters 0.0381m, 0.0254m and 0.0127m each 2m in length was built as closed loop liquid circulation system. The drag reduction ability of the water soluble mucilage was tested successfully with a maximum DR of 39% achieved in 0.0381m ID and 1.5m length pipe. The drag reduction ability of the oil soluble mucilage gives maximum DR of 47% achieved in 0.0381m ID and 1.5m length pipe. While gypsum powder reduces drag around 26% and 60% in water and diesel solutions respectively achieved in 0.0381m ID and 1.5m length pipe. The statistical drag reduction correlation was modeled with experimental data using STATISTICA software. As a conclusion, new environmentally friendly drag reducing agents were introduced to the field as an alternative to existing commercial additives and its effectiveness in improving the flow was proven experimentally.

ABSTRAK

Pengangkutan cecair melalui saluran paip dianggap sebagai salah satu sektor yang menggunakan kuasa yang banyak dalam industri disebabkan mod gelora cecair itu diangkut. Geseran yang disebabkan oleh aliran gelora di dalam paip menjadi aspek utama bagi penyelidik untuk meneroka bidang mekanik bendalir. Seretan geseran yang terbentuk dalam saluran paip yang mengangkut cecair boleh dikurangkan secara drastik dengan menambah sedikit ejen mengurangkan seretan. Pengurangan seretan adalah fenomena di mana pusingan mengubah strukturnya untuk berinteraksi dengan ejen yang ditambah dalam system pengangkutan untuk menjimatkan kuasa mengepam. Beberapa dekad yang lalu, aditif tiruan telah digunakan untuk menyelesaikan masalah tersebut. Kebanyakan aditif ini adalah tidak mesra alam dengan tahap ketoksikan yang tinggi. Oleh itu, dalam kajian ini dua ejen mengurangkan seretan yang novel serta mesra alam telah diperkenalkan. Tesis ini merangkumi prestasi aditif semulajadi dan serbuk sebagai ejen mengurangkan seretan dalam pengangkutan air dan diesel melalui saluran paip. Dua agen pengurang seretan baru yang diperkenalkan dalam kajian ini adalah aditif semulajadi yang diekstrak daripada daun *Hibiscus rosa-sinensis* (sisa pertanian) dan gipsum merah (bahan buangan dari industri pembuatan titanium dioksida). Lendir yang diekstrak larut dalam air kemudiannya diubahsuai untuk larut dalam diesel melalui kaedah pengubahsuaian kebolehlarutan fasa. Objektif kajian ini adalah untuk menganalisis kesan ejen mengurangkan seretan yang diperkenalkan berdasarkan kepekatan larutan, nombor Reynolds bendalir, diameter paip dan panjang paip yang diuji. Bagi mencapai objektif kajian ini, rig eksperimen yang terdiri daripada tiga diameter paip bergalvani yang berlainan iaitu 0.0381m, 0.0254m dan 0.0127m masing-masing dengan panjang 2m telah dibina sebagai sistem peredaran cecair tertutup. Keupayaan mengurangkan seretan oleh lendir yang larut dalam air telah diuji dengan jayanya dengan DR maksimum 39% yang dicapai dalam 0.0381m diameter dan 1.5m panjang paip. Keupayaan mengurangkan seretan oleh lendir yang larut dalam diesel menunjukkan DR maksimum 47% yang dicapai dalam 0.0381m diameter dan 1.5m panjang paip. Serbuk gipsum pulak mengurangkan seretan sebanyak 26% and 60% masing-masing dalam air dan diesel di dalam paip 0.0381m diameter dan 1.5m panjang paip. Korelasi statistik pengurangan seretan telah dimodelkan menggunakan perisian STATISTICA dengan data-data dari eksperimen. Sebagai kesimpulan, ejen-ejen mengurangkan seretan yang baru serta mesra alam telah berjaya diperkenalkan untuk menggantikan aditif yang sedia ada dan digunakan secara komersil disamping keberkesanannya untuk meningkatkan aliran telah dibuktikan melalui eksperimen.

TABLE OF CONTENTS

		Page
STATEMENT OF AWARD		ii
SUPERVISOR'S DECLARATION		iii
STUDENT'S DECLARATION		iv
DEDICATION		v
ACKNOWLEDGEMENTS		vi
ABSTRACT		vii
ABSTRAK		viii
TABLE OF CONTENTS		ix
LIST OF TABLES		xii
LIST OF FIGURES		xv
LIST OF SYMBOLS		xix
LIST OF ABBREVIATIONS		xx
LIST OF APPENDICES		xxi
CHAPTER 1	INTRODUCTION	
1.1	Background	1
1.2	Problem Statement	2
1.3	Objectives of Research	3
1.4	Scopes of Research	3
1.5	Study Contributions	4
1.6	Overview of the Thesis	4
CHAPTER 2	LITERATURE REVIEW	
2.1	Introduction	5
2.2	Types of Flow	
	2.2.1 Laminar Flow	6
	2.2.2 Transitional Flow	7
	2.2.3 Turbulent Flow	7

2.3	Energy Losses in Pipelines	8
2.4	Drag Reduction	
2.4.1	Introduction	11
2.4.2	Drag Reducing Agents (DRA)	12
2.4.3	Drag Reduction Mechanisms	23
2.4.4	Commercial Applications	26

CHAPTER 3 MATERIALS AND METHOD

3.1	Introduction	28
3.2	Raw Materials	
3.2.1	Hibiscus Leaves	28
3.2.2	Red Gypsum Powders	29
3.2.3	Grafting Chemicals	30
3.2.4	Transported Liquid	36
3.3	Closed Loop Liquid Circulation System	37
3.4	Mucilage Preparation	
3.4.1	Mucilage Extraction	39
3.4.2	Mucilage Grafting	40
3.5	Red Gypsum Preparation	
3.5.1	Particle Size Analysis	42
3.6	Experimental Procedure	
3.6.1	Solution Preparation and Testing in Rig	43
3.7	Physical Properties Tests	
3.7.1	Viscosity	44
3.8	Experimental Calculations	
3.8.1	Reynolds Number	45
3.8.2	Friction Factor	45
3.8.3	Percentage Drag Reduction	46

CHAPTER 4 RESULTS AND DISCUSSION

4.1	Property Tests	47
4.2	Verification of Closed Loop Liquid Circulation System	50
4.3	Additives Drag Reduction Performance in Water and Diesel	

4.3.1	Effect of Solution Velocity	52
4.3.2	Effect of Additives Concentration	61
4.3.3	Effect of Pipe Diameter	68
4.3.4	Effect of Testing Section Length	72
4.4	Mucilage Degradation	76
4.5	Statistical Model (Correlations)	79

CHAPTER 5 CONCLUSION AND RECOMMENDATIONS

5.1	DRA Performance	81
5.2	Recommendations	82

REFERENCES 83

APPENDICES

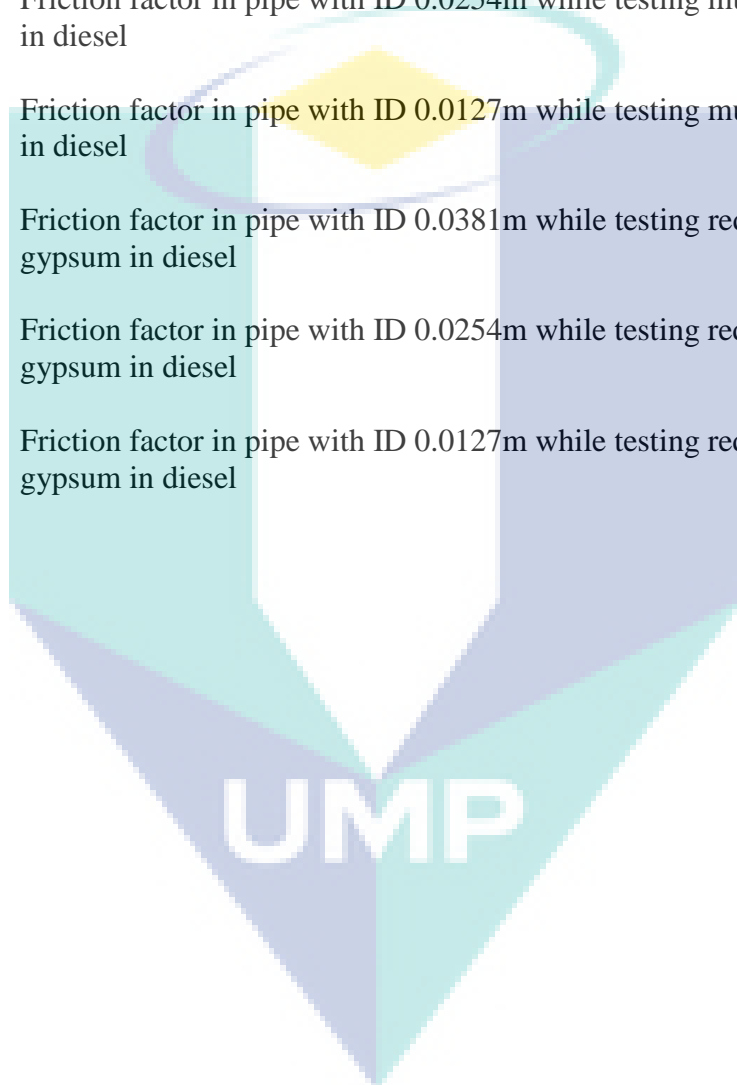
A1	Amount of mucilage in transporting liquids	96
A2	Amount of red gypsum in transporting liquids	98
B1	System verification in transporting water	100
B2	System verification in transporting diesel	112
C1	Percentage drag reduction by mucilage	124
C2	Percentage drag reduction by red gypsum	130
D1	Friction factor in pipe while testing mucilage in water	136
D2	Friction factor in pipe while testing red gypsum in water	169
D3	Friction factor in pipe while testing mucilage in diesel	202
D4	Friction factor in pipe while testing red gypsum in diesel	235
E	Steps for statistical correlation estimation	268
F	List of publications	272

LIST OF TABLES

Table No.	Title	Page
3.1	Properties of red gypsum	30
3.2	Properties of acrylonitrile	31
3.3	Specifications of nitric acid	32
3.4	Properties of isopropanol	34
3.5	Properties of acetone	35
3.6	Properties of dimethylformamide	36
3.7	Measured physical properties of transported liquids	37
3.8	Percent mixing and the viscosity of resulted mucilage	40
3.9	Amount of water soluble mucilage in transporting water	96
3.10	Amount of grafted mucilage in transporting diesel	96
3.11	Amount of red gypsum in transporting water	98
3.12	Amount of red gypsum in transporting diesel	98
4.1	Viscosity of the DRAs ($T = 25^{\circ}\text{C}$)	49
4.2	System verification of pipe with ID 0.0381m in transporting water before DRA addition	100
4.3	System verification of pipe with ID 0.0254m in transporting water before DRA addition	104
4.4	System verification of pipe with ID 0.0127m in transporting water before DRA addition	108
4.5	System verification of pipe with ID 0.0381m in transporting diesel before DRA addition	112
4.6	System verification of pipe with ID 0.0254m in transporting diesel before DRA addition	116
4.7	System verification of pipe with ID 0.0127m in transporting diesel before DRA addition	120

4.8	Percentage drag reduction by mucilage in transporting water via pipe with ID 0.0381m	124
4.9	Percentage drag reduction by mucilage in transporting water via pipe with ID 0.0254m	125
4.10	Percentage drag reduction by mucilage in transporting water via pipe with ID 0.0127m	126
4.11	Percentage drag reduction by mucilage in transporting diesel via pipe with ID 0.0381m	127
4.12	Percentage drag reduction by mucilage in transporting diesel via pipe with ID 0.0254m	128
4.13	Percentage drag reduction by mucilage in transporting diesel via pipe with ID 0.0127m	129
4.14	Percentage drag reduction by red gypsum in transporting water via pipe with ID 0.0381m	130
4.15	Percentage drag reduction by red gypsum in transporting water via pipe with 0.0254m	131
4.16	Percentage drag reduction by red gypsum in transporting water via pipe with ID 0.0127m	132
4.17	Percentage drag reduction by red gypsum in transporting diesel via pipe with ID 0.0381m	133
4.18	Percentage drag reduction by red gypsum in transporting diesel via pipe with ID 0.0254m	134
4.19	Percentage drag reduction by red gypsum in transporting diesel via pipe with ID 0.0127m	135
4.20	Friction factor in pipe with ID 0.0381m while testing mucilage in water	136
4.21	Friction factor in pipe with ID 0.0254m while testing mucilage in water	147
4.22	Friction factor in pipe with ID 0.0127m while testing mucilage in water	158
4.23	Friction factor in pipe with ID 0.0381m while testing red gypsum in water	169

4.24	Friction factor in pipe with ID 0.0254m while testing red gypsum in water	180
4.25	Friction factor in pipe with ID 0.0127m while testing red gypsum in water	191
4.26	Friction factor in pipe with ID 0.0381m while testing mucilage in diesel	202
4.27	Friction factor in pipe with ID 0.0254m while testing mucilage in diesel	213
4.28	Friction factor in pipe with ID 0.0127m while testing mucilage in diesel	224
4.29	Friction factor in pipe with ID 0.0381m while testing red gypsum in diesel	235
4.30	Friction factor in pipe with ID 0.0254m while testing red gypsum in diesel	246
4.31	Friction factor in pipe with ID 0.0127m while testing red gypsum in diesel	257



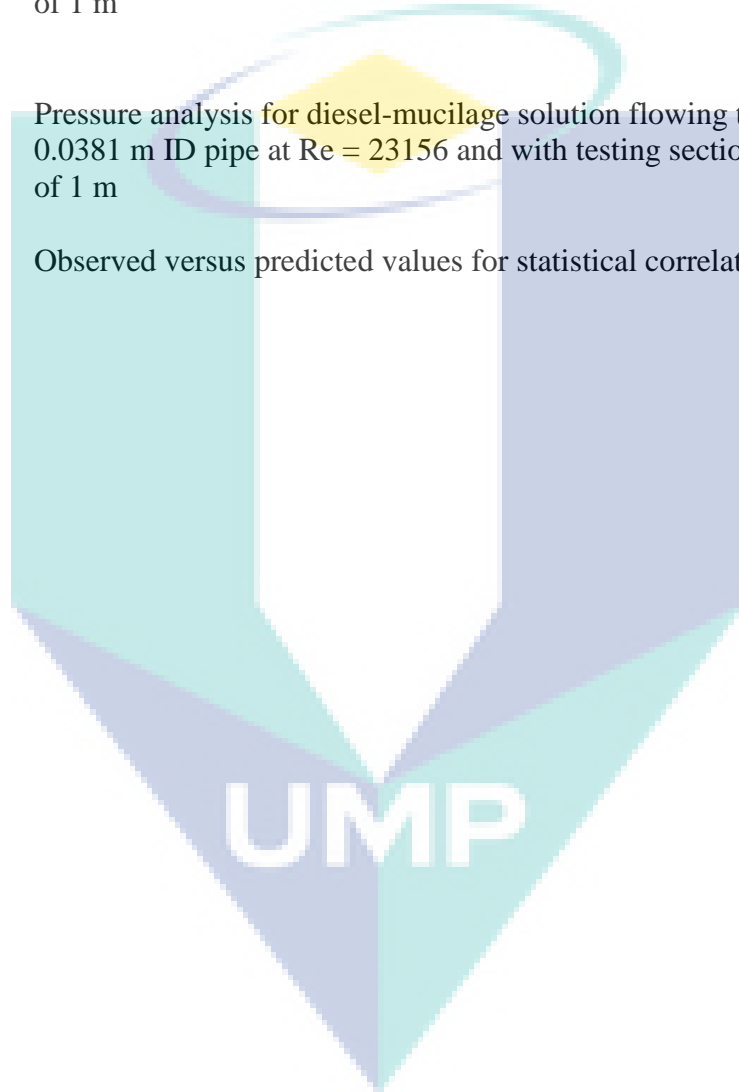
LIST OF FIGURES


Figure No.	Title	Page
2.1	Flow regions	6
3.1	Leaves of <i>Hibiscus rosa-sinensis</i>	29
3.2	Crushed red gypsum	30
3.3	Structural formula of acrylonitrile	31
3.4	Structural formula of nitric acid	32
3.5	Structural formula of hydroquinone	33
3.6	Structural formula of isopropanol	33
3.7	Structural formula of acetone	35
3.8	Structural formula of dimethylformamide	36
3.9	Schematic diagram of closed loop liquid circulation system	38
3.10	Built-up experimental rig	39
3.11	Process summary in obtaining mucilage from hibiscus leaves	40
3.12	Grafted powder of mucilage	41
3.13	Typical system of Mastersizer	42
3.14	Viscometer	44
4.1	Effect of mucilage concentration on viscosity	48
4.2	Effect of red gypsum concentration on viscosity	48
4.3	Friction factor of water flow for $L/D = 39.4$	51
4.4	Friction factor of diesel flow for $L/D = 39.4$	51
4.5	The effect of Reynolds number on drag reduction at different natural mucilage concentration in water along 0.0381m diameter and 1.5m length pipe	53

4.6	The effect of Reynolds number on drag reduction at different grafted mucilage concentration in diesel along 0.0381m diameter and 1.5m length pipe	54
4.7	The effect of Reynolds number on drag reduction at different natural mucilage concentration in water along 0.0254m diameter and 1.5m length pipe	55
4.8	The effect of Reynolds number on drag reduction at different grafted mucilage concentration in diesel along 0.0254m diameter and 1.5m length pipe	55
4.9	The effect of Reynolds number on drag reduction at different natural mucilage concentration in water along 0.0127m diameter and 1.5m length pipe	56
4.10	The effect of Reynolds number on drag reduction at different grafted mucilage concentration in diesel along 0.0127m diameter and 1.5m length pipe	57
4.11	The effect of Reynolds number on drag reduction at different gypsum concentration in water along 0.0381m diameter and 1.5m length pipe	58
4.12	The effect of Reynolds number on drag reduction at different gypsum concentration in diesel along 0.0381m diameter and 1.5m length pipe	59
4.13	The effect of Reynolds number on drag reduction at different gypsum concentration in water along 0.0254m diameter and 1.5m length pipe	60
4.14	The effect of Reynolds number on drag reduction at different gypsum concentration in diesel along 0.0254m diameter and 1.5m length pipe	60
4.15	The effect of natural mucilage concentration in water on drag reduction at different Reynolds number along 0.0381m diameter and 1.0m length pipe	62
4.16	The effect of grafted mucilage concentration in diesel on drag reduction at different Reynolds number along 0.0381m diameter and 1.0m length pipe	62
4.17	The effect of natural mucilage concentration in water on drag reduction at different Reynolds number along 0.0254m diameter and 1.0m length pipe	63


4.18	The effect of grafted mucilage concentration in diesel on drag reduction at different Reynolds number along 0.0254m diameter and 1.0m length pipe	63
4.19	The effect of natural mucilage concentration in water on drag reduction at different Reynolds number along 0.0127m diameter and 1.0m length pipe	64
4.20	The effect of grafted mucilage concentration in diesel on drag reduction at different Reynolds number along 0.0127m diameter and 1.0m length pipe	65
4.21	The effect of gypsum concentration in water on drag reduction at different Reynolds number along 0.0381m diameter and 1.0m length pipe	66
4.22	The effect of gypsum concentration in diesel on drag reduction at different Reynolds number along 0.0381m diameter and 1.0m length pipe	67
4.23	The effect of gypsum concentration in water on drag reduction at different Reynolds number along 0.0254m diameter and 1.0m length pipe	68
4.24	The effect of gypsum concentration in diesel on drag reduction at different Reynolds number along 0.0254m diameter and 1.0m length pipe	68
4.25	The effect of pipe diameter on drag reduction while testing 100ppm natural mucilage in water along 2m pipe length	70
4.26	The effect of pipe diameter on drag reduction while testing 100ppm grafted mucilage in diesel along 2m pipe length	71
4.27	The effect of pipe diameter on drag reduction while testing 100ppm red gypsum in water along 2m pipe length	71
4.28	The effect of pipe diameter on drag reduction while testing 100ppm red gypsum in diesel along 2m pipe length	72
4.29	The effect of pipe length on drag reduction while testing natural mucilage in water at $Re=92791$ along 0.0381m ID pipe	74
4.30	The effect of pipe length on drag reduction while testing grafted mucilage in diesel at $Re=24442$ along 0.0381m ID pipe	75
4.31	The effect of pipe length on drag reduction while testing red gypsum in water at $Re=92791$ along 0.0381m ID pipe	75

4.32	The effect of pipe length on drag reduction while testing red gypsum in diesel at $Re=24442$ along 0.0381m ID pipe	76
4.33	Pressure analysis for diesel-mucilage solution flowing through 0.0127 m ID pipe at $Re = 13893$ and with testing section length of 1 m	77
4.34	Pressure analysis for diesel-mucilage solution flowing through 0.0254 m ID pipe at $Re = 25085$ and with testing section length of 1 m	78
4.35	Pressure analysis for diesel-mucilage solution flowing through 0.0381 m ID pipe at $Re = 23156$ and with testing section length of 1 m	78
4.36	Observed versus predicted values for statistical correlation	80



LIST OF SYMBOLS

m	Meter
ppm	Part per million
ρ	Fluid density
D	Internal diameter
μ	Dynamic viscosity of fluid
h_f	Head loss due to friction
L	Pipe length
V	Average velocity
g	Acceleration due to gravity
f	Darcy friction factor
Δp	Pressure loss
D_h	Hydraulic diameter
τ_w	Wall shear stress
k_s	Sand-grain roughness
wppm	Weight part per million
mL	Milliliter
μm	Micrometer
g	Gram
%DR	Percentage drag reduction
%DI	Percent degree of increase
C	Concentration

LIST OF ABBREVIATIONS

Re	Reynolds number
DRA	Drag Reducing Agent
DR	Drag Reduction
PEO	Poly(ethylene oxide)
MW	Molecular weight
MWD	Molecular weight distribution
GG	Guar gum
RDA	Rotating disk apparatus
AM	Acrylamide
Fen	Fenugreek
CAN	Ceric ammonium nitrate
MDRA	Maximum drag reduction asymptote
DNS	Direct numerical simulation
CFD	Computational fluid dynamics
IUPAC	International Union of Pure and Applied Chemistry
AN	Acrylonitrile
SEM	Scanning Electron Microscopy
ID	Internal diameter
ΔL	Length difference

LIST OF APPENDICES

Appendix	Title	Page
A1	Amount of mucilage in transporting liquids	96
A2	Amount of red gypsum in transporting liquids	98
B1	System verification in transporting water	100
B2	System verification in transporting diesel	112
C1	Percentage drag reduction by mucilage	124
C2	Percentage drag reduction by red gypsum	130
D1	Friction factor in pipe while testing mucilage in water	136
D2	Friction factor in pipe while testing red gypsum in water	169
D3	Friction factor in pipe while testing mucilage in diesel	202
D4	Friction factor in pipe while testing red gypsum in diesel	235
E	Steps for statistical correlation estimation	268
F	List of publications	272

The logo for UMP (Universitas Muhammadiyah Purwokerto) is a large, downward-pointing triangle. It is composed of four smaller triangles meeting at the center: a light blue triangle on the top-left, a light purple triangle on the top-right, a light green triangle on the bottom-left, and a light blue triangle on the bottom-right. The letters 'UMP' are written in a bold, white, sans-serif font across the center of the triangle.

UMP

CHAPTER 1

INTRODUCTION

1.1 BACKGROUND

Due to the continuously shrinking resources of energy in the modern world, power consumption and saving has become a very tactical issue in most of industrial applications. Electrical power is consumed in significant amounts for pumping petroleum liquids through pipelines over long distances. As the liquid moves through the pipe, it experiences a mechanical force (drag) that resists its movement. Drag is identifiable as mechanical force that exists and more accurately known as friction near wall region that decreases the fluid's velocity.

Several techniques were suggested by many authors to overcome the pumping power dissipation problem when transporting liquid in turbulent mode through pipelines. The main target was to reduce the drag force and hence reduce the pressure drop. One of the first and most effective solutions was by installing supporting pumping stations along the pipelines to regain the lost pumping power during transportation. Although this solution helped in improving the flow in pipelines, it added another problem to the system. Maintenance cost plus the energy consumed by the pumping stations added another obstacle in the way of exploring the field of drag.

Since the early 40's, a new technique was suggested to improve the flow in pipelines and to reduce the number of pump stations along the strategic pipelines. Toms (1949) was the pioneer of the idea with an extra energy input to the systems to reduce drag. He discovered that skin-friction could be reduced with the addition of dilute

polymer solutions in very minute amount. The extra energy input is known as drag reducing agent (DRA).

Since then, the drag reduction science has evolved tremendously, and numerous research efforts have been conducted in order to make practical use of this finding. For several decades, DRA has been used in the petroleum industry, to reduce the friction loss in pipelines. Polymers, surfactants and fibers are used as DRAs although artificial viscoelastic polymer is the most preferred additive in industrial applications.

In the present investigation, two new types of drag reducing agents were introduced namely natural polymer extracted from leaves of hibiscus plant (agricultural waste) and red gypsum which is also a waste from titanium dioxide manufacturing industry. These DRAs are commercially cheap and environmentally friendly compared to the existing synthetic DRA in the market. An experimental rig was built to test the flow of petroleum products and water in pipelines. Classical variables such as the pipe diameter, pipe length, additive concentrations and the liquid flow rate were tested in the built closed loop liquid circulation system using both DRA mentioned.

1.2 PROBLEM STATEMENT

Most economic and suitable ways of transporting water and petroleum products over long distances is through pipelines compared to other means of transportation. The cost of transportation through pipelines is high due to high pumping power consumption. Consequently, many supporting pumping stations needed to be built along the way of pipelines to overcome the drag and maintain the fluid flow rate. The formation of eddies induces drag which is manifested in higher pressure drop across the length of the pipe. The cost of pumping increases by additional pump stations and maintenance requirements. In order to solve this problem, the DRA was introduced as the one of efficient ways to reduce costs and achieve a higher volumetric flow rate at the same time.

Surfactants, fibers and synthetic polymers have been used as DRA in the industry for a long time and the applications were successful in improving the flow in

pipelines. Most of the artificial polymers are not biodegradable and cannot be considered as an environmentally friendly product. The biodegradable polymers are mostly insoluble additives, offering lower resistance to flow. Hence the application of these artificial polymer additives has generated interest among researchers for practical applications.

Hence, in this present research, two new flow improvers have been introduced: a natural polymer extracted from hibiscus leaves and suspended solid (red gypsum) which is a waste from titanium dioxide manufacturing industry.

1.3 OBJECTIVES OF RESEARCH

1. To investigate the drag reduction efficiency of the natural mucilage and red gypsum in water and diesel under turbulent flow in pipes.
2. To formulate oil soluble mucilage as it is insoluble in diesel.
3. To investigate the effect of the following classical variables on the overall flow efficiency; liquid flow rate, additive concentration, pipe diameter and testing section length.

1.4 SCOPES OF RESEARCH

- i. To evaluate the performance of *Hibiscus rosa-sinensis* mucilage and red gypsum powder as flow improver in the range of 0 - 1000ppm by weight in water and diesel.
- ii. To determine the applicability of phase solubility inversion method for solubility of *Hibiscus rosa-sinensis* mucilage in diesel to use as DRA.
- iii. To determine the influence of the testing section length range from 0.5 to 2.0m for three diameters 0.0381m, 0.0254m and 0.0127m pipe on the performance of DRAs in the turbulent range of Reynolds number.

1.5 STUDY CONTRIBUTIONS

Two new drag reducing agents, natural mucilage from the leaves of *Hibiscus rosa-sinensis* and red gypsum will be introduced. These two DRA, natural mucilage and red gypsum are agriculture and industrial waste respectively. Therefore, using these DRA as flow improver in transporting liquid through pipelines which have been the backbone energy transport infrastructure will be economical and environmental friendly as an alternative to the existing synthetic additives. Hence, the cost to locate pumping stations along the pipeline network or to use synthetic additive as DRA will reduce.

1.6 OVERVIEW OF THE THESIS

This thesis comprises of five main chapters with the introduction in Chapter 1. Literature reviews on related researches have been discussed in Chapter 2 while Chapter 3, discusses on methodology, apparatus and experimental equipments used. Discussions on the results obtained have been explained in Chapter 4, and Chapter 5 holds the conclusion from current research and recommendations for future work. The list of references and the appendices are given at the end.

The logo of UMP (Universiti Malaysia Perlis) is a large, stylized 'V' shape. The left side of the 'V' is light blue, the right side is light green, and the bottom point is a darker blue. The letters 'UMP' are written in white, bold, sans-serif font across the bottom of the 'V'.

UMP

CHAPTER 2

LITERATURE REVIEW

The review of the work undertaken by previous researches related to drag reduction is presented. As an introduction to the understanding of drag reduction in turbulent flow, general types of flow will be discussed. Then, energy losses in pipelines followed by types of drag reducing agents (DRA), the mechanisms involved and finally the commercial applications of DRA will be discussed in detail.

2.1 INTRODUCTION

The transportation of liquids through pipelines is considered as one of high-power consuming sectors in the industry due to the turbulent mode these liquids are transported. Since the early forties in the previous century, several techniques were suggested to overcome this problem. One of these techniques was the injection of certain chemical additives into the core of the main flow to improve the flow. The unique physical properties of the injected chemicals such as, the density and visco-elasticity, made a large number of these additives commercially visible. It is important to know the mode of the liquid media flowing through the pipeline and the degree of turbulence to understand the effectiveness of any chemical additive, and that will help approaching the mechanism controlling the drag reduction.

2.2 TYPES OF FLOW

Fluid flow in pipelines basically classified into three categories or regimes which is laminar, transitional and turbulent flow. Each flow possesses its own

characteristics and the factor that determines the type of flow is the Reynolds number (Re). Therefore, the understanding on the definition of Re is important.

Reynolds number (Re) is a dimensionless number that gives a measure on the types of flow in fluid mechanics. The Re by definition is a ratio of inertial forces to viscous forces (Batchelor, 1967) depends upon the fluid property and pipe dimension as shown in Eq. (2.1) (Reynolds, 1883).

$$Re = \frac{\rho V D}{\mu} \quad (2.1)$$

Where: ρ is the fluid density (kg/m^3), V is the fluid velocity (m/s), D is the hydraulic diameter or internal diameter of pipe (m) and μ is the dynamic viscosity of the fluid ($\text{Pa}\cdot\text{s}$ or $\text{N}\cdot\text{s/m}^2$ or $\text{kg}/(\text{m}\cdot\text{s})$).

2.2.1 Laminar Flow

Laminar flow or favorably known as streamline flow, occurs when the fluid flows in parallel layers as shown in Fig. 2.1. There is no interference between the layers, therefore, no energy losses to the surroundings. Laminar flow occurs at low Re up to 2000 where viscous forces are dominant, and is characterized by smooth, constant fluid motion.

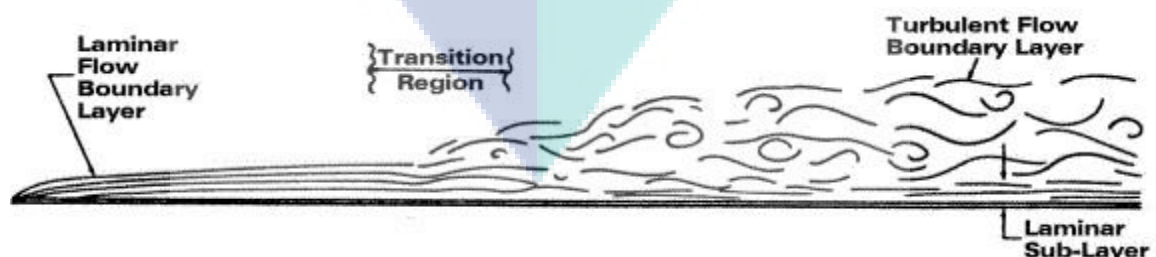


Figure 2.1: Flow regions

2.2.2 Transitional Flow

The process of a laminar boundary layer becoming turbulent is referred to a transitional flow region as shown in Fig. 2.1. Sudden changes in the amplitudes of the disturbance introduce nonlinearity effects. Therefore, Re ranges from 2000-4000 considered as transitional flow.

2.2.3 Turbulent Flow

Turbulent flow in pipeline characterizes at high Re above 4000 and is dominated by inertial forces, which tend to produce chaotic eddies, vortices and other flow instabilities such as pressure and velocity fluctuation. A constant source of energy supply is required to sustain turbulent flow or else, turbulence dissipates rapidly as the kinetic energy is converted into internal energy by viscous shear stress.

Davidson (2004) stated that turbulent flow occurs when the fluid velocity is enough to develop a randomly chaotic component of motion. Turbulence is normally accompanied by an increase in friction and pressure drop as a result of generating eddies in the transverse and horizontal direction as the fluid flows along its boundaries. Attention is placed on the description of turbulence structure as shown in Fig 2.1. There are three different zones or layers of turbulent flow regimes, laminar sublayer, buffer zone and fully turbulent core zone. The turbulent core zone is the largest space that holds most of the fluid in the pipe. This is the zone of the eddy currents and random motion of fluid.

Industrial application usually transports fluids in pipelines under turbulent mode, which is the main source of drag. Detailed inspection exposes that, at low velocities, the fluid flow is streamlined, but as the velocity increases above critical values it turns to chaos (Cengel and Cimbala, 2006). The region where fluctuating random movement of fluids known as eddies and the reverse current created when the fluid flows past an obstacle. The moving fluid creates a space devoid of downstream. Fluid behind the obstacle flows into the void creating a swirl of fluid on each edge of the obstacle, followed by a short reverse flow of fluid behind the obstacle.

Eddies tend to collide between each other cause sudden exchange of momentum (Warhaft, 1997). Eddies always change its shape and size as they move along the flow. They dissipate their energy through the viscous shear and eventually disappears while new eddies formed continuously. These continuous formations slow down the fluid particles, and this phenomenon is known as frictional drag.

There is a wide range of eddies in different size within turbulent region. Usually smaller eddies are unstable, and this pass its energy into even smaller structure. This causes a continual cascade of pumping energy from the large scale down to the smallest. The eddies are destroyed only in the final stages of this process when structures are very small (Davidson, 2004). In fluid mechanics, drag phenomenon referred as eddies which suppresses the fluid rate and increases pressure drop. Therefore, any attempt of reduction in pumping power losses to minimize the pressure drop along pipelines framed as drag reduction.

2.3 ENERGY LOSSES IN PIPELINES

Skin friction is the main cause for energy loss in pipelines, and the friction depends on the properties of pipe and flow type. In laminar flow, the fluid flows in parallel layers thus no change in momentum. Therefore, energy maintained constant until towards the end. Hence, there is less or almost zero energy loss. However, totally different situation arises in turbulent flow (Warhaft, 1997).

As illustrated in Fig. 2.1, a fraction of the laminar sublayer will move up to the buffer zone, it will begin to form eddies. These eddies tend to collide with each other resulting in momentum transfers between fluid particles, thus causing friction. As fluid flows along the pipelines, part of its energy dissipated to overcoming this resistance, with the results that the energy of fluid decreases continuously in the flow direction (Rashidi and Banerjee, 1990).

The flow of water under turbulent conditions in long unobstructed straight pipes of uniform diameter was studied by Darcy and Weisbach (Lester, 2002). Darcy-Weisbach suggested the following Eq. (2.2) which relates the head loss (or pressure

loss) due to friction along a given length of pipe to the average velocity of the flowing fluid.

$$h_f = f \frac{L V^2}{D 2g} \quad (2.2)$$

Where h_f is the head loss due to friction, L is the pipe length, D is the internal diameter of pipe, V is the average velocity of fluid, g is the acceleration due to gravity, and f is a dimensionless Darcy friction factor. Given that the h_f expresses the pressure loss Δp as the height of a column of liquid as in Eq. (2.3) and Eq. (2.4) where ρ is the fluid density.

$$\Delta P = \rho g h_f \quad (2.3)$$

$$\Delta P = f \frac{L \rho V^2}{D 2} \quad (2.4)$$

Where f can be found by solving the Colebrook equation as shown in Eq. (2.5).

$$\frac{1}{\sqrt{f}} = -2 \log_{10} \left(\frac{\varepsilon/D_h}{3.7} + \frac{2.51}{\text{Re} \sqrt{f}} \right) \quad (2.5)$$

Where f is the Darcy friction factor, ε is roughness height (m), D_h is the hydraulic diameter of pipe and Re is the Reynolds number.

Holland (1973) explains that the measure of energy loss or friction loss can be achieved by comparing the total energy at two points in the flow line, as a pressure gradient. The pressure gradient is usually expressed as the pressure difference relative to a selected horizontal datum divided by the distance between the two points, i.e. ($\Delta P/L$). The friction loss can be expressed in term of pressure drop per pipe length using the energy balance equation for a circular horizontal pipe in a steady fluid flow as follows (Eq. 2.6):

$$\tau_w = \frac{D\Delta P}{4L} \quad (2.6)$$

The friction loss in pipe flow can also be expressed as in Eq. (2.7):

$$f = \frac{2\tau_w}{\rho V^2} \quad (2.7)$$

Fanning friction factor for friction loss can be expressed as follows (Eq. 2.8):

$$f = \frac{\Delta P.D/4L}{\rho.V^2/2} \quad (2.8)$$

For a Newtonian fluid, the relation between the friction factor and the Re for a turbulent channel flow is given by Dean (1978) as in Eq. (2.9):

$$f = 0.073\text{Re}^{-0.25} \quad (2.9)$$

Due to the general similarity between the pipe and channel flow, Eq. (2.9) is likely similar to Blasius' relation for pipe flow with the only difference being that the value of the constant is 0.079 instead of 0.073.

The smooth pipe law and rough pipes relation were originally presented by Prandtl and Von Karman as in Eq. (2.10), and Eq. (2.11) respectively where f is the friction factor from (Moody) and ks represent sand-grain roughness (m). Nevertheless, the constants in both relations were adjusted Nikuradse (1932 and 1933) to fit his experimental data.

$$\sqrt{1/f} = 2.0\log(\text{Re}\sqrt{f}) - 0.8 = 2.0\log\left(\frac{\text{Re}\sqrt{f}}{2.51}\right) \quad (2.10)$$

$$\sqrt{1/f} = 2 \log \left(\frac{r}{k_s} \right) + 1.74 = 2 \log \left(7.41 \frac{r}{k_s} \right) \quad (2.11)$$

Most of the friction factor correlations used in the industry are based on turbulent boundary layer theory. The main reference for friction factors in pipes has been the work of Nikuradse (1950 and 1966) for flow in both smooth and sand roughened pipes, where friction factor relations were presented as Eqs.(2.10) and (2.11).

In Eq. (2.10) and Eq. (2.11), Nikuradse showed that, for low Re, the friction factor dependent on Re only, then at sufficiently high Re the friction value more dependent on wall roughness only. Then, Colebrook presented additional experimental results and developed a correlation for the friction factor as in Eq. (2.5) which is valid also in the transitional regime between the smooth and rough flow.

A recent study (Zagarola and Smits, 1998) of the flow at high Re in smooth pipes showed that the Prandtl law was not accurate for high Re. A friction factor correlation of the same form as the Prandtl law was presented. This correlation differs by as much as 5% at $Re \ 3 \times 10^7$ compared to Prandtl law. The Prandtl correlation was shown to predict too low values of the friction.

2.4 DRAG REDUCTION

2.4.1 Introduction

It was the accidental discovery by Toms (1949) that opened the door wide for the drag reduction research from the early forties of the last century. He discovered that addition of a small amount of additives, i.e. a few weight parts per million (wppm), can greatly reduce the turbulent frictional pressure drop of a fluid is known as drag reducing agent (DRA) and thus named after him as Toms Phenomenon. Since then, several techniques, additives and mechanism were suggested by a large number of authors to improve the flow in pipelines and reduce the energy losses. The addition of minute quantities of polymeric additives was highly recognized by the industry due to its high effectiveness and low addition concentrations (Motier *et al.*, 1996, Warholic *et al.*, 1999 and Mohamed, 2000). The main concern for a large number of these industries was the

additive's stability against shear forces and how to prevent the degradation. This is the reason for surfactant and even suspended solids were introduced as drag reducing agents later to overcome the polymeric additives degradation problem.

Drag Reducing Agents (DRA) can be classified into three major categories: polymers, surfactants and suspended solids. The earlier DRA was in the form of gel, and nowadays can be found in the form of slurries and powders (Daas, 2001).

2.4.2 Drag Reducing Agents (DRA)

(i) Polymers

Polymer defined as a substance with high molar masses. Structurally, it has a large number of repeating units known as monomers, covalently bonded together. Polymers grouped into two types, synthetic and natural polymers (Ophardt, 2003). Synthetic polymers are chemically derived through a polymerization process and manufactured in the industry. Plastics, synthetic fibers, and elastomer are examples of synthetic polymers. Naturally occurring polymers exists in plants and animals. Cellulose, starch, lignin, chitin and various polysaccharides are included in this group. The viscoelastic properties of polymers cause the field of drag reduction study expand. Mainly synthetic polymers have been widely used by researchers in this drag reducing study and very few explored it with natural polymers.

Toms (1949) was the first to reports that a significant reduction of the frictional pressure gradient in turbulent flow could be achieved by adding minute amounts of polymers into a solvent. Toms obtained 50% drag reduction (DR) compared with a pure solvent using poly (methylmethacrylate) in monochlorobenzene. These low concentration additives mostly show no effect in laminar flows (Sher and Hetsroni, 2008) as it is the streamlined flow. Since then, this field has attracted a number of researchers and industries due to its economic benefits. Many attempts on drag reducing polymers for possible applications in industry.

Subsequent studies (Shaver and Merrill, 1959; Savins, 1963; Fabula, 1963; Metzner and Park, 1964; Elata and Tirosh, 1965; Hershey and Zakin, 1965) confirmed

Toms phenomenon with several different polymers in turbulent flow through pipes with ranging internal pipe diameter. A detailed description of the drag reduction phenomenon is presented from Virk *et al.* (1967) who shows experimental evidence that drag reduction is limited by an asymptotic value; it can be concluded that models confirm the observations of Lumley (1969) who observed drag reduction in different polymers.

Recently, experiments conducted using polyalpha-olefin (polyisobutylene) in annular two-phase flow of oil and air (Mowla and Naderi, 2006) and about 40% DR is observed at certain experimental conditions. Besides that, polymer-induced turbulent drag reduction in a rotating disk apparatus was investigated using nonionic poly(ethylene oxide) (PEO) in a synthetic saline solution (Choi *et al.*, 2000). A maximum total drag reduction of 30% was obtained with 50 wppm of PEO. Although synthetic polymers of high molecular weight ($>10^5$) are very effective drag reducers; however, it gets degrade in turbulent flows and lose their effectiveness after a short interval of time or flow (Singh *et al.*, 2009).

Polymeric additives usually expose towards elongation strain as well as to strong shear stresses under turbulent flow, and this mechanical energy causes scission of the polymeric chains which decreasing the drag reducing effectiveness. Mechanical degradation in turbulent flow influenced by various factors including polymer molecular weight (MW), molecular weight distribution (MWD), temperature, polymer-solvent interactions, polymer concentration, turbulent intensity, method of preparation and storage, and flow geometry (Choi *et al.*, 2000). The majority of studies explored the influence of these factors on polymer degradation from changes in either the friction factor or intrinsic viscosity. Recently, Vanapalli *et al.* (2005) directly quantified polymer degradation within turbulent flows with measurements of the molar mass distributions via light scattering techniques.

It is known that most of the research work conducted by many researchers adopted synthetic polymers as a trustable polymeric DRA. Natural polymers did take less attention by the researchers worldwide due to its limited, unsustainable resources and also because most of the drag reducing natural polymers is driven from plant used for human food consumptions. Guar gum (GG), which extracted from the guar bean, is

the most well known biopolymers drag reducing agent (Turabi *et al.*, 2008 and Hong *et al.*, 2010).

Hong *et al.* (2010) observed maximum 30% DR with 200ppm virgin guar gum while studying the mechanical degradation of polysaccharide guar gum under turbulent flow. Tremendous reduction in frictional drag was observed even though only a minute amount (in ppm) of GG is dissolved in aqueous solutions (Choi *et al.*, 2002 and Lim *et al.*, 2003). Even drag reduction efficiency of GG has been investigated in a rotating disk apparatus (RDA) (Kim *et al.*, 2002). Anderson *et al.*, (1993) studied the combined effects of riblets and polymers in pipe flow, and it was found that 0-40% drag reduction with 100ppm guar gum in a pipe lined with 0.15mm V groove riblets.

Another biopolymer, which is widely used as DRA, is xanthan gum (Sohn *et al.*, 2001). Xanthan gum is an extracellular polysaccharide and the backbone of the polymer are similar to that of cellulose. It has been broadly used in a different field of industry, e.g. pharmaceutical areas, in the cosmetics, in oil drilling fluids and enhanced oil recovery. It's even possible for use in coal water mixtures (Podolsak *et al.*, 1996; Katzbauer, 1998 and Kim *et al.*, 2000).

Wyatt *et al.* (2011) studied the drag reduction effectiveness of dilute and entangled xanthan in turbulent pipe flow. They explored the drag reduction properties of the polyelectrolyte xanthan in differing solvent environments (salt free versus salt solution) and delivery configurations (homogeneous versus stock solution dilution). Drag reduction effectiveness increases as an entangled xanthan solution is diluted compared to solutions prepared in the dilute regime. Based on dynamic rheological measurements of the elastic modulus, residual entanglements and network structure are hypothesized to account for the observed change in drag reduction. Drag reduction effectiveness is unchanged by the presence of salt when the stock solution concentration is sufficiently above the critical concentration. It is observed that the drag reduction effectiveness decreases with time when diluted from an entangled stock solution but remains greater than the homogeneous case after more than 24h.

The study on polymers is connected with degradation where changes in the properties such as tensile strength, color and shape takes place. The advantage of natural polymer is their high mechanical stability against degradation when compared to flexible synthetic polymers with similar molecular weights; however they are highly susceptible to biological degradation (Sohn *et al.*, 2001). Certain industrial polymers (Chakrabarti, 1991a, 1991b and Deshmukh and Singh, 1987) such as hydroxypropylguar, guar gum and xanthan gum, have been found to be reasonably shear-stable DRA.

The major problems facing the usage of natural polymers in the industrial applications are the availability of the raw materials and the solubility of the resulting polymer in the transported media. The benefits of DRA use in existing systems increase production without any mechanical modification, reduction of operating costs such as pumping power and reduction of pipeline pressure while maintaining throughput.

One of the most important scopes in polymer science is the preparation and application of functional polymers. Merging (grafting) of the precise functional group into polymer imparts beneficial effects on its properties (Narayan, 1990 and Dalman *et al.*, 2003). It is experimentally proven that, incorporation of monomers onto the backbone of natural polysaccharides helps in improving some original properties of polysaccharides and also allows the product copolymers to show novel functionality (Singh *et al.*, 2000; Teramoto and Nishio, 2003). Singh *et al.* (2000) has grafted polysaccharides such as guar gum, xanthan gum, carboxymethyl cellulose and starch with acrylamide (AM) using ceric ion/HNO₃ acid as redox initiator. Recently, reports showing that synthesis of polyacrylamide and polyacrylonitrile grafted copolymers of mucilage obtained from food grade polysaccharides have been found (Mishra and Bajpai, 2005; Mishra *et al.*, 2003).

Mishra *et al.* (2006) synthesized polyacrylamide-grafted-fenugreek mucilage (Fen-g-PAM) copolymers by grafting acrylamide (AM) onto fenugreek mucilage (Fen) backbone by ceric ion initiated solution polymerization technique under nitrogen atmosphere. A total of 19 copolymer samples was prepared by varying concentrations of AM and ceric ammonium nitrate (CAN), reaction time and temperature. The variation

in reaction parameters affected the percent grafting, grafting efficiency and intrinsic viscosity of the copolymer samples. The copolymers were characterized using different techniques. The prepared copolymers were partially soluble in water and completely soluble in 1 N NaOH aqueous solution. Thermal properties of the copolymers seem to be much better than that of pure mucilage. Biodegradability studies showed a minor difference in the length of time taken for complete degradation of Fen and Fen-g-PAM. Therefore, it was concluded that the grafting of AM onto the backbone of natural polysaccharide only improves its properties without affecting its biodegradable nature.

Mishra and Pal (2007) in their recent findings has synthesized polyacrylonitrile-grafted copolymers of Okra mucilage (O-g-PAN), which used in the food industry as a good emulsifying and foam-stabilizing agent. Grafting of polyacrylonitrile onto Okra mucilage, a polysaccharide of vegetable origin, offer a new polymeric material with properties that can be exploited industrially. They prove that grafting only improves the properties of mucilage by introducing more reactive sites and without making any change in the molecular stability of chelating groups of polysaccharide. A redox initiator system of ceric ammonium nitrate/HNO₃ was efficiently used to graft PAN onto the mucilage.

While studying the effect of monomer/starch feed ratios and moisture content during reactive extrusion of starch-poly-acrylamide graft copolymers, Finkenstadt and Willett (2005) demonstrated that graft copolymer properties can be controlled with proper selection of acrylamide/starch ratio and moisture content during reactive extrusion. Increasing the acrylamide/starch ratio leads to graft copolymers with more grafts of higher molecular weight, even as the grafting efficiency decreases. Increasing moisture content gives more grafts of lower molecular weight as well as decreased conversion and graft efficiency.

Cellulose is frequently modified in the preparation of a wide range of new materials that have proved to be very useful in several and diverse fields of application (Onishi *et al.*, 2004 and Kato *et al.*, 1999). One method of modifying cellulose that has been studied extensively is graft copolymerization (Ouajai *et al.*, 2004). Great numbers of grafting methods have been developed, but the free radical methods of generating

radicals on the cellulose backbone before grafting have received the greatest attention (Fernandez *et al.*, 1990). The use of ceric ions to generate free radicals, which initiate grafting reactions has been one of the most reported methods (Gupta and Khandekar, 2002).

(ii) *Surfactants*

Surfactants are known as surface active agents who capable of reducing surface tension of a liquid. This organic compound is amphiphilic which contain both hydrophobic (tails) and hydrophilic (heads) portions. Depending on the electric charge of head group, surfactants can be classified as anionic, cationic, nonionic or zwitterionic (Zhang, 2005). Anionic surfactant has negatively charged head. Cationic surfactant has positively charged head whereas nonionic surfactant does not carry any net charges. In contrast to nonionic surfactant, zwitterionic surfactant has two oppositely charged groups.

Meantime of using polymers as DRA, several studies have qualitatively shown that surfactants have the potential to be used as DRA. Mysels (1949) observed drag reduction in the increased gasoline flow rate in a pipeline with the addition of aluminum soaps (anionic surfactant). Surfactants have been extensively reviewed by Gyr and Bewersdorff (1995), Zakin *et al.* (1996) and Myska and Zakin (1997).

The well known Maximum Drag Reduction Asymptote (MDRA) for dilute polymer solutions is proposed by Virk. A fairly good power law approximation to this implicit equation is given by (Aguilar *et al.*, 2001) that ' $f = 0.58\text{Re}^{-0.58}$ '. This asymptotic correlation has been confirmed by a great amount of experimental data with regards to dilute polymer solutions, and it was shown to be independent of pipe diameter, concentration, molecular weight, coil size and etc. There is almost a unanimous consensus that the MDRA for surfactants should be higher than that of polymers (Aguilar *et al.*, 2001). Zakin *et al.* (1996), proposed a new MDRA for surfactants. This MDRA is approximately valid in the range between $4000 < \text{Re} < 130,000$ where $f = 0.315\text{Re}^{-0.55}$.

Though anionic surfactants are found to be mechanically stable flow improver (Savins, 1967), their use is not favored due to its vulnerability to calcium and magnesium ions normally present in water, and their foam-forming characteristics (Zakin *et al.*, 1971). Cationic surfactants show much broader effective temperature window of applicability and thus have larger potential for practical applications (Zakin and Lui, 1983) compared with nonionic surfactants which have a narrow temperature window of applicability around their cloud points (Chou, 1991).

Myska and Zakin (1997) studied the differences in the flow behavior of polymeric and cationic surfactant drag reducing additives. These include the influence of preshearing, the effect of mechanical shear on degradation, the influence of tube diameter, maximum drag reduction effectiveness, and the shape of their mean velocity profiles. Polymer solutions are generally shear thinning while cationic surfactant show increases in viscosity when sheared, indicating the formation of a shear induced structure. Polymer solutions degrade irreversibly when sheared and lose their drag reduction effectiveness whereas cationic surfactants degrade under high shear, but the structures are “repairable” and they regain their drag reducing ability where shear is induced. Dilute polymer solutions become drag reducing when a critical shear rate is exceeded but surfactant solutions generally show a gradual departure from the laminar flow curve and are drag reducing until a critical shear rate is reached. When compare the friction factors for both, cationic surfactant and aluminum disoap systems reached significantly below those predicted by the maximum drag reduction asymptote for high polymers. Turbulent mean velocity profiles for cationic surfactants can be radically steeper than that predicted with elastic sublayer model for high polymers. A three dimensional entangled threadlike network formed in surfactant solutions may cause a different drag reduction mechanism from that for high polymer solutions.

Myska and Mik (2003) have presented experimental results involving the use of drag reducing surfactants in a small house heating system as an application in daily life. They reported no significant reduction in heat transfer. However, they recommend proper precautions be taken concerning biodegradation of surfactant in long operation heating systems. Signification of the surfactant adhesion on the surface in that already long operating system was not as estimated. The large surface of tiny particles of the

dust and other impurities was the main reason for not being successful in energy saving, therefore; the system recommended being cleaned before applying the surfactant. Small hydronic heating systems with automatic electric or gas heaters do not run with large Re and low intensity of turbulence to make use of considerable drag reduction effectiveness of the surfactant. These considered as large barrier in the experiment.

While testing the cationic surfactant as DRA, Indartono *et al.* (2005) investigated the temperature and the diameter effect on hydrodynamic characteristic. Olelylhydroxyethyle methyl ammonium chloride found to be has the clear DRA capability until $70^{\circ}C$, and they suggested that temperature has a significant influence in changing the hydrodynamic entrance length of surfactant drag reducing flows. For ionic surfactants, increase in temperature usually causes shrinking of micelles (Israelachvili, 1991). Evans and Miller (1992) explained this as resulting from the unbinding of counterions from the micellar surface due to thermal motion, which causing less screened headgroup electrostatic repulsions.

Lu *et al.* (1998) studied the effect of variations in counterion to surfactant ratio on rheology and microstructures of drag reducing cationic surfactant systems. Rheology, drag reduction and cryo-TEM experiments were performed on Arquad 16-50/NaSal and Ethoquad O/12/NaSal surfactant systems at different counterion-to-surfactant ratios and at constant, low surfactant concentrations, 5mM, appropriate for drag reduction. The molar ratio of counterion-to-surface was varied from 0.6-2.5. All the surfactant systems described were viscoelastic and drag reducing. It was found that the viscoelasticity and drag reducing effectiveness increase with the increase in counterion/surfactant ratio. Network was found to present in the solutions with high ratios, and they were viscoelastic. However, in order to induce network formation for solutions at low ratio, shear was needed. Cryo-TEM images confirmed the existence of threadlike micelles, which formed entanglement networks, and showed that the micellar network became denser with increasing counterion/surfactant ratio in one surfactant series. Both increase in the counterion/surfactant ratio and the shear rate resulted in shorter relaxation times. For some of those systems, abrupt increases in viscosity are observed in certain shear rates which are time effects affecting microstructure rearrangements rather than the formation of shear induced structures.

Meanwhile, Chapman (2005) determined for both Zwitterionic and nonionic surfactant at 20% by weight ethylene glycol/water that could be used in district cooling systems for a range of temperature. Drag reduction of other solvent such as water 30% by weight glycerol/water and 25% propylene glycol/water were also suggested. The main aim of the Chapman's project was to find more environmentally friendly surfactants with the drag reducing ability equal to that of cationic surfactants. Addition of sodium nitrile has also contributed in drag reduction as being an effective means of resistance on corrosion in the metal pipes when used in combination with zwitterionic/nonionic or zwitterionic/anionic surfactant solutions.

Due to the unique DR properties that mixed surfactant solutions show, there has been increasing interest in mixed surfactant solutions such as cationic and anionic (Salkar *et al.*, 1998; Marques *et al.*, 1999 and 2003; Schubert *et al.*, 2003) and zwitterionic and anionic (Li *et al.*, 1998). When different surfactants are mixed together, the physicochemical properties of the mixtures usually differ greatly from those of the neat surfactants due to the synergistic interactions between amphiphiles, i.e. nonideal mixing. Such synergy is most often observed as enhanced interface properties, increased surface activity, compared to the individual surfactants.

The drag reduction (DR) and heat transfer efficiency reduction (ER) of nonionic surfactant as a function of fluid velocity, temperature and surfactant concentration were investigated by Cho *et al.*, (2007). From the experimental results, it was concluded that existing alkyl ammonium surfactant (CTAC; cetyl trimethyl ammonium chloride) had highest DR at lower temperature ranging from 50-60⁰C and the new amine oxide and betaine surfactant (SAOB, stearyl amine oxide + betaine had highest DR at higher temperature ranging from 70-80⁰C within the tested concentration of 1000 – 2000 ppm concentration.

Hadri and Guillou (2010) studied the drag reduction by surfactant in closed turbulent flow. In general, CTAC/NaSal (CetylTrimethyl Ammonium Chloride and Sodium Salicylate) of 75ppm reduced drag up to 75%. At the same time, the spatial velocity distribution was measured and analyzed using particle image velocimetry (PIV). PIV's results show that the turbulence characteristics of the very low-

concentrated surfactant solutions are strongly affected, whereas, the flow is fully turbulent; the turbulent kinetic energy for the surfactant solution is lower and the Reynolds stress is negligible.

Unique models for the drag reduction in surfactant micellar solutions have also been proposed. This kind of additive can sometimes exhibit behavior different from polymer additives, such as an increased drag reduction, above Virk's maximum asymptote (Gyr and Bewersdorff, 1995). Fichman and Hetsroni (2004) discussed the applicability of electrokinetic mechanism, exclusive for ionic surfactants micellar solutions.

(iii) *Suspended solids*

The study on drag reduction caused by the addition of suspended solid matter was initiated by the fact that turbid streams of water were found to flow faster than clear ones (Shenoy, 1984). Vanoni (1946) was the first who undertaken comprehensive experimental works in this study. Suspended solids (insoluble in liquid media) refer to small solid particles which remain in suspension in water as a colloid or due to the motion of the water. Recently, the classification of suspended solids as DRA opened the door wide for more research regarding the availability of the solubility condition in the drag reduction phenomena (Toorman, 2002; Zhu and Peskin, 2007 and Inaba *et al.* (2000). The capability of insoluble material to act as DRA was one of the motivations in the present investigation. Shenoy (1984) classified suspensions into two types, namely granular or nearly spherical particles and fibers.

Few types of suspended solids that have been used as DRA are glass beads, sand and polystyrene (Molerus and Heucke, 1999). Glass spheres and plastic beads (Barresi, 1997) were used to study the interaction between particles and turbulent flow in a stirred tank. He found that the turbulence was modified by suspended solids and concluded that large changes in turbulence depends on high particle loading and smaller but heavier glass sphere particles.

Radin *et al.* (1975) studied the effects of particle shape and size, concentration, fluid viscosity, and tube diameter on friction factor. Their central objective was to determine under what conditions drag reduction would occur. It has been evidenced that the presence of solid particles can modify the energy spectra of the fluid phase (Schreck and Kleis, 1993). It can cause either an increase or a decrease of the turbulence intensity, mainly depending on the relative size of the particles with respect to the fluid length scale (Gore and Crowe, 1989a).

Besides that, paper pulp such as Kraft hardwood pulp (Luetzgen *et al.*, 1991) and wood pulp (Kazi *et al.*, 1999) have contributed to the study of drag reduction mainly due to their environmental friendly behavior and low cost. The use of pulp fibers as DRA was earlier mentioned by Moller (1976). The behavioral study on pulp suspension was conducted by Inaba *et al.* (2000) whereby they constructed an experimental system. Drag reduction was measured based on the velocity profile of laminar and turbulent flow. Results showed that the velocity profile of turbulent flow in the presence of fiber did not follow the values of the velocity distribution law equation without fibers.

The mechanisms of fiber suspension suggest that the drag reduction occurred in turbulent core and not near the wall. An increase in the effective viscosity, in the turbulent core, has been observed during fiber suspensions away from the wall. Thus, turbulent fluctuations damped, while the viscosity in the viscous sub layer will be lowered. This mechanism, however, may not account for the large degree of drag reduction observed in some dilute suspensions where the effective viscosity of the suspensions is nearly the same as that of the carrier fluid alone (Luetzgen *et al.*, 1991).

Prediction of the flow and orientation of semi-dilute, rigid fiber suspensions in a tapered channel was presented through numerical modeling (Krochak *et al.*, 2009). They investigated the effect of the two-way flow/fiber coupling for a low Reynolds number flow using the constitutive model of Shaqfeh and Fredrickson (1990). The results of the numerical predictions showed that the streamlines of the flow are altered and that velocity profiles change from Jeffery-Hamel, to something resembling a plug flow when the fiber phase was considered in the fluid momentum equations. This phenomenon was found when the suspension enters the channel in either a pre-aligned,

or in a fully random orientation state. When the suspension entered the channel with an aligned orientation state, fiber orientation was shown to be only marginally changed when the two-way coupling was included. However, when the suspensions enters the channel with a random orientation state, significant differences were found between coupled and uncoupled predictions of fiber orientation. In such case, the suspension was shown to align much more quickly when the mutual coupling accounted for, and profiles of the orientation anisotropy were considerably different both qualitatively and quantitatively.

Alumina and sand with polyamide is another example of suspended solids which has proven their ability as DRA (Hayder, 2006). An experimental closed loop liquid circulation system was built up to test the effectiveness. Evidently demonstrated that, in the presence of 2000 ppm of polyamide, maximum drag reduction up to 53% could be achieved and 40% in a solution with 2000 ppm sand powder.

2.4.3 Drag Reduction Mechanisms

Despite the extensive research in the area of drag reduction over the past decades, there is no universally accepted model that explains the real mechanism for friction reduction. A comprehensive mechanism would have to address the role of the DRAs structure and composition, as well as interactions between additives-solvent in the drag reduction phenomena. During the last 50 years, numerous papers have been written, discussing several experimental, numerical and theoretical aspects of drag reduction of turbulent flows by polymer additives. A general review of drag reduction is given by Lumley (1969) and more work by Hoyt (1972).

Two principal theoretical concepts have been put forward to explain the phenomenon of drag reduction by polymers. The first can be attributed to Lumley (1969, 1973), who proposed that the stretching of randomly coiled polymers increase the effective viscosity. By consequence, small eddies are damped which leads to a thickening of the viscous sublayer and thus reduce drag. Lumley also postulated that the influence of polymers on turbulence becomes important only when the time scale of

the polymers such as relaxation time is larger than the time scale of the flow, which known as the onset of drag reduction.

In contrast to Lumley, Gadd (1971) and de Gennes (1990) proposed a new theory where drag reduction is caused by the elastic properties rather than viscous. Gadd's observation on experimental works made him conclude that polymers were active at the centre of the pipe and viscous forces do not play any role. He argued that the elastic property of polymer cause shear waves to prevent the formation of turbulent velocity fluctuations at smaller scales. De Gennes (1990) and Joseph (1990) strengthen the results that elasticity is the main reason for drag reduction. De Gennes' explanation is that the shear waves, which are caused by the elasticity of the polymers, prevent the production of turbulent velocity fluctuations at smaller scales.

Direct numerical simulation (DNS) has been used to analyze quantitatively the turbulence transport mechanism. With DNS, the instantaneous flow structures near the wall can be calculated accurately, which are difficult to measure precisely in experiments. The instantaneous extra stress associated with the deformation of macromolecule/network structures can be calculated which has not yet been directly measured in experimental conditions. The quantitative data obtained by DNS are helpful in analyzing the mechanism of drag-reduction. Moreover, in contrast to experiments, the effects of various physical properties can be easily isolated and studied by numerical simulations. Orlandi (1995) and Toonder *et al.* (1997) carried out DNS using extensional viscosity models for a channel, and a pipe flow, respectively. Their results qualitatively agree with most experimental observations.

Dubief *et al.*, (2005) used DNS and numerical experiments to access further in the mechanisms of polymeric drag reduction. Investigating the polymer body force shows that, polymers reduce turbulence by opposing the downwash and upwash flows generated by near-wall vortices, while they enhance streamwise velocity fluctuations in the near-wall region. The numerical experiments allow characterizing the importance of each component of the polymer body force on the drag-reducing and turbulence-enhancing properties. The exact localization of polymer's drag reducing activity is now fundamental for the development of a predictive model for polymeric drag reduction.

With advances in instrumentation and visualization techniques, another category of analyzing drag reduction mechanism arose, in which changes in coherent turbulent structure due to polymers are examined. The visualization of the mixing layer shows that the addition of the polymer will enhance coherent structure. The measurement of the turbulent intensities and Reynolds stresses by LDA shows that polymer additives do not simply suppress the turbulent fluctuation as we expected (Xueming *et al.*, 2002). On the contrary, the peaks of these quantities in polymer solution are higher than their counterparts in a Newtonian fluid at the downstream of the mixing layer. In pipe flow, the axial turbulence intensity increases, while the radial turbulence intensity reduces. This means that the turbulence structures gets altered rather than suppressed.

Of all the possible explanations for the polymer drag reduction, some studied on mechanisms involved while using solid particles. Several theoretical, numerical and experimental studies have tried to model two-phase flows, but this is a hard task whenever particle-particle interactions have also to be taken into account. Luetzgen *et al.* (1991) said that drag reduction by fiber suspension in turbulent flow is due to the structural changes of turbulent. Profound indication of an altered turbulence structure is the observation that increased turbulent dispersion and decreased momentum transfer can occur simultaneously when fibers are added into the turbulent water flow. In addition, the presence of entangled fibers in a flow may force a redirection of turbulent bursts, which could alter the structure of turbulence and resistance to elongation of fluid elements with fibers may also contribute to the changed turbulence structure.

On top of that, changes in the velocity profile near the wall were noticed as suspended pulp fibers were evenly dispersed in the pipe (Inaba *et al.*, 2000). Based on the observations, it was concluded that the mechanism of drag reduction in presence of fibers occurred near the pipe wall and not in the turbulent core as mentioned by other researchers. This statement was later supported by Dong *et al.* (2003) that the concentration results scaled by the fiber length show a linear region near the wall.

Besides that, Koichi *et al.* (2005) investigate drag reducing flows by nylon fibers to discuss the mechanism of drag reduction with fiber suspensions and to develop the prediction method of the drag reduction range. As for the prediction method, they

introduced time scale ratio of drag reducing additives like fibers to coherent fine scale eddy. Since the time scale of a given fiber is considered to be constant, the time scale ratio depends only on the time scale of the coherent fine eddy for a given fiber. The time scale of the coherent fine eddy can characterize the range of drag reduction for pipes of different diameters very well. The drag reduction occurs in a specific range for low fiber concentration, while the drag reduction range shift to the small time scale of the coherent fine scale eddies for high fiber concentration. The characteristic time of the fiber as a drag reducer becomes longer in proportion to the second power of the fiber aspect ratio for low concentration.

Barresi (1997) while investigating the interaction between turbulent liquid flow and solid particles, qualitatively explained the observed behavior considering that turbulence modification in two-phase systems contributed by different mechanisms, and depending on the particle size (or Re), dissipation of turbulent kinetic energy or generation of additional turbulence by shedding vortices can be relevant. Energy dissipation through particle collisions becomes important in dense suspensions, which can explain the observed dependence of selectivity on concentration.

2.4.4 Commercial Applications

In general, commercial application of DRAs is due to 3 important factors, environmentally friendly, availability and economic cost. This mostly related to long distance transportation of water and petroleum products in pipelines, oil well operations, sewage and water disposal, fire fighting system and water heating and cooling in the heat exchanger. The well known application of the DRA was in 1979 at the Trans-Alaska pipelines which transporting crude oil. Injecting a concentrated solution of high molecular weight polymer as low as 1 ppm downstream of pumping stations, reduce the power consumptions (Ragsdale, 2007). The pipeline is 800 miles long with 48-inch diameter. Prasetyo (2002) reported that the use of DRA allowed an Indonesian pipeline system to overcome capacity constraint quickly, bring on stream additional crude production and eliminate some pumping capacity at substantial savings. Polymer DRAs were also successfully applied in other crude oil pipelines such as Iraq-Turkey, Bass Strait in Australia, Mumbai Offshore (Nijis, 1995), and North Sea Offshore (Dujmovich

and Gallegos, 2005) and in finished hydrocarbon product lines (Motier and Carreir, 1989). In each case, the polymer composition had to be designed for the particular hydrocarbon to be transported.

Besides that, polymer additives have been used successfully in commercial applications that involve fluid flow in pipes or conduits (Sellin *et al.*, 1982). On the other hand, the DRA was used as a corrosion inhibitor in the gas pipelines of Gulf of Mexico. The field trial was conducted and as a result, peak gas production rate increases by 10 to 15 % and peak pressure drop decreases up to 20 % (Chen *et al.*, 2000). Other examples of commercial application of DRA in the industry are Philips (2006) and Creamer (2008).

Polymer DRAs have also been proposed for the following applications: oil field operations (Hellsten and Oskarsson, 2004 and Sullivan *et al.*, 2007), slurry or hydraulic capsule pipeline transportation (Golda, 1986 and Wul *et al.*, 1998) suppression of atherosclerosis (Mostardi *et al.*, 1978 and Unthank *et al.*, 1992), prevention of lethality from hemorrhagic shock (Kameneva *et al.*, 2004), increased water flow and water jet focusing in firefighting equipment (Fabula, 1971 and Figueredo and Sabadini, 2003), prevention of overflows of water in sewage systems after heavy rains (Dembek and Bewersdorff, 1981), increase of volumetric flow rate of water in hydro-power and irrigation systems (Singh *et al.*, 1985) and as anti-misting agents in jet fuel (Zakin *et al.*, 2007).

CHAPTER 3

MATERIALS AND METHOD

3.1 INTRODUCTION

In this chapter, the experimental materials and apparatuses, setup and procedures will be explained in details. Experimental work is carried out to obtain the data for the pressure drop of aqueous solution before and after addition of drag reducers. The main purpose of the pressure drop measurements was to obtain the percent drag reduction (% DR). The drag reduction rig was designed and installed to operate at different ranges of pipe diameter, length, liquid flow rates and additive's concentrations.

3.2 RAW MATERIALS

3.2.1 Hibiscus Leaves

Hibiscus rosa-sinensis is widely grown throughout the tropics and subtropics as a patterned plant with large flowers, generally red but lack any scent. Traditionally, the flower is used in local Chinese medicine. In South East Asia's area, this flower is widely planted, and only the flower part of the plant is used for demonstration while the rest of the 85% of the plant is considered as an agricultural waste. In the present work, this waste (leaves) will be used to extract the new DRA (natural mucilage). Figure 3.1 shows the hibiscus leaves used in this study.



Figure 3.1: Leaves of *Hibiscus rosa-sinensis*

3.2.2 Red Gypsum Powders

The suspended solid tested in this experiment is crushed red gypsum. It's a waste from titanium dioxide manufacturing industry which dumped every year on open land. According to the Huntsman Tioxide Responsible Care Report for 2004, the co-products for which a market cannot be found are disposed to land in an environmentally controlled manner and approximately 965,000 tonnes per annum of gypsum wastes are disposed to land from all Huntsman Tioxide sites globally. From the Huntsman Tioxide Responsible Care Performance Report Grimsby 2004, Grimsby site waste emissions of about 54, 860 tonnes gypsum disposed to land. If not properly managed, they cause danger to our health and environment. The total accumulation of red gypsum in Malaysia is at least 340, 000 tonnes per annum. Table 3.1 shows the properties of red gypsum collected from Tioxide (Malaysia) Sdn. Bhd. while Figure 3.2 shows the apparent physical appearance of the red gypsum used in this study.

Fauziah *et al.* (1996) studied the characterization and land application of red gypsum. The study indicated that, under scanning electron microscopy (SEM), the gypsum crystals are present as tabular crystals of radiating elongated crystals in a matrix of calcite and iron oxides. The calcium content of red gypsum is 18.9% with the trace elements such as As, B, Cd, Cr, Cu, Ni and Pb which present in low concentrations. Dissolution kinetics studies proved that the rate of red gypsum dissolution increases with decreasing particle size. Land application was the proposed disposal option of red gypsum; however, there is some concern that heavy metals presents in this waste

product may be consumed by plants, or pollute surface water or even leach into the ground water.

Table 3.1: Properties of red gypsum

Properties	Appearance
Color	Dark red
Empirical Formula	$\text{CaSO}_4 \cdot 2\text{H}_2\text{O}$
Solubility (g/L) @ 20 ⁰ C	2.1
Molar mass (g/mol) (based on molecular formula)	172.2
Density (g/ml) (measured in the current study)	2.8
pH	7.80

Source: Adriano *et al.* (1980); Fauziah *et al.* (1996) and Gazquez *et al.* (2009)



Figure 3.2: Crushed red gypsum

3.2.3 Grafting Chemicals

(a) Acrylonitrile

Acrylonitrile ($\text{C}_3\text{H}_3\text{N}$) is a colorless and volatile liquid that is soluble in water and most common organic solvents such as acetone, benzene and toluene. It is an important monomer in manufacturing useful plastics. The molecular structure of acrylonitrile consists of a vinyl group linked to a nitrile. The IUPAC (International Union of Pure and Applied Chemistry) name of acrylonitrile is 2-propenenitrile. Acrylonitrile or known as cyanoethene and vinylcyanide, which is highly flammable and toxic (Kotz *et al.*, 2006), bought from Fisher Scientific. Figure 3.3 shows the structural formula of acrylonitrile and Table 3.2 shows the physical properties of

acrylonitrile. Acrylonitrile may cause cancer and irritating to respiratory system and skin.

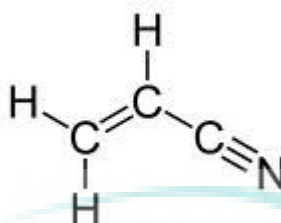


Figure 3.3: Structural formula of acrylonitrile

Source: Kotz *et al.* (2006)

Table 3.2: Properties of acrylonitrile

Properties	Value
Purity	99%
Molar mass (based on molecular formula)	53.06 g/mol
Boiling point	77.5-79.6 ⁰ C
Melting point	-83.5 ⁰ C
Density (25 ⁰ C)	0.81 g/cm ³

Source: Leonard *et al.* (1999)

(b) Nitric Acid

Nitric acid (HNO₃) is colorless when pure and, at room temperature, it tends to develop a yellow color rapidly due to decomposition. Nitric acid is commonly used as a strong oxidizing agent and for the production of fertilizers, explosives and etc. (EFMA, 1998). This liquid is highly corrosive and toxic strong acid bought from Fisher Scientific. Figure 3.4 shows the structural formula of nitric acid and Table 3.3 shows the specifications of nitric acid.

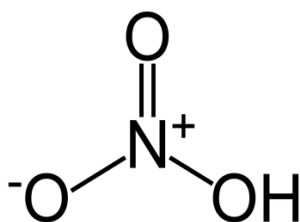


Figure 3.4: Structural formula of nitric acid

Table 3.3: Specifications of nitric acid

Specification	Composition
Assay (acidimetric)	Min. 65%
Chloride (Cl)	Max. 0.001%
Copper (Cu)	Max. 0.0005%
Sulphate (SO ₄)	Max. 0.001%
Cadmium (Cd)	Max. 0.0005%
Lead (Pb)	Max. 0.002%
Calcium (Ca)	Max. 0.005%
Cobalt (Co)	Max. 0.0005%
Chromium (Cr)	Max. 0.0005%
Iron (Fe)	Max. 0.0005%
Potassium (K)	Max. 0.005%
Magnesium (Mg)	Max. 0.0005%
Manganese (Mn)	Max. 0.0005%
Sodium (Na)	Max. 0.005%
Nickel (Ni)	Max. 0.0005%
Zinc (Zn)	Max. 0.0005%

Source: MSDS (2009)

(c) **Hydroquinone**

Hydroquinone (C₆H₆O₂) also known as quinol with IUPAC name benzene-1,4-diol is an aromatic organic compound that is a type of phenol purchased from Fisher Scientific. Its structural formula shown in Figure 3.5 has two hydroxyl groups bonded to a benzene ring in a para position. This white granular solid has a variety of uses principally associated with its action as a reducing agent which is soluble in water (Hudnall, 2000). As a polymerization inhibitor, hydroquinone prevents polymerization of monomers that are susceptible to radical-initiated polymerization.

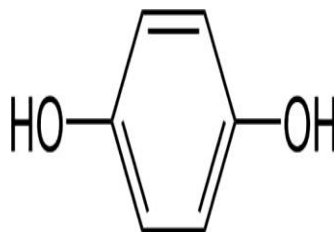


Figure 3.5: Structural formula of hydroquinone

Source: Kari (1989)

(d) Isopropanol

Isopropanol also known as 2-propanol or isopropyl alcohol with molecular formula C_3H_8O is a colorless chemical compound with a strong odor (Logsdon and Loke, 2000). The preferred IUPAC name for isopropanol is propan-2-ol. Like acetone, it dissolves a wide range of nonpolar compounds. It also evaporates quickly and is relatively non-toxic, compared to alternative solvents. Therefore, it is widely used as a solvent and as a cleaning fluid. Isopropyl used in this study purchased from Fisher Scientific. The structural formula of isopropanol is shown (Figure 3.6). Table 3.4 illustrates the physical properties of isopropanol.

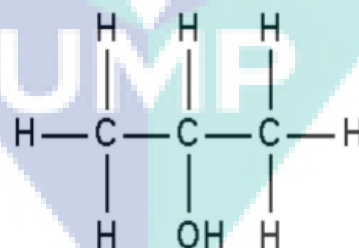


Figure 3.6: Structural formula of isopropanol

Table 3.4: Properties of isopropanol

Properties	Value
Purity	Min 99.7%
Molar mass	60.10 g/mol
Melting point	-89 ⁰ C
Boiling point	82 ⁰ C
Flash point	12 ⁰ C
Specification	Composition
Assay (GC)	Min. 99.7%
Identity IR Spectrum	Passes test
Free acid (as CH ₃ CH ₂ CH ₂ COOH)	Max. 0.002%
Aluminum (Al)	Max. 0.00005%
Boron (Bo)	Max. 0.000002%
Cadmium (Cd)	Max. 0.000005%
Chromium (Cr)	Max. 0.000002%
Iron (Fe)	Max. 0.00001%
Magnesium (Mg)	Max. 0.00001%
Nickel (Ni)	Max. 0.000002%
Zinc (Zn)	Max. 0.00001%
Acetone (GC)	Max. 0.01%
Ethanol (GC)	Max. 0.01%
Methanol (GC)	Max. 0.1%
Barium (Ba)	Max. 0.00001%
Calcium (Ca)	Max. 0.00005%
Cobalt (Co)	Max. 0.000002%
Copper (Cu)	Max. 0.000002%
Lead (Pb)	Max. 0.00001%
Manganese (Mn)	Max. 0.000002%
Tin (Sn)	Max. 0.00001%
Water	Max. 0.1%

Source: MSDS (2009)

(e) Acetone

Acetone (C₃H₆O) is an organic compound with IUPAC name propanone. It's the simplest example of ketones which is a colorless liquid. Acetone is miscible with water and serves as an important solvent in its own right, typically as the solvent of choice for cleaning purposes (Bradberry, 2007). Figure 3.7 shows the molecular structure of acetone. Physical properties of acetone purchased from Fisher Scientific have been shown in Table 3.5.

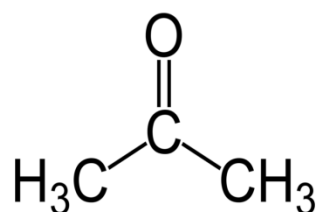


Figure 3.7: Structural formula of acetone

Table 3.5: Properties of acetone

Properties	Value
Purity	Min 99.5%
Molar mass	58.08 g/mol
Melting point	-95 ⁰ C
Boiling point	56 ⁰ C
Flash point	-20 ⁰ C
Specification:	Composition
Assay (GC)	Min. 99.5%
Ethanol (GC)	Max. 0.01%
Water	Max. 0.2%
Boron (B)	Max. 0.000002%
Calcium (Ca)	Max. 0.00005%
Cobalt (Co)	Max. 0.000002%
Copper (Cu)	Max. 0.000002%
Magnesium (Mg)	Max. 0.00001%
Lead (Pb)	Max. 0.00001%
Tin (Sn)	Max. 0.00001%
Identity IR Spectrum	Passes test
2-Propanol	Max. 0.05%
Methanol (GC)	Max. 0.05%
Aluminum (Al)	Max. 0.00005%
Barium (Ba)	Max. 0.00001%
Cadmium (Cd)	Max. 0.000005%
Chromium (Cr)	Max. 0.000002%
Iron (Fe)	Max. 0.00001%
Manganese (Mn)	Max. 0.000002%
Nickel (Ni)	Max. 0.000002%
Zinc (Zn)	Max. 0.00001%

Source: MSDS (2009)

(f) *Dimethylformamide*

Dimethylformamide (C₃H₇NO) purchased from Fisher Scientific is a colorless, high-boiling, polar liquid with a faint, characteristic odor. It is freely miscible with water, alcohol, ether, ketone, ester, carbon disulfide and chlorinated and aromatic hydrocarbons. It is either immiscible or only partly miscible with aliphatic hydrocarbons. The primary use of dimethylformamide is as a solvent with low evaporate rate. The IUPAC name for dimethylformamide is N,N-dimethylmethanamide. The molecular structure of dimethylformamide is shown in Figure 3.8 whereas Table 3.6 contains the physical properties of dimethylformamide.

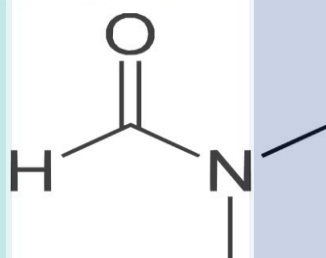


Figure 3.8: Structural formula of dimethylformamide

Source: BASF (1999)

Table 3.6: Properties of dimethylformamide

Properties	Value
Purity	99.6%
Acidity/Alkalinity	0.00005meq/g

Source: BASF (1999)

3.2.4 Transported Liquid

In this experimental work, two types of liquids were tested to compare the results of drag reduction, i.e. water and diesel. Petroleum products are the most commonly transported fluids via pipelines in the industry. Therefore, in this study, diesel, which is a fraction obtained from petroleum distillation, was used as a

transported liquid, to test the efficiency of DRA. The measured physical properties of water and diesel are shown in Table 3.7.

Table 3.7: Measured physical properties of transported liquids

Transported Liquid	Properties	Value
Diesel	Viscosity ($\mu_{\text{diesel @ 25}^\circ\text{C}}$)	0.003016 Pa.s
	Density ($\rho_{\text{diesel @ 25}^\circ\text{C}}$)	836.25 kg/m ³
Water	Viscosity ($\mu_{\text{water @ 25}^\circ\text{C}}$)	0.001 Pa.s
	Density ($\rho_{\text{water @ 25}^\circ\text{C}}$)	1000 kg/m ³

3.3 CLOSED LOOP LIQUID CIRCULATION SYSTEM

The drag reduction experimental study for four independent variables, which are pipe diameter (D), testing section length, volumetric flow rate (with reference to Reynolds number) and the additive concentrations was carried out in a built up closed loop liquid circulatory system. Figure 3.9 shows the schematic diagram of a closed loop liquid circulation system used to test the drag reduction phenomenon in this experiment while Figure 3.10 shows the photo of the built up experimental rig.

The rig mainly consists of liquid tank (101), precision pump (102) model PPM-158 with a maximum load 10.5m³/h and pipes 104, 105 and 106 with different diameters of 0.0381m, 0.0254m and 0.0127m respectively. The tank connected with discharge pipe (109) and recirculation pipe (108). The recirculation pipe is used to control the diesel flow rate entering the system. Each testing section is supported with a ball valve. These valves are used to close and open the testing section stream and not to control the flow rate entering to the section in order not to disturb the developed turbulent flow entering to each testing section. In each pipe, the first testing point starts after 50D (D=diameter of pipe) to ensure the flow is constant turbulent. After 50D is where the first transmitter sensor is located, i.e. 1.91m, 1.27m and 0.635m for pipe with ID of 0.0381m, 0.0254m and 0.0127m respectively.

The maximum capacity of the liquid tank is 180 Liters (0.5m x 0.6m x 0.6m). The main piping system starts by connecting the liquid tank to the pump by 0.0381m ID pipe as the core delivering exit. Then the piping system delivers the liquid pump out through 0.55m horizontal pipe with 0.0381m ID. This is where the ultrasonic flow meter located before the liquids transferred through vertical pipe of 0.0381m ID. Flow rates were measured using Burket 8035 Minisonic flow meter (103). From this vertical pipe, liquids delivered into three different pipes each with ID of 0.0381m, 0.0254m and 0.0127m respectively. These three pipes are the exact place to measure pressure readings and called as testing section.

The testing sections were made of four parts, and each section is 0.5m in length. Each pipe is supplied with five pressure measurement holes. A pressure transmitter sensor located at each pressure testing hole (PT101 to PT105 for the 0.0381 m I.D pipe), (PT201 to PT205 for the 0.0254 m I.D. pipe) and (PT301 to PT305 for the 0.0127 m I.D pipe). All the pressure transmitters connect to an interface which gives computational pressure readings straight to the computer. The pressure measurements are taken every two seconds. SCADA interface was designed and installed in the computer for the pressure reading visualization in each testing point.

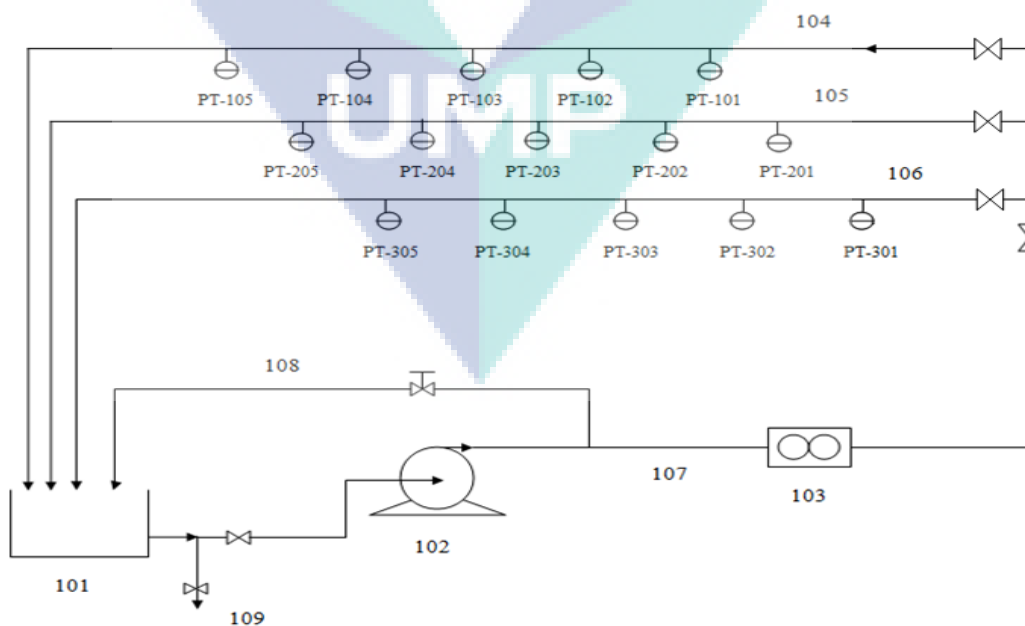


Figure 3.9: Schematic diagram of closed loop liquid circulation system

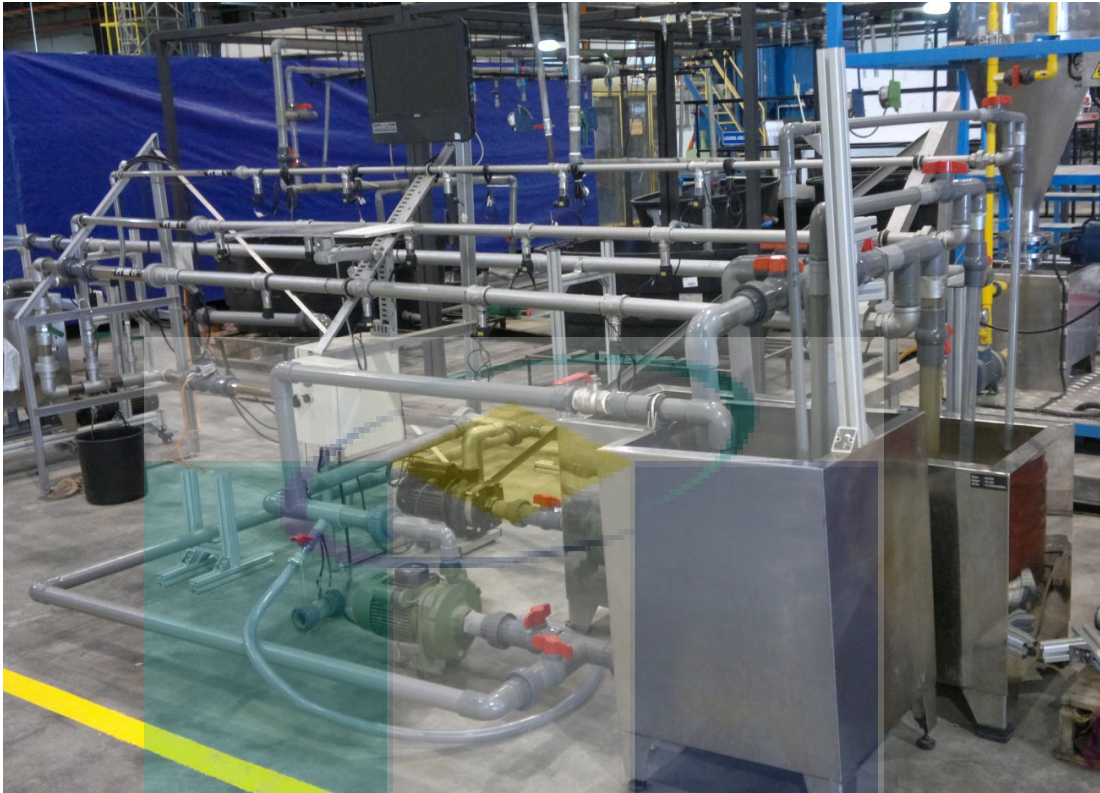


Figure 3.10: Built-up experimental rig

3.4 MUCILAGE PREPARATION

Natural additive solution's preparation include from the extraction of mucilage to grafting method which is suitable for this study.

3.4.1 Mucilage Extraction

Young, fresh leaves of *Hibiscus rosa-sinensis* (25%wt) chopped into small size pieces and soaked in three times its weight of distilled water (75%wt) for 12 hours. The resulting mucilage was highly viscous (0.0206 Pa.s) with greenish color. Percent mixing chosen depends on the high viscosity and the amount of the resulting mucilage as shown in Table 3.8. Adding large amounts of water gives more mucilage but highly diluted. Therefore, sample 2 was chosen as the best mixing ratio in this experiment. Figure 3.11 shows the process summary.

Table 3.8: Percent mixing and the viscosity of resulted mucilage

Sample	Weight of leaves, g	Amount of water, mL	Viscosity of mucilage, Pa.s	Amount of mucilage, mL
1	50	100	0.0225	20
2	50	150	0.0206	100
3	50	200	0.0149	100
4	50	300	0.0123	200

**Figure 3.11:** Process summary in obtaining mucilage from hibiscus leaves

3.4.2 Mucilage Grafting

The target of the present work is to use the mucilage as drag reducing agent in hydrocarbon media; this is why grafting procedure is needed for the extracted mucilage to change its solubility from aqueous to hydrocarbon media. Previously, many graft copolymers have been synthesized through the grafting of polyacrylamide chains onto guar gum and xanthan gum. Their shear stability and drag reduction efficiencies have been studied. Furthermore, by variation in the number and length of grafted polyacrylamide chains onto the backbone, it has been found that the graft copolymers having fewer and longer chains are more efficient as DRA (Singh *et al.*, 2000).

Polyacrylonitrile-grafted copolymers of hibiscus leaf's mucilage (HI-g-PAN) were synthesized under nitrogen atmosphere by grafting acrylonitrile (AN) monomer onto the hibiscus leaf mucilage (HI) backbone using nitric acid as the initiator in radical polymerization method. Acrylonitrile considered as the best monomer instead of

acrylamide because of its high possibility of monomer to be intact with polysaccharide by the presence of the vinyl group ($-\text{CH}=\text{CH}_2$) in acrylonitrile.

One gram of mucilage was dissolved in distilled water (200mL) and then flushed with nitrogen for about 20 min. Then required amount of AN was added into the solution. The solution stirred for 30 min while being bubbled with nitrogen. Next, required amount of nitric acid was injected. Nitrogen flushing was continued for additional 20 min. After that, the container was sealed and immersed in constant temperature (60°C) water bath. The reaction was continued for 24h and then terminated by injecting saturated hydroquinone. The product was precipitated with excess isopropanol and filtered through glass filter. Finally, the precipitate was again slurried in acetone followed by filtration and the final product was dried in a vacuum oven. HI-g-PAN was separated from PAN (homopolymers) by mixing with a quantity of dimethylformamide. The grafting method and an optimum amount of chemical addition was adopted from previous researchers (Mishra *et al.*, 2006). Figure 3.12 shows the grafted powder of mucilage.



Figure 3.12: Grafted powder of mucilage

3.5 RED GYPSUM PREPARATION

Red gypsum preparation includes only crushing steps. The range of size of the particles was measured as mentioned in the following section.

3.5.1 Particle Size Analysis

The red gypsum used in this study is within the range of 15-30 μm . The size of the particles measured using MALVERN Mastersizer 2000 of model APA 2000 and more specifically, measures the distribution of different sizes within a sample. Mastersizer uses Mie theory, which accurately predicts the light scattering behavior of all materials under all conditions. Mie theory was developed to predict the way light is scattered by spherical particles and deals with the way light passes through, or is adsorbed by the particle. This theory is more accurate with known refractive index and its absorption.

The Mastersizer works by using the optical unit to capture the actual scattering pattern from a field of particles. Then, using the theories described, it can calculate the size of particles that created that pattern. There are three distinct procedures involved in measuring a sample on the Mastersizer. Firstly, the sample was prepared and dispersed to the correct concentration and then delivered to the optical unit. Secondly, there is a capturing of the scattering pattern from the prepared sample which is known as the “measurement”. Finally, once the measurement is complete, the raw data contained in the measurement can be analyzed by the Malvern software. Figure 3.13 shows a typical system with its key modules.

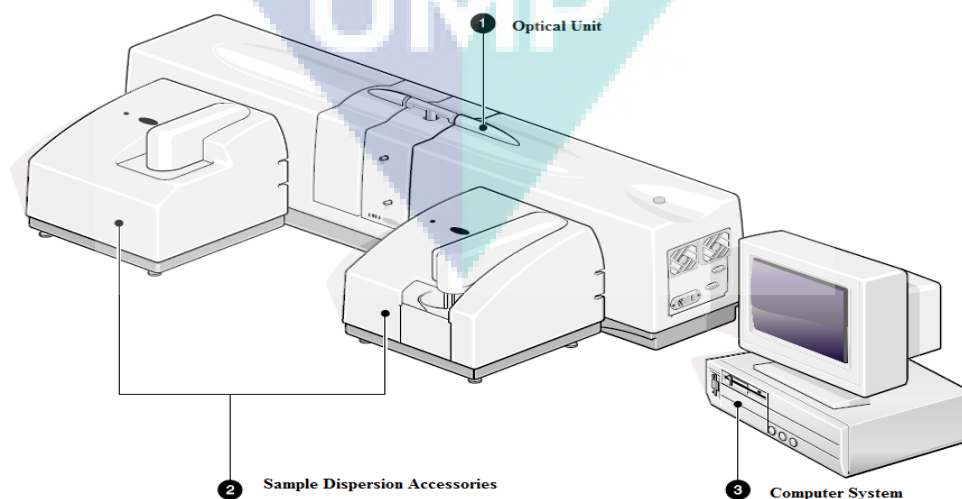


Figure 3.13: Typical system of Mastersizer

3.6 EXPERIMENTAL PROCEDURE

3.6.1 Solution Preparation and Testing in Rig

The drag reduction solutions were prepared in a beaker before adding it into the experimental tank according to their concentration. The solution concentration varied from 50ppm to 1000ppm for each DRA and all these concentrations were taken on a weight/weight basis. For example, the amount of gypsum needed to prepare exactly 50ppm of solution is equal to 1.67g. This sample is then mixed with diesel, which inside the tank to be tested. The same procedure is applied to make the entire required sample's concentration. These steps were repeated for mucilage solution, as well. The amount of mucilage and red gypsum needed to prepare for each concentration were shown in details at Table 3.9 –Table 3.10 at Appendix A1 and Table 3.11 – Table 3.12 at Appendix A2 respectively.

To test the DRA, the tank at first was filled with the testing liquid, pumping starts and the liquid was allowed to flow inside the pipelines. After that, the required flow rate was set by adjusting the valve at recirculation pipe. Next, the pressure readings at each pipe and testing section were recorded. Finally, prepared solution added into the liquid tank, and the same above-mentioned procedures were repeated. Pressure readings used to calculate pressure drops and percent drag reduction (%DR) to study the performance of DRAs. The same procedures were followed for each independent variable.

3.7 PHYSICAL PROPERTY TEST

Basic tests have been conducted to the water soluble mucilage, grafted mucilage and red gypsum after preparation in order to forecast the drag reducing capacity of each DRA. Besides that, the tests clearly show the effects of additive at different concentration on original properties of transported liquid. The viscosity was measured at 25°C.

3.7.1 Viscosity

Viscosities for all the samples were measured using BROOKFIELD DV-III Ultra Programmable Rheometer. Figure 3.14 shows the rheometer used in this study. First, the rheometer switched on, and appropriate spindle was chosen. In this study, SC4-27 spindle was used. After that, the sample placed in the sample cup, tightened the holder and the system connected to temperature bath to measure viscosity at a constant temperature of 25⁰C. The readings were set to auto zero, and spindle is installed after auto zero completion. Next, the motor on, spindle code set to 27, and RPM fixed at 200RPM. By allowing the sample for three minutes while the spindle rotates in, the readings will be shown in the rheometer.



Figure 3.14: Viscometer

3.8 EXPERIMENTAL CALCULATIONS

3.8.1 Reynolds Number

The Reynolds Number (Re) was calculated using the solution's density (ρ), fluid's average velocity (V), pipe diameter (D) and solution viscosity (μ), for each testing as follows (Reynolds, 1883):

$$Re = \frac{\rho VD}{\mu} \quad (3.1)$$

Where: Re = dimensionless

ρ = Solution's density (kg/m^3)

μ = Solution's viscosity (Pa.s)

D = Pipe diameter (m)

V = Average velocity (m/s)

Examples of Re calculation for each case has been tabulated in Appendix B1 and Appendix B2.

3.8.2 Friction Factor

Fanning friction factor calculated using the following equation (Kim and Kim, 1991):

$$f = \frac{\tau_w}{\rho.V^2/2} \quad (3.2)$$

Where: f = Friction factor (dimensionless)

$\tau_w = D(\Delta P)/4L$

ΔP = Pressure drop

L = Pipe length (m)

ρ = Solution's density (kg/m^3)

D = Pipe diameter (m)

V = Average velocity (m/s)

Examples of friction factor calculations for each case tabulated in Appendix B1-B2 before DRA addition and in Appendix D1-D4 after DRA addition.

3.8.3 Percentage Drag Reduction

Percentage drag reduction through a testing section calculated using the differential pressure drop before and after DRA's addition as shown in the following equation (Mowla and Naderi, 2008):

$$\%DR = \frac{\Delta P_b - \Delta P_a}{\Delta P_b} \times 100 \quad (3.3)$$

Where: ΔP_a = Pressure drop after DRA addition

ΔP_b = Pressure drop before DRA addition

Calculated values for %DR have been tabulated in Appendix C1-C2.

The logo for UMP (Universitas Muhammadiyah Purwokerto) is a large, downward-pointing arrow shape. It is composed of four quadrants: the top-left and bottom-right are light blue, the top-right and bottom-left are light purple, and the center is white. The letters 'UMP' are written in a bold, white, sans-serif font across the white center of the arrow.

UMP

CHAPTER 4

RESULTS AND DISCUSSION

The performances of natural mucilage and suspended solid as DRA in improving the flow in pipelines were investigated in closed loop liquid circulation system. Classical parameters such as pipe diameter, pipe length, additive concentration and liquid flow rate were tested. Comparisons and discussions of the results obtained will be presented here in detail while the rest of the experimental data will be tabulated in appendices.

4.1 PROPERTY TEST

Rheological tests are carried out with samples at different concentrations to evaluate their effect on the flow characteristics of the transported liquid. The results of the tests are tabulated in Table 4.1. Viscosity is the major factors affecting the drag reduction performance. Figures 4.1-4.2 shows the effect of additive concentration on the viscosity of the transported liquids (diesel and water). The viscosity of the two investigated solutions increases with increase in concentration. The figures also show that the total viscosity of the diesel solution is much higher than the water solution.

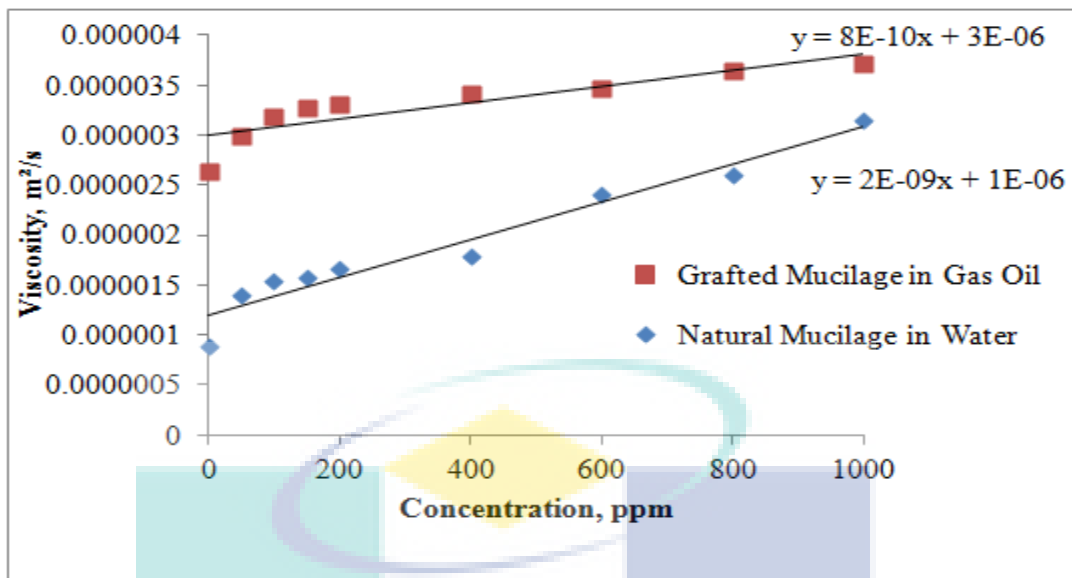


Figure 4.1: Effect of mucilage concentration on viscosity

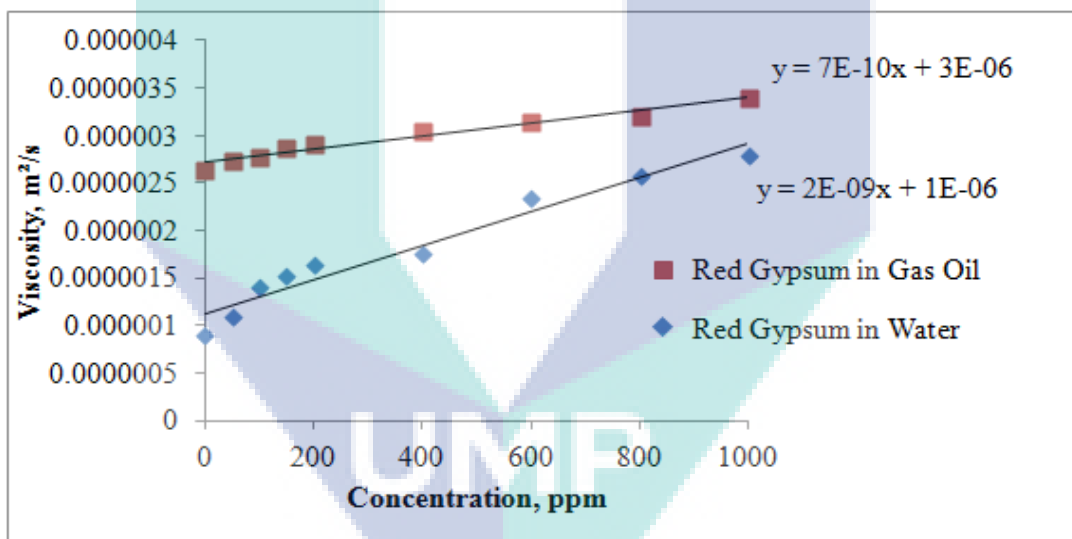


Figure 4.2: Effect of red gypsum concentration on viscosity

Table 4.1: Viscosity of the DRAs (T = 25°C)

Properties	Water + Natural Mucilage								
Concentrations, ppm	0	50	100	150	200	400	600	800	1000
Viscosity, m²/s	0.00000089	1.4E-06	1.55E-06	1.58E-06	1.67E-06	1.79E-06	2.4E-06	2.61E-06	3.15E-06
Properties	Water + Red Gypsum								
Concentrations, ppm	0	50	100	150	200	400	600	800	1000
Viscosity, m²/s	0.00000089	1.09E-06	1.41E-06	1.52E-06	1.64E-06	1.76E-06	2.34E-06	2.58E-06	2.78E-06
Properties	Diesel + Grafted Mucilage								
Concentrations, ppm	0	50	100	150	200	400	600	800	1000
Viscosity, m²/s	0.00000263	2.99E-06	3.18E-06	3.27E-06	3.31E-06	3.41E-06	3.47E-06	3.64E-06	3.71E-06
Properties	Diesel + Red Gypsum								
Concentrations, ppm	0	50	100	150	200	400	600	800	1000
Viscosity, m²/s	0.00000263	2.73E-06	2.76E-06	2.87E-06	2.9E-06	3.04E-06	3.13E-06	3.2E-06	3.4E-06

4.2 VERIFICATION OF CLOSED LOOP LIQUID CIRCULATION SYSTEM

Verification and validation of the built-up liquid circulation system before the start of any experimental work is necessary to validate the experimental data extracted from the system and compared it to the standards. The friction factor for the additives-free liquid flowing through the pipelines was calculated using Eq. (3.2). The data were compared graphically with the standard asymptotes suggested by Blasius (Eq. 4.1), Virk (Eq. 4.2) and laminar flow (Eq. 4.3). Theoretically, additive-free liquid must obey the Blasius correlation in turbulent flow while the possible maximum drag reduction after addition of DRA should be exactly between the Blasius' and Virk's correlation.

$$f = 0.0791 \text{Re}^{-0.25} \quad (4.1)$$

$$f = 0.59 \text{Re}^{-0.58} \quad (4.2)$$

$$f = \frac{16}{\text{Re}} \quad (4.3)$$

The experimental friction factor of water and diesel is compared with Blasius equation given by (4.1) in figures 4.3 and 4.4 respectively for $L/D = 39.4$. The values are in good agreement with Blasius rather than with Virk's equation. Since the present values are based on several repeated experiments (7 times), the values from the experimental setup are reliable for undertaking drag reduction studies. The experimental data is tabulated as Appendix B1 for water and Appendix B2 for diesel solutions.

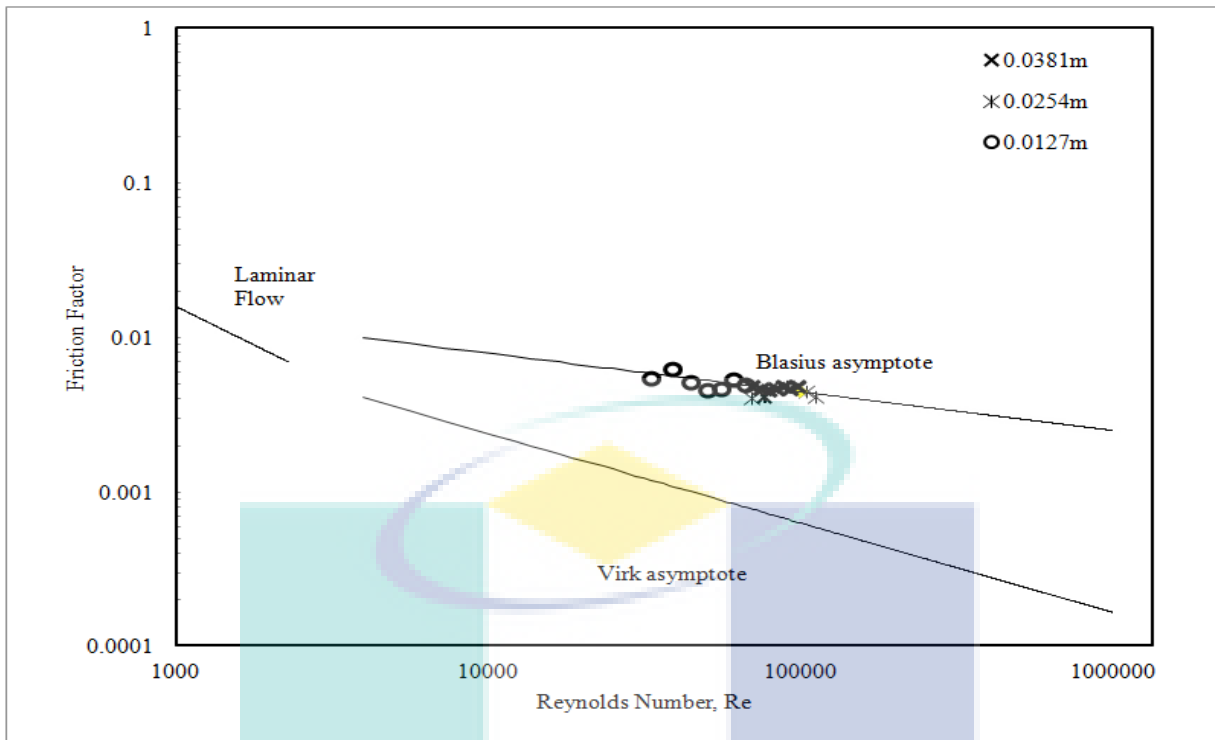


Figure 4.3: Friction factor of water flow for $L/D = 39.4$

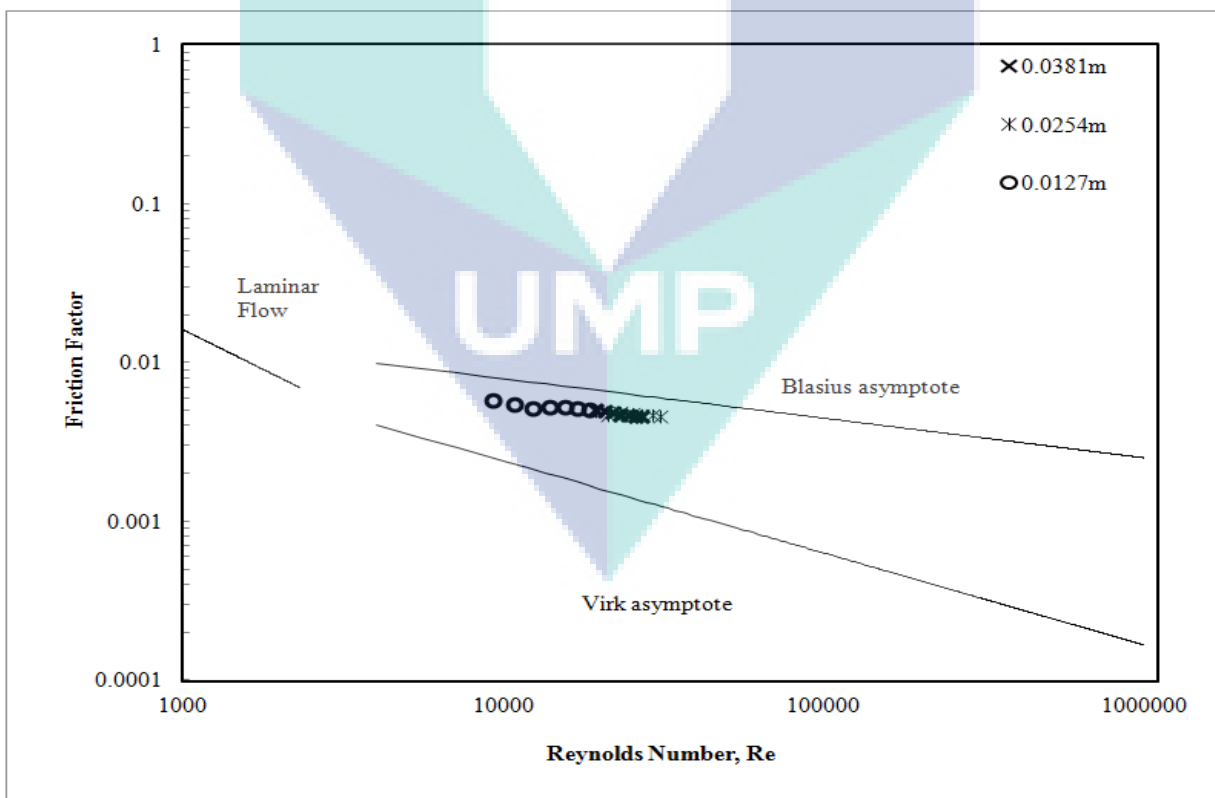


Figure 4.4: Friction factor of diesel flow for $L/D = 39.4$

4.3 ADDITIVES DRAG REDUCTION PERFORMANCE IN WATER AND DIESEL

4.3.1 Effect of Solution Velocity

Selected experimental data showing the effect of liquid (diesel and water solutions) velocity (represented by the dimensionless Reynolds number, Re) on the percent drag reduction (%DR) are presented graphically in Figures 4.5-4.10 for 0.0381m, 0.0254m and 0.0127m ID respectively and at 1.5m pipe length. The rest of the data has been tabulated in Appendix C1.

Figure 4.5 shows that the %DR increases by increasing the value of Re . Three distinguishable parts appear for all concentrations, i.e. the %DR increase rapidly in the range of Re varying between 69,000 and 83,000, reaching maximum values of DR 33%, 34%, 36%, 39%, 41% and 46% respectively at $Re=88152$ for 50ppm, 100ppm, 400ppm, 800ppm and 1000ppm and $Re=83512$ for 200ppm solution. A further increase in the Re show that the value of %DR remains constant or reduces though not significantly. The trend is in good agreement with the observations of other authors such as Kamel and Shah (2009) and (Kim *et al.*, 2009). Increasing Re means increasing the degree of turbulence inside the pipe, and that will provide a more suitable medium for the additives to interfere within the turbulence structures inside surface of the pipe for reducing friction or enhancing %DR.

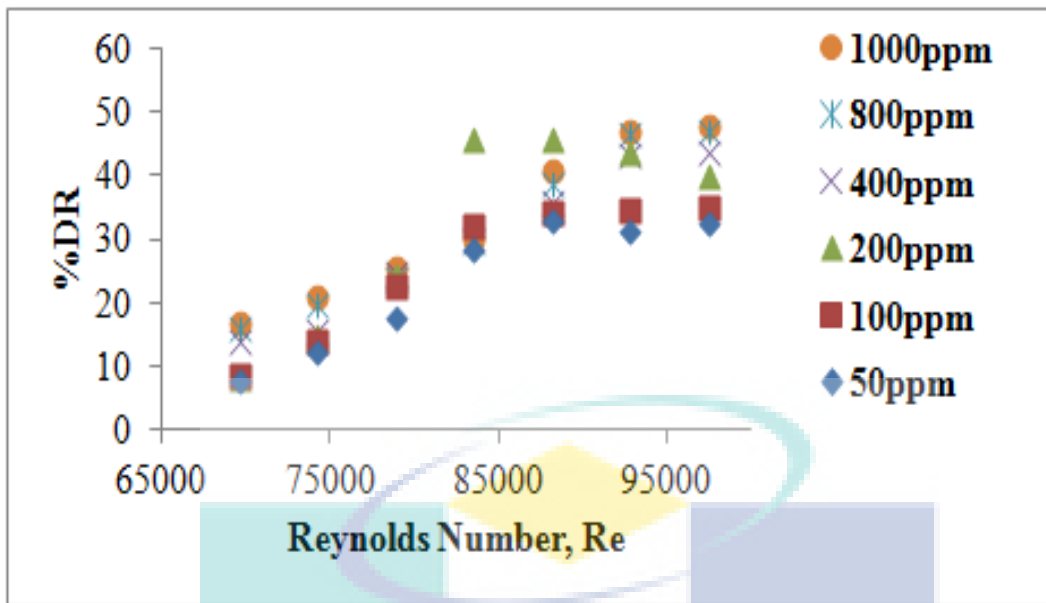


Figure 4.5: The effect of Reynolds number on drag reduction at different natural mucilage concentration in water along 0.0381m diameter and 1.5m length pipe

At the optimum value, the degree of turbulence is balanced with the effect of DRA for natural mucilage in water with no significant change in the %DR shown in figure 4.5. At values of Re greater than the optimum the %DR will reduce, as the degree of turbulence is higher than the effect of additive. Such observations are supported by the results published by (Vlachogiannis *et al.*, 2003 and Kim *et al.*, 2000) who stated that the drag reducing agent effectiveness diminishes significantly when exposed to turbulent flow for an extended period of time.

Figure 4.6 shows the effect of the grafted mucilage Re on the %DR in the diesel solution flowing in a pipe of ID 0.0381m and 1.5m long. It can be observed that the %DR increases with Re for diesel solution undertaken at various concentrations, without any distinguishable optimum value. The Reynolds number range for water solution is between 69,000 and 97,000 whereas for the diesel solution investigated is between 19,000 and 27,000. The high viscosity of the diesel solution requires larger power to undertake experiments for Reynolds number greater than 27,000. Experiments could not be undertaken due to practical limitations. Possibly, an optimum value can be observed for diesel solution, if undertaken at higher Reynolds number.

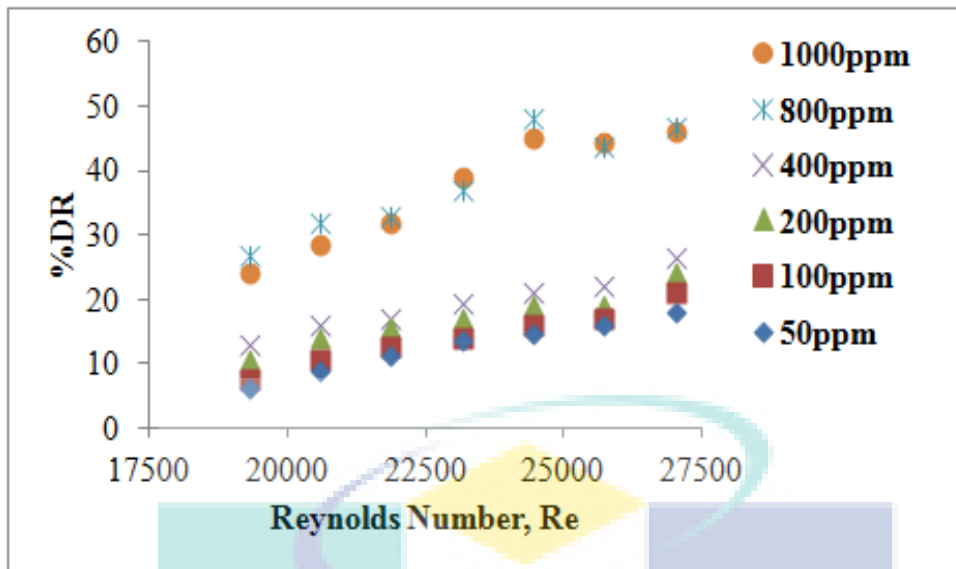


Figure 4.6: The effect of Reynolds number on drag reduction at different grafted mucilage concentration in diesel along 0.0381m diameter and 1.5m length pipe

Figure 4.7 and Figure 4.8 shows the same investigated variable effect on the %DR of the water and diesel solution within the same additive concentrations mentioned in Figure 4.5 and Figure 4.6 but this time for the other pipe diameter which is 0.0254m ID at 1.5m pipe length. It can be noticed clearly that the same behavior repeats itself again with the two media investigated, i.e. the three parts of the Re-%DR curve trend are clearer in the water solution media compared to the grafted mucilage solution media which shows the same, inclined trend that shows almost a linear increase in the %DR without reaching its maximum %DR at its optimum Re.

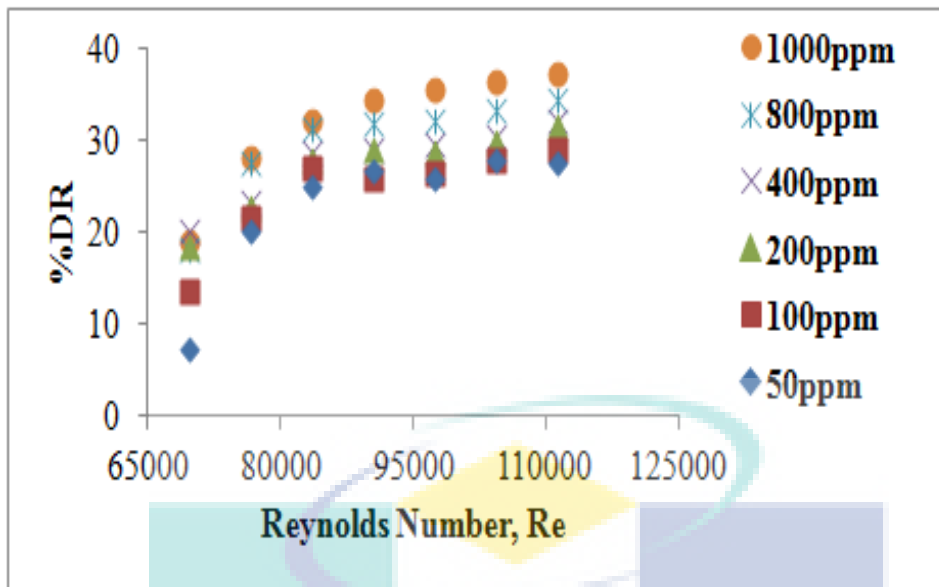


Figure 4.7: The effect of Reynolds number on drag reduction at different natural mucilage concentration in water along 0.0254m diameter and 1.5m length pipe

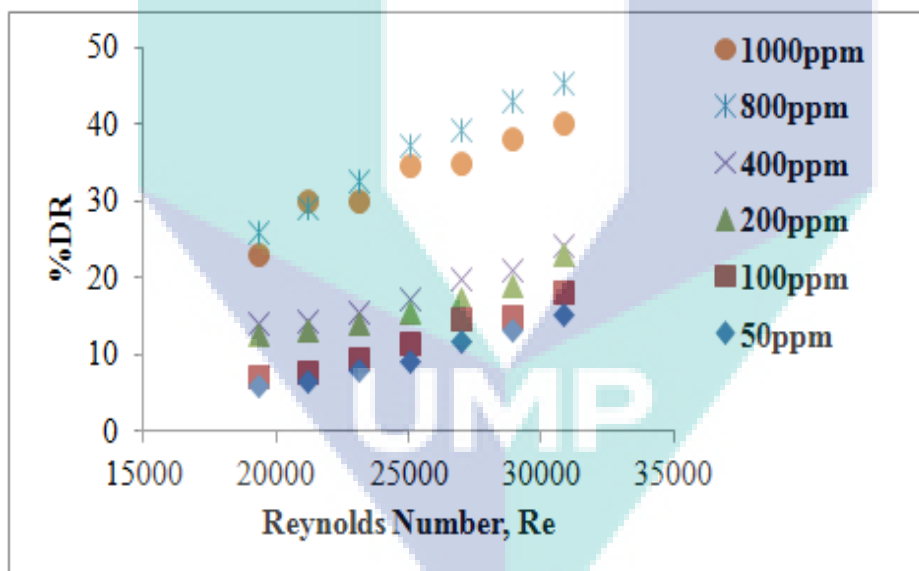


Figure 4.8: The effect of Reynolds number on drag reduction at different grafted mucilage concentration in diesel along 0.0254m diameter and 1.5m length pipe

Testing the %DR for the natural and grafted mucilage additive with a pipe having ID of 0.0127m changed the nature of the curve when compared with pipes of larger diameters as shown in figures 4.9 and 4.10. Figure 4.9 shows the %DR increases with Re without reaching a clear and distinguishable maximum drag reduction peak.

The same trend can be seen in Figure 4.10 for the grafted mucilage flowing in diesel solution within the same operating conditions of Figure 4.9. It is explained that the degree of turbulence is higher in smaller pipe (0.127m ID) at the same flow rate compared with other two pipes and that will provide higher shear rate on the additive molecules which will alter the drag reduction performance of the additives especially for the water soluble mucilage. As described earlier, several factors are controlling the drag reduction performance of the additives; one of these factors is the pipe geometry, such as the pipe diameter and length. It is explained that by reducing the pipe diameter to 0.0127 m I.D, the pipe diameter effect will dominate the other factors controlling the drag reduction performance of the additive, i.e. the increase in the turbulence will be so intensive that will shift the optimum Re and additive concentration where the real maximum %DR is achieved. Such behavior can be considered as a real test of the drag reduction performance of the proposed additives in severe handling conditions where the grafted mucilage showed higher and better ability to perform in high shear stress flow conditions compared to the water soluble mucilage.

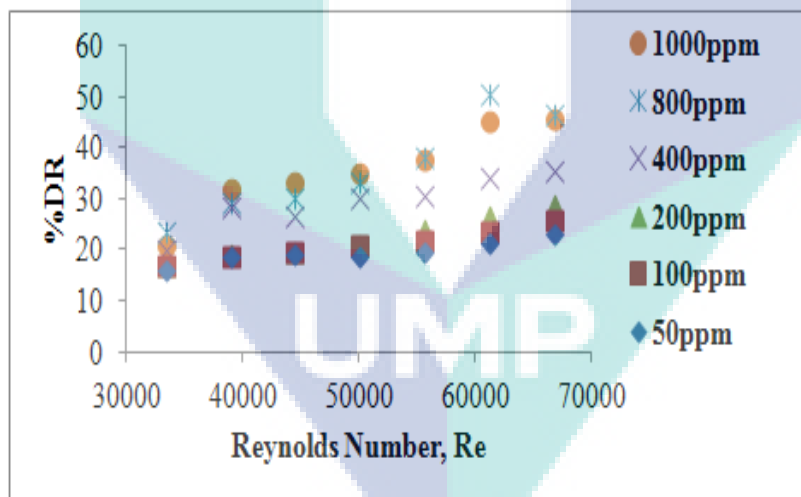


Figure 4.9: The effect of Reynolds number on drag reduction at different natural mucilage concentration in water along 0.0127m diameter and 1.5m length pipe

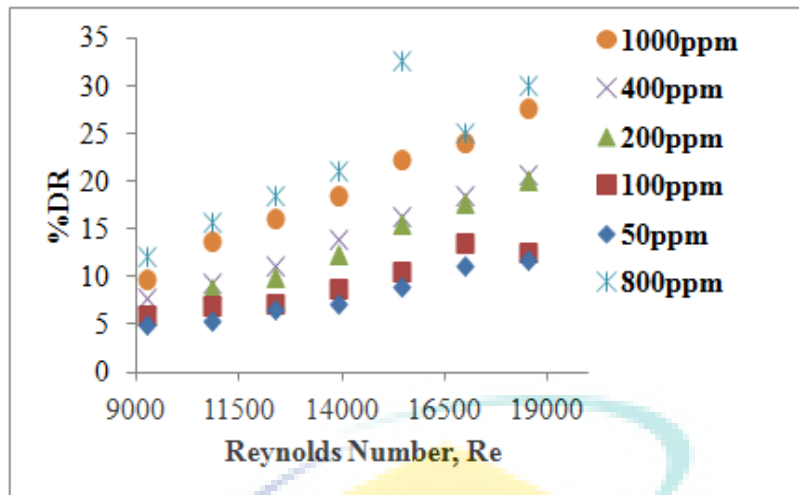


Figure 4.10: The effect of Reynolds number on drag reduction at different grafted mucilage concentration in diesel along 0.0127m diameter and 1.5m length pipe

The red gypsum introduced as insoluble drag reducing agent in this present study. The red gypsum powder investigated is a waste from the titanium dioxide industry. Graphical representation of the liquid velocity (Re) effect on %DR is shown in Figures 4.11-4.14 for specified operating conditions of selected data. The rest of the data has been tabulated in Appendix C1. The basic idea of adopting insoluble drag reducing agent (powders) is to avoid the solubility condition for any chemicals to be distinguished as DRA (polymers and surfactants).

Figure 4.11 shows the effect of Re on %DR when transporting water with gypsum for 50-1000ppm concentration range. Generally, the figure shows that the %DR increases linearly with Re reaching maximum DR (19%, 21%, 24%, 24%, 26% and 26% respectively for 50ppm, 100ppm, 200ppm, 400ppm, 800ppm and 1000ppm solution) without any optimum drag reduction peak. It is very interesting to see that the trend of the curve is not as the one introduced in the previous section describing mucilage (soluble additives) drag reduction performance. The basic idea is that the powder particles will interfere within the eddies formed in the pipelines and due to the very high density differences between the solid particles (2800 kg/m^3) and the carrying liquid (1000 kg/m^3); the structure of the eddy will be different. The power needed to start its formation by the eddy will be higher due to the existence of the solid powders within the main structures of the eddy during the flow, and that will prevent the eddies

from completing its regular shape and absorbing more energy from the main stream. As mentioned before, increasing the Re means increasing the degree of turbulence inside the pipe and for the case of the gypsum powder, increasing the degree of turbulence will increase the amount of solid particles involve and interfering within the eddies and reducing the drag.

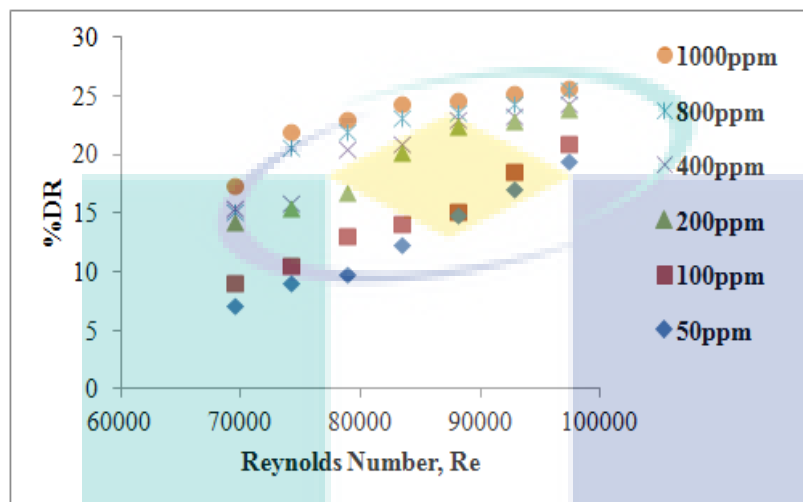


Figure 4.11: The effect of Reynolds number on drag reduction at different gypsum concentration in water along 0.0381m diameter and 1.5m length pipe

Figure 4.12 shows the same linearity as the one mentioned in Figure 4.11 where the %DR increases with Re of grafted mucilage in diesel in 0.0381m ID and 1.5m length pipe. The graph shows that the diesel-gypsum solution has a larger increase in %DR. It is important to state that the energy from the main flow absorbed to form an eddy will be higher in the diesel media compared to the water media. The relation between the density of the particles investigated and involved in the drag reduction process and the viscosity of the media is controlling (see table 4.1). It is noted that the interference of the solid particles in the diesel media will be higher than that with the water media i.e. the solid particle suspension status will be more stable within the diesel media. This may be due to the viscose turbulent structures formed when the diesel flows through the pipe that have the higher carrying force compared with the water media and that will allow a larger number of solid particles to interfere successfully with the eddies. The larger number of the solid particles involved in the flow regime, the higher the drag reduction performance.

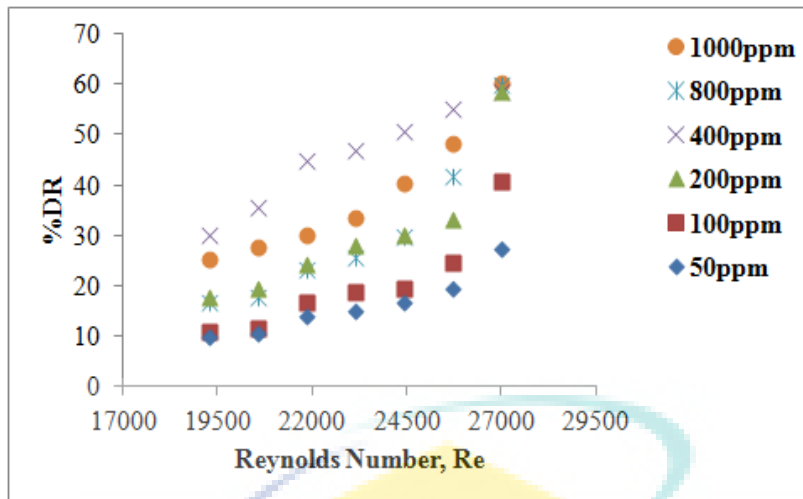


Figure 4.12: The effect of Reynolds number on drag reduction at different gypsum concentration in diesel along 0.0381m diameter and 1.5m length pipe

Figures 4.13 and 4.14 show the Re-%DR relationship for gypsum transported in water and diesel respectively through 0.0254m ID and 1.5m length pipe. The same trend is observed in Figure 4.13 and 4.14 as in Figure 4.11 and 4.12. The graph in Figure 4.13 shows two different parts, the first part where the entire solution concentrations give close values of the %DR within the range of $Re=69594-83512$. From $Re=90472$ to 111350 for all the investigated solution concentration, there are huge differences in %DR value obtained between 50-100ppm and 200-1000ppm, for example; the percent of increase in DR values for 100ppm and 200ppm at $Re=111350$ is 94%. These figures highlight another side of the relation between the degree of turbulence and the suspended solid. It is clear that for all the concentration range investigated the %DR was close in the first range as mentioned and the difference will be higher at higher Re and that is due to drag reduction onset point that needs certain Re to occur. The drag reduction onset point is the point when the drag reducing agent reaches its first optimum balance with the turbulent structures inside the pipe. A further increase in the value of Re will bring the other factor controlling in the action which is the additive concentration. This is why the values of the %DR in the first range of Re were close and start to be more distinguishable within higher values of Re.

For the case of diesel solution shown in Figure 4.14, the same behavior described in Figure 4.13 was observed in the concentration range 50 to 800ppm while the 1000ppm curve was higher than the other curves in all Re ranges. It is believed that,

for high viscosity solutions and high additive concentration 1000ppm, the onset point will not be as clear as the other concentration due to the large number of particles already exist in the main flow and that will lead to the conclusion that the onset point already occurred at the lower range of Re (which was not covered in the present work).

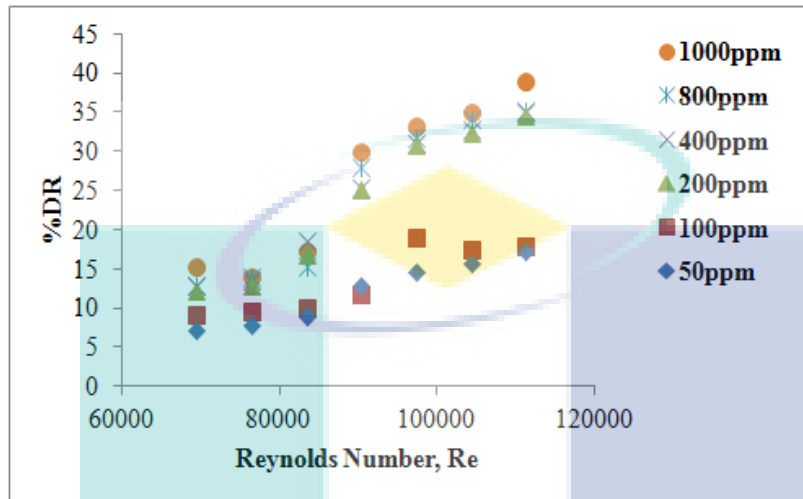


Figure 4.13: The effect of Reynolds number on drag reduction at different gypsum concentration in water along 0.0254m diameter and 1.5m length pipe

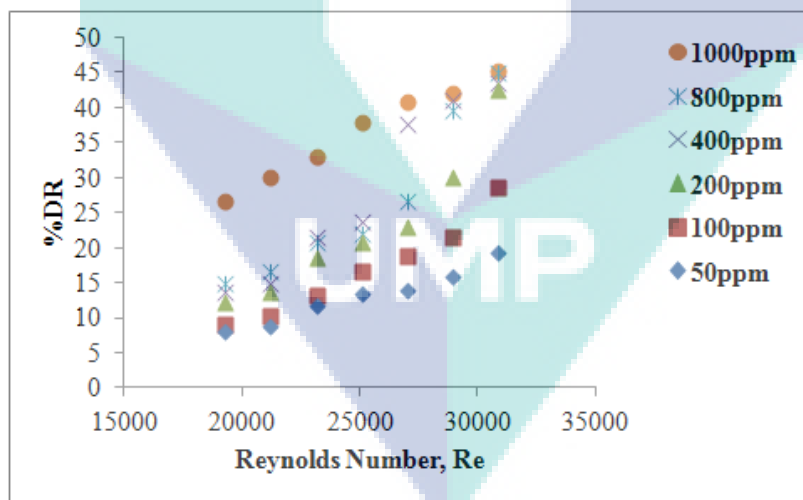


Figure 4.14: The effect of Reynolds number on drag reduction at different gypsum concentration in diesel along 0.0254m diameter and 1.5m length pipe

4.3.2 Effect of Additives Concentration

The additive concentration is one of the effective factors controlling the drag reduction performance. The limitations of additive concentration are taken to guarantee the liquid transported within the same properties. The concentration range investigated was 50-1000ppm for all the additives used in the present work. Figures 4.15-4.20 shows some selected experimental work results for the water soluble and oil soluble mucilage (grafted mucilage) solutions flowing through different pipe diameters and Re and all for the 1m testing section. The rest of the experimental data can be found in Appendix C1.

Generally, it can be noticed that the %DR increases by increasing the mucilage concentration and that agrees with the large number of published results such as Kamel and Shah (2009), Kim *et al.* (2009), Mostafa (2010), Bewersdorff (1993) and Nakken *et al.* (2004). The increasing trend for each experimental set is not uniform. Figure 4.15 shows the effect of natural mucilage concentration in water solution flowing along 0.0381m ID and 1m pipe length. At the optimum concentration (400ppm), maximum DR of 14%, 16%, 16%, 25%, 27% 29% and 29% achieved with respective Re (69594, 74233, 78873, 83512, 88152, 92791 and 97431). Generally it can be observed that the %DR increases by increasing the additive concentration for each Re individually but by comparing the same behavior with the Re range investigated, the points start to intersect, and a more general conclusion cannot be observed, i.e. it is hard to state that %DR increases by increasing the additive concentration and by increasing Re at the same time. The same thing can be seen when testing grafted mucilage flowing with diesel solution (Figure 4.16) at the same operating conditions mentioned in Figure 4.15.

Increasing the additive concentration means increasing the number of polymeric molecules interfering within the turbulence inside the pipe and that will make the stretching of the liquid globe forming the eddy harder due to the additional viscoelastic properties introduced by the additive to the main eddy body. It is important to highlight that the addition of the polymer additives must be within certain acceptable range where the changes in the apparent physical properties is kept within the minimum range.

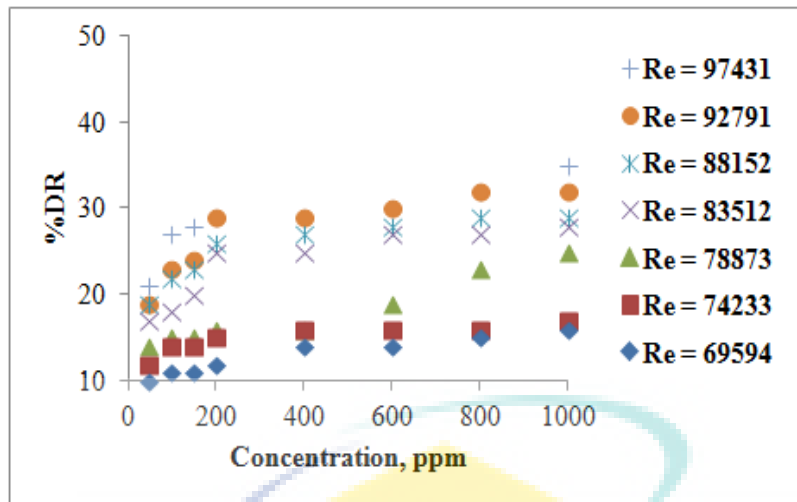


Figure 4.15: The effect of natural mucilage concentration in water on drag reduction at different Reynolds number along 0.0381m diameter and 1.0m length pipe

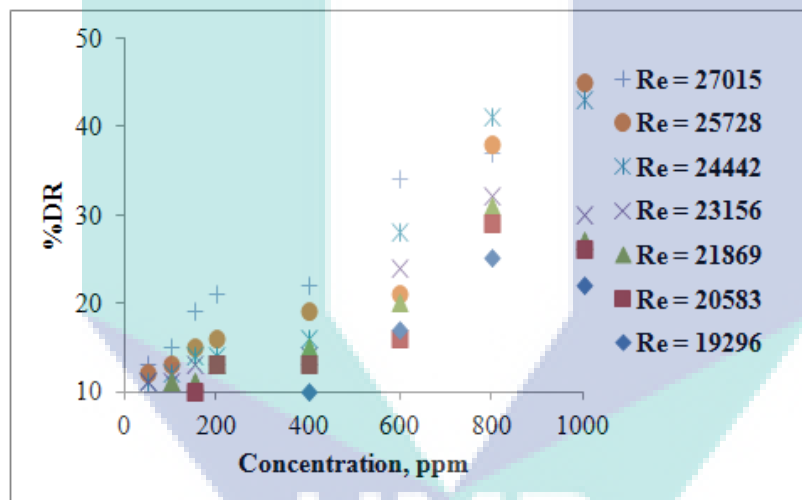


Figure 4.16: The effect of grafted mucilage concentration in diesel on drag reduction at different Reynolds number along 0.0381m diameter and 1.0m length pipe

For the same solution investigated, reducing the pipe diameter to 0.0254m, the clearer and distinguishable effect can be seen as shown in Figure 4.17 and 4.18, where the %DR is clearly increasing with increasing the concentration and Re at the same time. This behavior strongly highlights the complicated interaction between all the variables in the drag reduction science, and how a general conclusion can be driven by adopting all the acting variables at the same time, i.e. clearer effect of additive concentration was observed by reducing the pipe diameter from 0.0381m to 0.0254m.

Reducing the pipe diameter will increase the degree of turbulence, and that will provide more suitable and less severe media (optimum) for the drag reducers to perform than in the large pipe.

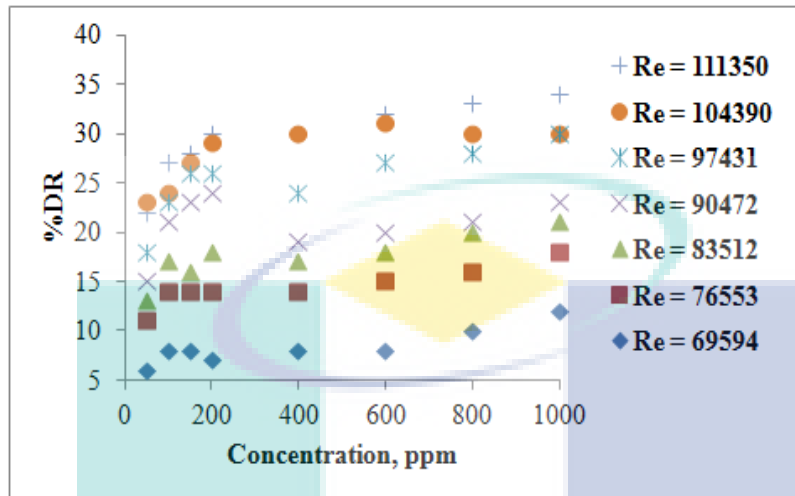


Figure 4.17: The effect of natural mucilage concentration in water on drag reduction at different Reynolds number along 0.0254m diameter and 1.0m length pipe

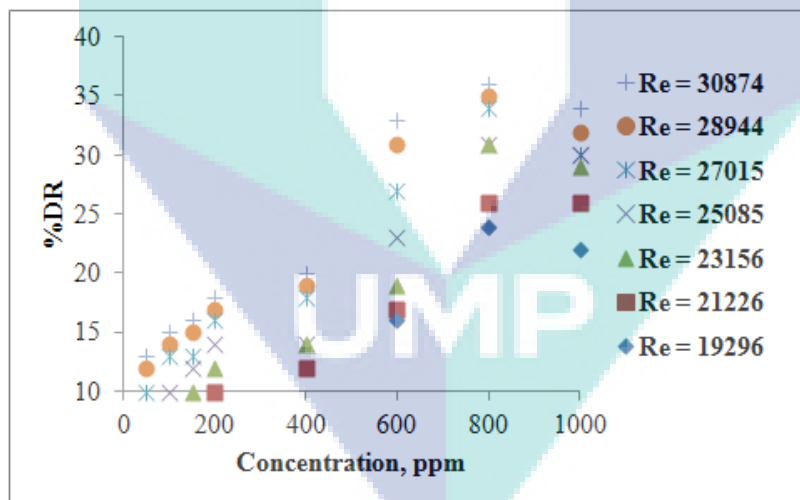


Figure 4.18: The effect of grafted mucilage concentration in diesel on drag reduction at different Reynolds number along 0.0254m diameter and 1.0m length pipe

Further reduction in the pipe diameter (0.0127m) again resulted in a mixed and intersected point as shown in the Figure 4.19 for mucilage soluble in the water, while it is still can be noticed that the same and distinguishable concentration effect on the %DR for the grafted mucilage in the diesel (Figure 4.20) solution flowing in 0.0127m ID.

These two figures highlight another new factor affecting the drag reduction performance which is the physical properties of the transported solution. Again reducing the pipe diameter means increasing the velocity inside the pipe, on the other hand, it means increasing the degree of turbulence and that provide a higher shear stress flow medium compared to the larger pipe. The grafted mucilage shows stable and distinguishable performance compared to the unstable drag reduction performance of the water mucilage. It is very clear that the high viscosity of the grafted mucilage solution played the role in resisting the high shear forces exerted by the turbulence structure inside the pipe, and that means a higher range of Re is needed to see the same behavior of the water soluble mucilage.

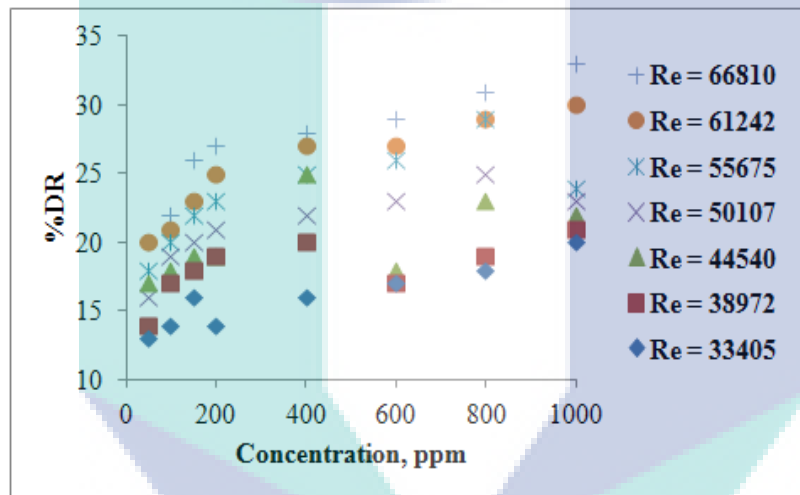


Figure 4.19: The effect of natural mucilage concentration in water on drag reduction at different Reynolds number along 0.0127m diameter and 1.0m length pipe

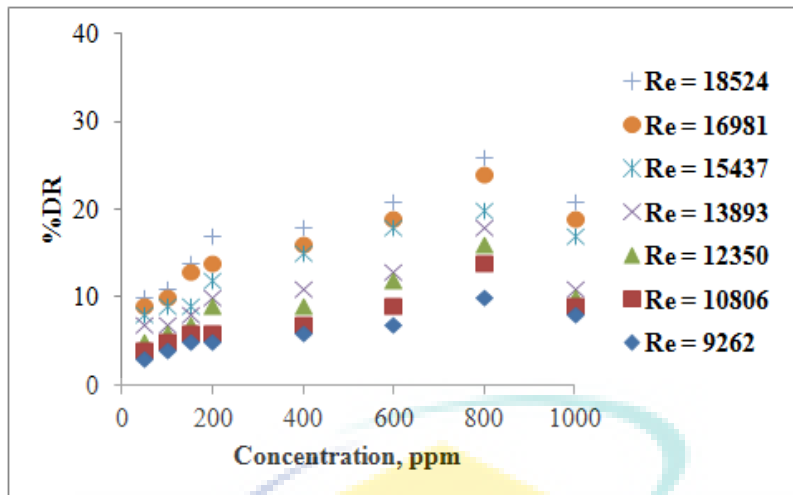


Figure 4.20: The effect of grafted mucilage concentration in diesel on drag reduction at different Reynolds number along 0.0127m diameter and 1.0m length pipe

For the red gypsum powder concentration effect, Figures 4.21-4.24 shows the concentration-%DR curve for water and diesel solution within mentioned operating conditions. In Figure 4.21, the %DR increases as solution concentration increase. This result shows a general agreement on drag reduction (Vaseleski and Metzner, 1974; Sharma *et al.*, 1979, Wang *et al.*, 1998; Lin *et al.*, 2006; Develter and Duoffrey, 1998). Maximum DR of 14%, 19%, 20%, 20%, 20%, 22% and 22% respectively for each Re= 69594, 74233, 78873, 83512, 88152, 92791 and 97431 at optimum water solution of 400ppm, were obtained. Further increase in solution concentration gives stable value in %DR. The concentration of solid suspension is related to the solid distribution in turbulent eddies, and that can be considered as the main factor controlling its drag reduction performance. Increasing the gypsum concentration means increasing the number of solids particles or aggregates involved in the drag reduction operation and that will cover wider spectra of turbulence all over the pipes. In the Figure 4.21, the %DR increase was lower in the powder concentration range above the 400 ppm; such behavior indicates that the 400 ppm concentration is the optimum concentration to suppress the turbulent eddies and any increase in the additive concentration will not contribute significantly to the flow enhancement. In other words, the eddy (within the point operating conditions) will carry the maximum solid particle load and any further increase in the number of particles will not be involved in suppressing the same eddy

especially knowing that the additive is insoluble and not degradable so replacing the damaged additive molecules doesn't occur.

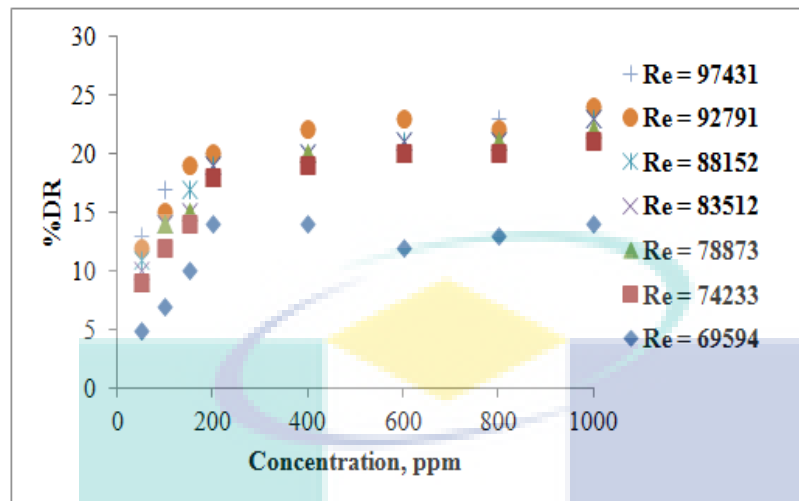


Figure 4.21: The effect of gypsum concentration in water on drag reduction at different Reynolds number along 0.0381m diameter and 1.0m length pipe

Figure 4.22 shows the effect of the gypsum powder suspended in the diesel solution on %DR within the investigated range of Re at the same operating conditions mentioned in Figure 4.21. Although the %DR increases with solution concentration, the performance of water solution is clearer than the diesel solution. In diesel solution, the points start to intersect, and a more general conclusion cannot be made, i.e. it is hard to state that %DR increases by increasing the additive concentration and by increasing Re at the same time.

UMP

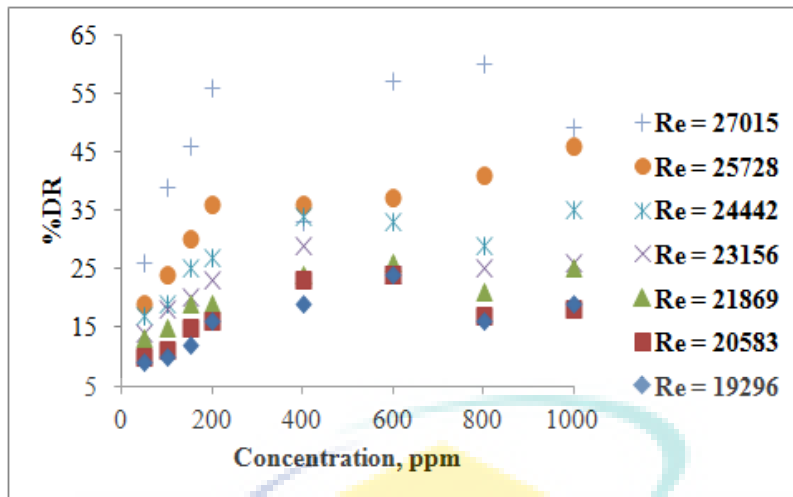


Figure 4.22: The effect of gypsum concentration in diesel on drag reduction at different Reynolds number along 0.0381m diameter and 1.0m length pipe

Figure 4.23 shows the same curve trend as mentioned in Figure 4.21 but here the effect is clearer in smaller pipe diameter (0.0254m). The behavior of water solution in smaller pipe is more distinguishable than larger pipe diameter (0.0381m). Figures 4.24 and 4.22 shares the same behavior trend in performance where the %DR observed is not uniform and indistinguishable with the increase in solution concentration for all the investigated Re. Solution at higher Re, which over its degree of turbulence, will cause the reduction static due to the decrement of additive efficiency. This arises due to the impairing ratio of solid concentration and degree of turbulence within the transported pipelines.

UMP

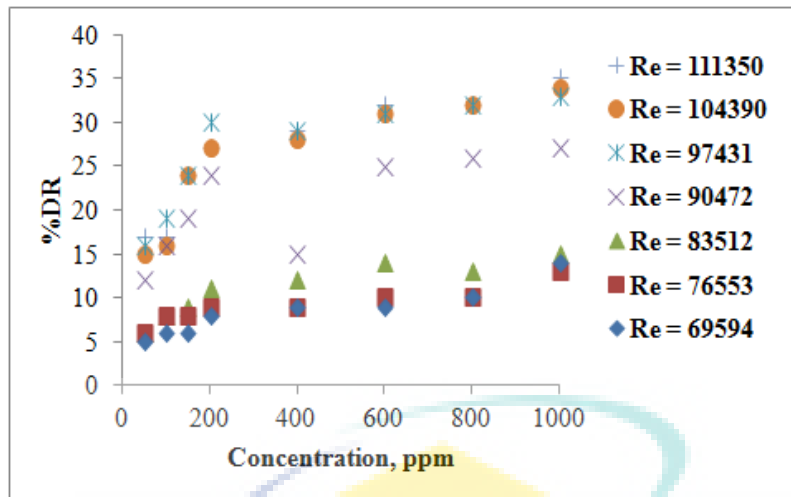


Figure 4.23: The effect of gypsum concentration in water on drag reduction at different Reynolds number along 0.0254m diameter and 1.0m length pipe

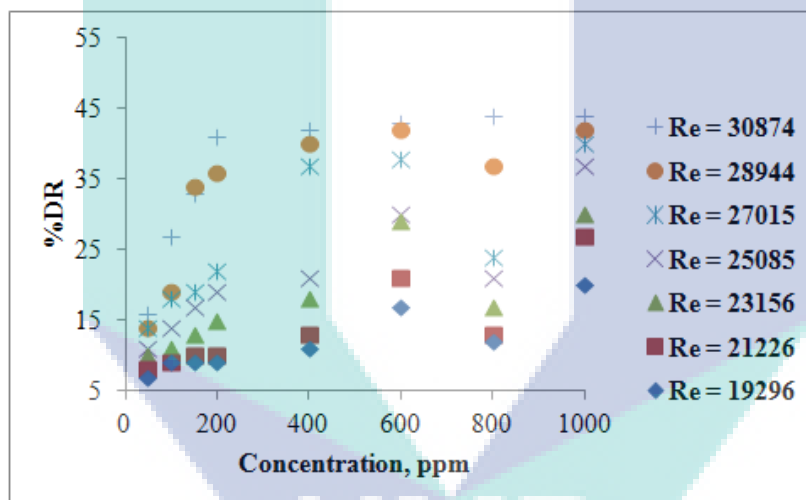


Figure 4.24: The effect of gypsum concentration in diesel on drag reduction at different Reynolds number along 0.0254m diameter and 1.0m length pipe

4.3.3 Effect of Pipe Diameter

One of the key factors controlling the drag reduction performance of any additives is the geometry of the pipe itself. The pipe size can be considered as one of the effective parameters that control the degree of turbulence and that will also control the drag reduction performance of the proposed additives. In the present work, three pipe diameters were studied which are 0.0381m ID, 0.0254m ID and 0.0127m ID respectively.

Figures 4.25-4.28 shows a graphical representation for selected experimental data introducing the effects of pipe diameter on drag reduction performance at 100ppm additive concentration in 2m testing section length. Due to the experimental rig capacity limitations, it doesn't allow covering exactly the same Re range for all the three pipes within the range of Re employed (69594-97431, 69594-111350 and 33405-66810 for 0.0381m, 0.0254m and 0.0127m ID respectively in water solution and 19296-27015, 19296-30874 and 9262-18524 for 0.0381m, 0.0254m and 0.0127m ID respectively in diesel solution).

Generally, it can be noticed that the 0.0381m ID pipe is showing higher %DR compared with the other two diameters in both solutions. A maximum DR of 36%, 25%, 39% and 44% is achieved respectively in 2m length pipe of 100ppm water-mucilage, diesel-mucilage, water-gypsum and diesel-gypsum solutions.

It is very important to highlight that the degree of turbulence is controlled by the space available for the liquid to flow. Figure 4.25 shows that the %DR for the 0.0381m ID pipe is clearly higher than the 0.0254m ID pipe and which is higher than 0.0127m ID pipe. Increasing the pipe diameter means increasing the space available for the turbulence structure to form and that will provide less intense shearing media for the liquid to form larger and slower eddies compared to the smaller pipe diameters. The low shearing eddies will provide a more suitable medium for the additives to suppress those eddies. While in smaller pipes within the same flow rate compared to larger pipes, the velocity will be higher, and that will produce much more faster eddies with high shearing force that will reduce the efficiency of the drag reducer, i.e. will reduce the ability of the drag reducer to suppress the eddies formed in the core of the flow.

Although the flow inside these three pipe diameters is maintained in turbulent mode, but the degree of turbulence is different in each pipe. In smaller pipe, the energy absorbed by eddies from the main stream will be higher than larger pipes (larger pressure drop), when the degree of turbulence becomes higher, frequent collisions occur between eddies which will produce smaller eddies. This provides an extra number of eddies absorbing energy from the main stream to complete their shape. The same phenomenon occurs in larger pipe, but the wider space within pipe causes few collisions

to occur between eddies. Therefore, lower amount of energy absorbed from the main stream. The important role of additives is to suppress eddy formation and prevent it from completing its shape to reduce the amount of absorbed energy from the main flow and that's explains also the lower pressure drop observed in larger pipes. As in smaller pipe, smaller eddies formed; therefore the additives can perform better. The results of the pipe diameter effect agree well with the results published by Virk *et al.* (1967), Radin *et al.* (1975), Matthys and Sabersky (1982), Al-Sarkhi and Hanratty (2001) and Robert (2002). While Mowla and Naderi (2006) in their research proved the exact opposite results, i.e. in smaller pipe diameter, higher %DR achieved. Decreasing of pipe diameter means the relative roughness (ϵ/D) is decreased which will result in a higher degree of turbulence represents better the effect of the DRA.

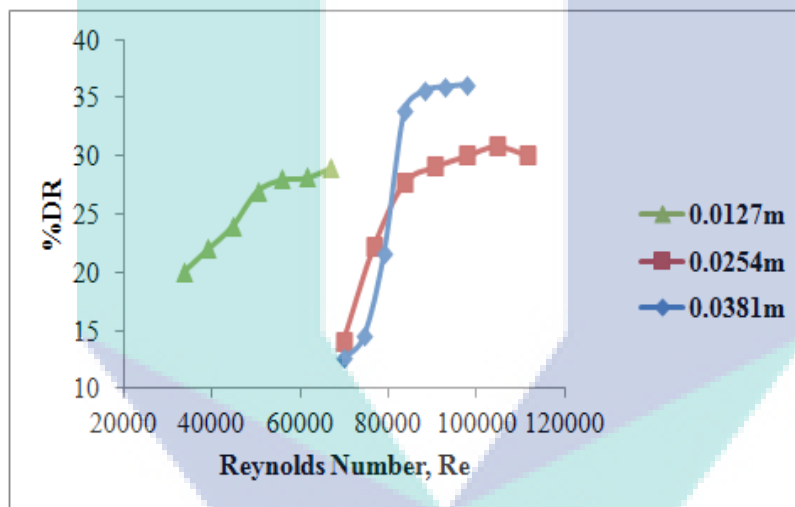


Figure 4.25: The effect of pipe diameter on drag reduction while testing 100ppm natural mucilage in water along 2m pipe length

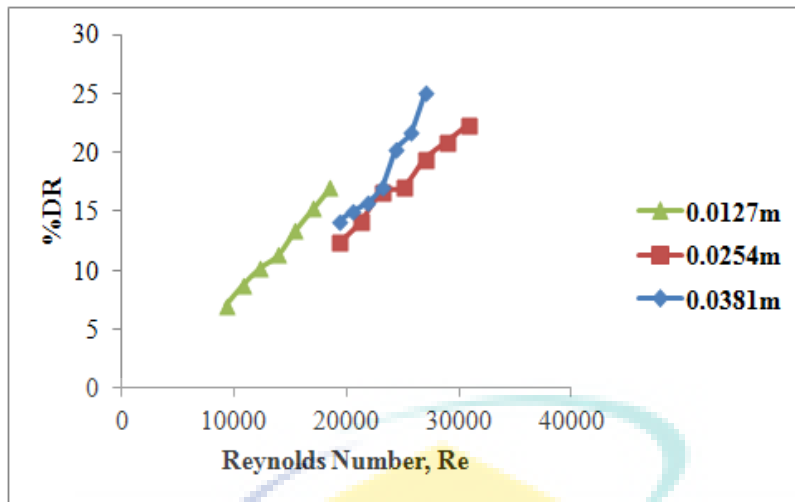


Figure 4.26: The effect of pipe diameter on drag reduction while testing 100ppm grafted mucilage in diesel along 2m pipe length

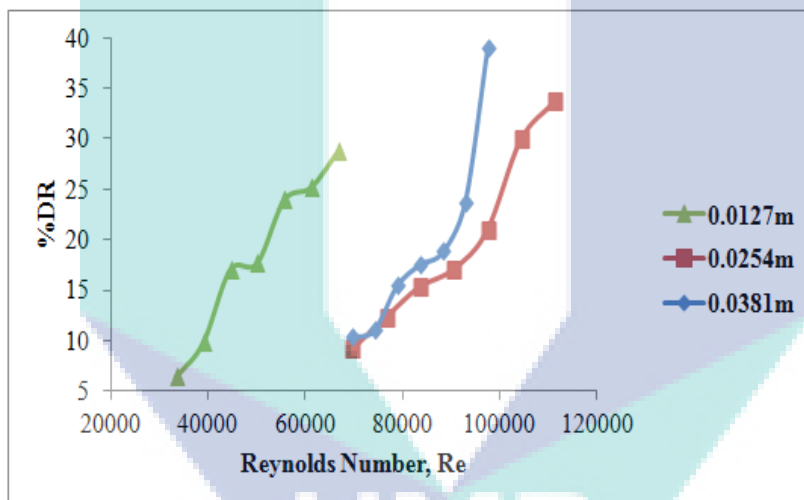


Figure 4.27: The effect of pipe diameter on drag reduction while testing 100ppm red gypsum in water along 2m pipe length

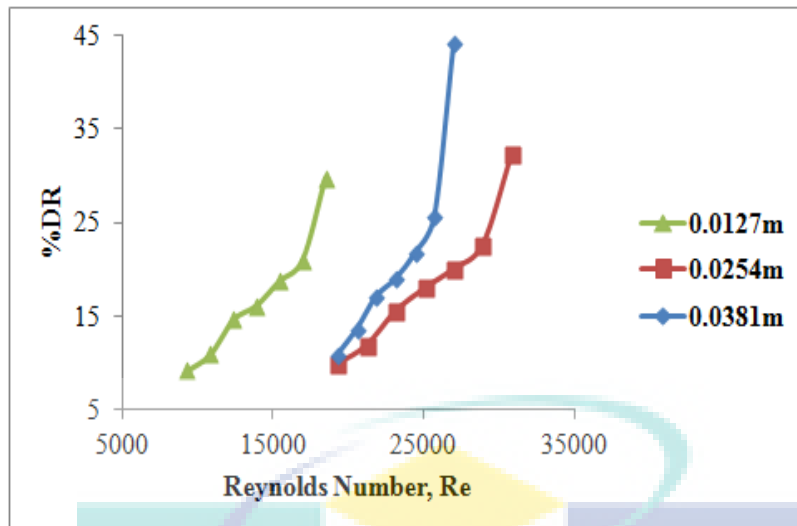


Figure 4.28: The effect of pipe diameter on drag reduction while testing 100ppm red gypsum in diesel along 2m pipe length

4.3.4 Effect of Testing Section Length

The effect of pipe length was studied by many authors (Berman and George, 1974; Berman, 1977a, 1977b; Berman and Yuen, 1977; Berman *et al.*, 1978) and it was criticized and adjusted by others, and it was the key factors in some of the studies about the additive resistance to shear forces. This section covers the study on drag reducing capacity of newly introduced additives over the testing section length (four testing section lengths: 0.5, 1.0, 1.5 and 2.0m) were adopted). Figures 4.29-4.32 shows the graphical presentation of selected experimental data of the testing section length effect on the drag reduction performance of the new additives.

Figure 4.29 shows the effect of testing section length on %DR at different water soluble mucilage concentrations. It is observed that the %DR increases when testing section length increase. Generally, the rate of increase in %DR is slower after 1.5m pipe length; therefore, 1.5m concerned as optimum pipe length for effective drag reduction. An optimum DR of 31%, 35%, 44%, 43%, 47% and 47% achieved when testing 50ppm, 100ppm, 200ppm, 400ppm, 800ppm and 1000ppm solution respectively. It is believed that the reduction in the drag reduction performance of the additive after reaching the 1.5 m length pipe is due to the turbulent flow development and its effect on the additive effectiveness. It is known that the turbulent structure develops continuously with time

and distance. Increasing the pipe length means increasing the distance and time for the same liquid globe forming the turbulent structure (eddy) to develop in shape and that may add more complicated structures to the main flow that the additives will not have the ability to overcome. Another factor that might cause the reduction in performance is the polymer additive partial degradation due to the long exposure to shear forces. When drag reducing polymers is introduced into a piping system, they degrade mechanically when passing through the pipe and the molecular weight decreases as a result of cleavage of the long polymer chains (Choi et al., 2000a, b, 2002), and drag reduction rate quickly reduced. Although still showing drag reducing ability, but not much. Alternative explanation provided that, instead of polymer degradation, some or all of the degradation is associated with a decrease in the amount of polymer aggregated or entangled (Vlachogiannis *et al.*, 2003). Length effect on %DR must be an indication about how important is this parameter on the drag reduction study. As the testing section lengthen, the polymer given longer time, to perform better by lining/forming long polymer molecules near the walls of the pipe to reduce the skin friction. The elongation of polymer through turbulent flow as a function of pipe length is the most accurate reason for the stated results.

Figure 4.30 shows the graphical representation of the pipe length effect on %DR in 0.0381m ID pipe at $Re=24442$ for the grafted mucilage in all the mentioned solution concentration. The %DR increases linearly with testing section length until maximum %DR without reaching an optimum pipe length. The performance of the oil soluble mucilage is not as clear as observed in Figure 4.29 for water soluble mucilage. Again, the factor of the apparent physical properties of the transported liquid appears. It is believed that, for high viscous solutions (diesel solution), the dynamic behavior of the transported liquid will be different where the development of the turbulent structures inside the pipe will be slower with the length. Generally, it is expected that the length where the peak point appears, will be beyond the 2m pipe length, i.e. the flow system needs a long pipe to reach the optimum pipe length where the %DR start to show more stable and even lower values.

The effect of pipe length is a clear clue to the effectiveness of solid particles. More real expression is the degree of sustainability of the solid molecules along the

transportation length with all the shear stresses exposed. One of the key reasons behind using the insoluble suspended solids as drag reducing agents is its resistance to shear degradation when transported with liquids in turbulent flow. This is why it is important to highlight that the additive degradation part will not be discussed when describing the solid particle effect. It is important to notice that the 1000 ppm curve showed irregular and odd behavior compared with the other concentrations investigated and that can be considered normal in the drag reduction experiments due to chaotic media these additives are working.

Figures 4.31 and 4.32 shows the effect of testing section length on the percentage drag reduction for a specified solution concentration. It can be noticed that, %DR increases by increasing the pipe length and it is not consistent with all the solution concentrations. Most of the curves showed that the %DR increases by increasing the pipe length with some irregular behaviors in some points. It is very important to highlight that the suspended solid drag reduction effectiveness is directly linked to the degree of turbulence and its effectiveness will not be reduced by time or length because it is not a degradable additive. This is why, a maximum %DR point was not reached and the only part left controlling the drag reduction performance by eliminating the degradation part is the developed turbulent eddies with length.

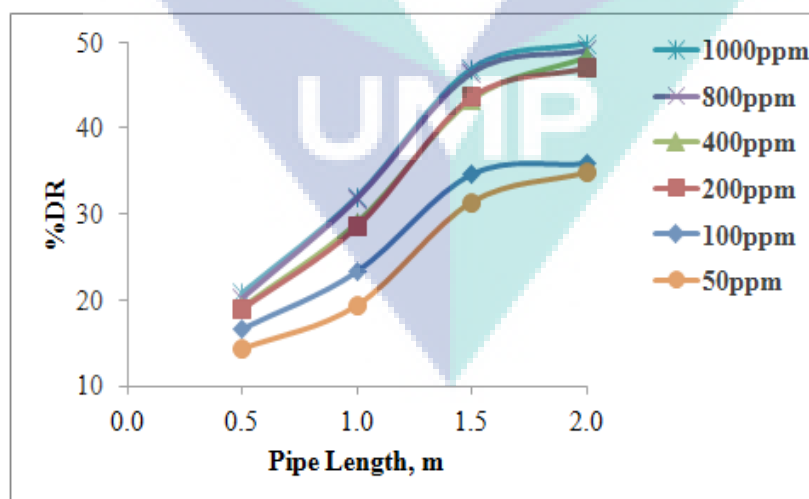


Figure 4.29: The effect of pipe length on drag reduction while testing natural mucilage in water at $Re=92791$ along 0.0381m ID pipe

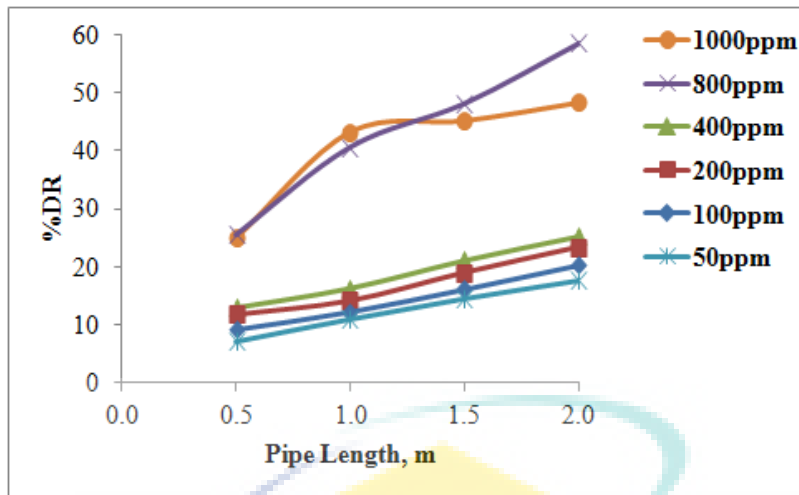


Figure 4.30: The effect of pipe length on drag reduction while testing grafted mucilage in diesel at $Re=24442$ along 0.0381m ID pipe

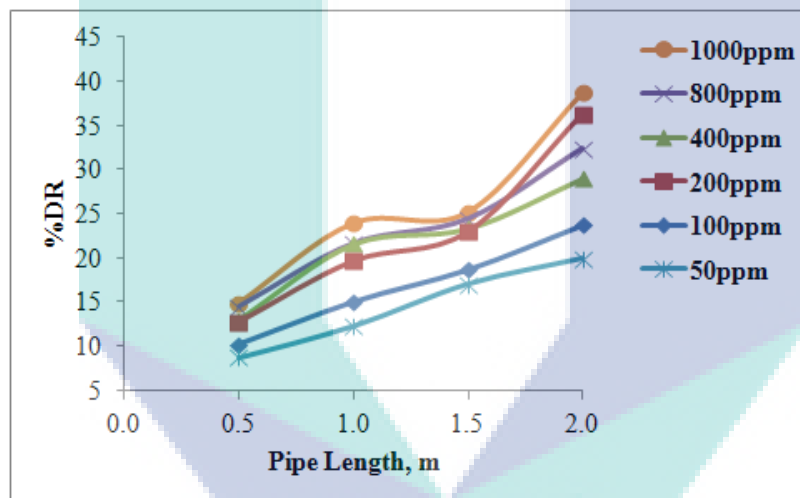


Figure 4.31: The effect of pipe length on drag reduction while testing red gypsum in water at $Re=92791$ along 0.0381m ID pipe

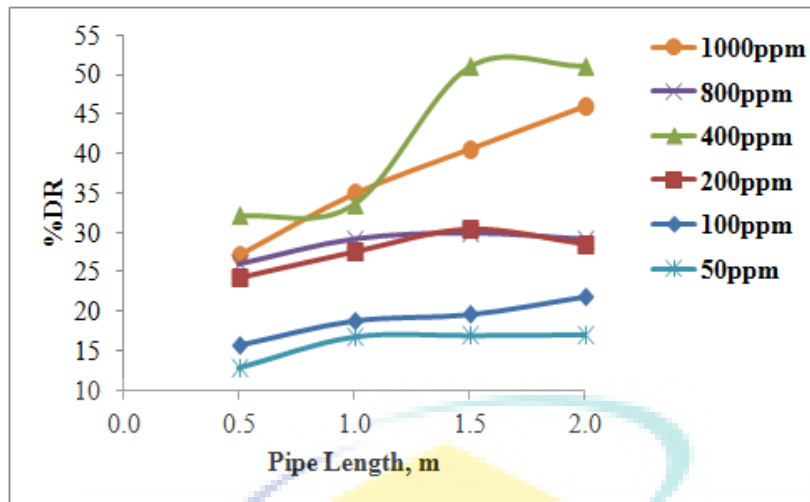


Figure 4.32: The effect of pipe length on drag reduction while testing red gypsum in diesel at $Re=24442$ along 0.0381m ID pipe

4.4 MUCILAGE DEGRADATION

Mechanical degradation of the polymer additives is considered the most important factor that limits the use and the value of the additive. In the present work, the pressure readings were recorded every one second and for two hundred seconds in each experiment. The records were taken for all the experiments conducted before and after the addition of the additive. Figures 4.33-4.35 shows selected results of the pressure drop readings for the first 1 m testing section length of each pipe. It is noted that the pressure drop readings for the grafted mucilage-diesel solutions continue to be within the same trend and line even after 200 seconds (3.33 minutes) of continuous recirculation of the solution in such a short circulation system and under the server shearing conditions of the centrifugal pump. The reason behind circulating the solutions for only 200 seconds is to avoid the effect of temperature rise that can occur due to the extensive shear force exposed by the centrifugal pump, i.e. circulating the solution for a long time will increase the solution temperature (solution temperature maintained at 25°C) and that will reduce the solution viscosity which will lead to false pressure drop readings.

The biodegradability of natural polymers reduces their shelflife and needs to be suitably controlled. To overcome the disadvantage, grafting methods have been

introduced (Deshmukh and Singh, 1986, 1987; Deshmukh *et al.*, 1985) so that grafting technique enables the mucilage to perform better in hydrophobic liquid by changing its properties. The advantage of polysaccharide polymers is their high mechanical stability against degradation when compared to flexible synthetic polymers with similar molecular weights; however they are highly susceptible to biological degradation. High mechanical stability means the polymer still subject to mechanical degradation but after some extended time. Viscosity of the polymer is another factor that explains the high mechanical stability. As the viscosity of natural mucilage and grafted mucilage is slightly higher at higher concentrations (Table 4.1) makes the molecular rupture occur slowly when the polymer circulated through pump continuously. This indicates the advantage of highly concentrated polymers.

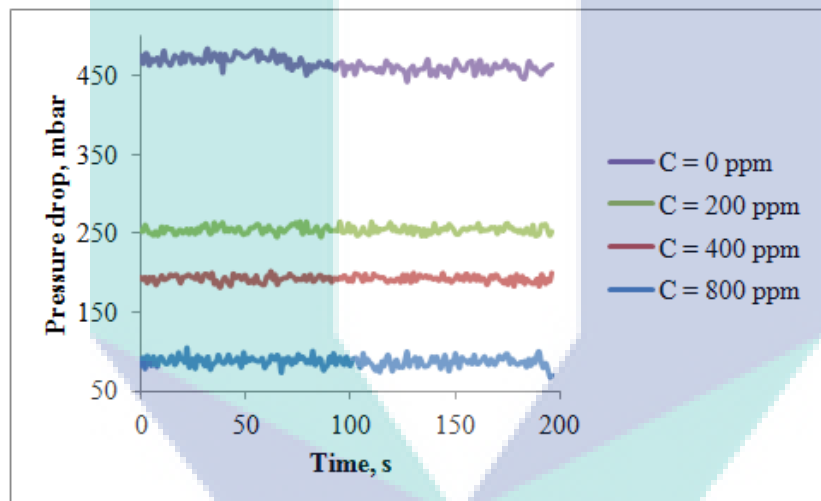


Figure 4.33: Pressure analysis for diesel-mucilage solution flowing through 0.0127 m ID pipe at $Re = 13893$ and with testing section length of 1 m

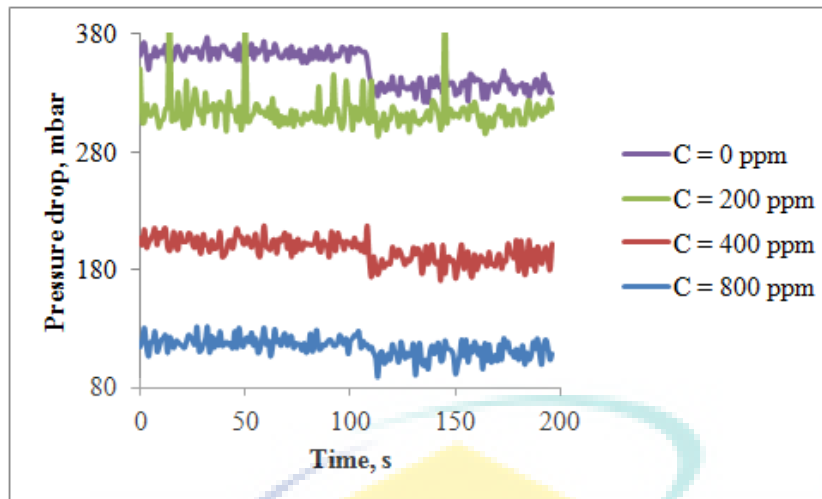


Figure 4.34: Pressure analysis for diesel-mucilage solution flowing through 0.0254 m ID pipe at $Re = 25085$ and with testing section length of 1 m

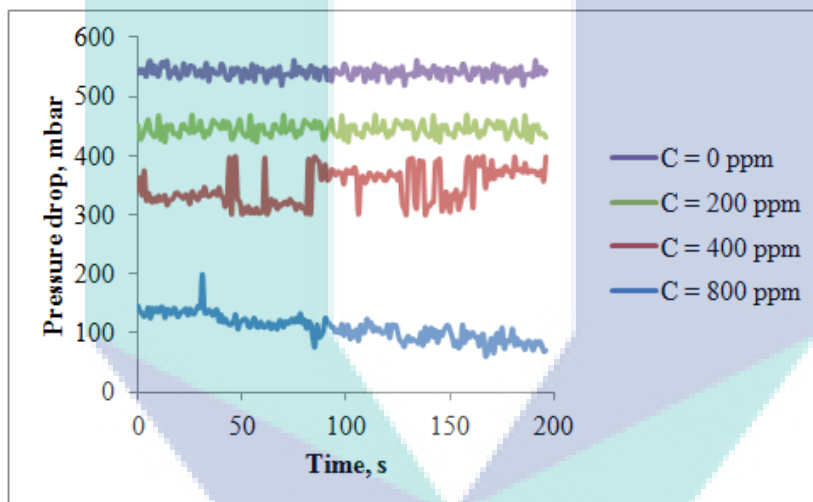


Figure 4.35: Pressure analysis for diesel-mucilage solution flowing through 0.0381 m ID pipe at $Re = 23156$ and with testing section length of 1 m.

4.5 STATISTICAL MODEL (CORRELATIONS)

Dimensional analysis is used to group all the significant quantities into a dimensionless friction factor to reduce the number of variables and to make the results applicable to all the similar situations. Choosing the suitable variables that control the friction factor (f) in the study of drag reduction is very important as it is influenced by the solution's physical properties, pipe dimensions and flow properties. Three dimensionless groups were adopted which are:

1. The Reynolds number (Re)
2. The fanning friction factor (f)
3. The pipe dimensions and the concentration group (L/D) and C where C is a dimensionless factor (in ppm)

$$F = a \times \left[\left(\frac{k}{\log f} \right) + s \right] \times \left[\left(\frac{L}{D} \right) \times (1 + C) \times Re \right]^b \quad (4.4)$$

Detailed description of the dimensional analysis correlation is shown in Appendix E. The fundamental problem is to find the values of constants (a , k , s and b) that give the best fitting of the experimental data. In this present work, the least square method has been used to determine the value of constants using a computer program 'STATISTICA'. The value of the constants for experimental work is as follows: $a = 0.3398$, $k = -0.1503$, $s = -0.0506$ and $b = -0.0008$ with best variance (V) and (R) values of 0.991678786 and 0.995830701 respectively. The maximum drag reduction in this present study is represented by the following Eq. (4.5) and the observed values versus predicted values are shown in the Figure 4.36.

$$F = 0.3399 \times \left[\left(\frac{-0.1502}{\log f} \right) - 0.0506 \right] \times \left[\left(\frac{L}{D} \right) \times (1 + C) \times Re \right]^{-0.0008} \quad (4.5)$$

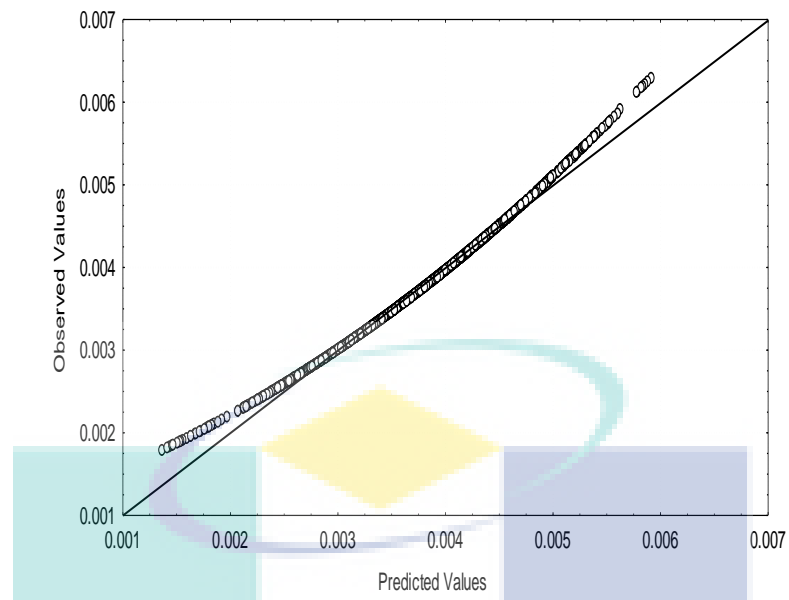


Figure 4.36: Observed versus predicted values for statistical correlation

UMP

CHAPTER 5

CONCLUSION AND RECOMMENDATION

5.1 DRA PERFORMANCE

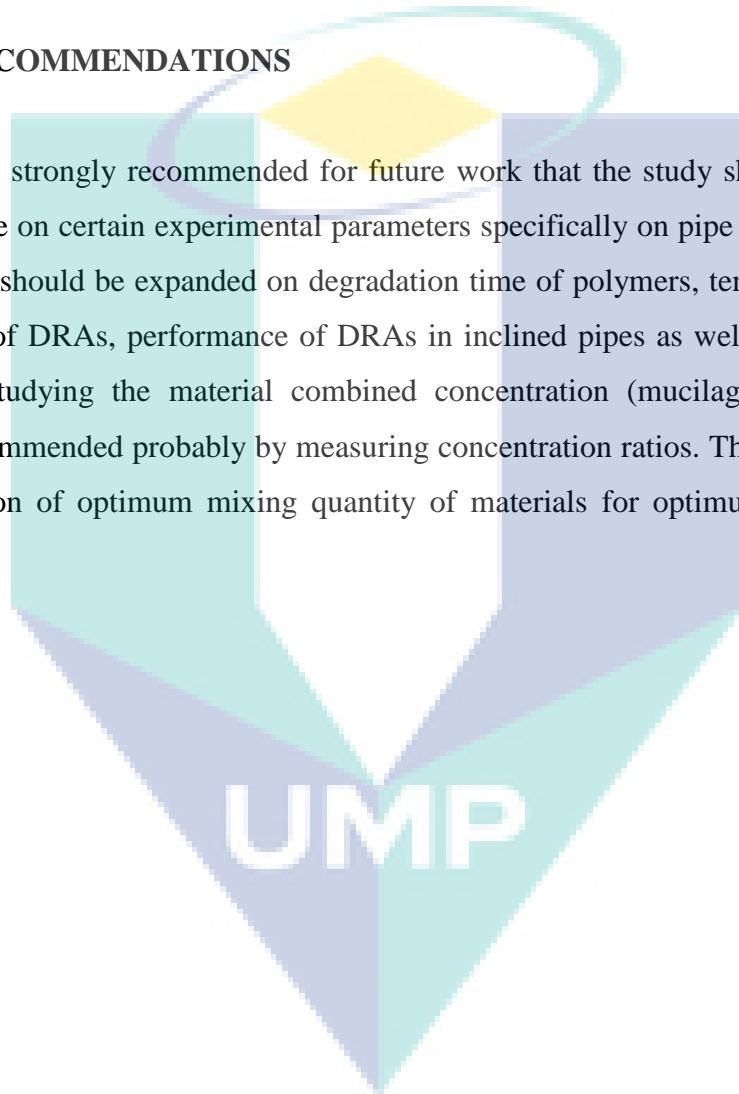
In this present work, two novel and environmentally friendly DRAs are introduced successfully (hibiscus leaves' mucilage and red gypsum powder). The drag reduction ability of the water soluble hibiscus leaves' mucilage was tested and maximum DR of 39% achieved with 400ppm solution of $Re = 88152$ in 0.0381m ID and 1.5m length pipe. The solubility of the hibiscus leaves' mucilage was converted to oil-soluble by applying the grafting process. The drag reduction ability of the oil soluble hibiscus leaves' mucilage was tested and maximum DR of 47% achieved in 0.0381m ID and 1.5m length pipe. The gypsum powder from the titanium dioxide manufacturing industry was tested as the insoluble DRA in the present work. The drag reduction ability of the gypsum powder was tested and maximum DR of 26% and 60% in water and diesel solutions respectively achieved in 0.0381m ID and 1.5m length pipe.

Generally, the %DR increases by increasing the solution velocity for both the tested DRAs until specific optimum or maximum %DR value is reached. The %DR increases by increasing the solution concentrations. Pipe geometry (pipe internal diameter and testing section length) directly proportional to the %DR as well where the %DR increase as the pipe diameter and testing section length increase. The relationship between the %DR and investigated parameters (solution velocity, additive concentration, pipe diameter and testing section length) is always related lead us to conclude that these additives improve the performance.

A statistical correlation was introduced in this present study ($F = a \times [(k/\log f) + s] \times [(L/D) \times (1+C) \times Re]^b$) where this dimensionless relation was tested with the experimental data for the maximum drag reduction performance. All the experimental data showed a good fit with the resulted correlation ($f = 0.3399 \times [(-0.1502/\log f) - 0.0506] \times [(L/D) \times (1+C) \times Re]^{-0.0008}$) as displayed in Figure 4.36. This correlation is one of the engineering contribution as the results fit well.

5.2 RECOMMENDATIONS

It is strongly recommended for future work that the study should be done in a larger scope on certain experimental parameters specifically on pipe sizes. Besides that, the studies should be expanded on degradation time of polymers, temperature effect on efficiency of DRAs, performance of DRAs in inclined pipes as well as vertical piping systems. Studying the material combined concentration (mucilage and gypsum) is highly recommended probably by measuring concentration ratios. This will enhance the identification of optimum mixing quantity of materials for optimum drag reductions occur.



REFERENCES

- Adriano, D.C., Page, A.L., Elseewi, A.A., Chang, A.C. and Straughan, I. 1980. Utilization and disposal of fly ash and other coal residues in terrestrial ecosystems: a review. *Journal of Environmental Quality*. **9**(3): 333-344.
- Aguilar, G., Gasljevic, K. and Matthys, E.F. 2001. Asymptotes of maximum friction and heat transfer reductions for drag-reducing surfactant solutions. *International Journal of Heat and Mass Transfer*. **44**(15): 2835-2843.
- Al-Sarkhi, A. and Hanratty, T.J. 2001. Effect of pipe diameter on the performance of drag-reducing polymers in annular gas-liquid flows. *Chemical Engineering Research and Design*. **79**(4): 402-408.
- Anderson, G.W., Rohr, J.J. and Stanley, S.D. 1993. The combined drag effects of riblets and polymers in pipe flow. *Journal of Fluids Engineering*. **115**(2): 213-221.
- Barresi, A.A. 1997. Experimental investigation of interaction between turbulent liquid flow and solid particles and its effects on fast reactions. *Chemical Engineering Science*. **52**(5): 807-814.
- BASF. 1999. *Dimethylformamide*. Technical Data Sheet.
- Batchelor, G.K. 1967. An introduction to fluid dynamics. *Journal of Fluid Mechanics*. **28**(4): 822-824.
- Berman, N.S. 1977a. Drag reduction of the highest molecular weight fractions of polyethylene oxide. *Physics of Fluids*. **20**(5): 715-718.
- Berman, N.S. 1977b. Flow time scales and drag reduction. *Physics of Fluids*. **20**(10): 168-174.
- Berman, N.S. and George, W.K. 1974. Onset of drag reduction in dilute polymer solutions. *Physics of Fluids*. **17**(1): 250-251.
- Berman, N.S. and Yuen, J. 1977. The study of drag reduction using narrow fractions of polyox, *2nd International Conference on Drag Reduction*.
- Berman, N.S., Griswold, S.T., Elihu, S. and Yuen, J. 1978. An observation of the effect of integral scale on drag reduction. *AIChE Journal*. **24**(1): 124-130.
- Bewersdorff. 1993. *Polymer physics: from suspensions to nanocomposites and beyond* (Editors Utracki, L.A. and Jamieson, A.M.) (online). <http://onlinelibrary.wiley.com/book/10.1002/9780470600160> (16 August 2011).
- Bradberry, S. 2007. Acetone. *Medicine*. **35**(11): 581 (Poisoning Part 2 and 3).
- Cengel, Y.A. and Cimbala, J.M. 2006. *Fluid Mechanics Fundamentals and Application*. New York: McGraw-Hill.

Chakrabarti, S., Seidl, B., Vorwerk, J. and Brunn, P.O. 1991(a). The rheology of hydroxy-propylguar (HPG) solutions and its influence on the flow through a porous medium and turbulent tube flow, respectively (Part 1). *Rheologica Acta*. **30**(2): 114-123.

Chakrabarti, S., Seidl, B., Vorwerk, J. and Brunn, P.O. 1991(b). Correlations between porous medium flow data and turbulent tube flow results for aqueous hydroxypropylguar solutions (Part 2). *Rheologica Acta*. **30**(2): 124-130.

Chapman, B., 2005. Study of drag reduction by zwitterionic and non-ionic surfactants in low temperature ethylene glycol/water recirculation systems. Ohio State University. <https://kb.osu.edu/dspace/bitstream/1811/313/1/BrianChapman.pdf>

Chen, H.J., Kouba, G.E., Fouchi, M.S., Fu, B. and Rey, D.G. 2000. DRA for gas pipelining successful in Gulf of Mexico trial (online). [http:// www.accessmylibrary.com/coms2/summary_0286-27976076_ITM](http://www.accessmylibrary.com/coms2/summary_0286-27976076_ITM) (1 March 2009).

Cho, S.H., Tae, C.S. and Zaheeruddin, M. 2007. Effect of fluid velocity, temperature, and concentration of non-ionic surfactants on drag reduction. *Energy Conversion and Management*. **48**(3): 913-918.

Choi, H.J., Kim, C.A., Sohn, J.I. and Jhon, M.S. 2000a. An exponential decay function for polymer degradation in turbulent drag reduction. *Polymer Degradation and Stability*. **69**(3): 341-346.

Choi, H.J., Kim, C.A., Sung, J.H., Kim, C.B., Chun, W. and Jhon, M.S. 2000b. Universal drag reduction characteristics of saline water-soluble poly(ethylene oxide) in a rotating disk apparatus. *Colloid and Polymer Science*. **278**(7): 701-705.

Choi, H.J., Lim, S.T., Lai, P.Y. and Chan, C.K. 2002. Turbulent drag reduction and degradation of DNA. *Physical Review Letters*. **89**(8): 1-4.

Chou, L.C. 1991. *Drag reducing cationic surfactant solutions for district heating and cooling systems*. Ph.D. Thesis. The Ohio State University, Columbus, Ohio.

Clamond, D. 2009. Efficient resolution of the Colebrook equation. *Industrial and Engineering Chemistry Research*. **48**(7): 3665-3671.

Creamer, T. 2008. Construction of vital R11, 2bn fuel pipeline to start in September. *Engineering News*. 23 April.

Daas, M.A. 2001. *Modeling the effects of oil viscosity and pipe inclination on flow characteristics and drag reduction in slug flow*. Ph.D. Thesis. Ohio University.

Dalman, Y., Puskar, Judit E., and Marganitis, A. 2003. *Macromolecules*. **36**: 2198.

Davidson, P.A. 2004. *Turbulence: An Introduction for Scientists and Engineers*. New York: Oxford.

de Gennes, P.G. 1990. *Introduction to polymer dynamics*, Cambridge University Press.

- Dean, R.C. 1978. Editorial. *Journal of Fluids Engineering*. **100**(1): 2. doi:10.1115/1.3448608
- Dembek, G. and Bewersdorff, H.W. 1981. Short-time increase of sewer capacity by addition of water-soluble polymers. *GWF, Wasser/Abwasser*. **122**(9): 392-395.
- Deshmukh, S.R., Chaturvedi, P.N. and Singh, R.P. 1985. The turbulent drag reduction by graft copolymers of guar gum and polyacrylamide. *Journal of Applied Polymer Science*. **30**(10): 4013-4018.
- Deshmukh, S.R. and Singh, R.P. 1986. Drag reduction characteristics of graft copolymers of xanthan gum and polyacrylamide. *Journal of Applied Polymer Science*. **32**(8): 6163-6176.
- Deshmukh, S.R. and Singh, R.P. 1987. Drag reduction effectiveness, shear stability and biodegradation resistance of guar gum-based graft copolymers. *Journal of Applied Polymer Science*. **33**(6): 1963-1975.
- Develter, P. and Duoffrey, G., 1998. Flow of wood pulp fibre suspensions in open channels. *Appita Journal*. **51**: 356-362.
- Dong, S., Feng, X., Salcudean, M. and Gartshore, I. 2003. Concentration of pulp fibers in 3D turbulent channel flow. *International Journal of Multiphase Flow*. **29**(1):1-21.
- Dubief, Y., Terrapon, V.E., White, C.M., Shaqfeh, E.S.G., Moin, P. and Lele, S.K. 2005. New answers on the interaction between polymers and vortices in turbulent flows. *Flow, Turbulence and Combustion*. **74**(4): 311-329.
- Dujmovich, T. and Gallegos, A. 2005. Drag reducers improve throughput, cut costs. *Offshore* **65**(12): 1-4.
- EFMA. 1998. *Guidelines for transporting nitric acid in tanks*. Belgium: European Fertilizer Manufacturers Association.
- Elata, C. and Tirosh, J. 1965. Frictional drag reduction. Israel Inst. of Technical Informal report on Contract 62558-4093 for Office of Naval Research.
- Evans, D.E. and Miller, D.D. 1992. "Organized Solutions in Polar Solvents", In: Friberg, S. E.; Lindman, B. (Ed.s) Organized solutions, *Surfactant Science Series*. Marcel Dekker, New York, **44**: 33-44.
- Fabula, A.G. 1963. The Toms phenomenon in the turbulent flow of very dilute polymer solutions. *4th International Congress on Rheology, Brown U., Providence, Rhode Island*.
- Fabula, A.G. 1971. Fire-fighting benefits of polymeric friction reduction. *Journal of Basic Engineering*. **93**(3): 453-455.

- Fauziah, I., Zaayah, S. and Jamal, T. 1996. Characterization and land application of red gypsum: a waste product from the titanium dioxide industry. *Science of the Total Environment*. **188**(2-3): 243-251.
- Fernandez, M.J, Casinos, I. and Guzman, G.M. 1990. Effect of the way of addition of the reactants in the graft copolymerization of a vinyl acetate-methyl acrylate mixture onto cellulose. *Journal of Polymer Science Part A: Polymer Chemistry*. **28**(9): 2275-2292.
- Fichman, M. and Hetsroni, G. 2004. Electrokinetic aspects of turbulent drag reduction in surfactant solutions. *Physics of Fluids*. **16**(12): 4346-4352.
- Figueredo, R.C.R. and Sabadini, E. 2003. Firefighting foam stability: the effect of the drag reducer poly(ethylene) oxide. *Colloids and Surfaces A: Physicochemical and Engineering Aspects*. **215**(1-3): 77-86.
- Finkenstadt, V.L. and Willett, J.L. 2005. Reactive extrusion of starch-polyacrylamide graft copolymers: effects of monomer/starch ratio and moisture content. *Macromolecular Chemistry and Physics*. **206**(16): 1648-1652.
- Gadd, G.E. 1971. Reduction of turbulent drag in liquids. *Nature Phys. Science*. **230**:29.
- Gampert, B. and Wagner, P. 1985. The influence of polymer additives on velocity and temperature fields. *Springer-Verlag, New York*.
- Gazquez, M.J., Mantero, J., Bolivar, J.P., Garcia-Tenorio, R. and Galan, F. 2009. Characterization and valorization of norm wastes: application to the TiO₂ production industry. *1st Spanish National Conference on Advances in Materials Recycling and Eco-Energy Madrid*, 79-82.
- Golda, J. 1986. Hydraulic transport of coal in pipes with drag reducing additives. *Chemical Engineering Communications*. **43**(1-3): 53-67.
- Gore, R.A. and Crowe, C.T. 1989a. Effect of particle size on modulating turbulent intensity. *International Journal of Multiphase Flow*. **15**(2): 279-285.
- Gupta K.C. and Khandekar, K. 2002. Graft copolymerization of acrylamide-methylacrylate comonomers onto cellulose using ceric ammonium nitrate. *Journal of Applied Polymer Science*. **86**(10): 2631-2642.
- Gyr, A. and Bewersdorff, H.-W. 1995. *Fluid Mechanics and Its Applications*. Drag reduction of turbulent flows by additives. **32**. Dordrecht: Kluwer Academic Publishers.
- Hadri, F. and Guillou, S. 2010. Drag reduction by surfactant in closed turbulent flow. *International Journal of Engineering Science and Technology*. **2**(12): 6876-6879.
- Hayder, A.A.B. 2006. Studying the effect of polycrylamide on increasing the percentage drag reduction established by using two types of suspended solids in water. *Proceedings of the 11th APCChE Congress 2006, Kuala Lumpur*, 27-30.

Hellsten, M. and Oskarsson, H. 2004. A drag-reducing agent for use in injection water at oil recovery. Application: WO/2004/007630 (Patent).

Hershey, H.C. and Zakin, J.L. 1965. A study of turbulent drag reduction of solutions of high polymers in organic solvents. *Preprint 21B, Symposium on Mechanics of Viscoelastic Fluids, Part II, 58th Meeting, AIChE., Philadelphia.*

Holland, F.A. 1973. *Fluid flow for chemical engineering*. 1st ed. London: Edward Arnold.

Hong, C.H., Zhang, K., Choi, H.J. and Yoon, S.M. 2010. Mechanical degradation of polysaccharide guar gum under turbulent flow. *Journal of Industrial and Engineering Chemistry*. **16**(2): 178-180.

Hoyt, J.W. 1972. A freeman scholar lecture: The effect of additives on fluid friction. *ASME Journal of Basic Engineering*. **94**(2): 258-285.

Hudnall, P.M. 2000. Hydroquinone. *Ullmann's Encyclopedia of Industrial Chemistry*, http://onlinelibrary.wiley.com/doi/10.1002/14356007.a13_499/full, (26 Jun 2010).

Hunston, L. and Reischman, M.M. 1975. The role of polydispersity in the mechanism of drag reduction. *Physics of Fluids*. **18**: 1626.

Hunston, D.L. and Zakin, J.L. 1980. Flow-assisted degradation in dilute polystyrene solutions. *Polymer Engineering and Science*. **20**(7): 517-523.

Inaba, H., Haruki, N. and Horibe, A. 2000. Flow drag and heat transfer reduction of flowing water containing fibrous material in a straight pipe. *International Journal of Thermal Sciences*. **39**(1): 18-29.

Indartono, Y.S., Usui, H., Suzuki, H. and Komoda, Y. 2005. Temperature and diameter effect on hydrodynamic characteristic of surfactant drag-reducing flows. *Korea-Australia Rheology Journal*. **17**(4): 157-164.

Israelachvili, J.N. 1991. *Intermolecular and surface forces*. 2nd ed. London: Academic Press.

Joseph, D.D. 1990. Fluid dynamics of viscoelastic liquids. *Springer Verlag New York Inc. Applied mathematical sciences*. **84**.

Kamel, A. and Shah, S.N. 2009. Effects of salinity and temperature on drag reduction characteristics of polymers in straight circular pipes. *Journal of Petroleum Science and Engineering*. **67**(1-2): 23-33.

Kameneva, M.V., Wu, Z.J., Uraysh, A., Repko, B., Litwak, K.N., Billiar, T.R., Fink, M.P., Simmons, R.L., Griffith, B.P. and Borovetz, H.S. 2004. Blood soluble drag-reducing polymers prevent lethality from hemorrhagic shock in acute animal experiments. *Biorheology*. **41**(1): 53-64.

Kari, F.W. 1989. Toxicology and carcinogenesis studies of hydroquinone (CAS No. 123-31-9) in F344/N rats and B6C3F₁ mice (Gavage Studies). National Toxicology Program Technical Report. U.S. Department of Health and Human Services: TR 366. NIH Publication No. 90-2821.

Kato, K., Vasilets, V.N., Fursa, M.N., Meguro, M., Ikada, Y. and Nakame, K. 1999. Surface oxidation of cellulose fibers by vacuum ultraviolet irradiation. *Journal of Polymer Science Part A: Polymer Chemistry*. **37**(3): 357-361.

Katzbauer, B. 1998. Properties and applications of xanthan gum. *Polymer Degradation and Stability*. **59**(1-3): 81-84.

Kazi, M.S.N., Duffy, G.G. and Chen, X.D. 1999. Heat transfer in the drag reducing regime of wood pulp fibre suspensions. *Chemical Engineering Journal*. **73**(3): 247-253.

Kim, S.C. and Kim, C.B. 1991. A drag reduction in cwm transportation with polymer additives. *The Korean Society of Mechanical Engineers: Journal of Mechanical Science and Technology*. **5**(1): 53-58.

Kim, C.A., Kim, J.T., Lee, K., Choi, H.J. and Jhon, M.S. 2000. Mechanical degradation of dilute polymer solutions under turbulent flow. *Polymer*. **41**(21): 7611-7615.

Kim, C.A., Lim, S.T., Choi, H.J., Sohn, J.-I. and Jhon, M.S. 2002. Characterization of drag reducing guar gum in a rotating disk flow. *Journal of Applied Polymer Science*. **83**(13): 2938-2944.

Kim, N.J., Lee, J.Y., Yoon, S.M., Kim, C.B. and Hur, B.K. 2000. Drag reduction rates and degradation effects in synthetic polymer solution with surfactant additives. *Journal of Industrial and Engineering Chemistry*. **6**(6): 412-418 (online). <http://www.cheric.org/research/tech/periodicals/view.php?seq=280208&jourid=13&mode=ref> (20 July 2010).

Kim, N.J., Kim, S., Lim, S.H., Chen, K. and Chun, W. 2009. Measurement of drag reduction in polymer added turbulent flow. *International Communications in Heat and Mass Transfer*. **36**(10): 1014-1019.

Koichi, N., Mamoru, T., Hideaki, K., Yutaka, Y. and Toshio, M. 2005. Drag reduction with fiber suspensions in water flows. *Transactions of the Japan Society of Mechanical Engineers. B*. **71**(710): 2494-2499.

Kotz, J.C., Treichel, P. and Weaver, G.C. 2006. *Chemistry and chemical reactivity*. 6th ed. USA: Cengage Learning.

Krochak, P.J., Olson, J.A. and Martinez, D.M. 2009. Fiber suspension flow in a tapered channel: The effect of flow/fiber coupling. *International Journal of Multiphase Flow*. **35**(7): 676-688.

- Leonard, A., Gerber, G.B., Stecca, C., Rueff, J., Borba, H., Farmer, P.B., Sram, R.J., Czeizel, A.E. and Kalina, I. 1999. Mutagenicity, carcinogenicity, and teratogenicity of acrylonitrile. *Mutation Research/Reviews in Mutation Research*. **436**(3): 263-283.
- Lester, T.G. 2002. Calculating pressure drops in piping systems. *ASHRAE Journal*. 41-43.
- Li, F., Li, G.Z. and Chen, J.B. 1998. Synergism in mixed zwitterionic-anionic surfactant solutions and the aggregation numbers of the mixed micelles. *Colloids and Surfaces A: Physicochemical and Engineering Aspects*. **145**(1-3): 167-174.
- Lim, S.T., Choi, H.J., Lee, S.Y., So, J.S. and Chan, C.K. 2003. λ -DNA induced turbulent drag reduction and its characteristics. *Macromolecules*. **36**(14): 5348-5354.
- Lin, J.Z., Gao, Z.Y., Zhou, K. and Chan, T.L. 2006. Mathematical modeling of turbulent fiber suspension and successive iteration solution in the channel flow. *Applied Mathematical Modeling*. **30**(9): 1010-1020.
- Logsdon, J.E. and Loke, R.A. 2000. Isopropyl alcohol. *Kirk-Othmer Encyclopedia of Chemical Technology* (online) <http://onlinelibrary.wiley.com/doi/10.1002/0471238961.0919151612150719.a01/abstract> (1 August 2010).
- Lu, B., Zheng, Y., Davis, H.T., Scriven, L.E., Talmon, Y. and Zakin, J.L. 1998. Effect of variations in counterion to surfactant ratio on rheology and microstructures of drag reducing cationic surfactant systems. *Rheologica Acta*. **37**(6): 528-548.
- Luetgen, C.O., Lindsay, J.D. and Stratton, R.A. 1991. Turbulent dispersion in pulp flow: Preliminary results and implications for the mechanisms of fiber-turbulence interactions. Technical Paper. IPST Technical Paper Series. IPST Georgia: 408.
- Lumley, J.L. 1969. Drag reduction by additives. *Annual Review of Fluid Mechanics*. **1**(1): 367-384.
- Lumley, J.L. 1973. Drag reduction in turbulent flow by polymer additives. *Journal of Polymer Science: Macromolecular Reviews*. **7**(1): 263-290.
- Marques, E.F., Regev, O., Khan, A. and Lindman, B. 2003. Self-organization of double-chained and pseudodouble-chained surfactants: counterion and geometry effects. *Advances in Colloid and Interface*. **100-102**: 83-104.
- Marques, E.F., Regev, O., Khan, A., Miguel, M.D.G. and Lindman, B. 1999. Vesicle formation and general phase behavior in the catanionic mixture SDS-DDAB water. The cationic-rich side. *Journal of Physical Chemistry B*. **103**: 8353-8363.
- Matthys, E.F. and Sabersky, R.H. 1982. A method of predicting the 'diameter effect' for heat transfer and friction of drag-reducing fluids. *International Journal of Heat and Mass Transfer*. **25**(9): 1343-1351.

Metzner, A.B. and Park, M.G. 1964. Turbulent flow characteristics of viscoelastic fluids. *Journal of Fluid Mechanics*. **20**(2): 291-303.

Mishra, A., and Bajpai, M. 2005. Synthesis and characterization of polyacrylamide grafted copolymers of Kundoor mucilage. *Journal of Applied Polymer Science*. **98**(3): 1186–1191.

Mishra, A. and Pal, S. 2007. Polyacrylonitrile-grafted Okra mucilage: A renewable reservoir to polymeric materials. *Carbohydrate Polymers*. **68**(1): 95-100.

Mishra, A., Rajani, S., and Gupta, R.K. 2003. P. psyllium-g-polyacrylonitrile: synthesis and characterization. *Colloid and Polymer Science*. **281**(2): 187-189.

Mishra, A., Yadav, A., Pal, S. and Singh, A. 2006. Biodegradable graft copolymers of fenugreek mucilage and polyacrylamide: A renewable reservoir to biomaterials. *Carbohydrate Polymers*. **65**(1): 58-63.

Mohamed, G.E.H. 2000. *Flow control: passive, active and reactive flow management*. Cambridge University Press.

Molerus, O. and Heucke, U. 1999. Pneumatic transport of coarse grained particles in horizontal pipes. *Powder Technology*. **102**(2): 135-150.

Moller, K. 1976. A correlation of pipe friction data for paper pulp suspensions. *Industrial and Engineering Chemistry Process Design and Development*. **15**(1): 16-19.

Mostafa, A.E.S. 2010. Effect of polymer on drag reduction in a sudden enlargement of pipe cross section. *International Journal of Fluid Mechanics Research*. **37**(2): 101-110.

Mostardi, R.A., Thomas, L.C., Greene, H. L., VanEssen, F. and Nokes, R.F. 1978. Suppression of atherosclerosis in rabbits using drag reducing polymers. *Biorheology*. **15**(1): 1-14.

Motier, J.F. and Carreir, A.M. 1989. *Recent studies on polymer drag reduction in commercial pipelines. Drag reduction in fluid flows: Techniques for friction control*. R.L. Sellin and R.T. Moses eds. 197-204. Chichester, England: Ellis Horwood limited Press.

Motier, J.F., Chou, L.C. and Kommareddi, N. 1996. *Proceedings of ASME: Fluids Engineering Division Summer Meeting, SanDiego, CA*. **2**: 229.

Mowla, D. and Naderi, A. 2006. Experimental study of drag reduction by a polymeric additive in slug two-phase flow of crude oil and air in horizontal pipes. *Chemical Engineering Science*. **61**(5): 1549-1554.

Mowla, D. and Naderi, A. 2008. Experimental investigation of drag reduction in annular two-phase flow of oil and air. *Iranian Journal of Science and Technology, Transaction B, Engineering*. **32**(B6): 601-609.

MSDS. 2009. *Thermo Fisher Scientific – Acetone*. Revision Number 3. Material Safety Data Sheet.

MSDS. 2009. *Thermo Fisher Scientific – Isopropanol*. Revision Number 1. Material Safety Data Sheet.

MSDS. 2009. *Thermo Fisher Scientific – Nitric acid (65 – 70%)*. Revision Number 2. Material Safety Data Sheet.

Myska, J. and Mik, V. 2003. Application of drag reducing surfactant in the heating circuit. *Journal of Energy and Buildings*. **35**(8):813–819.

Mysels, K.J. 1949. *Flow of Thickened Fluids*. U.S. Patent 2,492,173.

Myska, J. and Zakin, J.L. 1997. Differences in the flow behaviors of polymeric and cationic surfactant drag-reducing additives. *Industrial and Engineering Chemistry Research*. **36**(12): 5483–5487.

Nakken, T., Tande, M. and Nystrom, B. 2004. Effects of molar mass, concentration and thermodynamic conditions on polymer-induced flow drag reduction. *European Polymer Journal*. **40**(1): 181-186.

Narayan, R. 1990. *Emerging technologies for materials and chemicals from biomass*. Editors Rowell, R.M., Schults, T.P. and Narayan, R. ACS Symp. Ser. 476. Washington, DC: American Chemical Society.

Nikuradse, J. 1932. Laws of turbulent flow in smooth pipes (English translation), VDI Forschungsheft vol. 356. NASA TT F-10: p.359.

Nikuradse, J. 1933. Stromungsgesetze in rauhen rohren, VDI Forschungsheft, vol. 361 (English translation: Laws of flow in rough pipes). Techh. Rep. NACA Technical Memorandum 1292. Washington, D.C, USA: National Advisory Commission for Aeronautics.

Nijis, L. 1995. New generation drag reducer. *The 2nd International Pipeline Technology Conference, Ostend, Belgium*. Elsevier B.V.

Onishi, Y., Butler, G.B. and Hogen-Esch, T.E. 2004. 1,2-propanediol-cellulose-acrylamide Graft Copolymers. *Journal of Applied Polymer Science*. **92**(5): 3022-3029.

Ophardt, C.E. 2003. *Polymers. Introduction to the study of chemistry*. Virtual ChemBook. Elmhurst College.

Orlandi, P. 1995. A tentative approach to the direct simulation of drag reduction by polymers. *Journal of Non-Newtonian Fluid Mechanics*. **60**(2-3): 277–301.

Oujai, S., Hodzic, A. and Shanks, R.A. 2004. Morphological and grafting modifications of natural cellulose fibers. *Journal of Applied Polymer Science*. **94**(6): 2456-2465.

Philips, C. 2006. Sustainable Development Report. USA: ConocoPhillips.

Podolsak, A.K., Tiu, C., Saeki, T. and Usui, H. 1996. Rheological properties and some applications for rhaman and xanthan gum solutions. *Polymer International*. **40**(3): 155-167.

Prasetyo, I. 2002. DRA increases Indonesia pipeline capacity to allow accelerated field production. (Pipelines). (drag-reducing agent). *The Oil and Gas Journal* (online). <http://www.accessmylibrary.com/article-1G1-92806452/dra-increases-indonesia-pipeline.html> (6 March 2010).

Radin, I., Zakin, J.L. and Patterson, G.K. 1975. Drag reduction in solid-fluid systems. *AIChE Journal*. **21**(2): 358-371.

Ragsdale, R. 2007. Chemical additive enables Alyeska Pipeline Service Co. to achieve huge cost savings. *30 Strong: With DRA pipeline less of a drag* (online). <http://www.scribd.com/doc/43951206/30-Strong> (16 June 2010).

Rashidi, M. and Banerjee, S. 1990. The effect of boundary conditions and shear rate on streak formation and break down in turbulent channel flows. *Physics of Fluids A2: Fluid Dynamics*. **2**(10): 1827-1831.

Reynolds, O. 1883. An experimental investigation of the circumstances which determine whether the motion of water shall be direct or sinuous, and of the law of resistance in parallel channels. *Philosophical Transactions of the Royal Society of London*, **174**: 935-982.

Robert, B. 2002. A simple model for drag reduction.

Salkar, R.A., Mukesh, D.S., Samant, D. and Manohar, C. 1998. Mechanism of micelle to vesicle transition in cationic-anionic surfactant mixtures. *Langmuir*. **14**(14): 3778-3782.

Savins, J.G. 1963. Drag reduction characteristics of solutions of macromolecules in turbulent pipe flow. *Symposium on Non-Newtonian Fluid Mechanics, 56th Annual A.I.Ch.E. Meeting, Houston, Texas*.

Savins, J.G. 1967. A stress-controlled drag-reduction phenomenon. *Rheologica Acta*. **6**(4): 323-330.

Schreck, S. and Kleis, S.J. 1993. Modification of grid-generated turbulence by solid particles. *Journal of Fluid Mechanics*. **249**: 665-688.

Schubert, B.A., Kaler, E.W. and Wagner, N.J. 2003. The microstructure and rheology of mixed cationic/anionic wormlike micelles. *Langmuir*. **19**: 4079-4089.

Sellin, R.H.J., Hoyt, J.W., Pollert, J. and Scrivener, O. 1982. The effect of drag-reducing additives on fluid flows and their industrial applications: Part 2. Present applications and future proposals. *Journal of Hydraulic Research*. **20**(3): 235-292.

Shaqfeh, E.S.G. and Fredrickson, G.H. 1990. The hydrodynamic stress in a suspension of rods. *Physics of Fluids A: Fluid Dynamics*. **2**(1): 7–24.

Sharma, R.S., Seshadri, V. and Malhotra, R.C. 1979. Drag reduction by centre-line injection of fibres in a polymeric solution. *The Chemical Engineering Journal*. **18**(1): 73-79.

Shaver, R.G. and Merrill, E.W. 1959. Turbulent flow of pseudoplastic polymer solutions in straight cylindrical tubes. *AIChE. Journal*. **5**(2): 181-188.

Shenoy, A.V. 1984. A review on drag reduction with special reference to micellar systems. *Colloid and Polymer Science*. **262**(4): 319-337.

Sher, I. and Hetsroni, G. 2008. A mechanistic model of turbulent drag reduction by additives. *Chemical Engineering Science*. **63**(7): 1771-1778.

Singh, R.P., Karmakar, G.P., Rath, S.K., Karmakar, N.C., Pandey, S.R., Tripathy, T., Panda, J., Kanan, K., Jain, S.K. and Lan, N.T. 2000. Biodegradable drag reducing agents and flocculants based on polysaccharides: materials and applications. *Polymer Engineering and Science*. **40**(1): 46-60.

Singh, R.P., Pal, S., Krishnamoorthy, S., Adhikary, P. and Ali, Sk.A. 2009. High-technology materials based on modified polysaccharides. *Pure and Applied Chemistry*. **81**(3): 525-547.

Singh, R.P., Singh, J., Deshmukh, S.R. and Kumar, A. 1985. The effect of grafted and ungrafted guar gum on turbulent flow of water and on hydraulic conductivity of soil. *Influence Polym. Addit. Velocity Temp. Fields, Symp.*, 131-139.

Sohn, J.-I., Kim, C.A., Choi, H.J., Jhon, M.S. 2001. Drag-reduction effectiveness of xanthan gum in a rotating disk apparatus. *Carbohydrate Polymers*. **45**(1): 61-68.

Sullivan, P., Nelson, E.B., Anderson, V. and Hughes, T. 2007. *Oilfield applications of giant micelles*. Editors Zana, R. and Kaler, E.W. Surfactant science series (Giant micelles: properties and applications). **140**: 453-472. Boca Raton: CRC Press.

Teramoto, Y. and Nishio, Y. 2003. Cellulose diacetate-graft-poly(lactic acid)s: synthesis of wide-ranging compositions and their thermal and mechanical properties. *Polymer*. **44**(9): 2701-2709.

Toms, B.A. 1949. Observation on the flow of linear polymer solutions through straight tubes at large Reynold numbers. *In Proc. Intl. Rheological Congress, Holland*, 135-141.

Toonder, J.M.J.D., Hulsen, M.A., Kuiken, G.D.C. and Nieuwstadt, F.T.M. 1997. Drag reduction by polymer additives in a turbulent pipe flow: numerical and laboratory experiments. *Journal of Fluid Mechanics*. **337**: 193-231.

- Toorman, E.A. 2002. Modelling of turbulent flow with suspended cohesive sediment, in Winterwerp, J.C. and Kranenburg, C. (Ed.) (2002). Fine sediment dynamics in the marine environment. *Proceedings in Marine Science*, **5**: 155-169. Amsterdam: Elsevier Science.
- Turabi, E., Sumnu, G. and Sahin, S. 2008. Rheological properties and quality of rice cakes formulated with different gums and an emulsifier blend. *Food Hydrocolloids*. **22**(2): 305-312.
- Unthank, J.L., Lalka, S.G., Nixon, J.C. and Sawchuk, A.P. 1992. Improvement of flow through arterial stenoses by drag reducing agents. *Journal of Surgical Research*. **53**(6): 625-630.
- Vanapalli, S.A., Islam, M.T. and Solomon, M.J. 2005. Scission-induced bounds on maximum polymer drag reduction in turbulent flow. *Physics of Fluids*. **17**(9): 095108-095118.
- Vanoni, V.A. 1946. Transportation of suspended sediment by water. *Trans. ASCE*. **111**(Paper 2267): 67-133.
- Vaseleski, R.C. and Metzner, A.B. 1974. Drag reduction in the turbulent flow of fiber suspensions. *AIChE Journal*. **20**(2): 301-306.
- Virk, P.S., Merrill, E.W., Mickley, H.S, Smith, K.A. and Mollo-Christensen, E.L. 1967. The Toms phenomena: turbulent pipe flow of dilute polymer solution. *Journal of Fluid Mechanics*. **30**(02): 305-328.
- Vlachogiannis, M., Liberatore, M.W., McHugh, A.J., and Hanratty, T.J. 2003. Effectiveness of a drag reducing polymer: relation to molecular weight distribution and structuring. *Physics of Fluids*. **15**(12):3786-3794.
- Wade, J.H.T. and Kumar, P. 1972. Electronic microscope studies of polymer degradation. *Journal of Hydronautics* **6**(1): 40-45.
- Wang, Z.Y., Larsen, P., Nestmann, F. and Dittrich, A. 1998. Resistance and drag reduction of flows of clay suspensions. *Journal of Hydraulic Engineering*. **124**(1): 41-49.
- Warhaft, Z. 1997. *Transition and Turbulence*. The Engine and the Atmosphere: An Introduction to Engineering. Cambridge University Press.
- Warholic, M.D., Massah, H. and Hanratty, T.J. 1999. Influence of drag-reducing polymers on turbulence: effects of Reynolds number, concentration and mixing. *Experiment in Fluids*. **27**(5): 461-472.
- White, D.A. 1970. Preliminary experiments on polymer degradation in a turbulent shear field. *Chemical Engineering Science*. **25**(8): 1255-1258.

- Wul, G., Xu, J. and Miles, J. 1998. Polymer drag reduction in large diameter coal log pipeline. *Proceedings of the International Technical Conference on Coal Utilization and Fuel Systems*. **23**: 889-900.
- Wyatt, N.B., Gunther, C.M. and Liberatore, M.W. 2011. Drag reduction effectiveness of dilute and entangled xanthan in turbulent pipe flow. *Journal of Non-Newtonian Fluid Mechanics*. **166**(1-2): 25-31.
- Xueming, S., Jianzhong, L., Tao, W. and Yulin, L. 2002. Experimental research on drag reduction by polymer additives in a turbulent pipe flow. *The Canadian Journal of Chemical Engineering*. **80**(2): 293-298.
- Zagarola, M.V. and Smits, A.J. 1998. Mean-flow scaling of turbulent pipe flow. *Journal of Fluid Mechanics*. **373**: 33-79.
- Zakin, J.L. and Lui, H.L. 1983. Variables affecting drag reduction by nonionic surfactant additives. *Chemical Engineering Communications*. **23**(1-3): 77-88.
- Zakin, J.L., Myska, J. and Chara, Z. 1996. New limiting drag reduction and velocity profile asymptotes for nonpolymeric additives systems. *AIChE Journal*. **42**(12): 3544-3546.
- Zakin, J.L., Poreh, M., Brosh, A. and Warshavsky, M. 1971. *Chem. Eng. Prog. Sym. Ser.* **67**: 85-89.
- Zakin, J.L., Zhang, Y. and Ge, W. 2007. Drag Reduction by surfactant giant micelles. Surfactant science series (Giant micelles: properties and applications). Editors Zana, R. and Kaler, E.W. **140**: 489. Boca Raton: CRC Press.
- Zhang, Y. 2005. *Correlations among surfactant drag reduction, additive chemical structures, rheological properties and microstructures in water and water/co-solvent systems*. Ph.D. Thesis. The Ohio State University.
- Zhu, L. and Peskin, C.S. 2007. Drag of a flexible fiber in a 2D moving viscous fluid. *Computers and Fluids*. **36**(2): 398-406.

APPENDIX A1

AMOUNT OF MUCILAGE IN TRANSPORTING LIQUIDS

Table 3.9: Amount of water soluble mucilage in transporting water

Concentration, ppm	Volume of Water, m ³	Amount of water soluble mucilage, g
50	0.21	10.5
100	0.21	21.0
150	0.21	31.5
200	0.21	42.0
400	0.21	84.0
600	0.21	126.0
800	0.21	168.0
1000	0.21	210.0

Sample calculation for 50ppm:

Volume of water: 0.21m³

Weight of water = Density of water x Volume of water

$$= 1000\text{kg/m}^3 \times 0.21\text{m}^3$$

$$= 210\text{kg}$$

$$= 210000\text{g}$$

$$\frac{1}{1000000} = \frac{X}{210000\text{g}}$$

$$X = \frac{210000}{1000000} = 0.21\text{g}$$

Therefore, 1ppm = 0.21g mucilage

So, for 50ppm = 0.21 x 50 = 10.5g of water soluble mucilage

Table 3.10: Amount of grafted mucilage in transporting diesel

Concentration, ppm	Volume of Diesel, m ³	Amount of grafted mucilage, g
50	0.04	1.67
100	0.04	3.34
150	0.04	5.02
200	0.04	6.68
400	0.04	13.36
600	0.04	20.04
800	0.04	26.72
1000	0.04	33.4

Sample calculation for 50ppm:

Volume of diesel: 0.04m^3

Weight of diesel = Density of diesel x Volume of diesel

$$= 836.25\text{kg/m}^3 \times 0.04\text{m}^3$$

$$= 33.45\text{kg}$$

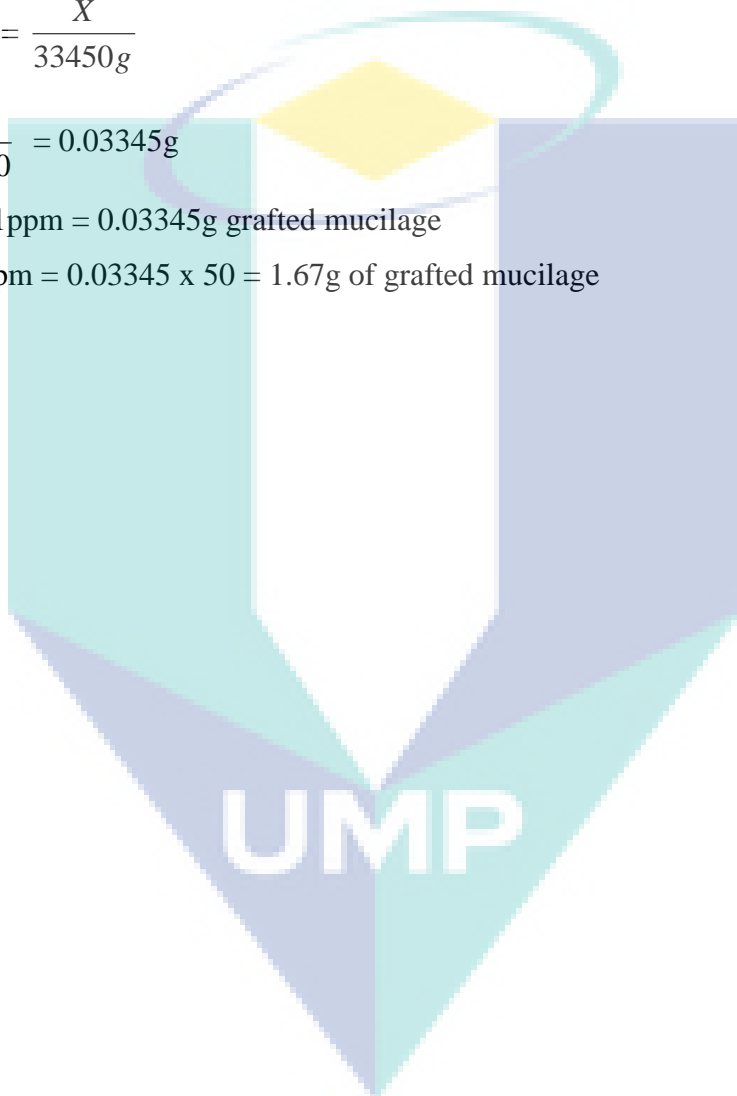
$$= 33450\text{g}$$

$$\frac{1}{1000000\text{g}} = \frac{X}{33450\text{g}}$$

$$X = \frac{33450}{1000000} = 0.03345\text{g}$$

Therefore, 1ppm = 0.03345g grafted mucilage

So, for 50ppm = $0.03345 \times 50 = 1.67\text{g}$ of grafted mucilage



APPENDIX A2

AMOUNT OF RED GYPSUM IN TRANSPORTING LIQUIDS

Table 3.11: Amount of red gypsum in transporting water

Concentration, ppm	Volume of Water, m ³	Amount of red gypsum, g
50	0.21	10.5
100	0.21	21.0
150	0.21	31.5
200	0.21	42.0
400	0.21	84.0
600	0.21	126.0
800	0.21	168.0
1000	0.21	210.0

Sample calculation for 50ppm:

Volume of water: 0.21m³

Weight of water = Density of water x Volume of water

$$= 1000\text{kg/m}^3 \times 0.21\text{m}^3$$

$$= 210\text{kg}$$

$$= 210000\text{g}$$

$$\frac{1}{1000000\text{g}} = \frac{X}{210000\text{g}}$$

$$X = \frac{210000}{1000000} = 0.21\text{g}$$

Therefore, 1ppm = 0.21g red gypsum

So, for 50ppm = 0.21 x 50 = 10.5g of red gypsum

Table 3.12: Amount of red gypsum in transporting diesel

Concentration, ppm	Volume of Diesel, m ³	Amount of red gypsum, g
50	0.04	1.67
100	0.04	3.34
150	0.04	5.02
200	0.04	6.68
400	0.04	13.36
600	0.04	20.04
800	0.04	26.72
1000	0.04	33.4

Sample calculation for 50ppm:

Volume of diesel: 0.04m^3

Weight of diesel = Density of diesel x Volume of diesel

$$= 836.25\text{kg/m}^3 \times 0.04\text{m}^3$$

$$= 33.45\text{kg}$$

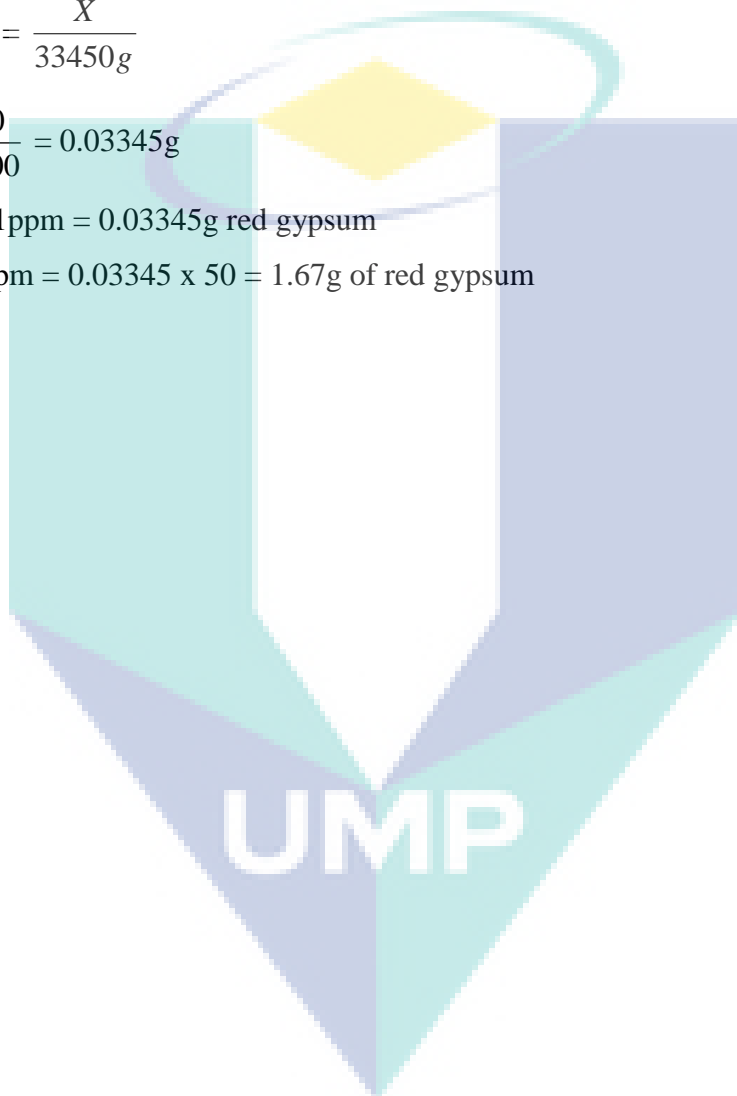
$$= 33450\text{g}$$

$$\frac{1}{1000000\text{g}} = \frac{X}{33450\text{g}}$$

$$X = \frac{33450}{1000000} = 0.03345\text{g}$$

Therefore, 1ppm = 0.03345g red gypsum

So, for 50ppm = $0.03345 \times 50 = 1.67\text{g}$ of red gypsum



APPENDIX B1

SYSTEM VERIFICATION IN TRANSPORTING WATER

Table 4.2: System verification of pipe with ID 0.0381m in transporting water before DRA addition

Flow rate(Q), m ³ /h	Flow rate(Q), m ³ /s	Pipe diameter (D), m	Area (A), m ²	Velocity (v =Q/A), m/s	Length (L), m	L/D
10.5	0.002917	0.0381	0.001141	2.557244	0.5	13.1
10.5	0.002917	0.0381	0.001141	2.557244	1.0	26.2
10.5	0.002917	0.0381	0.001141	2.557244	1.5	39.4
10.5	0.002917	0.0381	0.001141	2.557244	2.0	52.5
10.0	0.002778	0.0381	0.001141	2.435471	0.5	13.1
10.0	0.002778	0.0381	0.001141	2.435471	1.0	26.2
10.0	0.002778	0.0381	0.001141	2.435471	1.5	39.4
10.0	0.002778	0.0381	0.001141	2.435471	2.0	52.5
9.5	0.002639	0.0381	0.001141	2.313697	0.5	13.1
9.5	0.002639	0.0381	0.001141	2.313697	1.0	26.2
9.5	0.002639	0.0381	0.001141	2.313697	1.5	39.4
9.5	0.002639	0.0381	0.001141	2.313697	2.0	52.5
9.0	0.002500	0.0381	0.001141	2.191924	0.5	13.1
9.0	0.002500	0.0381	0.001141	2.191924	1.0	26.2
9.0	0.002500	0.0381	0.001141	2.191924	1.5	39.4
9.0	0.002500	0.0381	0.001141	2.191924	2.0	52.5

Pressure drop (ΔP), kg/(ms ²)	Wall shear stress (τ_w), kg/(ms ²)	Fanning friction factor (C_f)	Reynolds number, Re	Blasius	Virk	Laminar flow
	$\tau_w = D\Delta P/4L$	$C_f = 2\tau_w / \rho v^2$		$f = 0.0791Re^{-0.25}$	$f = 0.59Re^{-0.58}$	$f = 16/Re$
784	14.94	0.004567690	97431.00	0.004477	0.000754	0.000164
1609	15.33	0.004687126	97431.00	0.004477	0.000754	0.000164
2503	15.89	0.004860939	97431.00	0.004477	0.000754	0.000164
3291	15.67	0.004793453	97431.00	0.004477	0.000754	0.000164
695	13.24	0.004464203	92791.43	0.004532	0.000776	0.000172
1443	13.74	0.004634421	92791.43	0.004532	0.000776	0.000172
2206	14.01	0.004723277	92791.43	0.004532	0.000776	0.000172
3089	14.71	0.004960405	92791.43	0.004532	0.000776	0.000172
611	11.64	0.004348637	88151.86	0.004591	0.000799	0.000182
1294	12.33	0.004604858	88151.86	0.004591	0.000799	0.000182
2070	13.14	0.004910900	88151.86	0.004591	0.000799	0.000182
2791	13.29	0.004966058	88151.86	0.004591	0.000799	0.000182
521	9.93	0.004131539	83512.29	0.004653	0.000825	0.000192
1114	10.61	0.004417020	83512.29	0.004653	0.000825	0.000192
1792	11.38	0.004736864	83512.29	0.004653	0.000825	0.000192
2458	11.71	0.004872996	83512.29	0.004653	0.000825	0.000192

Flow rate(Q), m ³ /h	Flow rate(Q), m ³ /s	Pipe diameter (D), m	Area (A), m ²	Velocity (v =Q/A), m/s	Length (L), m	L/D
8.5	0.002361	0.0381	0.001141	2.070150	0.5	13.1
8.5	0.002361	0.0381	0.001141	2.070150	1.0	26.2
8.5	0.002361	0.0381	0.001141	2.070150	1.5	39.4
8.5	0.002361	0.0381	0.001141	2.070150	2.0	52.5
8.0	0.002222	0.0381	0.001141	1.948377	0.5	13.1
8.0	0.002222	0.0381	0.001141	1.948377	1.0	26.2
8.0	0.002222	0.0381	0.001141	1.948377	1.5	39.4
8.0	0.002222	0.0381	0.001141	1.948377	2.0	52.5
7.5	0.002083	0.0381	0.001141	1.826603	0.5	13.1
7.5	0.002083	0.0381	0.001141	1.826603	1.0	26.2
7.5	0.002083	0.0381	0.001141	1.826603	1.5	39.4
7.5	0.002083	0.0381	0.001141	1.826603	2.0	52.5

Pressure drop (ΔP), kg/(ms ²)	Wall shear stress (τ_w), kg/(ms ²)	Fanning friction factor (C_f)	Reynolds number, Re	Blasius	Virk	Laminar flow
	$\tau_w = D\Delta P/4L$	$C_f = 2\tau_w / \rho v^2$		$f = 0.0791\text{Re}^{-0.25}$	$f = 0.59\text{Re}^{-0.58}$	$f = 16/\text{Re}$
500	9.53	0.004445200	78872.72	0.004720	0.000852	0.000203
1016	9.68	0.004516323	78872.72	0.004720	0.000852	0.000203
1563	9.93	0.004631899	78872.72	0.004720	0.000852	0.000203
2096	9.98	0.004658570	78872.72	0.004720	0.000852	0.000203
489	9.32	0.004907814	74233.15	0.004792	0.000883	0.000216
992	9.45	0.004978069	74233.15	0.004792	0.000883	0.000216
1408	8.94	0.004710431	74233.15	0.004792	0.000883	0.000216
1965	9.36	0.004930396	74233.15	0.004792	0.000883	0.000216
400	7.62	0.004567690	69593.57	0.004870	0.000917	0.000230
873	8.32	0.004984492	69593.57	0.004870	0.000917	0.000230
1291	8.20	0.004914073	69593.57	0.004870	0.000917	0.000230
1657	7.89	0.004730414	69593.57	0.004870	0.000917	0.000230

Table 4.3: System verification of pipe with ID 0.0254m in transporting water before DRA addition

Flow rate(Q), m ³ /h	Flow rate(Q), m ³ /s	Pipe diameter (D), m	Area (A), m ²	Velocity (v =Q/A), m/s	Length (L), m	L/D
8.0	0.002222	0.0254	0.000507	4.383847	0.5	19.7
8.0	0.002222	0.0254	0.000507	4.383847	1.0	39.4
8.0	0.002222	0.0254	0.000507	4.383847	1.5	59.1
8.0	0.002222	0.0254	0.000507	4.383847	2.0	78.7
7.5	0.002083	0.0254	0.000507	4.109857	0.5	19.7
7.5	0.002083	0.0254	0.000507	4.109857	1.0	39.4
7.5	0.002083	0.0254	0.000507	4.109857	1.5	59.1
7.5	0.002083	0.0254	0.000507	4.109857	2.0	78.7
7.0	0.001944	0.0254	0.000507	3.835866	0.5	19.7
7.0	0.001944	0.0254	0.000507	3.835866	1.0	39.4
7.0	0.001944	0.0254	0.000507	3.835866	1.5	59.1
7.0	0.001944	0.0254	0.000507	3.835866	2.0	78.7
6.5	0.001806	0.0254	0.000507	3.561876	0.5	19.7
6.5	0.001806	0.0254	0.000507	3.561876	1.0	39.4
6.5	0.001806	0.0254	0.000507	3.561876	1.5	59.1
6.5	0.001806	0.0254	0.000507	3.561876	2.0	78.7

Pressure drop (ΔP), kg/(ms ²)	Wall shear stress (τ_w), kg/(ms ²)	Fanning friction factor (C_f)	Reynolds number, Re	Blasius	Virk	Laminar flow
	$\tau_w = D\Delta P/4L$	$C_f = 2\tau_w / \rho v^2$		$f = 0.0791Re^{-0.25}$	$f = 0.59Re^{-0.58}$	$f = 16/Re$
3038	38.58	0.004015232	111349.72	0.004330	0.000698	0.000144
6317	40.11	0.004174494	111349.72	0.004330	0.000698	0.000144
9664	40.91	0.004257538	111349.72	0.004330	0.000698	0.000144
14229	45.18	0.004701509	111349.72	0.004330	0.000698	0.000144
2996	38.05	0.004505284	104390.36	0.004401	0.000724	0.000153
6003	38.12	0.004513555	104390.36	0.004401	0.000724	0.000153
9072	38.40	0.004547389	104390.36	0.004401	0.000724	0.000153
12210	38.77	0.004590247	104390.36	0.004401	0.000724	0.000153
2601	33.03	0.004490008	97431.00	0.004477	0.000754	0.000164
5451	34.61	0.004704928	97431.00	0.004477	0.000754	0.000164
8532	36.12	0.004909490	97431.00	0.004477	0.000754	0.000164
10300	32.70	0.004445126	97431.00	0.004477	0.000754	0.000164
2201	27.95	0.004406525	90471.65	0.004561	0.000787	0.000177
4884	31.01	0.004889020	90471.65	0.004561	0.000787	0.000177
7110	30.10	0.004744872	90471.65	0.004561	0.000787	0.000177
9036	28.69	0.004522644	90471.65	0.004561	0.000787	0.000177

Flow rate(Q), m ³ /h	Flow rate(Q), m ³ /s	Pipe diameter (D), m	Area (A), m ²	Velocity (v =Q/A), m/s	Length (L), m	L/D
6.0	0.001667	0.0254	0.000507	3.287885	0.5	19.7
6.0	0.001667	0.0254	0.000507	3.287885	1.0	39.4
6.0	0.001667	0.0254	0.000507	3.287885	1.5	59.1
6.0	0.001667	0.0254	0.000507	3.287885	2.0	78.7
5.5	0.001528	0.0254	0.000507	3.013895	0.5	19.7
5.5	0.001528	0.0254	0.000507	3.013895	1.0	39.4
5.5	0.001528	0.0254	0.000507	3.013895	1.5	59.1
5.5	0.001528	0.0254	0.000507	3.013895	2.0	78.7
5.0	0.001389	0.0254	0.000507	2.739904	0.5	19.7
5.0	0.001389	0.0254	0.000507	2.739904	1.0	39.4
5.0	0.001389	0.0254	0.000507	2.739904	1.5	59.1
5.0	0.001389	0.0254	0.000507	2.739904	2.0	78.7

Pressure drop (ΔP), kg/(ms ²)	Wall shear stress (τ_w), kg/(ms ²)	Fanning friction factor (C_f)	Reynolds number, Re	Blasius	Virk	Laminar flow
	$\tau_w = D\Delta P/4L$	$C_f = 2\tau_w / \rho v^2$		$f = 0.0791Re^{-0.25}$	$f = 0.59Re^{-0.58}$	$f = 16/Re$
2010	25.53	0.004722766	83512.29	0.004653	0.000825	0.000192
4083	25.93	0.004796780	83512.29	0.004653	0.000825	0.000192
6147	26.02	0.004814402	83512.29	0.004653	0.000825	0.000192
7651	24.29	0.004494264	83512.29	0.004653	0.000825	0.000192
1685	21.40	0.004711698	76552.93	0.004755	0.000867	0.000209
2964	18.82	0.004144057	76552.93	0.004755	0.000867	0.000209
4513	19.11	0.004206507	76552.93	0.004755	0.000867	0.000209
6487	20.60	0.004534834	76552.93	0.004755	0.000867	0.000209
1255	15.94	0.004246260	69593.57	0.004870	0.000917	0.000230
2439	15.49	0.004126147	69593.57	0.004870	0.000917	0.000230
4001	16.94	0.004512427	69593.57	0.004870	0.000917	0.000230
5763	18.30	0.004874741	69593.57	0.004870	0.000917	0.000230

Table 4.4: System verification of pipe with ID 0.0127m in transporting water before DRA addition

Flow rate(Q), m ³ /h	Flow rate(Q), m ³ /s	Pipe diameter (D), m	Area (A), m ²	Velocity (v =Q/A), m/s	Length (L), m	L/D
2.4	0.000667	0.0127	0.000127	5.260617	0.5	39.4
2.4	0.000667	0.0127	0.000127	5.260617	1.0	78.7
2.4	0.000667	0.0127	0.000127	5.260617	1.5	118.1
2.4	0.000667	0.0127	0.000127	5.260617	2.0	157.5
2.2	0.000611	0.0127	0.000127	4.822232	0.5	39.4
2.2	0.000611	0.0127	0.000127	4.822232	1.0	78.7
2.2	0.000611	0.0127	0.000127	4.822232	1.5	118.1
2.2	0.000611	0.0127	0.000127	4.822232	2.0	157.5
2.0	0.000556	0.0127	0.000127	4.383847	0.5	39.4
2.0	0.000556	0.0127	0.000127	4.383847	1.0	78.7
2.0	0.000556	0.0127	0.000127	4.383847	1.5	118.1
2.0	0.000556	0.0127	0.000127	4.383847	2.0	157.5
1.8	0.000500	0.0127	0.000127	3.945462	0.5	39.4
1.8	0.000500	0.0127	0.000127	3.945462	1.0	78.7
1.8	0.000500	0.0127	0.000127	3.945462	1.5	118.1
1.8	0.000500	0.0127	0.000127	3.945462	2.0	157.5

Pressure drop (ΔP), kg/(ms ²)	Wall shear stress (τ_w), kg/(ms ²)	Fanning friction factor (C_f)	Reynolds number, Re	Blasius	Virk	Laminar flow
	$\tau_w = D\Delta P/4L$	$C_f = 2\tau_w / \rho v^2$		$f = 0.0791Re^{-0.25}$	$f = 0.59Re^{-0.58}$	$f = 16/Re$
10961	69.60	0.005030146	66809.83	0.004920	0.000939	0.000239
20507	65.11	0.004705465	66809.83	0.004920	0.000939	0.000239
28123	59.53	0.004302004	66809.83	0.004920	0.000939	0.000239
37466	59.48	0.004298409	66809.83	0.004920	0.000939	0.000239
9847	62.53	0.005377885	61242.34	0.005028	0.000987	0.000261
17588	55.84	0.004802795	61242.34	0.005028	0.000987	0.000261
23009	48.70	0.004188746	61242.34	0.005028	0.000987	0.000261
30203	47.95	0.004123800	61242.34	0.005028	0.000987	0.000261
7125	45.24	0.004708448	55674.86	0.005149	0.001043	0.000287
15857	50.35	0.005239429	55674.86	0.005149	0.001043	0.000287
20707	43.83	0.004561302	55674.86	0.005149	0.001043	0.000287
28674	45.52	0.004737194	55674.86	0.005149	0.001043	0.000287
5639	35.81	0.004600552	50107.37	0.005287	0.001109	0.000319
13672	43.41	0.005577119	50107.37	0.005287	0.001109	0.000319
16833	35.63	0.004577709	50107.37	0.005287	0.001109	0.000319
22195	35.23	0.004526922	50107.37	0.005287	0.001109	0.000319

Flow rate(Q), m ³ /h	Flow rate(Q), m ³ /s	Pipe diameter (D), m	Area (A), m ²	Velocity (v =Q/A), m/s	Length (L), m	L/D
1.6	0.000444	0.0127	0.000127	3.507078	0.5	39.4
1.6	0.000444	0.0127	0.000127	3.507078	1.0	78.7
1.6	0.000444	0.0127	0.000127	3.507078	1.5	118.1
1.6	0.000444	0.0127	0.000127	3.507078	2.0	157.5
1.4	0.000389	0.0127	0.000127	3.068693	0.5	39.4
1.4	0.000389	0.0127	0.000127	3.068693	1.0	78.7
1.4	0.000389	0.0127	0.000127	3.068693	1.5	118.1
1.4	0.000389	0.0127	0.000127	3.068693	2.0	157.5
1.2	0.000333	0.0127	0.000127	2.630308	0.5	39.4
1.2	0.000333	0.0127	0.000127	2.630308	1.0	78.7
1.2	0.000333	0.0127	0.000127	2.630308	1.5	118.1
1.2	0.000333	0.0127	0.000127	2.630308	2.0	157.5

Pressure drop (ΔP), kg/(ms ²)	Wall shear stress (τ_w), kg/(ms ²)	Fanning friction factor (C_f)	Reynolds number, Re	Blasius	Virk	Laminar flow
	$\tau_w = D\Delta P/4L$	$C_f = 2\tau_w / \rho v^2$		$f = 0.0791\text{Re}^{-0.25}$	$f = 0.59\text{Re}^{-0.58}$	$f = 16/\text{Re}$
5018	31.86	0.005181358	44539.89	0.005445	0.001187	0.000359
10856	34.47	0.005604705	44539.89	0.005445	0.001187	0.000359
14555	30.81	0.005009610	44539.89	0.005445	0.001187	0.000359
19047	30.24	0.004916766	44539.89	0.005445	0.001187	0.000359
4730	30.04	0.006379079	38972.40	0.005630	0.001283	0.000411
8226	26.12	0.005546967	38972.40	0.005630	0.001283	0.000411
12177	25.77	0.005474140	38972.40	0.005630	0.001283	0.000411
15693	24.91	0.005291062	38972.40	0.005630	0.001283	0.000411
3006	19.09	0.005517971	33404.92	0.005851	0.001403	0.000479
5641	17.91	0.005177457	33404.92	0.005851	0.001403	0.000479
8739	18.50	0.005347255	33404.92	0.005851	0.001403	0.000479
12667	20.11	0.005813052	33404.92	0.005851	0.001403	0.000479

APPENDIX B2

SYSTEM VERIFICATION IN TRANSPORTING DIESEL

Table 4.5: System verification of pipe with ID 0.0381m in transporting diesel before DRA addition

Flow rate(Q), m ³ /h	Flow rate(Q), m ³ /s	Pipe diameter (D), m	Area (A), m ²	Velocity (v =Q/A), m/s	Length (L), m	L/D
10.5	0.002917	0.0381	0.001141	2.557244	0.5	13.1
10.5	0.002917	0.0381	0.001141	2.557244	1.0	26.2
10.5	0.002917	0.0381	0.001141	2.557244	1.5	39.4
10.5	0.002917	0.0381	0.001141	2.557244	2.0	52.5
10.0	0.002778	0.0381	0.001141	2.435471	0.5	13.1
10.0	0.002778	0.0381	0.001141	2.435471	1.0	26.2
10.0	0.002778	0.0381	0.001141	2.435471	1.5	39.4
10.0	0.002778	0.0381	0.001141	2.435471	2.0	52.5
9.5	0.002639	0.0381	0.001141	2.313697	0.5	13.1
9.5	0.002639	0.0381	0.001141	2.313697	1.0	26.2
9.5	0.002639	0.0381	0.001141	2.313697	1.5	39.4
9.5	0.002639	0.0381	0.001141	2.313697	2.0	52.5
9.0	0.002500	0.0381	0.001141	2.191924	0.5	13.1
9.0	0.002500	0.0381	0.001141	2.191924	1.0	26.2
9.0	0.002500	0.0381	0.001141	2.191924	1.5	39.4
9.0	0.002500	0.0381	0.001141	2.191924	2.0	52.5

Pressure drop (ΔP), kg/(ms ²)	Wall shear stress (τ_w), kg/(ms ²)	Fanning friction factor (C_f)	Reynolds number, Re	Blasius	Virk	Laminar flow
	$\tau_w = D\Delta P/4L$	$C_f = 2\tau_w / \rho v^2$		$f = 0.0791Re^{-0.25}$	$f = 0.59Re^{-0.58}$	$f = 16/Re$
625	11.91	0.004354361	27014.81	0.006170	0.001587	0.000592
1272	12.12	0.004430998	27014.81	0.006170	0.001587	0.000592
1969	12.50	0.004572660	27014.81	0.006170	0.001587	0.000592
2786	13.27	0.004852500	27014.81	0.006170	0.001587	0.000592
573	10.92	0.004401267	25728.39	0.006246	0.001632	0.000622
1154	10.99	0.004431991	25728.39	0.006246	0.001632	0.000622
1810	11.49	0.004634260	25728.39	0.006246	0.001632	0.000622
2418	11.52	0.004643221	25728.39	0.006246	0.001632	0.000622
526	10.02	0.004476737	24441.97	0.006326	0.001682	0.000655
1093	10.41	0.004651211	24441.97	0.006326	0.001682	0.000655
1647	10.46	0.004672488	24441.97	0.006326	0.001682	0.000655
2209	10.52	0.004700148	24441.97	0.006326	0.001682	0.000655
482	9.18	0.004570725	23155.55	0.006412	0.001735	0.000691
986	9.39	0.004675036	23155.55	0.006412	0.001735	0.000691
1485	9.43	0.004694002	23155.55	0.006412	0.001735	0.000691
2003	9.54	0.004748528	23155.55	0.006412	0.001735	0.000691

Flow rate(Q), m ³ /h	Flow rate(Q), m ³ /s	Pipe diameter (D), m	Area (A), m ²	Velocity (v =Q/A), m/s	Length (L), m	L/D
8.5	0.002361	0.0381	0.001141	2.070150	0.5	13.1
8.5	0.002361	0.0381	0.001141	2.070150	1.0	26.2
8.5	0.002361	0.0381	0.001141	2.070150	1.5	39.4
8.5	0.002361	0.0381	0.001141	2.070150	2.0	52.5
8.0	0.002222	0.0381	0.001141	1.948377	0.5	13.1
8.0	0.002222	0.0381	0.001141	1.948377	1.0	26.2
8.0	0.002222	0.0381	0.001141	1.948377	1.5	39.4
8.0	0.002222	0.0381	0.001141	1.948377	2.0	52.5
7.5	0.002083	0.0381	0.001141	1.826603	0.5	13.1
7.5	0.002083	0.0381	0.001141	1.826603	1.0	26.2
7.5	0.002083	0.0381	0.001141	1.826603	1.5	39.4
7.5	0.002083	0.0381	0.001141	1.826603	2.0	52.5

Pressure drop (ΔP), kg/(ms ²)	Wall shear stress (τ_w), kg/(ms ²)	Fanning friction factor (C_f)	Reynolds number, Re	Blasius	Virk	Laminar flow
	$\tau_w = D\Delta P/4L$	$C_f = 2\tau_w / \rho v^2$		$f = 0.0791Re^{-0.25}$	$f = 0.59Re^{-0.58}$	$f = 16/Re$
450	8.57	0.004784072	21869.13	0.006505	0.001794	0.000732
901	8.58	0.004789388	21869.13	0.006505	0.001794	0.000732
1380	8.76	0.004890385	21869.13	0.006505	0.001794	0.000732
1880	8.95	0.004996697	21869.13	0.006505	0.001794	0.000732
399	7.60	0.004788682	20582.71	0.006604	0.001858	0.000777
802	7.64	0.004812685	20582.71	0.006604	0.001858	0.000777
1230	7.81	0.004920700	20582.71	0.006604	0.001858	0.000777
1692	8.06	0.005076723	20582.71	0.006604	0.001858	0.000777
371	7.07	0.005066108	19296.30	0.006711	0.001929	0.000829
743	7.08	0.005072935	19296.30	0.006711	0.001929	0.000829
1120	7.11	0.005097970	19296.30	0.006711	0.001929	0.000829
1508	7.18	0.005148040	19296.30	0.006711	0.001929	0.000829

Table 4.6: System verification of pipe with ID 0.0254m in transporting diesel before DRA addition

Flow rate(Q), m ³ /h	Flow rate(Q), m ³ /s	Pipe diameter (D), m	Area (A), m ²	Velocity (v =Q/A), m/s	Length (L), m	L/D
8.0	0.002222	0.0254	0.000507	4.383847	0.5	19.7
8.0	0.002222	0.0254	0.000507	4.383847	1.0	39.4
8.0	0.002222	0.0254	0.000507	4.383847	1.5	59.1
8.0	0.002222	0.0254	0.000507	4.383847	2.0	78.7
7.5	0.002083	0.0254	0.000507	4.109857	0.5	19.7
7.5	0.002083	0.0254	0.000507	4.109857	1.0	39.4
7.5	0.002083	0.0254	0.000507	4.109857	1.5	59.1
7.5	0.002083	0.0254	0.000507	4.109857	2.0	78.7
7.0	0.001944	0.0254	0.000507	3.835866	0.5	19.7
7.0	0.001944	0.0254	0.000507	3.835866	1.0	39.4
7.0	0.001944	0.0254	0.000507	3.835866	1.5	59.1
7.0	0.001944	0.0254	0.000507	3.835866	2.0	78.7
6.5	0.001806	0.0254	0.000507	3.561876	0.5	19.7
6.5	0.001806	0.0254	0.000507	3.561876	1.0	39.4
6.5	0.001806	0.0254	0.000507	3.561876	1.5	59.1
6.5	0.001806	0.0254	0.000507	3.561876	2.0	78.7

Pressure drop (ΔP), kg/(ms ²)	Wall shear stress (τ_w), kg/(ms ²)	Fanning friction factor (C_f)	Reynolds number, Re	Blasius	Virk	Laminar flow
	$\tau_w = D\Delta P/4L$	$C_f = 2\tau_w / \rho v^2$		$f = 0.0791\text{Re}^{-0.25}$	$f = 0.59\text{Re}^{-0.58}$	$f = 16/\text{Re}$
2862	36.35	0.004523311	30874.07	0.005967	0.001469	0.000518
5811	36.90	0.004592061	30874.07	0.005967	0.001469	0.000518
8810	37.30	0.004641319	30874.07	0.005967	0.001469	0.000518
11789	37.43	0.004658046	30874.07	0.005967	0.001469	0.000518
2533	32.17	0.004554906	28944.44	0.006064	0.001525	0.000553
5197	33.00	0.004672690	28944.44	0.006064	0.001525	0.000553
7951	33.66	0.004765898	28944.44	0.006064	0.001525	0.000553
10626	33.74	0.004776987	28944.44	0.006064	0.001525	0.000553
2184	27.74	0.004508409	27014.81	0.006170	0.001587	0.000592
4513	28.66	0.004658070	27014.81	0.006170	0.001587	0.000592
6830	28.91	0.004699700	27014.81	0.006170	0.001587	0.000592
9116	28.94	0.004704517	27014.81	0.006170	0.001587	0.000592
1982	25.17	0.004745082	25085.18	0.006285	0.001656	0.000638
3997	25.38	0.004784584	25085.18	0.006285	0.001656	0.000638
6035	25.55	0.004816106	25085.18	0.006285	0.001656	0.000638
8084	25.67	0.004838451	25085.18	0.006285	0.001656	0.000638

Flow rate(Q), m ³ /h	Flow rate(Q), m ³ /s	Pipe diameter (D), m	Area (A), m ²	Velocity (v =Q/A), m/s	Length (L), m	L/D
6.0	0.001667	0.0254	0.000507	3.287885	0.5	19.7
6.0	0.001667	0.0254	0.000507	3.287885	1.0	39.4
6.0	0.001667	0.0254	0.000507	3.287885	1.5	59.1
6.0	0.001667	0.0254	0.000507	3.287885	2.0	78.7
5.5	0.001528	0.0254	0.000507	3.013895	0.5	19.7
5.5	0.001528	0.0254	0.000507	3.013895	1.0	39.4
5.5	0.001528	0.0254	0.000507	3.013895	1.5	59.1
5.5	0.001528	0.0254	0.000507	3.013895	2.0	78.7
5.0	0.001389	0.0254	0.000507	2.739904	0.5	19.7
5.0	0.001389	0.0254	0.000507	2.739904	1.0	39.4
5.0	0.001389	0.0254	0.000507	2.739904	1.5	59.1
5.0	0.001389	0.0254	0.000507	2.739904	2.0	78.7

Pressure drop (ΔP), kg/(ms ²)	Wall shear stress (τ_w), kg/(ms ²)	Fanning friction factor (C_f)	Reynolds number, Re	Blasius	Virk	Laminar flow
	$\tau_w = D\Delta P/4L$	$C_f = 2\tau_w / \rho v^2$		$f = 0.0791Re^{-0.25}$	$f = 0.59Re^{-0.58}$	$f = 16/Re$
1704	21.64	0.004787776	23155.55	0.006412	0.001735	0.000691
3467	22.02	0.004870663	23155.55	0.006412	0.001735	0.000691
5211	22.06	0.004880497	23155.55	0.006412	0.001735	0.000691
6971	22.13	0.004896653	23155.55	0.006412	0.001735	0.000691
1389	17.64	0.004644550	21225.92	0.006553	0.001825	0.000754
2781	17.66	0.004649565	21225.92	0.006553	0.001825	0.000754
4385	18.56	0.004887533	21225.92	0.006553	0.001825	0.000754
5880	18.67	0.004915398	21225.92	0.006553	0.001825	0.000754
1208	15.34	0.004887578	19296.30	0.006711	0.001929	0.000829
2450	15.56	0.004956360	19296.30	0.006711	0.001929	0.000829
3744	15.85	0.005049418	19296.30	0.006711	0.001929	0.000829
5028	15.96	0.005085832	19296.30	0.006711	0.001929	0.000829

Table 4.7: System verification of pipe with ID 0.0127m in transporting diesel before DRA addition

Flow rate(Q), m ³ /h	Flow rate(Q), m ³ /s	Pipe diameter (D), m	Area (A), m ²	Velocity (v =Q/A), m/s	Length (L), m	L/D
2.4	0.000667	0.0127	0.000127	5.260617	0.5	39.4
2.4	0.000667	0.0127	0.000127	5.260617	1.0	78.7
2.4	0.000667	0.0127	0.000127	5.260617	1.5	118.1
2.4	0.000667	0.0127	0.000127	5.260617	2.0	157.5
2.2	0.000611	0.0127	0.000127	4.822232	0.5	39.4
2.2	0.000611	0.0127	0.000127	4.822232	1.0	78.7
2.2	0.000611	0.0127	0.000127	4.822232	1.5	118.1
2.2	0.000611	0.0127	0.000127	4.822232	2.0	157.5
2.0	0.000556	0.0127	0.000127	4.383847	0.5	39.4
2.0	0.000556	0.0127	0.000127	4.383847	1.0	78.7
2.0	0.000556	0.0127	0.000127	4.383847	1.5	118.1
2.0	0.000556	0.0127	0.000127	4.383847	2.0	157.5
1.8	0.000500	0.0127	0.000127	3.945462	0.5	39.4
1.8	0.000500	0.0127	0.000127	3.945462	1.0	78.7
1.8	0.000500	0.0127	0.000127	3.945462	1.5	118.1
1.8	0.000500	0.0127	0.000127	3.945462	2.0	157.5

Pressure drop (ΔP), kg/(ms ²)	Wall shear stress (τ_w), kg/(ms ²)	Fanning friction factor (C_f)	Reynolds number, Re	Blasius	Virk	Laminar flow
	$\tau_w = D\Delta P/4L$	$C_f = 2\tau_w / \rho v^2$		$f = 0.0791\text{Re}^{-0.25}$	$f = 0.59\text{Re}^{-0.58}$	$f = 16/\text{Re}$
9201	58.43	0.005049278	18524.44	0.006780	0.001975	0.000864
18546	58.88	0.005088790	18524.44	0.006780	0.001975	0.000864
27849	58.95	0.005094278	18524.44	0.006780	0.001975	0.000864
37163	59.00	0.005098531	18524.44	0.006780	0.001975	0.000864
7932	50.37	0.005180291	16980.74	0.006929	0.002077	0.000942
14668	46.57	0.004789744	16980.74	0.006929	0.002077	0.000942
23054	48.80	0.005018760	16980.74	0.006929	0.002077	0.000942
30792	48.88	0.005027468	16980.74	0.006929	0.002077	0.000942
6634	42.13	0.005242425	15437.04	0.007096	0.002195	0.001036
13324	42.30	0.005264552	15437.04	0.007096	0.002195	0.001036
19657	41.61	0.005177889	15437.04	0.007096	0.002195	0.001036
26511	42.09	0.005237486	15437.04	0.007096	0.002195	0.001036
5379	34.16	0.005247752	13893.33	0.007286	0.002334	0.001152
10945	34.75	0.005338971	13893.33	0.007286	0.002334	0.001152
16374	34.66	0.005324824	13893.33	0.007286	0.002334	0.001152
21067	33.44	0.005138241	13893.33	0.007286	0.002334	0.001152

Flow rate(Q), m ³ /h	Flow rate(Q), m ³ /s	Pipe diameter (D), m	Area (A), m ²	Velocity (v =Q/A), m/s	Length (L), m	L/D
1.6	0.000444	0.0127	0.000127	3.507078	0.5	39.4
1.6	0.000444	0.0127	0.000127	3.507078	1.0	78.7
1.6	0.000444	0.0127	0.000127	3.507078	1.5	118.1
1.6	0.000444	0.0127	0.000127	3.507078	2.0	157.5
1.4	0.000389	0.0127	0.000127	3.068693	0.5	39.4
1.4	0.000389	0.0127	0.000127	3.068693	1.0	78.7
1.4	0.000389	0.0127	0.000127	3.068693	1.5	118.1
1.4	0.000389	0.0127	0.000127	3.068693	2.0	157.5
1.2	0.000333	0.0127	0.000127	2.630308	0.5	39.4
1.2	0.000333	0.0127	0.000127	2.630308	1.0	78.7
1.2	0.000333	0.0127	0.000127	2.630308	1.5	118.1
1.2	0.000333	0.0127	0.000127	2.630308	2.0	157.5

Pressure drop (ΔP), kg/(ms ²)	Wall shear stress (τ_w), kg/(ms ²)	Fanning friction factor (C_f)	Reynolds number, Re	Blasius	Virk	Laminar flow
	$\tau_w = D\Delta P/4L$	$C_f = 2\tau_w / \rho v^2$		$f = 0.0791Re^{-0.25}$	$f = 0.59Re^{-0.58}$	$f = 16/Re$
4153	26.37	0.005127890	12349.63	0.007503	0.002499	0.001296
8501	26.99	0.005248278	12349.63	0.007503	0.002499	0.001296
12449	26.35	0.005123775	12349.63	0.007503	0.002499	0.001296
16674	26.47	0.005147029	12349.63	0.007503	0.002499	0.001296
3374	21.42	0.005441339	10805.93	0.007758	0.002700	0.001481
6287	19.96	0.005069606	10805.93	0.007758	0.002700	0.001481
9622	20.37	0.005172551	10805.93	0.007758	0.002700	0.001481
13778	21.87	0.005555036	10805.93	0.007758	0.002700	0.001481
2650	16.83	0.005817015	9262.22	0.008063	0.002952	0.001727
5525	17.54	0.006063963	9262.22	0.008063	0.002952	0.001727
7931	16.79	0.005803112	9262.22	0.008063	0.002952	0.001727
10934	17.36	0.006000305	9262.22	0.008063	0.002952	0.001727

APPENDIX C1
PERCENTAGE DRAG REDUCTION BY MUCILAGE

Table 4.8: Percentage drag reduction by mucilage in transporting water via pipe with ID 0.0381m

Re	50ppm				0.5	100ppm			0.5	150ppm				0.5	200ppm		
	0.5	1.0	1.5	2.0		1.0	1.5	2.0		1.0	1.5	2.0	1.0		1.5	2.0	
97431.00	14.83	21.28	32.76	35.51	17.90	26.61	35.11	36.09	19.56	28.18	36.53	39.94	19.79	28.79	40.22	47.95	
92791.43	14.40	19.45	31.39	34.78	16.71	23.39	34.67	35.89	17.84	23.94	35.65	38.90	18.90	28.55	43.68	47.07	
88151.86	13.38	18.82	33.21	34.40	16.33	21.56	34.18	35.57	17.10	22.56	33.74	38.03	17.88	25.88	46.02	46.92	
83512.29	13.00	16.67	28.47	21.27	14.39	17.72	32.39	33.86	15.95	19.90	37.46	37.82	16.56	25.00	45.96	43.40	
78872.72	12.87	14.43	17.88	18.89	13.84	14.85	22.79	21.65	14.44	15.13	20.36	23.37	13.39	15.86	24.35	24.79	
74233.15	12.26	12.34	12.56	13.35	11.23	13.82	13.93	14.46	12.27	14.01	14.81	15.75	12.73	14.67	14.95	16.03	
69593.57	8.21	9.90	7.67	11.26	9.29	10.87	8.63	12.62	10.18	11.29	8.74	13.36	11.71	12.04	8.32	13.90	

Re	400ppm				0.5	600ppm			0.5	800ppm				0.5	1000ppm		
	0.5	1.0	1.5	2.0		1.0	1.5	2.0		1.0	1.5	2.0	1.0		1.5	2.0	
97431.00	20.06	29.43	43.84	48.84	20.65	30.00	45.18	49.03	21.59	32.32	47.17	49.56	21.77	34.78	47.85	50.05	
92791.43	19.15	29.00	43.30	48.19	19.87	29.75	45.70	48.94	20.10	31.80	46.50	49.10	20.83	32.04	46.93	49.84	
88151.86	18.44	26.67	36.11	47.63	19.07	28.03	38.56	46.00	19.50	28.98	38.94	47.26	19.86	29.06	41.05	48.83	
83512.29	17.30	25.41	30.04	33.56	18.04	26.77	30.84	35.51	18.85	27.32	29.68	36.92	19.05	27.92	30.22	39.89	
78872.72	13.94	16.44	24.87	25.33	14.99	19.04	24.30	25.94	17.12	23.24	24.08	27.00	17.84	24.83	25.67	27.19	
74233.15	13.11	15.52	15.50	16.70	14.03	15.78	19.35	17.31	14.79	15.93	19.89	21.24	15.30	17.05	21.17	22.05	
69593.57	12.07	13.89	14.02	14.72	12.75	14.12	14.97	16.00	13.00	15.10	16.07	16.95	13.68	15.87	16.84	17.18	

Table 4.9: Percentage drag reduction by mucilage in transporting water via pipe with ID 0.0254m

Re	50ppm				100ppm				150ppm				200ppm			
	0.5	1.0	1.5	2.0	0.5	1.0	1.5	2.0	0.5	1.0	1.5	2.0	0.5	1.0	1.5	2.0
111349.72	16.13	21.61	27.69	31.16	16.98	26.60	29.04	30.15	17.14	28.05	31.19	31.95	17.03	29.90	31.70	33.02
104390.36	15.59	23.36	28.01	30.12	14.80	24.22	27.88	30.87	15.58	26.88	29.12	31.03	16.12	29.28	30.05	32.76
97431.00	14.77	17.70	25.95	29.10	13.75	23.38	26.64	30.00	14.90	25.53	27.43	30.46	15.55	26.03	28.87	32.28
90471.65	12.18	14.73	26.77	28.90	12.89	20.62	25.98	29.11	13.32	23.30	28.26	29.94	14.10	23.95	29.08	31.92
83512.29	11.00	13.35	25.03	27.77	12.37	17.09	27.14	27.69	12.78	16.39	27.90	29.02	13.96	17.74	28.01	30.31
76552.93	11.16	10.81	20.09	21.18	7.35	13.99	21.56	22.20	7.94	14.17	21.72	23.30	6.28	13.90	22.86	24.76
69593.57	3.31	5.55	7.39	7.17	3.98	8.00	13.50	14.02	5.10	8.08	17.07	17.88	6.62	7.39	18.47	18.90
Re	400ppm				600ppm				800ppm				1000ppm			
	0.5	1.0	1.5	2.0	0.5	1.0	1.5	2.0	0.5	1.0	1.5	2.0	0.5	1.0	1.5	2.0
111349.72	17.94	30.31	32.10	34.63	18.39	31.78	33.35	36.92	22.03	33.31	34.41	39.90	23.87	33.87	37.43	41.17
104390.36	17.09	29.82	30.59	33.75	18.32	30.91	31.77	36.49	21.90	29.94	33.37	37.72	23.31	30.11	36.65	39.92
97431.00	16.53	24.48	29.67	33.14	17.99	26.76	31.10	35.50	20.31	28.29	32.30	36.68	20.87	29.70	35.57	38.88
90471.65	15.49	19.05	29.06	32.29	17.13	19.93	30.18	33.39	18.83	21.17	31.94	34.41	19.33	22.74	34.41	35.26
83512.29	15.87	16.80	28.65	31.18	16.29	17.72	29.94	32.27	14.40	19.98	31.38	32.98	16.65	21.27	32.30	34.45
76552.93	7.14	14.21	23.33	26.84	8.12	15.20	25.53	28.35	8.22	16.23	27.77	30.16	9.49	17.65	28.19	31.37
69593.57	6.30	7.94	20.10	20.92	7.75	8.11	21.17	22.99	7.94	10.15	18.13	24.47	10.82	12.26	19.17	26.64

Table 4.10: Percentage drag reduction by mucilage in transporting water via pipe with ID 0.0127m

Re	50ppm				100ppm				150ppm				200ppm			
	0.5	1.0	1.5	2.0	0.5	1.0	1.5	2.0	0.5	1.0	1.5	2.0	0.5	1.0	1.5	2.0
66809.83	14.11	20.18	23.06	25.69	19.03	22.49	25.77	29.00	19.88	25.55	27.79	30.79	21.33	27.00	29.03	45.65
61242.34	13.78	19.55	21.63	23.75	17.81	20.92	23.81	28.17	18.54	23.20	25.70	31.18	19.10	25.42	26.54	43.84
55674.86	13.30	17.61	19.77	22.80	15.38	20.16	21.80	27.98	16.60	21.65	23.42	29.11	18.32	22.57	23.91	40.97
50107.37	11.09	15.70	18.84	21.95	13.89	18.75	21.03	27.00	15.43	19.62	20.96	28.73	16.40	20.94	21.05	40.00
44539.89	10.44	16.73	19.38	21.03	13.50	18.11	19.67	24.00	14.05	18.77	19.84	25.54	14.78	19.16	19.88	37.00
38972.40	10.03	14.19	18.59	19.81	11.86	16.90	18.63	22.00	12.80	18.00	18.61	22.66	13.97	19.00	19.08	33.00
33404.92	9.81	13.32	16.01	17.66	10.73	14.22	16.89	20.00	12.29	15.52	16.89	20.91	12.01	14.43	17.16	28.00
Re	400ppm				600ppm				800ppm				1000ppm			
	0.5	1.0	1.5	2.0	0.5	1.0	1.5	2.0	0.5	1.0	1.5	2.0	0.5	1.0	1.5	2.0
66809.83	20.19	27.95	35.50	49.08	22.10	29.23	36.62	49.88	22.65	31.18	46.55	51.14	23.91	33.02	45.87	52.17
61242.34	18.64	26.63	34.35	48.94	22.28	27.11	34.06	49.39	23.33	29.04	50.59	49.80	23.80	29.77	45.21	51.90
55674.86	18.90	25.20	30.90	48.02	20.95	25.69	32.29	48.66	21.76	28.73	38.22	49.37	24.48	23.66	37.92	51.11
50107.37	17.87	22.39	30.22	47.00	20.21	23.00	31.77	47.91	19.07	24.71	33.40	48.00	21.22	23.01	35.00	49.09
44539.89	16.73	24.58	26.81	45.00	18.93	18.10	26.15	44.75	18.01	23.38	30.32	44.00	19.80	21.56	33.39	46.15
38972.40	14.85	19.62	28.33	41.00	15.59	17.17	22.76	40.15	16.78	18.64	29.25	41.00	19.11	20.87	32.20	40.42
33404.92	14.16	15.51	20.11	37.00	15.12	16.92	20.94	37.73	16.23	17.56	23.44	39.00	18.12	20.20	21.19	35.26

Table 4.11: Percentage drag reduction by mucilage in transporting diesel via pipe with ID 0.0381m

Re	50ppm				100ppm				150ppm				200ppm			
	0.5	1.0	1.5	2.0	0.5	1.0	1.5	2.0	0.5	1.0	1.5	2.0	0.5	1.0	1.5	2.0
27014.81	11.88	13.08	18.00	23.67	13.90	15.00	20.88	25.00	15.07	18.83	23.33	26.61	16.39	20.90	24.09	27.26
25728.39	10.00	11.86	16.03	19.33	11.04	12.87	16.89	21.66	13.04	14.97	18.22	22.98	14.00	16.04	19.10	23.15
24441.97	7.16	11.00	14.51	17.60	9.22	12.26	16.10	20.23	10.31	13.88	17.05	22.70	11.78	14.15	18.96	23.31
23155.55	4.85	10.75	13.70	16.05	6.05	11.43	14.00	17.05	8.20	13.00	15.34	19.88	10.04	13.43	17.08	21.05
21869.13	4.00	8.31	11.36	14.88	4.53	10.90	12.70	15.70	6.00	11.17	13.00	17.06	7.80	13.04	15.66	19.88
20582.71	3.37	7.04	9.00	14.00	4.00	8.07	10.50	14.98	4.66	10.40	12.30	16.10	4.92	12.87	14.00	16.97
19296.30	2.78	4.66	6.14	12.87	3.03	5.61	7.41	14.12	3.10	6.02	7.75	15.04	4.33	8.00	10.43	16.50

Re	400ppm				600ppm				800ppm				1000ppm			
	0.5	1.0	1.5	2.0	0.5	1.0	1.5	2.0	0.5	1.0	1.5	2.0	0.5	1.0	1.5	2.0
27014.81	16.90	21.78	26.44	29.91	20.14	34.03	36.22	45.95	22.52	36.91	46.92	48.31	19.00	45.03	46.00	43.37
25728.39	15.60	18.97	22.05	27.18	18.00	20.69	35.84	39.78	20.34	37.88	43.60	45.68	18.12	44.98	44.41	40.00
24441.97	12.99	16.32	21.10	25.22	15.76	28.04	30.00	38.57	25.44	40.56	48.05	58.40	25.00	43.18	45.11	48.22
23155.55	11.27	13.59	19.27	23.87	14.38	23.77	28.10	32.90	15.48	32.15	37.00	41.55	15.04	30.01	38.85	39.04
21869.13	8.01	15.16	17.12	21.69	10.11	19.89	27.45	29.00	14.10	30.97	32.90	35.14	13.90	27.00	32.00	33.17
20582.71	6.30	13.01	15.93	20.55	12.07	16.47	23.69	29.88	12.69	28.58	31.84	32.76	12.00	26.12	28.31	30.03
19296.30	5.00	9.89	12.74	18.38	5.55	17.18	19.90	25.14	7.32	25.11	26.79	28.79	7.11	22.40	24.00	24.94

Table 4.12: Percentage drag reduction by mucilage in transporting diesel via pipe with ID 0.0254m

Re	50ppm				100ppm				150ppm				200ppm			
	0.5	1	1.5	2	0.5	1	1.5	2	0.5	1	1.5	2	0.5	1	1.5	2
30874.07	9.03	13.00	15.09	20.00	10.90	15.04	18.00	22.29	12.23	16.00	20.40	24.11	14.70	18.17	22.86	25.64
28944.44	8.61	11.81	13.00	19.08	9.04	13.69	15.01	20.86	11.16	15.06	18.12	22.50	13.00	17.03	19.00	23.37
27014.81	6.70	9.83	11.72	17.55	8.77	13.00	14.60	19.40	9.03	13.39	16.16	20.66	10.04	15.60	17.30	21.16
25085.18	4.55	8.51	9.04	15.87	6.05	10.09	11.29	17.03	7.80	12.00	14.03	19.97	8.76	13.83	15.51	20.03
23155.55	3.60	6.79	7.80	15.10	4.00	8.12	9.45	16.62	5.02	10.05	13.76	18.03	6.50	12.26	14.11	19.92
21225.92	2.33	6.00	6.54	13.24	3.42	6.77	7.64	14.05	4.49	7.90	12.87	16.00	5.01	10.03	13.04	16.43
19296.30	1.99	4.11	5.96	10.60	2.76	6.00	7.00	12.27	3.10	7.33	11.00	13.65	3.38	8.04	12.67	15.50

Re	400ppm				600ppm				800ppm				1000ppm			
	0.5	1	1.5	2	0.5	1	1.5	2	0.5	1	1.5	2	0.5	1	1.5	2
30874.07	15.57	20.19	24.06	27.61	16.10	32.85	35.03	44.83	19.05	35.88	45.21	46.44	18.00	33.58	40.00	41.80
28944.44	13.98	18.56	20.92	25.87	15.17	30.57	33.55	39.96	18.56	35.32	43.00	43.80	17.68	31.65	38.14	40.38
27014.81	11.32	17.67	19.93	23.68	13.66	26.91	30.18	36.59	16.10	33.69	39.19	40.78	16.00	30.00	34.99	36.11
25085.18	9.91	14.31	17.33	21.98	12.83	22.58	26.93	32.31	14.75	31.09	37.07	39.09	14.05	29.76	34.52	35.04
23155.55	7.22	13.66	15.54	21.00	11.27	19.26	24.24	29.61	12.96	30.54	32.48	33.77	12.00	29.04	30.09	30.87
21225.92	6.09	11.78	14.34	18.91	10.92	17.34	22.48	27.58	11.94	26.09	29.17	30.65	10.03	25.50	29.86	30.00
19296.30	4.66	9.13	13.98	17.88	4.98	15.90	19.23	24.35	7.42	23.86	25.97	28.30	7.00	22.00	22.89	25.00

Table 4.13: Percentage drag reduction by mucilage in transporting diesel via pipe with ID 0.0127m

Re	50ppm				100ppm				150ppm				200ppm			
	0.5	1	1.5	2	0.5	1	1.5	2	0.5	1	1.5	2	0.5	1	1.5	2
18524.44	4.00	10.07	11.67	14.67	8.16	11.27	12.50	17.00	9.75	14.22	17.66	19.32	11.40	16.70	20.00	21.91
16980.74	5.30	9.00	11.02	13.00	7.21	10.40	13.49	15.20	8.20	12.70	15.70	17.67	10.00	14.08	17.66	17.76
15437.04	3.76	7.60	9.00	11.23	5.20	8.84	10.56	13.38	6.58	9.00	13.29	16.68	9.12	12.27	15.45	18.17
13893.33	3.08	6.55	7.19	10.50	4.00	7.11	8.71	11.26	5.04	8.23	11.28	14.00	7.09	10.00	12.29	17.03
12349.63	2.03	4.90	6.50	9.34	2.78	5.93	7.09	10.20	4.00	6.51	7.91	11.45	5.41	8.81	9.86	14.00
10805.93	1.77	4.11	5.41	7.20	2.10	5.10	7.00	8.76	2.88	6.00	7.60	10.33	4.07	6.21	8.71	12.89
9262.22	1.29	3.40	5.03	6.93	1.67	4.03	5.98	7.00	1.90	4.78	5.61	7.89	2.80	5.05	5.90	8.77
Re	400ppm				600ppm				800ppm				1000ppm			
	0.5	1	1.5	2	0.5	1	1.5	2	0.5	1	1.5	2	0.5	1	1.5	2
18524.44	12.77	18.11	20.75	23.82	14.98	21.41	26.83	27.94	18.41	25.77	30.06	32.65	15.06	21.00	27.66	30.00
16980.74	11.50	15.97	18.54	18.01	14.31	19.43	25.04	26.13	16.43	24.41	24.99	30.84	13.37	18.90	24.00	26.12
15437.04	10.06	14.88	16.37	19.35	13.05	17.68	21.15	22.72	10.33	20.01	32.67	37.19	11.55	16.54	22.34	19.91
13893.33	8.48	11.05	13.86	17.60	11.38	12.99	18.11	19.69	12.99	18.38	21.04	22.85	10.09	10.97	18.51	20.00
12349.63	7.01	9.32	11.11	15.99	9.07	11.85	15.67	18.60	11.43	15.76	18.43	19.90	8.76	10.06	16.00	17.07
10805.93	4.99	7.17	9.32	13.63	6.57	9.44	13.80	15.84	8.00	13.64	15.71	17.67	6.13	8.79	13.60	14.50
9262.22	4.00	6.34	7.77	10.54	4.11	7.39	10.45	12.32	5.72	10.05	12.01	15.33	4.21	8.11	9.78	12.44

APPENDIX C2

PERCENTAGE DRAG REDUCTION BY RED GYPSUM

Table 4.14: Percentage drag reduction by red gypsum in transporting water via pipe with ID 0.0381m

Re	50ppm				0.5	100ppm			0.5	150ppm				0.5	200ppm			
	0.5	1.0	1.5	2.0		1.0	1.5	2.0		1.0	1.5	2.0	1.0		1.5	2.0		
97431.00	9.04	12.84	19.40	26.03	10.69	17.40	20.89	39.00	12.03	19.03	23.16	43.07	13.12	19.94	23.90	56.44		
92791.43	8.69	12.27	17.02	19.92	10.14	14.96	18.60	23.65	11.76	18.72	21.10	30.73	12.70	19.59	22.89	36.23		
88151.86	8.00	10.95	14.79	16.80	9.50	14.05	15.15	18.78	11.28	16.95	18.45	24.91	11.85	19.18	22.36	27.46		
83512.29	6.78	10.44	12.27	14.09	8.43	13.80	14.07	17.55	9.90	15.42	16.94	18.71	10.18	18.66	20.17	22.98		
78872.72	6.12	8.95	9.78	12.36	7.04	13.66	13.00	15.45	9.57	14.70	15.60	17.00	9.71	18.47	16.80	19.18		
74233.15	5.69	8.56	9.03	9.87	6.95	12.39	10.48	11.07	8.04	14.00	14.19	14.33	8.63	18.01	15.43	16.10		
69593.57	5.17	5.34	7.11	8.91	6.03	7.41	9.04	10.39	7.71	10.22	12.05	13.18	8.20	13.78	14.19	15.95		

Re	400ppm				0.5	600ppm			0.5	800ppm				0.5	1000ppm			
	0.5	1.0	1.5	2.0		1.0	1.5	2.0		1.0	1.5	2.0	1.0		1.5	2.0		
97431.00	13.96	21.86	24.40	44.57	14.42	22.93	24.88	45.09	14.93	23.34	25.50	37.30	15.11	24.42	25.70	46.00		
92791.43	12.93	21.55	23.31	29.00	13.08	22.80	23.76	30.92	14.48	21.62	24.41	32.38	14.80	23.90	25.16	38.72		
88151.86	12.23	20.19	22.95	28.80	12.80	21.05	23.08	30.17	13.33	21.17	23.64	30.00	13.72	23.43	24.65	32.75		
83512.29	10.87	19.93	20.96	24.10	11.39	20.73	21.04	24.80	12.40	20.99	23.20	25.60	12.69	22.70	24.40	26.88		
78872.72	9.94	19.57	20.51	20.95	10.57	20.14	20.74	21.81	10.90	20.56	21.92	22.05	11.59	21.69	22.98	24.30		
74233.15	9.38	18.76	15.93	16.72	10.00	19.60	20.03	21.00	10.56	19.95	20.57	21.54	11.18	21.17	22.00	22.87		
69593.57	8.94	14.03	15.42	16.00	9.83	12.29	15.90	16.53	10.03	13.40	15.11	17.33	10.66	14.01	17.34	18.02		

Table 4.15: Percentage drag reduction by red gypsum in transporting water via pipe with ID 0.0254m

Re	50ppm				100ppm				150ppm				200ppm			
	0.5	1.0	1.5	2.0	0.5	1.0	1.5	2.0	0.5	1.0	1.5	2.0	0.5	1.0	1.5	2.0
111349.72	7.07	16.86	17.08	22.04	7.93	16.71	17.83	33.71	8.30	24.42	25.76	39.25	11.55	27.11	34.51	45.33
104390.36	6.98	15.34	15.71	20.10	7.85	16.40	17.44	29.89	7.92	24.11	24.62	36.43	11.12	26.93	32.29	40.02
97431.00	6.86	16.44	14.41	18.68	7.49	18.72	18.90	20.83	7.65	23.61	24.17	26.75	9.78	30.38	30.75	34.63
90471.65	6.51	12.27	12.70	14.83	7.02	15.65	11.66	17.00	7.32	19.40	20.45	22.36	9.21	24.13	25.00	30.07
83512.29	6.03	5.87	8.90	11.73	6.74	8.13	9.82	15.27	6.90	9.20	14.97	17.65	7.65	10.96	16.70	26.51
76552.93	4.95	5.60	7.79	10.15	5.80	7.79	9.44	12.22	6.11	7.91	10.21	14.61	7.32	8.78	12.85	18.82
69593.57	4.90	5.24	7.04	7.33	5.31	6.01	9.00	9.06	5.80	6.42	9.84	12.04	6.74	8.03	12.10	13.29
Re	400ppm				600ppm				800ppm				1000ppm			
	0.5	1.0	1.5	2.0	0.5	1.0	1.5	2.0	0.5	1.0	1.5	2.0	0.5	1.0	1.5	2.0
111349.72	12.54	28.75	34.88	46.70	12.82	31.61	34.93	46.91	13.30	31.90	35.21	44.30	19.76	35.12	38.76	47.00
104390.36	11.96	28.39	32.74	41.13	12.43	31.07	34.10	36.55	12.84	31.56	33.95	36.71	19.31	33.65	34.83	40.79
97431.00	10.80	29.17	30.99	34.96	11.71	30.98	31.15	35.40	12.15	32.39	31.56	35.86	19.00	33.41	33.04	36.61
90471.65	9.73	14.55	25.21	31.50	10.46	25.43	27.48	32.78	11.96	26.17	27.90	33.00	18.33	27.00	29.77	33.67
83512.29	8.22	12.28	18.50	27.00	8.97	13.89	18.79	27.61	9.44	12.94	15.16	27.90	14.55	15.17	17.21	29.55
76552.93	7.85	9.32	13.39	19.12	8.21	9.78	13.65	21.17	8.70	9.94	13.78	21.56	10.10	13.31	13.90	20.14
69593.57	7.11	8.94	12.73	13.56	7.75	9.30	13.11	14.60	8.32	9.51	12.67	15.11	8.76	13.52	15.20	15.76

Table 4.16: Percentage drag reduction by red gypsum in transporting water via pipe with ID 0.0127m

Re	50ppm				100ppm				150ppm				200ppm			
	0.5	1.0	1.5	2.0	0.5	1.0	1.5	2.0	0.5	1.0	1.5	2.0	0.5	1.0	1.5	2.0
66809.83	4.95	18.72	19.00	19.61	5.71	25.66	26.71	28.71	6.01	31.18	31.76	34.33	6.80	34.07	34.72	40.18
61242.34	4.38	17.10	17.82	18.94	5.22	22.92	23.77	25.18	5.86	27.79	29.04	30.25	6.17	32.81	34.10	36.47
55674.86	3.77	8.29	13.90	18.22	4.01	9.20	14.43	23.92	4.55	9.75	17.69	25.51	4.61	11.54	19.50	28.72
50107.37	2.64	5.43	7.12	16.80	3.00	5.67	7.84	17.67	3.47	5.98	9.11	23.42	4.00	6.22	10.01	25.29
44539.89	2.16	3.15	4.77	13.64	2.72	3.34	4.98	17.05	3.02	3.87	5.17	19.39	3.50	4.01	8.00	21.74
38972.40	1.43	2.79	3.35	8.67	2.10	2.93	4.05	9.83	2.61	3.34	4.90	13.27	2.99	3.67	6.78	16.59
33404.92	1.05	1.70	3.02	4.23	1.46	2.03	3.45	6.46	2.30	2.51	4.57	9.11	2.57	2.90	6.10	12.76
Re	400ppm				600ppm				800ppm				1000ppm			
	0.5	1.0	1.5	2.0	0.5	1.0	1.5	2.0	0.5	1.0	1.5	2.0	0.5	1.0	1.5	2.0
66809.83	7.19	34.22	34.93	40.23	7.39	34.87	35.51	40.54	7.84	35.04	38.00	40.87	13.20	35.61	38.17	40.50
61242.34	6.57	33.10	34.50	36.88	6.78	33.69	34.94	27.10	7.00	34.00	36.44	37.11	11.95	30.20	35.51	38.04
55674.86	6.02	14.40	20.79	29.02	6.45	14.88	21.18	29.32	6.78	16.93	21.56	33.49	11.26	18.50	21.00	34.41
50107.37	5.67	6.75	9.43	23.20	5.83	6.17	10.54	25.77	5.97	6.65	11.49	26.00	9.59	9.95	16.00	26.70
44539.89	4.56	5.11	8.13	22.16	4.73	5.63	8.75	22.80	4.92	5.98	9.82	23.34	9.12	8.94	12.24	24.15
38972.40	4.00	4.65	6.81	16.78	3.22	4.80	7.32	16.94	4.10	5.00	7.76	17.56	7.34	8.16	10.17	18.01
33404.92	3.11	3.74	5.22	8.31	3.57	4.05	6.93	12.87	3.89	4.50	7.21	13.02	4.45	7.09	9.00	12.32

Table 4.17: Percentage drag reduction by red gypsum in transporting diesel via pipe with ID 0.0381m

Re	50ppm				100ppm				150ppm				200ppm			
	0.5	1.0	1.5	2.0	0.5	1.0	1.5	2.0	0.5	1.0	1.5	2.0	0.5	1.0	1.5	2.0
27014.81	16.61	26.03	27.56	29.03	20.05	39.00	40.68	44.12	23.40	45.70	49.76	52.31	43.10	56.44	58.55	58.44
25728.39	14.64	19.00	19.60	19.92	18.76	23.65	24.85	25.65	19.05	30.05	31.18	34.27	33.98	36.23	33.21	38.23
24441.97	12.78	16.80	16.99	17.08	15.71	18.78	19.56	21.78	16.09	25.14	27.80	28.00	24.22	27.46	30.31	28.46
23155.55	10.86	14.09	15.32	16.33	12.33	17.55	18.94	19.05	15.44	20.12	25.71	27.11	20.08	22.98	28.11	24.56
21869.13	9.40	13.21	14.03	14.36	9.90	15.45	16.77	17.15	13.35	18.91	23.99	20.19	17.65	19.18	24.46	21.98
20582.71	7.95	9.87	10.71	11.07	8.01	11.07	11.70	13.66	12.23	14.55	16.77	17.04	13.77	16.10	19.75	16.91
19296.30	6.19	9.01	10.05	10.39	6.82	10.03	10.89	10.91	9.06	12.27	12.26	13.21	10.10	15.51	17.88	15.95

Re	400ppm				600ppm				800ppm				1000ppm			
	0.5	1.0	1.5	2.0	0.5	1.0	1.5	2.0	0.5	1.0	1.5	2.0	0.5	1.0	1.5	2.0
27014.81	28.77	33.14	58.71	59.06	43.48	56.92	59.00	59.68	48.11	59.71	59.99	62.00	44.05	49.00	60.30	61.87
25728.39	34.10	36.00	55.32	54.18	35.00	36.87	56.63	56.04	35.66	40.51	42.00	43.51	42.31	46.42	48.31	49.18
24441.97	32.12	33.57	50.93	51.07	25.76	33.05	34.88	53.37	26.08	29.14	29.87	29.14	27.11	34.90	40.55	46.00
23155.55	23.66	28.91	47.06	49.55	23.10	23.87	48.53	52.18	22.67	24.80	25.87	26.80	24.76	26.13	33.80	40.09
21869.13	21.78	24.13	44.80	46.31	17.04	25.60	46.22	47.16	18.89	20.77	23.46	23.14	20.07	24.70	30.19	36.60
20582.71	19.74	22.50	35.72	40.58	13.20	24.05	40.05	45.53	14.19	16.82	17.99	18.02	14.87	18.06	27.75	33.20
19296.30	17.45	19.02	30.10	37.27	16.03	23.67	36.30	40.80	12.70	16.11	17.02	16.29	13.08	18.79	25.52	30.04

Table 4.18: Percentage drag reduction by red gypsum in transporting diesel via pipe with ID 0.0254m

Re	50ppm				100ppm				150ppm				200ppm			
	0.5	1.0	1.5	2.0	0.5	1.0	1.5	2.0	0.5	1.0	1.5	2.0	0.5	1.0	1.5	2.0
30874.07	13.93	15.66	19.32	23.90	18.33	26.84	28.81	32.28	21.00	32.92	39.92	41.80	30.71	40.85	42.66	44.34
28944.44	12.80	14.21	16.04	17.85	16.30	19.11	21.65	22.60	18.11	33.80	34.06	34.97	24.60	35.87	30.23	37.99
27014.81	12.16	13.87	14.12	16.61	14.67	17.90	18.92	20.02	17.05	19.06	20.78	23.15	18.66	21.80	23.14	25.71
25085.18	10.11	11.06	13.45	15.00	12.94	14.30	16.71	17.96	15.77	17.03	18.15	20.05	15.83	18.81	20.76	22.86
23155.55	7.98	9.75	11.80	13.31	9.00	11.21	13.22	15.51	12.20	13.37	16.48	18.00	13.37	15.12	18.55	20.61
21225.92	7.02	8.19	8.99	9.87	7.92	9.09	10.31	11.86	9.81	10.00	12.19	12.01	8.19	10.08	13.71	14.56
19296.30	5.93	7.33	8.10	9.09	6.14	8.62	9.04	9.90	8.09	8.78	9.88	13.60	7.07	9.30	12.29	14.00
Re	400ppm				600ppm				800ppm				1000ppm			
	0.5	1.0	1.5	2.0	0.5	1.0	1.5	2.0	0.5	1.0	1.5	2.0	0.5	1.0	1.5	2.0
30874.07	31.00	42.33	43.55	45.07	33.07	43.10	44.65	48.30	34.94	43.87	45.17	50.87	33.79	43.78	45.33	48.79
28944.44	25.67	40.09	41.18	42.99	26.00	41.78	41.69	44.13	28.55	36.71	39.64	40.21	28.00	42.19	42.19	45.13
27014.81	20.09	36.78	37.70	40.50	22.00	38.11	40.30	41.08	20.18	23.59	26.77	28.09	22.17	40.33	40.89	41.77
25085.18	17.74	21.08	23.88	28.17	17.00	30.02	32.91	33.19	17.90	20.66	22.16	24.78	17.68	37.10	37.95	39.86
23155.55	15.17	18.30	21.50	25.30	15.21	28.65	30.17	30.80	15.56	17.45	20.80	22.01	16.54	30.17	33.12	36.78
21225.92	9.23	13.40	15.11	27.11	10.04	20.66	26.57	29.00	11.23	13.17	16.61	17.69	13.39	26.80	30.10	34.60
19296.30	8.00	10.50	13.79	20.91	9.18	17.41	23.10	25.12	10.88	11.67	14.90	15.11	12.08	20.09	26.81	30.00

Table 4.19: Percentage drag reduction by red gypsum in transporting diesel via pipe with ID 0.0127m

Re	50ppm				100ppm				150ppm				200ppm			
	0.5	1.0	1.5	2.0	0.5	1.0	1.5	2.0	0.5	1.0	1.5	2.0	0.5	1.0	1.5	2.0
18524.44	12.84	14.41	17.55	19.66	15.78	20.24	23.55	29.81	16.59	21.55	24.80	30.02	25.54	33.10	36.45	39.51
16980.74	11.71	13.83	15.17	17.02	14.56	17.76	19.94	21.00	15.11	20.00	22.18	26.13	20.12	26.71	28.43	32.82
15437.04	10.57	12.27	13.40	15.51	12.27	15.18	16.88	18.77	14.36	17.83	19.17	24.40	15.53	19.33	21.91	23.99
13893.33	9.55	10.70	11.85	14.44	10.98	12.72	14.76	16.16	12.00	14.16	16.54	19.55	12.26	16.70	17.37	20.34
12349.63	7.39	8.99	10.02	12.29	8.19	10.09	12.18	14.64	10.31	11.05	14.89	18.00	10.11	13.78	15.98	17.61
10805.93	6.82	8.00	8.52	9.04	7.07	8.88	10.03	10.94	10.02	10.68	12.00	15.11	7.75	30.60	12.09	33.25
9262.22	5.13	6.91	7.78	8.68	5.67	7.81	8.87	9.18	5.90	9.10	10.16	13.37	6.16	9.02	10.63	12.27

Re	400ppm				600ppm				800ppm				1000ppm			
	0.5	1.0	1.5	2.0	0.5	1.0	1.5	2.0	0.5	1.0	1.5	2.0	0.5	1.0	1.5	2.0
18524.44	25.96	34.05	37.76	40.06	27.20	36.00	39.03	41.50	30.62	37.66	40.62	43.16	29.17	37.95	39.87	43.90
16980.74	22.17	28.00	30.04	36.77	22.85	28.92	33.11	37.02	24.30	30.05	34.41	37.75	24.01	32.50	36.33	40.03
15437.04	16.64	22.03	26.15	30.04	16.99	22.71	30.09	33.00	17.04	21.77	23.35	25.40	18.44	25.70	34.70	36.76
13893.33	13.66	17.04	20.70	27.65	14.05	26.64	28.83	30.16	15.63	18.89	20.36	21.19	16.32	24.18	30.01	33.17
12349.63	11.03	15.12	17.75	23.32	12.00	15.00	20.04	27.91	12.67	15.50	17.30	20.03	14.05	19.30	23.17	30.91
10805.93	8.00	16.03	17.02	20.61	8.93	16.87	19.54	22.15	9.34	11.09	13.44	18.84	10.11	18.04	21.11	26.00
9262.22	7.21	11.20	13.38	16.11	7.73	13.05	16.10	18.30	7.91	10.65	12.18	13.29	8.04	16.10	18.82	21.17

APPENDIX D1
FRICITION FACTOR IN PIPE WHILE TESTING MUCILAGE IN WATER

Table 4.20: Friction factor in pipe with ID 0.0381m while testing mucilage in water

Flow rate, m ³ /h	Concentration, ppm	Pressure drop, kg/(ms ²)			After	
		Before	After	%DR	Wall shear stress, τ_w (kg/(ms ²))	Fanning friction factor, C_f
					$\tau_w = D\Delta P/4L$	$C_f = 2\tau_w / \rho v^2$
10.5	50	784	668	14.83	12.72	0.003890302
10.5	100	784	644	17.90	12.26	0.003750074
10.5	150	784	631	19.56	12.01	0.003674250
10.5	200	784	629	19.79	11.98	0.003663744
10.5	400	784	627	20.06	11.94	0.003651412
10.5	600	784	622	20.65	11.85	0.003624462
10.5	800	784	615	21.59	11.71	0.003581526
10.5	1000	784	613	21.77	11.68	0.003573304
10.5	50	1609	1267	21.28	12.06	0.003689706
10.5	100	1609	1181	26.61	11.25	0.003439882
10.5	150	1609	1156	28.18	11.01	0.003366294
10.5	200	1609	1146	28.79	10.91	0.003337702
10.5	400	1609	1135	29.43	10.82	0.003307705
10.5	600	1609	1126	30.00	10.73	0.003280988
10.5	800	1609	1089	32.32	10.37	0.003172247
10.5	1000	1609	1049	34.78	10.00	0.003056944
10.5	50	2503	1683	32.76	10.69	0.003268495
10.5	100	2503	1624	35.11	10.31	0.003154263

Flow rate, m ³ /h	Concentration, ppm	Pressure drop, kg/(ms ²)			After	
		Before	After	%DR	Wall shear stress, τ_w (kg/(ms ²))	Fanning friction factor, C_f
					$\tau_w = D\Delta P/4L$	$C_f = 2\tau_w / \rho v^2$
10.5	150	2503	1589	36.53	10.09	0.003085238
10.5	200	2503	1496	40.22	9.50	0.002905869
10.5	400	2503	1406	43.84	8.93	0.002729903
10.5	600	2503	1372	45.18	8.71	0.002664767
10.5	800	2503	1322	47.17	8.40	0.002568034
10.5	1000	2503	1305	47.85	8.29	0.002534980
10.5	50	3291	2122	35.51	10.11	0.003091298
10.5	100	3291	2103	36.09	10.02	0.003063496
10.5	150	3291	1977	39.94	9.41	0.002878948
10.5	200	3291	1713	47.95	8.16	0.002494992
10.5	400	3291	1684	48.84	8.02	0.002452331
10.5	600	3291	1677	49.03	7.99	0.002443223
10.5	800	3291	1660	49.56	7.91	0.002417818
10.5	1000	3291	1644	50.05	7.83	0.002394330
10.0	50	695	595	14.40	11.33	0.003821358
10.0	100	695	579	16.71	11.03	0.003718235
10.0	150	695	571	17.84	10.88	0.003667790
10.0	200	695	564	18.90	10.74	0.003620469
10.0	400	695	562	19.15	10.70	0.003609309
10.0	600	695	557	19.87	10.61	0.003577166
10.0	800	695	555	20.10	10.58	0.003566899

Flow rate, m ³ /h	Concentration, ppm	Pressure drop, kg/(ms ²)			After	
		Before	After	%DR	Wall shear stress, τ_w (kg/(ms ²))	Fanning friction factor, C_f
					$\tau_w = D\Delta P/4L$	$C_f = 2\tau_w / \rho v^2$
10.0	1000	695	550	20.83	10.48	0.003534310
10.0	50	1443	1162	19.45	11.07	0.003733026
10.0	100	1443	1105	23.39	10.53	0.003550430
10.0	150	1443	1098	23.94	10.45	0.003524941
10.0	200	1443	1031	28.55	9.82	0.003311294
10.0	400	1443	1025	29.00	9.76	0.003290439
10.0	600	1443	1014	29.75	9.66	0.003255681
10.0	800	1443	984	31.80	9.37	0.003160675
10.0	1000	1443	981	32.04	9.34	0.003149553
10.0	50	2206	1514	31.39	9.61	0.003240640
10.0	100	2206	1441	34.67	9.15	0.003085717
10.0	150	2206	1420	35.65	9.01	0.003039429
10.0	200	2206	1242	43.68	7.89	0.002660150
10.0	400	2206	1251	43.30	7.94	0.002678098
10.0	600	2206	1198	45.70	7.61	0.002564740
10.0	800	2206	1180	46.50	7.49	0.002526953
10.0	1000	2206	1171	46.93	7.43	0.002506643
10.0	50	3089	2015	34.78	9.59	0.003235176
10.0	100	3089	1980	35.89	9.43	0.003180115
10.0	150	3089	1887	38.90	8.99	0.003030807
10.0	200	3089	1635	47.07	7.79	0.002625542
10.0	400	3089	1600	48.19	7.62	0.002569986

Flow rate, m ³ /h	Concentration, ppm	Pressure drop, kg/(ms ²)			After	
		Before	After	%DR	Wall shear stress, τ_w (kg/(ms ²))	Fanning friction factor, C_f
					$\tau_w = D\Delta P/4L$	$C_f = 2\tau_w / \rho v^2$
10.0	600	3089	1577	48.94	7.51	0.002532783
10.0	800	3089	1572	49.10	7.49	0.002524846
10.0	1000	3089	1549	49.84	7.38	0.002488139
9.5	50	611	529	13.38	10.08	0.003766790
9.5	100	611	511	16.33	9.74	0.003638505
9.5	150	611	507	17.10	9.65	0.003605020
9.5	200	611	502	17.88	9.56	0.003571101
9.5	400	611	498	18.44	9.49	0.003546749
9.5	600	611	494	19.07	9.42	0.003519352
9.5	800	611	492	19.50	9.37	0.003500653
9.5	1000	611	490	19.86	9.33	0.003484998
9.5	50	1294	1050	18.82	10.01	0.003738224
9.5	100	1294	1015	21.56	9.67	0.003612051
9.5	150	1294	1002	22.56	9.54	0.003566002
9.5	200	1294	959	25.88	9.14	0.003413121
9.5	400	1294	949	26.67	9.04	0.003376742
9.5	600	1294	931	28.03	8.87	0.003314116
9.5	800	1294	919	28.98	8.75	0.003270370
9.5	1000	1294	918	29.06	8.74	0.003266686
9.5	50	2070	1383	33.21	8.78	0.003279990
9.5	100	2070	1362	34.18	8.65	0.003232354

Flow rate, m ³ /h	Concentration, ppm	Pressure drop, kg/(ms ²)			After	
		Before	After	%DR	Wall shear stress, τ_w (kg/(ms ²))	Fanning friction factor, C_f
					$\tau_w = D\Delta P/4L$	$C_f = 2\tau_w / \rho v^2$
9.5	150	2070	1372	33.74	8.71	0.003253962
9.5	200	2070	1117	46.02	7.10	0.002650904
9.5	400	2070	1323	36.11	8.40	0.003137574
9.5	600	2070	1272	38.56	8.08	0.003017257
9.5	800	2070	1264	38.94	8.03	0.002998595
9.5	1000	2070	1220	41.05	7.75	0.002894975
9.5	50	2791	1831	34.40	8.72	0.003257734
9.5	100	2791	1798	35.57	8.56	0.003199631
9.5	150	2791	1730	38.03	8.24	0.003077466
9.5	200	2791	1481	46.92	7.06	0.002635984
9.5	400	2791	1462	47.63	6.96	0.002600725
9.5	600	2791	1507	46.00	7.18	0.002681671
9.5	800	2791	1472	47.26	7.01	0.002619099
9.5	1000	2791	1428	48.83	6.80	0.002541132
9.0	50	521	453	13.00	8.63	0.003594439
9.0	100	521	446	14.39	8.50	0.003537011
9.0	150	521	438	15.95	8.34	0.003472559
9.0	200	521	435	16.56	8.28	0.003447356
9.0	400	521	431	17.30	8.21	0.003416783
9.0	600	521	427	18.04	8.13	0.003386210
9.0	800	521	423	18.85	8.05	0.003352744

Flow rate, m ³ /h	Concentration, ppm	Pressure drop, kg/(ms ²)			After	
		Before	After	%DR	Wall shear stress, τ_w (kg/(ms ²))	Fanning friction factor, C_f
					$\tau_w = D\Delta P/4L$	$C_f = 2\tau_w / \rho v^2$
9.0	1000	521	422	19.05	8.03	0.003344481
9.0	50	1114	928	16.67	8.84	0.003680703
9.0	100	1114	917	17.72	8.73	0.003634324
9.0	150	1114	892	19.90	8.50	0.003538033
9.0	200	1114	836	25.00	7.96	0.003312765
9.0	400	1114	831	25.41	7.91	0.003294655
9.0	600	1114	816	26.77	7.77	0.003234584
9.0	800	1114	810	27.32	7.71	0.003210290
9.0	1000	1114	803	27.92	7.65	0.003183788
9.0	50	1792	1282	28.47	8.14	0.003388279
9.0	100	1792	1212	32.39	7.69	0.003202594
9.0	150	1792	1121	37.46	7.12	0.002962435
9.0	200	1792	968	45.96	6.15	0.002559801
9.0	400	1792	1254	30.04	7.96	0.003313910
9.0	600	1792	1239	30.84	7.87	0.003276015
9.0	800	1792	1260	29.68	8.00	0.003330963
9.0	1000	1792	1250	30.22	7.94	0.003305384
9.0	50	2458	1935	21.27	9.22	0.003836510
9.0	100	2458	1626	33.86	7.74	0.003222999
9.0	150	2458	1528	37.82	7.28	0.003030029
9.0	200	2458	1391	43.40	6.63	0.002758116
9.0	400	2458	1633	33.56	7.78	0.003237618

Flow rate, m ³ /h	Concentration, ppm	Pressure drop, kg/(ms ²)			After	
		Before	After	%DR	Wall shear stress, τ_w (kg/(ms ²))	Fanning friction factor, C_f
					$\tau_w = D\Delta P/4L$	$C_f = 2\tau_w / \rho v^2$
9.0	600	2458	1585	35.51	7.55	0.003142595
9.0	800	2458	1551	36.92	7.38	0.003073886
9.0	1000	2458	1478	39.89	7.04	0.002929158
8.5	50	500	436	12.87	8.30	0.003873103
8.5	100	500	431	13.84	8.21	0.003829985
8.5	150	500	428	14.44	8.15	0.003803313
8.5	200	500	433	13.39	8.25	0.003849988
8.5	400	500	430	13.94	8.20	0.003825539
8.5	600	500	425	14.99	8.10	0.003778865
8.5	800	500	414	17.12	7.89	0.003684182
8.5	1000	500	411	17.84	7.83	0.003652177
8.5	50	1016	869	14.43	8.28	0.003864618
8.5	100	1016	865	14.85	8.24	0.003845649
8.5	150	1016	862	15.13	8.21	0.003833004
8.5	200	1016	855	15.86	8.14	0.003800035
8.5	400	1016	849	16.44	8.09	0.003773840
8.5	600	1016	823	19.04	7.83	0.003656415
8.5	800	1016	780	23.24	7.43	0.003466730
8.5	1000	1016	764	24.83	7.27	0.003394920
8.5	50	1563	1284	17.88	8.15	0.003803715
8.5	100	1563	1207	22.79	7.66	0.003576289

Flow rate, m ³ /h	Concentration, ppm	Pressure drop, kg/(ms ²)			After	
		Before	After	%DR	Wall shear stress, τ_w (kg/(ms ²))	Fanning friction factor, C_f
					$\tau_w = D\Delta P/4L$	$C_f = 2\tau_w / \rho v^2$
8.5	150	1563	1245	20.36	7.90	0.003688844
8.5	200	1563	1182	24.35	7.51	0.003504031
8.5	400	1563	1174	24.87	7.46	0.003479945
8.5	600	1563	1183	24.30	7.51	0.003506347
8.5	800	1563	1187	24.08	7.54	0.003516537
8.5	1000	1563	1162	25.67	7.38	0.003442890
8.5	50	2096	1700	18.89	8.10	0.003778566
8.5	100	2096	1642	21.65	7.82	0.003649990
8.5	150	2096	1606	23.37	7.65	0.003569862
8.5	200	2096	1576	24.79	7.51	0.003503710
8.5	400	2096	1565	25.33	7.45	0.003478554
8.5	600	2096	1552	25.94	7.39	0.003450137
8.5	800	2096	1530	27.00	7.29	0.003400756
8.5	1000	2096	1526	27.19	7.27	0.003391905
8.0	50	489	429	12.26	8.17	0.004306116
8.0	100	489	434	11.23	8.27	0.004356666
8.0	150	489	429	12.27	8.17	0.004305625
8.0	200	489	427	12.73	8.13	0.004283049
8.0	400	489	425	13.11	8.09	0.004264399
8.0	600	489	420	14.03	8.01	0.004219247
8.0	800	489	417	14.79	7.94	0.004181948

Flow rate, m ³ /h	Concentration, ppm	Pressure drop, kg/(ms ²)			After	
		Before	After	%DR	Wall shear stress, τ_w (kg/(ms ²))	Fanning friction factor, C_f
					$\tau_w = D\Delta P/4L$	$C_f = 2\tau_w / \rho v^2$
8.0	1000	489	414	15.30	7.89	0.004156918
8.0	50	992	870	12.34	8.28	0.004363775
8.0	100	992	855	13.82	8.14	0.004290100
8.0	150	992	853	14.01	8.13	0.004280641
8.0	200	992	846	14.67	8.06	0.004247786
8.0	400	992	838	15.52	7.98	0.004205472
8.0	600	992	835	15.78	7.96	0.004192529
8.0	800	992	834	15.93	7.94	0.004185062
8.0	1000	992	823	17.05	7.84	0.004129308
8.0	50	1408	1231	12.56	7.82	0.004118800
8.0	100	1408	1212	13.93	7.70	0.004054268
8.0	150	1408	1199	14.81	7.62	0.004012816
8.0	200	1408	1198	14.95	7.60	0.004006221
8.0	400	1408	1190	15.50	7.55	0.003980314
8.0	600	1408	1136	19.35	7.21	0.003798962
8.0	800	1408	1128	19.89	7.16	0.003773526
8.0	1000	1408	1110	21.17	7.05	0.003713232
8.0	50	1965	1703	13.35	8.11	0.004272188
8.0	100	1965	1681	14.46	8.01	0.004217460
8.0	150	1965	1656	15.75	7.88	0.004153858
8.0	200	1965	1650	16.03	7.86	0.004140053
8.0	400	1965	1637	16.70	7.80	0.004107020

Flow rate, m ³ /h	Concentration, ppm	Pressure drop, kg/(ms ²)			After	
		Before	After	%DR	Wall shear stress, τ_w (kg/(ms ²))	Fanning friction factor, C_f
					$\tau_w = D\Delta P/4L$	$C_f = 2\tau_w / \rho v^2$
8.0	600	1965	1625	17.31	7.74	0.004076944
8.0	800	1965	1548	21.24	7.37	0.003883180
8.0	1000	1965	1532	22.05	7.29	0.003843243
7.5	50	400	367	8.21	6.99	0.004192683
7.5	100	400	363	9.29	6.91	0.004143352
7.5	150	400	359	10.18	6.84	0.004102699
7.5	200	400	353	11.71	6.73	0.004032814
7.5	400	400	352	12.07	6.70	0.004016370
7.5	600	400	349	12.75	6.65	0.003985310
7.5	800	400	348	13.00	6.63	0.003973891
7.5	1000	400	345	13.68	6.58	0.003942830
7.5	50	873	787	9.90	7.49	0.004491027
7.5	100	873	778	10.87	7.41	0.004442678
7.5	150	873	774	11.29	7.38	0.004421743
7.5	200	873	768	12.04	7.31	0.004384359
7.5	400	873	752	13.89	7.16	0.004292146
7.5	600	873	750	14.12	7.14	0.004280682
7.5	800	873	741	15.10	7.06	0.004231834
7.5	1000	873	734	15.87	7.00	0.004193453
7.5	50	1291	1192	7.67	7.57	0.004537164
7.5	100	1291	1180	8.63	7.49	0.004489989

Flow rate, m ³ /h	Concentration, ppm	Pressure drop, kg/(ms ²)			After	
		Before	After	%DR	Wall shear stress, τ_w (kg/(ms ²))	Fanning friction factor, C_f
					$\tau_w = D\Delta P/4L$	$C_f = 2\tau_w / \rho v^2$
7.5	150	1291	1178	8.74	7.48	0.004484583
7.5	200	1291	1184	8.32	7.52	0.004505222
7.5	400	1291	1110	14.02	7.05	0.004225120
7.5	600	1291	1098	14.97	6.97	0.004178437
7.5	800	1291	1084	16.07	6.88	0.004124382
7.5	1000	1291	1074	16.84	6.82	0.004086543
7.5	50	1657	1470	11.26	7.00	0.004197770
7.5	100	1657	1448	12.62	6.90	0.004133436
7.5	150	1657	1436	13.36	6.84	0.004098431
7.5	200	1657	1427	13.90	6.79	0.004072887
7.5	400	1657	1413	14.72	6.73	0.004034097
7.5	600	1657	1392	16.00	6.63	0.003973548
7.5	800	1657	1376	16.95	6.55	0.003928609
7.5	1000	1657	1372	17.18	6.54	0.003917729

Table 4.21: Friction factor in pipe with ID 0.0254m while testing mucilage in water

Flow rate, m ³ /h	Concentration, ppm	Pressure drop, kg/(ms ²)			After	
		Before	After	%DR	Wall shear stress, τ_w (kg/(ms ²))	Fanning friction factor, C_f
					$\tau_w = D\Delta P/4L$	$C_f = 2\tau_w / \rho v^2$
8.0	50	3038	2548	16.13	32.36	0.003367575
8.0	100	3038	2522	16.98	32.03	0.003333446
8.0	150	3038	2517	17.14	31.97	0.003327022
8.0	200	3038	2521	17.03	32.01	0.003331438
8.0	400	3038	2493	17.94	31.66	0.003294900
8.0	600	3038	2479	18.39	31.49	0.003276831
8.0	800	3038	2369	22.03	30.08	0.003130677
8.0	1000	3038	2313	23.87	29.37	0.003056796
8.0	50	6317	4952	21.61	31.44	0.003272385
8.0	100	6317	4637	26.60	29.44	0.003064078
8.0	150	6317	4545	28.05	28.86	0.003003548
8.0	200	6317	4428	29.90	28.12	0.002926320
8.0	400	6317	4402	30.31	27.95	0.002909205
8.0	600	6317	4309	31.78	27.37	0.002847839
8.0	800	6317	4213	33.31	26.75	0.002783970
8.0	1000	6317	4177	33.87	26.53	0.002760593
8.0	50	9664	6988	27.69	29.58	0.003078626
8.0	100	9664	6858	29.04	29.03	0.003021149
8.0	150	9664	6650	31.19	28.15	0.002929612
8.0	200	9664	6601	31.70	27.94	0.002907899

Flow rate, m ³ /h	Concentration, ppm	Pressure drop, kg/(ms ²)			After	
		Before	After	%DR	Wall shear stress, τ_w (kg/(ms ²))	Fanning friction factor, C_f
					$\tau_w = D\Delta P/4L$	$C_f = 2\tau_w / \rho v^2$
8.0	400	9664	6562	32.10	27.78	0.002890869
8.0	600	9664	6441	33.35	27.27	0.002837649
8.0	800	9664	6339	34.41	26.83	0.002792519
8.0	1000	9664	6047	37.43	25.60	0.002663942
8.0	50	14229	9795	31.16	31.10	0.003236519
8.0	100	14229	9939	30.15	31.56	0.003284004
8.0	150	14229	9683	31.95	30.74	0.003199377
8.0	200	14229	9531	33.02	30.26	0.003149071
8.0	400	14229	9301	34.63	29.53	0.003073377
8.0	600	14229	8976	36.92	28.50	0.002965712
8.0	800	14229	8552	39.90	27.15	0.002825607
8.0	1000	14229	8371	41.17	26.58	0.002765898
7.5	50	2996	2529	15.59	32.12	0.003802910
7.5	100	2996	2553	14.80	32.42	0.003838502
7.5	150	2996	2529	15.58	32.12	0.003803361
7.5	200	2996	2513	16.12	31.92	0.003779032
7.5	400	2996	2484	17.09	31.55	0.003735331
7.5	600	2996	2447	18.32	31.08	0.003679916
7.5	800	2996	2340	21.90	29.72	0.003518627
7.5	1000	2996	2298	23.31	29.18	0.003455102
7.5	50	6003	4601	23.36	29.21	0.003459188

Flow rate, m ³ /h	Concentration, ppm	Pressure drop, kg/(ms ²)			After	
		Before	After	%DR	Wall shear stress, τ_w (kg/(ms ²))	Fanning friction factor, C_f
					$\tau_w = D\Delta P/4L$	$C_f = 2\tau_w / \rho v^2$
7.5	100	6003	4549	24.22	28.89	0.003420372
7.5	150	6003	4389	26.88	27.87	0.003300311
7.5	200	6003	4245	29.28	26.96	0.003191986
7.5	400	6003	4213	29.82	26.75	0.003167613
7.5	600	6003	4147	30.91	26.34	0.003118415
7.5	800	6003	4206	29.94	26.71	0.003162196
7.5	1000	6003	4195	30.11	26.64	0.003154523
7.5	50	9072	6531	28.01	27.65	0.003273666
7.5	100	9072	6543	27.88	27.70	0.003279577
7.5	150	9072	6430	29.12	27.22	0.003223190
7.5	200	9072	6346	30.05	26.86	0.003180899
7.5	400	9072	6297	30.59	26.66	0.003156343
7.5	600	9072	6190	31.77	26.20	0.003102684
7.5	800	9072	6045	33.37	25.59	0.003029926
7.5	1000	9072	5747	36.65	24.33	0.002880771
7.5	50	12210	8532	30.12	27.09	0.003207664
7.5	100	12210	8441	30.87	26.80	0.003173238
7.5	150	12210	8421	31.03	26.74	0.003165893
7.5	200	12210	8210	32.76	26.07	0.003086482
7.5	400	12210	8089	33.75	25.68	0.003041038
7.5	600	12210	7755	36.49	24.62	0.002915266
7.5	800	12210	7604	37.72	24.14	0.002858806

Flow rate, m ³ /h	Concentration, ppm	Pressure drop, kg/(ms ²)			After	
		Before	After	%DR	Wall shear stress, τ_w (kg/(ms ²))	Fanning friction factor, C_f
					$\tau_w = D\Delta P/4L$	$C_f = 2\tau_w / \rho v^2$
7.5	1000	12210	7336	39.92	23.29	0.002757820
7.0	50	2601	2217	14.77	28.15	0.003826834
7.0	100	2601	2243	13.75	28.49	0.003872632
7.0	150	2601	2213	14.90	28.11	0.003820997
7.0	200	2601	2197	15.55	27.90	0.003791812
7.0	400	2601	2171	16.53	27.57	0.003747810
7.0	600	2601	2133	17.99	27.09	0.003682256
7.0	800	2601	2073	20.31	26.32	0.003578088
7.0	1000	2601	2058	20.87	26.14	0.003552944
7.0	50	5451	4486	17.70	28.49	0.003872156
7.0	100	5451	4177	23.38	26.52	0.003604916
7.0	150	5451	4059	25.53	25.78	0.003503760
7.0	200	5451	4032	26.03	25.60	0.003480235
7.0	400	5451	4117	24.48	26.14	0.003553162
7.0	600	5451	3992	26.76	25.35	0.003445889
7.0	800	5451	3909	28.29	24.82	0.003373904
7.0	1000	5451	3832	29.70	24.33	0.003307564
7.0	50	8532	6318	25.95	26.75	0.003635477
7.0	100	8532	6259	26.64	26.50	0.003601602
7.0	150	8532	6192	27.43	26.21	0.003562817
7.0	200	8532	6069	28.87	25.69	0.003492120

Flow rate, m ³ /h	Concentration, ppm	Pressure drop, kg/(ms ²)			After	
		Before	After	%DR	Wall shear stress, τ_w (kg/(ms ²))	Fanning friction factor, C_f
					$\tau_w = D\Delta P/4L$	$C_f = 2\tau_w / \rho v^2$
7.0	400	8532	6001	29.67	25.40	0.003452844
7.0	600	8532	5879	31.10	24.89	0.003382639
7.0	800	8532	5776	32.30	24.45	0.003323725
7.0	1000	8532	5497	35.57	23.27	0.003163185
7.0	50	10300	7303	29.10	23.19	0.003151594
7.0	100	10300	7210	30.00	22.89	0.003111588
7.0	150	10300	7163	30.46	22.74	0.003091140
7.0	200	10300	6975	32.28	22.15	0.003010239
7.0	400	10300	6887	33.14	21.86	0.002972011
7.0	600	10300	6644	35.50	21.09	0.002867106
7.0	800	10300	6522	36.68	20.71	0.002814654
7.0	1000	10300	6295	38.88	19.99	0.002716861
6.5	50	2201	1933	12.18	24.55	0.003869810
6.5	100	2201	1917	12.89	24.35	0.003838524
6.5	150	2201	1908	13.32	24.23	0.003819576
6.5	200	2201	1891	14.10	24.01	0.003785205
6.5	400	2201	1860	15.49	23.62	0.003723954
6.5	600	2201	1824	17.13	23.16	0.003651687
6.5	800	2201	1787	18.83	22.69	0.003576776
6.5	1000	2201	1776	19.33	22.55	0.003554744
6.5	50	4884	4165	14.73	26.45	0.004168868

Flow rate, m ³ /h	Concentration, ppm	Pressure drop, kg/(ms ²)			After	
		Before	After	%DR	Wall shear stress, τ_w (kg/(ms ²))	Fanning friction factor, C_f
					$\tau_w = D\Delta P/4L$	$C_f = 2\tau_w / \rho v^2$
6.5	100	4884	3877	20.62	24.62	0.003880904
6.5	150	4884	3746	23.30	23.79	0.003749878
6.5	200	4884	3714	23.95	23.59	0.003718100
6.5	400	4884	3954	19.05	25.11	0.003957662
6.5	600	4884	3911	19.93	24.83	0.003914638
6.5	800	4884	3850	21.17	24.45	0.003854015
6.5	1000	4884	3773	22.74	23.96	0.003777257
6.5	50	7110	5207	26.77	22.04	0.003474670
6.5	100	7110	5263	25.98	22.28	0.003512154
6.5	150	7110	5101	28.26	21.59	0.003403971
6.5	200	7110	5042	29.08	21.35	0.003365063
6.5	400	7110	5044	29.06	21.35	0.003366012
6.5	600	7110	4964	30.18	21.02	0.003312870
6.5	800	7110	4839	31.94	20.49	0.003229360
6.5	1000	7110	4663	34.41	19.74	0.003112162
6.5	50	9036	6425	28.90	20.40	0.003215600
6.5	100	9036	6406	29.11	20.34	0.003206102
6.5	150	9036	6331	29.94	20.10	0.003168564
6.5	200	9036	6152	31.92	19.53	0.003079016
6.5	400	9036	6118	32.29	19.43	0.003062282
6.5	600	9036	6019	33.39	19.11	0.003012533
6.5	800	9036	5927	34.41	18.82	0.002966402

Flow rate, m ³ /h	Concentration, ppm	Pressure drop, kg/(ms ²)			After	
		Before	After	%DR	Wall shear stress, τ_w (kg/(ms ²))	Fanning friction factor, C_f
					$\tau_w = D\Delta P/4L$	$C_f = 2\tau_w / \rho v^2$
6.5	1000	9036	5850	35.26	18.57	0.002927960
6.0	50	2010	1789	11.00	22.72	0.004203262
6.0	100	2010	1761	12.37	22.37	0.004138560
6.0	150	2010	1753	12.78	22.26	0.004119197
6.0	200	2010	1729	13.96	21.96	0.004063468
6.0	400	2010	1691	15.87	21.48	0.003973263
6.0	600	2010	1683	16.29	21.37	0.003953428
6.0	800	2010	1721	14.40	21.85	0.004042688
6.0	1000	2010	1675	16.65	21.28	0.003936426
6.0	50	4083	3538	13.35	22.47	0.004156410
6.0	100	4083	3385	17.09	21.50	0.003977010
6.0	150	4083	3414	16.39	21.68	0.004010587
6.0	200	4083	3359	17.74	21.33	0.003945831
6.0	400	4083	3397	16.80	21.57	0.003990921
6.0	600	4083	3359	17.72	21.33	0.003946790
6.0	800	4083	3267	19.98	20.75	0.003838383
6.0	1000	4083	3215	21.27	20.41	0.003776505
6.0	50	6147	4608	25.03	19.51	0.003609357
6.0	100	6147	4479	27.14	18.96	0.003507773
6.0	150	6147	4432	27.90	18.76	0.003471184
6.0	200	6147	4425	28.01	18.73	0.003465888

Flow rate, m ³ /h	Concentration, ppm	Pressure drop, kg/(ms ²)			After	
		Before	After	%DR	Wall shear stress, τ_w (kg/(ms ²))	Fanning friction factor, C_f
					$\tau_w = D\Delta P/4L$	$C_f = 2\tau_w / \rho v^2$
6.0	400	6147	4386	28.65	18.57	0.003435076
6.0	600	6147	4307	29.94	18.23	0.003372970
6.0	800	6147	4218	31.38	17.86	0.003303643
6.0	1000	6147	4162	32.30	17.62	0.003259350
6.0	50	7651	5526	27.77	17.55	0.003246207
6.0	100	7651	5532	27.69	17.57	0.003249802
6.0	150	7651	5431	29.02	17.24	0.003190029
6.0	200	7651	5332	30.31	16.93	0.003132053
6.0	400	7651	5265	31.18	16.72	0.003092953
6.0	600	7651	5182	32.27	16.45	0.003043965
6.0	800	7651	5128	32.98	16.28	0.003012056
6.0	1000	7651	5015	34.45	15.92	0.002945990
5.5	50	1685	1497	11.16	19.01	0.004185872
5.5	100	1685	1561	7.35	19.83	0.004365388
5.5	150	1685	1551	7.94	19.70	0.004337589
5.5	200	1685	1579	6.28	20.06	0.004415803
5.5	400	1685	1565	7.14	19.87	0.004375282
5.5	600	1685	1548	8.12	19.66	0.004329108
5.5	800	1685	1546	8.22	19.64	0.004324396
5.5	1000	1685	1525	9.49	19.37	0.004264558
5.5	50	2964	2644	10.81	16.79	0.003696084

Flow rate, m ³ /h	Concentration, ppm	Pressure drop, kg/(ms ²)			After	
		Before	After	%DR	Wall shear stress, τ_w (kg/(ms ²))	Fanning friction factor, C_f
					$\tau_w = D\Delta P/4L$	$C_f = 2\tau_w / \rho v^2$
5.5	100	2964	2549	13.99	16.19	0.003564303
5.5	150	2964	2544	14.17	16.15	0.003556844
5.5	200	2964	2552	13.90	16.21	0.003568033
5.5	400	2964	2543	14.21	16.15	0.003555186
5.5	600	2964	2513	15.20	15.96	0.003514160
5.5	800	2964	2483	16.23	15.77	0.003471476
5.5	1000	2964	2441	17.65	15.50	0.003412631
5.5	50	4513	3606	20.09	15.27	0.003361419
5.5	100	4513	3540	21.56	14.99	0.003299584
5.5	150	4513	3533	21.72	14.96	0.003292853
5.5	200	4513	3481	22.86	14.74	0.003244899
5.5	400	4513	3460	23.33	14.65	0.003225129
5.5	600	4513	3361	25.53	14.23	0.003132586
5.5	800	4513	3260	27.77	13.80	0.003038360
5.5	1000	4513	3241	28.19	13.72	0.003020692
5.5	50	6487	5113	21.18	16.23	0.003574356
5.5	100	6487	5047	22.20	16.02	0.003528101
5.5	150	6487	4976	23.30	15.80	0.003478218
5.5	200	6487	4881	24.76	15.50	0.003412009
5.5	400	6487	4746	26.84	15.07	0.003317685
5.5	600	6487	4648	28.35	14.76	0.003249209
5.5	800	6487	4531	30.16	14.38	0.003167128

Flow rate, m ³ /h	Concentration, ppm	Pressure drop, kg/(ms ²)			After	
		Before	After	%DR	Wall shear stress, τ_w (kg/(ms ²))	Fanning friction factor, C_f
					$\tau_w = D\Delta P/4L$	$C_f = 2\tau_w / \rho v^2$
5.5	1000	6487	4452	31.37	14.14	0.003112257
5.0	50	1255	1213	3.31	15.41	0.004105709
5.0	100	1255	1205	3.98	15.30	0.004077259
5.0	150	1255	1191	5.10	15.13	0.004029701
5.0	200	1255	1172	6.62	14.88	0.003965158
5.0	400	1255	1176	6.30	14.93	0.003978746
5.0	600	1255	1158	7.75	14.70	0.003917175
5.0	800	1255	1155	7.94	14.67	0.003909107
5.0	1000	1255	1119	10.82	14.21	0.003786815
5.0	50	2439	2304	5.55	14.63	0.003897146
5.0	100	2439	2244	8.00	14.25	0.003796055
5.0	150	2439	2242	8.08	14.24	0.003792754
5.0	200	2439	2259	7.39	14.34	0.003821225
5.0	400	2439	2245	7.94	14.26	0.003798531
5.0	600	2439	2241	8.11	14.23	0.003791516
5.0	800	2439	2191	10.15	13.92	0.003707343
5.0	1000	2439	2140	12.26	13.59	0.003620281
5.0	50	4001	3705	7.39	15.69	0.004178958
5.0	100	4001	3461	13.50	14.65	0.003903249
5.0	150	4001	3318	17.07	14.05	0.003742156
5.0	200	4001	3262	18.47	13.81	0.003678982

Flow rate, m ³ /h	Concentration, ppm	Pressure drop, kg/(ms ²)			After	
		Before	After	%DR	Wall shear stress, τ_w (kg/(ms ²))	Fanning friction factor, C_f
					$\tau_w = D\Delta P/4L$	$C_f = 2\tau_w / \rho v^2$
5.0	400	4001	3197	20.10	13.53	0.003605429
5.0	600	4001	3154	21.17	13.35	0.003557146
5.0	800	4001	3276	18.13	13.87	0.003694324
5.0	1000	4001	3234	19.17	13.69	0.003647395
5.0	50	5763	5350	7.17	16.99	0.004525222
5.0	100	5763	4955	14.02	15.73	0.004191302
5.0	150	5763	4733	17.88	15.03	0.004003137
5.0	200	5763	4674	18.90	14.84	0.003953415
5.0	400	5763	4557	20.92	14.47	0.003854945
5.0	600	5763	4438	22.99	14.09	0.003754038
5.0	800	5763	4353	24.47	13.82	0.003681892
5.0	1000	5763	4228	26.64	13.42	0.003576110

Table 4.22: Friction factor in pipe with ID 0.0127m while testing mucilage in water

Flow rate, m ³ /h	Concentration, ppm	Pressure drop, kg/(ms ²)			After	
		Before	After	%DR	Wall shear stress, τ_w (kg/(ms ²))	Fanning friction factor, C_f
					$\tau_w = D\Delta P/4L$	$C_f = 2\tau_w / \rho v^2$
2.4	50	10961	9414	14.11	59.78	0.004320392
2.4	100	10961	8875	19.03	56.36	0.004072909
2.4	150	10961	8782	19.88	55.77	0.004030153
2.4	200	10961	8623	21.33	54.76	0.003957216
2.4	400	10961	8748	20.19	55.55	0.004014560
2.4	600	10961	8539	22.10	54.22	0.003918484
2.4	800	10961	8478	22.65	53.84	0.003890818
2.4	1000	10961	8340	23.91	52.96	0.003827438
2.4	50	20507	16369	20.18	51.97	0.003755902
2.4	100	20507	15895	22.49	50.47	0.003647206
2.4	150	20507	15267	25.55	48.47	0.003503219
2.4	200	20507	14970	27.00	47.53	0.003434990
2.4	400	20507	14775	27.95	46.91	0.003390288
2.4	600	20507	14513	29.23	46.08	0.003330058
2.4	800	20507	14113	31.18	44.81	0.003238301
2.4	1000	20507	13736	33.02	43.61	0.003151721
2.4	50	28123	21638	23.06	45.80	0.003309962
2.4	100	28123	20876	25.77	44.19	0.003193378
2.4	150	28123	20308	27.79	42.98	0.003106477
2.4	200	28123	19959	29.03	42.25	0.003053132
2.4	400	28123	18139	35.50	38.39	0.002774793

Flow rate, m ³ /h	Concentration, ppm	Pressure drop, kg/(ms ²)			After	
		Before	After	%DR	Wall shear stress, τ_w (kg/(ms ²))	Fanning friction factor, C_f
					$\tau_w = D\Delta P/4L$	$C_f = 2\tau_w / \rho v^2$
2.4	600	28123	17824	36.62	37.73	0.002726610
2.4	800	28123	15032	46.55	31.82	0.002299421
2.4	1000	28123	15223	45.87	32.22	0.002328675
2.4	50	37466	27841	25.69	44.20	0.003194148
2.4	100	37466	26601	29.00	42.23	0.003051871
2.4	150	37466	25930	30.79	41.16	0.002974929
2.4	200	37466	20363	45.65	32.33	0.002336185
2.4	400	37466	19078	49.08	30.29	0.002188750
2.4	600	37466	18778	49.88	29.81	0.002154363
2.4	800	37466	18306	51.14	29.06	0.002100203
2.4	1000	37466	17920	52.17	28.45	0.002055929
2.2	50	9847	8490	13.78	53.91	0.004636812
2.2	100	9847	8093	17.81	51.39	0.004420083
2.2	150	9847	8021	18.54	50.94	0.004380825
2.2	200	9847	7966	19.10	50.59	0.004350709
2.2	400	9847	8012	18.64	50.87	0.004375447
2.2	600	9847	7653	22.28	48.60	0.004179692
2.2	800	9847	7550	23.33	47.94	0.004123224
2.2	1000	9847	7503	23.80	47.65	0.004097948
2.2	50	17588	14150	19.55	44.92	0.003863848
2.2	100	17588	13909	20.92	44.16	0.003798050

Flow rate, m ³ /h	Concentration, ppm	Pressure drop, kg/(ms ²)			After	
		Before	After	%DR	Wall shear stress, τ_w (kg/(ms ²)) $\tau_w = D\Delta P/4L$	Fanning friction factor, C_f $C_f = 2\tau_w / \rho v^2$
2.2	150	17588	13508	23.20	42.89	0.003688546
2.2	200	17588	13117	25.42	41.65	0.003581924
2.2	400	17588	12904	26.63	40.97	0.003523810
2.2	600	17588	12820	27.11	40.70	0.003500757
2.2	800	17588	12480	29.04	39.63	0.003408063
2.2	1000	17588	12352	29.77	39.22	0.003373003
2.2	50	23009	18032	21.63	38.17	0.003282720
2.2	100	23009	17531	23.81	37.11	0.003191406
2.2	150	23009	17096	25.70	36.19	0.003112238
2.2	200	23009	16902	26.54	35.78	0.003077053
2.2	400	23009	15105	34.35	31.97	0.002749912
2.2	600	23009	15172	34.06	32.11	0.002762059
2.2	800	23009	11369	50.59	24.06	0.002069659
2.2	1000	23009	12607	45.21	26.68	0.002295014
2.2	50	30203	23030	23.75	36.56	0.003144398
2.2	100	30203	21695	28.17	34.44	0.002962126
2.2	150	30203	20786	31.18	33.00	0.002837999
2.2	200	30203	16962	43.84	26.93	0.002315926
2.2	400	30203	15422	48.94	24.48	0.002105612
2.2	600	30203	15286	49.39	24.27	0.002087055
2.2	800	30203	15162	49.80	24.07	0.002070148
2.2	1000	30203	14528	51.90	23.06	0.001983548

Flow rate, m ³ /h	Concentration, ppm	Pressure drop, kg/(ms ²)			After	
		Before	After	%DR	Wall shear stress, τ_w (kg/(ms ²))	Fanning friction factor, C_f
					$\tau_w = D\Delta P/4L$	$C_f = 2\tau_w / \rho v^2$
2.0	50	7125	6177	13.30	39.23	0.004082224
2.0	100	7125	6029	15.38	38.29	0.003984289
2.0	150	7125	5942	16.60	37.73	0.003926846
2.0	200	7125	5820	18.32	36.96	0.003845860
2.0	400	7125	5778	18.90	36.69	0.003818551
2.0	600	7125	5632	20.95	35.77	0.003722028
2.0	800	7125	5575	21.76	35.40	0.003683890
2.0	1000	7125	5381	24.48	34.17	0.003555820
2.0	50	15857	13065	17.61	41.48	0.004316765
2.0	100	15857	12660	20.16	40.20	0.004183160
2.0	150	15857	12424	21.65	39.45	0.004105092
2.0	200	15857	12278	22.57	38.98	0.004056890
2.0	400	15857	11861	25.20	37.66	0.003919093
2.0	600	15857	11783	25.69	37.41	0.003893420
2.0	800	15857	11301	28.73	35.88	0.003734141
2.0	1000	15857	12105	23.66	38.43	0.003999780
2.0	50	20707	16613	19.77	35.16	0.003659533
2.0	100	20707	16193	21.80	34.27	0.003566938
2.0	150	20707	15857	23.42	33.56	0.003493045
2.0	200	20707	15756	23.91	33.35	0.003470695
2.0	400	20707	14309	30.90	30.29	0.003151860
2.0	600	20707	14021	32.29	29.68	0.003088458

Flow rate, m ³ /h	Concentration, ppm	Pressure drop, kg/(ms ²)			After	
		Before	After	%DR	Wall shear stress, τ_w (kg/(ms ²))	Fanning friction factor, C_f
					$\tau_w = D\Delta P/4L$	$C_f = 2\tau_w / \rho v^2$
2.0	800	20707	12793	38.22	27.08	0.002817972
2.0	1000	20707	12855	37.92	27.21	0.002831656
2.0	50	28674	22136	22.80	35.14	0.003657114
2.0	100	28674	20651	27.98	32.78	0.003411727
2.0	150	28674	20327	29.11	32.27	0.003358197
2.0	200	28674	16926	40.97	26.87	0.002796366
2.0	400	28674	14905	48.02	23.66	0.002462394
2.0	600	28674	14721	48.66	23.37	0.002432076
2.0	800	28674	14518	49.37	23.05	0.002398442
2.0	1000	28674	14019	51.11	22.25	0.002316014
1.8	50	5639	5014	11.09	31.84	0.004090351
1.8	100	5639	4856	13.89	30.83	0.003961536
1.8	150	5639	4769	15.43	30.28	0.003890687
1.8	200	5639	4714	16.40	29.94	0.003846062
1.8	400	5639	4631	17.87	29.41	0.003778434
1.8	600	5639	4499	20.21	28.57	0.003670781
1.8	800	5639	4564	19.07	28.98	0.003723227
1.8	1000	5639	4442	21.22	28.21	0.003624315
1.8	50	13672	11525	15.70	36.59	0.004701512
1.8	100	13672	11109	18.75	35.27	0.004531410
1.8	150	13672	10990	19.62	34.89	0.004482889

Flow rate, m ³ /h	Concentration, ppm	Pressure drop, kg/(ms ²)			After	
		Before	After	%DR	Wall shear stress, τ_w (kg/(ms ²))	Fanning friction factor, C_f
					$\tau_w = D\Delta P/4L$	$C_f = 2\tau_w / \rho v^2$
1.8	200	13672	10809	20.94	34.32	0.004409271
1.8	400	13672	10611	22.39	33.69	0.004328402
1.8	600	13672	10527	23.00	33.42	0.004294382
1.8	800	13672	10294	24.71	32.68	0.004199013
1.8	1000	13672	10526	23.01	33.42	0.004293824
1.8	50	16833	13662	18.84	28.92	0.003715268
1.8	100	16833	13293	21.03	28.14	0.003615017
1.8	150	16833	13305	20.96	28.16	0.003618221
1.8	200	16833	13290	21.05	28.13	0.003614101
1.8	400	16833	11746	30.22	24.86	0.003194325
1.8	600	16833	11485	31.77	24.31	0.003123371
1.8	800	16833	11211	33.40	23.73	0.003048754
1.8	1000	16833	10941	35.00	23.16	0.002975511
1.8	50	22195	17323	21.95	27.50	0.003533263
1.8	100	22195	16202	27.00	25.72	0.003304653
1.8	150	22195	15818	28.73	25.11	0.003226338
1.8	200	22195	13317	40.00	21.14	0.002716153
1.8	400	22195	11763	47.00	18.67	0.002399269
1.8	600	22195	11561	47.91	18.35	0.002358074
1.8	800	22195	11541	48.00	18.32	0.002354000
1.8	1000	22195	11299	49.09	17.94	0.002304656

Flow rate, m ³ /h	Concentration, ppm	Pressure drop, kg/(ms ²)			After	
		Before	After	%DR	Wall shear stress, τ_w (kg/(ms ²))	Fanning friction factor, C_f
					$\tau_w = D\Delta P/4L$	$C_f = 2\tau_w / \rho v^2$
1.6	50	5018	4494	10.44	28.54	0.004640424
1.6	100	5018	4341	13.50	27.56	0.004481875
1.6	150	5018	4313	14.05	27.39	0.004453377
1.6	200	5018	4276	14.78	27.15	0.004415553
1.6	400	5018	4178	16.73	26.53	0.004314517
1.6	600	5018	4068	18.93	25.83	0.004200527
1.6	800	5018	4114	18.01	26.13	0.004248195
1.6	1000	5018	4024	19.80	25.56	0.004155449
1.6	50	10856	9040	16.73	28.70	0.004667038
1.6	100	10856	8890	18.11	28.23	0.004589693
1.6	150	10856	8818	18.77	28.00	0.004552702
1.6	200	10856	8776	19.16	27.86	0.004530844
1.6	400	10856	8188	24.58	26.00	0.004227069
1.6	600	10856	8891	18.10	28.23	0.004590254
1.6	800	10856	8318	23.38	26.41	0.004294325
1.6	1000	10856	8515	21.56	27.04	0.004396331
1.6	50	14555	11734	19.38	24.84	0.004038747
1.6	100	14555	11692	19.67	24.75	0.004024220
1.6	150	14555	11667	19.84	24.70	0.004015703
1.6	200	14555	11661	19.88	24.68	0.004013699
1.6	400	14555	10653	26.81	22.55	0.003666533
1.6	600	14555	10749	26.15	22.75	0.003699597

Flow rate, m ³ /h	Concentration, ppm	Pressure drop, kg/(ms ²)			After	
		Before	After	%DR	Wall shear stress, τ_w (kg/(ms ²))	Fanning friction factor, C_f
					$\tau_w = D\Delta P/4L$	$C_f = 2\tau_w / \rho v^2$
1.6	800	14555	10142	30.32	21.47	0.003490696
1.6	1000	14555	9695	33.39	20.52	0.003336901
1.6	50	19047	15041	21.03	23.88	0.003882770
1.6	100	19047	14476	24.00	22.98	0.003736742
1.6	150	19047	14182	25.54	22.51	0.003661024
1.6	200	19047	12000	37.00	19.05	0.003097563
1.6	400	19047	10476	45.00	16.63	0.002704221
1.6	600	19047	10523	44.75	16.71	0.002716513
1.6	800	19047	10666	44.00	16.93	0.002753389
1.6	1000	19047	10257	46.15	16.28	0.002647678
1.4	50	4730	4256	10.03	27.02	0.005739257
1.4	100	4730	4169	11.86	26.47	0.005622520
1.4	150	4730	4125	12.80	26.19	0.005562557
1.4	200	4730	4069	13.97	25.84	0.005487922
1.4	400	4730	4028	14.85	25.58	0.005431786
1.4	600	4730	3993	15.59	25.35	0.005384581
1.4	800	4730	3936	16.78	25.00	0.005308669
1.4	1000	4730	3826	19.11	24.30	0.005160037
1.4	50	8226	7059	14.19	22.41	0.004759852
1.4	100	8226	6836	16.90	21.70	0.004609529
1.4	150	8226	6745	18.00	21.42	0.004548513

Flow rate, m ³ /h	Concentration, ppm	Pressure drop, kg/(ms ²)			After	
		Before	After	%DR	Wall shear stress, τ_w (kg/(ms ²))	Fanning friction factor, C_f
					$\tau_w = D\Delta P/4L$	$C_f = 2\tau_w / \rho v^2$
1.4	200	8226	6663	19.00	21.16	0.004493043
1.4	400	8226	6612	19.62	20.99	0.004458652
1.4	600	8226	6814	17.17	21.63	0.004594552
1.4	800	8226	6693	18.64	21.25	0.004513012
1.4	1000	8226	6509	20.87	20.67	0.004389315
1.4	50	12177	9913	18.59	20.98	0.004456497
1.4	100	12177	9908	18.63	20.97	0.004454308
1.4	150	12177	9911	18.61	20.98	0.004455402
1.4	200	12177	9854	19.08	20.86	0.004429674
1.4	400	12177	8727	28.33	18.47	0.003923316
1.4	600	12177	9406	22.76	19.91	0.004228226
1.4	800	12177	8615	29.25	18.24	0.003872954
1.4	1000	12177	8256	32.20	17.48	0.003711467
1.4	50	15693	12584	19.81	19.98	0.004242902
1.4	100	15693	12241	22.00	19.43	0.004127028
1.4	150	15693	12137	22.66	19.27	0.004092107
1.4	200	15693	10514	33.00	16.69	0.003545011
1.4	400	15693	9259	41.00	14.70	0.003121726
1.4	600	15693	9392	40.15	14.91	0.003166700
1.4	800	15693	9259	41.00	14.70	0.003121726
1.4	1000	15693	9350	40.42	14.84	0.003152414

Flow rate, m ³ /h	Concentration, ppm	Pressure drop, kg/(ms ²)			After	
		Before	After	%DR	Wall shear stress, τ_w (kg/(ms ²))	Fanning friction factor, C_f
					$\tau_w = D\Delta P/4L$	$C_f = 2\tau_w / \rho v^2$
1.2	50	3006	2711	9.81	17.22	0.004976658
1.2	100	3006	2683	10.73	17.04	0.004925892
1.2	150	3006	2637	12.29	16.74	0.004839812
1.2	200	3006	2645	12.01	16.80	0.004855262
1.2	400	3006	2580	14.16	16.39	0.004736626
1.2	600	3006	2551	15.12	16.20	0.004683654
1.2	800	3006	2518	16.23	15.99	0.004622404
1.2	1000	3006	2461	18.12	15.63	0.004518114
1.2	50	5641	4890	13.32	15.52	0.004487820
1.2	100	5641	4839	14.22	15.36	0.004441223
1.2	150	5641	4766	15.52	15.13	0.004373916
1.2	200	5641	4827	14.43	15.33	0.004430350
1.2	400	5641	4766	15.51	15.13	0.004374434
1.2	600	5641	4687	16.92	14.88	0.004301431
1.2	800	5641	4650	17.56	14.77	0.004268296
1.2	1000	5641	4502	20.20	14.29	0.004131611
1.2	50	8739	7340	16.01	15.54	0.004491160
1.2	100	8739	7263	16.89	15.37	0.004444104
1.2	150	8739	7263	16.89	15.37	0.004444104
1.2	200	8739	7239	17.16	15.32	0.004429666
1.2	400	8739	6982	20.11	14.78	0.004271922
1.2	600	8739	6909	20.94	14.62	0.004227540

Flow rate, m ³ /h	Concentration, ppm	Pressure drop, kg/(ms ²)			After	
		Before	After	%DR	Wall shear stress, τ_w (kg/(ms ²)) $\tau_w = D\Delta P/4L$	Fanning friction factor, C_f $C_f = 2\tau_w / \rho v^2$
1.2	800	8739	6691	23.44	14.16	0.004093858
1.2	1000	8739	6887	21.19	14.58	0.004214172
1.2	50	12667	10430	17.66	16.56	0.004786467
1.2	100	12667	10134	20.00	16.09	0.004650441
1.2	150	12667	10018	20.91	15.90	0.004597543
1.2	200	12667	9120	28.00	14.48	0.004185397
1.2	400	12667	7980	37.00	12.67	0.003662223
1.2	600	12667	7888	37.73	12.52	0.003619787
1.2	800	12667	7727	39.00	12.27	0.003545962
1.2	1000	12667	8201	35.26	13.02	0.003763370



UMP

APPENDIX D2
FRICITION FACTOR IN PIPE WHILE TESTING RED GYPSUM IN WATER

Table 4.23: Friction factor in pipe with ID 0.0381m while testing red gypsum in water

Flow rate, m ³ /h	Concentration, ppm	Pressure drop, kg/(ms ²)			After	
		Before	After	%DR	Wall shear stress, τ_w (kg/(ms ²))	Fanning friction factor, C_f
					$\tau_w = D\Delta P/4L$	$C_f = 2\tau_w / \rho v^2$
10.5	50	784	713	9.04	13.59	0.004154771
10.5	100	784	700	10.69	13.34	0.004079404
10.5	150	784	690	12.03	13.14	0.004018197
10.5	200	784	681	13.12	12.98	0.003968409
10.5	400	784	675	13.96	12.85	0.003930041
10.5	600	784	671	14.42	12.78	0.003909029
10.5	800	784	667	14.93	12.71	0.003885734
10.5	1000	784	666	15.11	12.68	0.003877512
10.5	50	1609	1402	12.84	13.36	0.004085299
10.5	100	1609	1329	17.40	12.66	0.003871566
10.5	150	1609	1303	19.03	12.41	0.003795166
10.5	200	1609	1288	19.94	12.27	0.003752513
10.5	400	1609	1257	21.86	11.98	0.003662520
10.5	600	1609	1240	22.93	11.81	0.003612368
10.5	800	1609	1233	23.34	11.75	0.003593151
10.5	1000	1609	1216	24.42	11.58	0.003542530
10.5	50	2503	2017	19.40	12.81	0.003917917
10.5	100	2503	1980	20.89	12.57	0.003845489

Flow rate, m ³ /h	Concentration, ppm	Pressure drop, kg/(ms ²)			After	
		Before	After	%DR	Wall shear stress, τ_w (kg/(ms ²))	Fanning friction factor, C_f
					$\tau_w = D\Delta P/4L$	$C_f = 2\tau_w / \rho v^2$
10.5	150	2503	1923	23.16	12.21	0.003735146
10.5	200	2503	1905	23.90	12.10	0.003699175
10.5	400	2503	1892	24.40	12.02	0.003674870
10.5	600	2503	1880	24.88	11.94	0.003651537
10.5	800	2503	1865	25.50	11.84	0.003621400
10.5	1000	2503	1860	25.70	11.81	0.003611678
10.5	50	3291	2434	26.03	11.59	0.003545717
10.5	100	3291	2008	39.00	9.56	0.002924006
10.5	150	3291	1874	43.07	8.92	0.002728913
10.5	200	3291	1434	56.44	6.83	0.002088028
10.5	400	3291	1824	44.57	8.69	0.002657011
10.5	600	3291	1807	45.09	8.61	0.002632085
10.5	800	3291	2063	37.30	9.83	0.003005495
10.5	1000	3291	1777	46.00	8.46	0.002588465
10.0	50	695	635	8.69	12.09	0.004076264
10.0	100	695	625	10.14	11.90	0.004011533
10.0	150	695	613	11.76	11.68	0.003939213
10.0	200	695	607	12.70	11.56	0.003897250
10.0	400	695	605	12.93	11.53	0.003886982
10.0	600	695	604	13.08	11.51	0.003880286
10.0	800	695	594	14.48	11.32	0.003817787

Flow rate, m ³ /h	Concentration, ppm	Pressure drop, kg/(ms ²)			After	
		Before	After	%DR	Wall shear stress, τ_w (kg/(ms ²))	Fanning friction factor, C_f
					$\tau_w = \Delta P / 4L$	$C_f = 2\tau_w / \rho v^2$
10.0	1000	695	592	14.80	11.28	0.003803501
10.0	50	1443	1266	12.27	12.06	0.004065778
10.0	100	1443	1227	14.96	11.69	0.003941112
10.0	150	1443	1173	18.72	11.17	0.003766858
10.0	200	1443	1160	19.59	11.05	0.003726538
10.0	400	1443	1132	21.55	10.78	0.003635704
10.0	600	1443	1114	22.80	10.61	0.003577773
10.0	800	1443	1131	21.62	10.77	0.003632459
10.0	1000	1443	1098	23.90	10.46	0.003526795
10.0	50	2206	1831	17.02	11.62	0.003919375
10.0	100	2206	1796	18.60	11.40	0.003844748
10.0	150	2206	1741	21.10	11.05	0.003726666
10.0	200	2206	1701	22.89	10.80	0.003642119
10.0	400	2206	1692	23.31	10.74	0.003622281
10.0	600	2206	1682	23.76	10.68	0.003601027
10.0	800	2206	1668	24.41	10.59	0.003570325
10.0	1000	2206	1651	25.16	10.48	0.003534901
10.0	50	3089	2474	19.92	11.78	0.003972292
10.0	100	3089	2358	23.65	11.23	0.003787269
10.0	150	3089	2140	30.73	10.19	0.003436072
10.0	200	3089	1970	36.23	9.38	0.003163250
10.0	400	3089	2193	29.00	10.45	0.003521887

Flow rate, m ³ /h	Concentration, ppm	Pressure drop, kg/(ms ²)			After	
		Before	After	%DR	Wall shear stress, τ_w (kg/(ms ²))	Fanning friction factor, C_f
					$\tau_w = D\Delta P/4L$	$C_f = 2\tau_w / \rho v^2$
10.0	600	3089	2134	30.92	10.16	0.003426647
10.0	800	3089	2089	32.38	9.95	0.003354226
10.0	1000	3089	1893	38.72	9.02	0.003039736
9.5	50	611	562	8.00	10.71	0.004000746
9.5	100	611	553	9.50	10.53	0.003935517
9.5	150	611	542	11.28	10.33	0.003858111
9.5	200	611	539	11.85	10.26	0.003833324
9.5	400	611	536	12.23	10.22	0.003816799
9.5	600	611	533	12.80	10.15	0.003792012
9.5	800	611	530	13.33	10.09	0.003768964
9.5	1000	611	527	13.72	10.04	0.003752004
9.5	50	1294	1152	10.95	10.98	0.004100626
9.5	100	1294	1112	14.05	10.59	0.003957876
9.5	150	1294	1075	16.95	10.24	0.003824335
9.5	200	1294	1046	19.18	9.96	0.003721646
9.5	400	1294	1033	20.19	9.84	0.003675137
9.5	600	1294	1022	21.05	9.73	0.003635535
9.5	800	1294	1020	21.17	9.72	0.003630010
9.5	1000	1294	991	23.43	9.44	0.003525940
9.5	50	2070	1764	14.79	11.20	0.004184578
9.5	100	2070	1756	15.15	11.15	0.004166898

Flow rate, m ³ /h	Concentration, ppm	Pressure drop, kg/(ms ²)			After	
		Before	After	%DR	Wall shear stress, τ_w (kg/(ms ²))	Fanning friction factor, C_f
					$\tau_w = D\Delta P/4L$	$C_f = 2\tau_w / \rho v^2$
9.5	150	2070	1688	18.45	10.72	0.004004839
9.5	200	2070	1607	22.36	10.21	0.003812822
9.5	400	2070	1595	22.95	10.13	0.003783848
9.5	600	2070	1592	23.08	10.11	0.003777464
9.5	800	2070	1581	23.64	10.04	0.003749963
9.5	1000	2070	1560	24.65	9.90	0.003700363
9.5	50	2791	2322	16.80	11.06	0.004131761
9.5	100	2791	2267	18.78	10.80	0.004033433
9.5	150	2791	2096	24.91	9.98	0.003729013
9.5	200	2791	2025	27.46	9.64	0.003602379
9.5	400	2791	1987	28.80	9.46	0.003535834
9.5	600	2791	1949	30.17	9.28	0.003467799
9.5	800	2791	1954	30.00	9.30	0.003476241
9.5	1000	2791	1877	32.75	8.94	0.003339674
9.0	50	521	486	6.78	9.25	0.003851421
9.0	100	521	477	8.43	9.09	0.003783250
9.0	150	521	469	9.90	8.94	0.003722517
9.0	200	521	468	10.18	8.91	0.003710949
9.0	400	521	464	10.87	8.85	0.003682441
9.0	600	521	462	11.39	8.79	0.003660957
9.0	800	521	456	12.40	8.69	0.003619228

Flow rate, m ³ /h	Concentration, ppm	Pressure drop, kg/(ms ²)			After	
		Before	After	%DR	Wall shear stress, τ_w (kg/(ms ²))	Fanning friction factor, C_f
					$\tau_w = D\Delta P/4L$	$C_f = 2\tau_w / \rho v^2$
9.0	1000	521	455	12.69	8.67	0.003607247
9.0	50	1114	998	10.44	9.50	0.003955883
9.0	100	1114	960	13.80	9.15	0.003807471
9.0	150	1114	942	15.42	8.97	0.003735915
9.0	200	1114	906	18.66	8.63	0.003592804
9.0	400	1114	892	19.93	8.50	0.003536708
9.0	600	1114	883	20.73	8.41	0.003501372
9.0	800	1114	880	20.99	8.38	0.003489887
9.0	1000	1114	861	22.70	8.20	0.003414356
9.0	50	1792	1572	12.27	9.98	0.004155651
9.0	100	1792	1540	14.07	9.78	0.004070387
9.0	150	1792	1488	16.94	9.45	0.003934439
9.0	200	1792	1431	20.17	9.08	0.003781438
9.0	400	1792	1416	20.96	8.99	0.003744017
9.0	600	1792	1415	21.04	8.99	0.003740228
9.0	800	1792	1376	23.20	8.74	0.003637912
9.0	1000	1792	1355	24.40	8.60	0.003581069
9.0	50	2458	2112	14.09	10.06	0.004186391
9.0	100	2458	2027	17.55	9.65	0.004017785
9.0	150	2458	1998	18.71	9.52	0.003961258
9.0	200	2458	1893	22.98	9.02	0.003753181
9.0	400	2458	1866	24.10	8.89	0.003698604

Flow rate, m ³ /h	Concentration, ppm	Pressure drop, kg/(ms ²)			After	
		Before	After	%DR	Wall shear stress, τ_w (kg/(ms ²))	Fanning friction factor, C_f
					$\tau_w = D\Delta P/4L$	$C_f = 2\tau_w / \rho v^2$
9.0	600	2458	1848	24.80	8.80	0.003664493
9.0	800	2458	1829	25.60	8.71	0.003625509
9.0	1000	2458	1797	26.88	8.56	0.003563135
8.5	50	500	469	6.12	8.94	0.004173154
8.5	100	500	465	7.04	8.85	0.004132258
8.5	150	500	452	9.57	8.61	0.004019795
8.5	200	500	451	9.71	8.60	0.004013571
8.5	400	500	450	9.94	8.58	0.004003347
8.5	600	500	447	10.57	8.52	0.003975343
8.5	800	500	446	10.90	8.49	0.003960673
8.5	1000	500	442	11.59	8.42	0.003930002
8.5	50	1016	925	8.95	8.81	0.004112113
8.5	100	1016	877	13.66	8.36	0.003899394
8.5	150	1016	867	14.70	8.25	0.003852424
8.5	200	1016	828	18.47	7.89	0.003682159
8.5	400	1016	817	19.57	7.78	0.003632479
8.5	600	1016	811	20.14	7.73	0.003606736
8.5	800	1016	807	20.56	7.69	0.003587767
8.5	1000	1016	796	21.69	7.58	0.003536733
8.5	50	1563	1410	9.78	8.95	0.004178899
8.5	100	1563	1360	13.00	8.63	0.004029752

Flow rate, m ³ /h	Concentration, ppm	Pressure drop, kg/(ms ²)			After	
		Before	After	%DR	Wall shear stress, τ_w (kg/(ms ²))	Fanning friction factor, C_f
					$\tau_w = \Delta P / 4L$	$C_f = 2\tau_w / \rho v^2$
8.5	150	1563	1319	15.60	8.38	0.003909322
8.5	200	1563	1300	16.80	8.26	0.003853740
8.5	400	1563	1242	20.51	7.89	0.003681896
8.5	600	1563	1239	20.74	7.87	0.003671243
8.5	800	1563	1220	21.92	7.75	0.003616586
8.5	1000	1563	1204	22.98	7.64	0.003567488
8.5	50	2096	1837	12.36	8.75	0.004082771
8.5	100	2096	1772	15.45	8.44	0.003938821
8.5	150	2096	1740	17.00	8.29	0.003866613
8.5	200	2096	1694	19.18	8.07	0.003765056
8.5	400	2096	1657	20.95	7.89	0.003682599
8.5	600	2096	1639	21.81	7.81	0.003642536
8.5	800	2096	1634	22.05	7.78	0.003631355
8.5	1000	2096	1587	24.30	7.56	0.003526537
8.0	50	489	461	5.69	8.79	0.004628559
8.0	100	489	455	6.95	8.67	0.004566721
8.0	150	489	450	8.04	8.57	0.004513225
8.0	200	489	447	8.63	8.51	0.004484269
8.0	400	489	443	9.38	8.44	0.004447461
8.0	600	489	440	10.00	8.38	0.004417032
8.0	800	489	437	10.56	8.33	0.004389549

Flow rate, m ³ /h	Concentration, ppm	Pressure drop, kg/(ms ²)			After	
		Before	After	%DR	Wall shear stress, τ_w (kg/(ms ²))	Fanning friction factor, C_f
					$\tau_w = D\Delta P/4L$	$C_f = 2\tau_w / \rho v^2$
8.0	1000	489	434	11.18	8.27	0.004359120
8.0	50	992	907	8.56	8.64	0.004551946
8.0	100	992	869	12.39	8.28	0.004361286
8.0	150	992	853	14.00	8.13	0.004281139
8.0	200	992	813	18.01	7.75	0.004081518
8.0	400	992	806	18.76	7.68	0.004044183
8.0	600	992	798	19.60	7.60	0.004002367
8.0	800	992	794	19.95	7.56	0.003984944
8.0	1000	992	782	21.17	7.45	0.003924212
8.0	50	1408	1281	9.03	8.13	0.004285079
8.0	100	1408	1260	10.48	8.00	0.004216777
8.0	150	1408	1208	14.19	7.67	0.004042020
8.0	200	1408	1191	15.43	7.56	0.003983611
8.0	400	1408	1184	15.93	7.52	0.003960059
8.0	600	1408	1126	20.03	7.15	0.003766931
8.0	800	1408	1118	20.57	7.10	0.003741495
8.0	1000	1408	1098	22.00	6.97	0.003674136
8.0	50	1965	1771	9.87	8.43	0.004443766
8.0	100	1965	1747	11.07	8.32	0.004384601
8.0	150	1965	1683	14.33	8.02	0.004223870
8.0	200	1965	1649	16.10	7.85	0.004136602
8.0	400	1965	1636	16.72	7.79	0.004106033

Flow rate, m ³ /h	Concentration, ppm	Pressure drop, kg/(ms ²)			After	
		Before	After	%DR	Wall shear stress, τ_w (kg/(ms ²))	Fanning friction factor, C_f
					$\tau_w = D\Delta P/4L$	$C_f = 2\tau_w / \rho v^2$
8.0	600	1965	1552	21.00	7.39	0.003895013
8.0	800	1965	1542	21.54	7.34	0.003868388
8.0	1000	1965	1516	22.87	7.22	0.003802814
7.5	50	400	379	5.17	7.23	0.004331541
7.5	100	400	376	6.03	7.16	0.004292259
7.5	150	400	369	7.71	7.03	0.004215521
7.5	200	400	367	8.20	7.00	0.004193140
7.5	400	400	364	8.94	6.94	0.004159339
7.5	600	400	361	9.83	6.87	0.004118686
7.5	800	400	360	10.03	6.86	0.004109551
7.5	1000	400	357	10.66	6.81	0.004080774
7.5	50	873	826	5.34	7.87	0.004718320
7.5	100	873	808	7.41	7.70	0.004615141
7.5	150	873	784	10.22	7.47	0.004475077
7.5	200	873	753	13.78	7.17	0.004297629
7.5	400	873	751	14.03	7.15	0.004285168
7.5	600	873	766	12.29	7.29	0.004371898
7.5	800	873	756	13.40	7.20	0.004316570
7.5	1000	873	751	14.01	7.15	0.004286165
7.5	50	1291	1199	7.11	7.61	0.004564683
7.5	100	1291	1174	9.04	7.46	0.004469841

Flow rate, m ³ /h	Concentration, ppm	Pressure drop, kg/(ms ²)			After	
		Before	After	%DR	Wall shear stress, τ_w (kg/(ms ²))	Fanning friction factor, C_f
					$\tau_w = D\Delta P/4L$	$C_f = 2\tau_w / \rho v^2$
7.5	150	1291	1135	12.05	7.21	0.004321928
7.5	200	1291	1108	14.19	7.03	0.004216766
7.5	400	1291	1092	15.42	6.93	0.004156323
7.5	600	1291	1086	15.90	6.89	0.004132736
7.5	800	1291	1096	15.11	6.96	0.004171557
7.5	1000	1291	1067	17.34	6.78	0.004061973
7.5	50	1657	1509	8.91	7.19	0.004308934
7.5	100	1657	1485	10.39	7.07	0.004238924
7.5	150	1657	1439	13.18	6.85	0.004106946
7.5	200	1657	1393	15.95	6.63	0.003975913
7.5	400	1657	1392	16.00	6.63	0.003973548
7.5	600	1657	1383	16.53	6.59	0.003948477
7.5	800	1657	1370	17.33	6.52	0.003910633
7.5	1000	1657	1358	18.02	6.47	0.003877994

Table 4.24: Friction factor in pipe with ID 0.0254m while testing red gypsum in water

Flow rate, m ³ /h	Concentration, ppm	Pressure drop, kg/(ms ²)			Wall shear stress, τ_w (kg/(ms ²))	After Fanning friction factor, C_f
		Before	After	%DR		
					$\tau_w = D\Delta P/4L$	$C_f = 2\tau_w / \rho v^2$
8.0	50	3038	2823	7.07	35.85	0.003731355
8.0	100	3038	2797	7.93	35.52	0.003696824
8.0	150	3038	2786	8.30	35.38	0.003681968
8.0	200	3038	2687	11.55	34.13	0.003551473
8.0	400	3038	2657	12.54	33.74	0.003511722
8.0	600	3038	2649	12.82	33.64	0.003500480
8.0	800	3038	2634	13.30	33.45	0.003481206
8.0	1000	3038	2438	19.76	30.96	0.003221822
8.0	50	6317	5252	16.86	33.35	0.003470674
8.0	100	6317	5261	16.71	33.41	0.003476936
8.0	150	6317	4774	24.42	30.32	0.003155082
8.0	200	6317	4604	27.11	29.24	0.003042788
8.0	400	6317	4501	28.75	28.58	0.002974327
8.0	600	6317	4320	31.61	27.43	0.002854936
8.0	800	6317	4302	31.90	27.32	0.002842830
8.0	1000	6317	4098	35.12	26.03	0.002708411
8.0	50	9664	8013	17.08	33.92	0.003530351
8.0	100	9664	7941	17.83	33.62	0.003498419
8.0	150	9664	7175	25.76	30.37	0.003160797
8.0	200	9664	6329	34.51	26.79	0.002788262

Flow rate, m ³ /h	Concentration, ppm	Pressure drop, kg/(ms ²)			After	
		Before	After	%DR	Wall shear stress, τ_w (kg/(ms ²))	Fanning friction factor, C_f
					$\tau_w = D\Delta P/4L$	$C_f = 2\tau_w / \rho v^2$
8.0	400	9664	6293	34.88	26.64	0.002772509
8.0	600	9664	6288	34.93	26.62	0.002770380
8.0	800	9664	6261	35.21	26.51	0.002758459
8.0	1000	9664	5918	38.76	25.05	0.002607317
8.0	50	14229	11093	22.04	35.22	0.003665297
8.0	100	14229	9432	33.71	29.95	0.003116631
8.0	150	14229	8644	39.25	27.45	0.002856167
8.0	200	14229	7779	45.33	24.70	0.002570315
8.0	400	14229	7584	46.70	24.08	0.002505904
8.0	600	14229	7554	46.91	23.98	0.002496031
8.0	800	14229	7926	44.30	25.16	0.002618741
8.0	1000	14229	7541	47.00	23.94	0.002491800
7.5	50	2996	2787	6.98	35.39	0.004190815
7.5	100	2996	2761	7.85	35.06	0.004151619
7.5	150	2996	2759	7.92	35.04	0.004148465
7.5	200	2996	2663	11.12	33.82	0.004004296
7.5	400	2996	2638	11.96	33.50	0.003966452
7.5	600	2996	2624	12.43	33.32	0.003945277
7.5	800	2996	2611	12.84	33.16	0.003926805
7.5	1000	2996	2417	19.31	30.70	0.003635314
7.5	50	6003	5082	15.34	32.27	0.003821175

Flow rate, m ³ /h	Concentration, ppm	Pressure drop, kg/(ms ²)			After		
		Before	After	%DR	Wall shear stress, τ_w (kg/(ms ²))	Fanning friction factor, C_f	
					$\tau_w = D\Delta P/4L$	$C_f = 2\tau_w / \rho v^2$	
7.5	100	6003	5019	16.40	31.87	0.003773332	
7.5	150	6003	4556	24.11	28.93	0.003425337	
7.5	200	6003	4386	26.93	27.85	0.003298054	
7.5	400	6003	4299	28.39	27.30	0.003232156	
7.5	600	6003	4138	31.07	26.28	0.003111193	
7.5	800	6003	4108	31.56	26.09	0.003089077	
7.5	1000	6003	3983	33.65	25.29	0.002994744	
7.5	50	9072	7647	15.71	32.37	0.003832995	
7.5	100	9072	7490	17.44	31.71	0.003754325	
7.5	150	9072	6838	24.62	28.95	0.003427822	
7.5	200	9072	6143	32.29	26.00	0.003079037	
7.5	400	9072	6102	32.74	25.83	0.003058574	
7.5	600	9072	5978	34.10	25.31	0.002996730	
7.5	800	9072	5992	33.95	25.37	0.003003551	
7.5	1000	9072	5912	34.83	25.03	0.002963534	
7.5	50	12210	9756	20.10	30.97	0.003667607	
7.5	100	12210	8560	29.89	27.18	0.003218222	
7.5	150	12210	7762	36.43	24.64	0.002918020	
7.5	200	12210	7324	40.02	23.25	0.002753230	
7.5	400	12210	7188	41.13	22.82	0.002702278	
7.5	600	12210	7747	36.55	24.60	0.002912512	
7.5	800	12210	7728	36.71	24.54	0.002905167	

Flow rate, m ³ /h	Concentration, ppm	Pressure drop, kg/(ms ²)			After	
		Before	After	%DR	Wall shear stress, τ_w (kg/(ms ²))	Fanning friction factor, C_f
					$\tau_w = D\Delta P/4L$	$C_f = 2\tau_w / \rho v^2$
7.5	1000	12210	7230	40.79	22.95	0.002717885
7.0	50	2601	2423	6.86	30.77	0.004181994
7.0	100	2601	2406	7.49	30.56	0.004153707
7.0	150	2601	2402	7.65	0.51	0.004146523
7.0	200	2601	2347	9.78	29.80	0.004050886
7.0	400	2601	2320	10.80	29.47	0.004005088
7.0	600	2601	2296	11.71	29.16	0.003964228
7.0	800	2601	2285	12.15	29.02	0.003944472
7.0	1000	2601	2107	19.00	26.76	0.003636907
7.0	50	5451	4555	16.44	28.92	0.003931438
7.0	100	5451	4431	18.72	28.13	0.003824166
7.0	150	5451	4164	23.61	26.44	0.003594095
7.0	200	5451	3795	30.38	24.10	0.003275571
7.0	400	5451	3861	29.17	24.52	0.003332501
7.0	600	5451	3762	30.98	23.89	0.003247341
7.0	800	5451	3685	32.39	23.40	0.003181002
7.0	1000	5451	3630	33.41	23.05	0.003133012
7.0	50	8532	7303	14.41	30.91	0.004202033
7.0	100	8532	6919	18.90	29.29	0.003981597
7.0	150	8532	6470	24.17	27.39	0.003722866
7.0	200	8532	5908	30.75	25.01	0.003399822

Flow rate, m ³ /h	Concentration, ppm	Pressure drop, kg/(ms ²)			After	
		Before	After	%DR	Wall shear stress, τ_w (kg/(ms ²))	Fanning friction factor, C_f
					$\tau_w = D\Delta P/4L$	$C_f = 2\tau_w / \rho v^2$
7.0	400	8532	5888	30.99	24.93	0.003388039
7.0	600	8532	5874	31.15	24.87	0.003380184
7.0	800	8532	5839	31.56	24.72	0.003360055
7.0	1000	8532	5713	33.04	24.19	0.003287395
7.0	50	10300	8376	18.68	26.59	0.003614776
7.0	100	10300	8155	20.83	25.89	0.003519206
7.0	150	10300	7545	26.75	23.95	0.003256055
7.0	200	10300	6733	34.63	21.38	0.002905779
7.0	400	10300	6699	34.96	21.27	0.002891110
7.0	600	10300	6654	35.40	21.13	0.002871551
7.0	800	10300	6606	35.86	20.98	0.002851104
7.0	1000	10300	6529	36.61	20.73	0.002817765
6.5	50	2201	2058	6.51	26.13	0.004119660
6.5	100	2201	2046	7.02	25.99	0.004097187
6.5	150	2201	2040	7.32	25.91	0.004083967
6.5	200	2201	1998	9.21	25.38	0.004000684
6.5	400	2201	1987	9.73	25.23	0.003977770
6.5	600	2201	1971	10.46	25.03	0.003945602
6.5	800	2201	1938	11.96	24.61	0.003879504
6.5	1000	2201	1798	18.33	22.83	0.003598809
6.5	50	4884	4285	12.27	27.21	0.004289137

Flow rate, m ³ /h	Concentration, ppm	Pressure drop, kg/(ms ²)			After	
		Before	After	%DR	Wall shear stress, τ_w (kg/(ms ²))	Fanning friction factor, C_f
					$\tau_w = D\Delta P/4L$	$C_f = 2\tau_w / \rho v^2$
6.5	100	4884	4120	15.65	26.16	0.004123889
6.5	150	4884	3937	19.40	25.00	0.003940550
6.5	200	4884	3705	24.13	23.53	0.003709300
6.5	400	4884	4173	14.55	26.50	0.004177668
6.5	600	4884	3642	25.43	23.13	0.003645742
6.5	800	4884	3606	26.17	22.90	0.003609564
6.5	1000	4884	3565	27.00	22.64	0.003568985
6.5	50	7110	6207	12.70	26.28	0.004142273
6.5	100	7110	6281	11.66	26.59	0.004191620
6.5	150	7110	5656	20.45	23.94	0.003774546
6.5	200	7110	5333	25.00	22.57	0.003558654
6.5	400	7110	5318	25.21	22.51	0.003548690
6.5	600	7110	5156	27.48	21.83	0.003440981
6.5	800	7110	5126	27.90	21.70	0.003421053
6.5	1000	7110	4993	29.77	21.14	0.003332324
6.5	50	9036	7696	14.83	24.43	0.003851936
6.5	100	9036	7500	17.00	23.81	0.003753794
6.5	150	9036	7016	22.36	22.27	0.003511381
6.5	200	9036	6319	30.07	20.06	0.003162685
6.5	400	9036	6190	31.50	19.65	0.003098011
6.5	600	9036	6074	32.78	19.28	0.003040121
6.5	800	9036	6054	33.00	19.22	0.003030171

Flow rate, m ³ /h	Concentration, ppm	Pressure drop, kg/(ms ²)			After	
		Before	After	%DR	Wall shear stress, τ_w (kg/(ms ²))	Fanning friction factor, C_f
					$\tau_w = D\Delta P/4L$	$C_f = 2\tau_w / \rho v^2$
6.5	1000	9036	5994	33.67	19.03	0.002999870
6.0	50	2010	1889	6.03	23.99	0.004437983
6.0	100	2010	1875	6.74	23.81	0.004404452
6.0	150	2010	1871	6.90	23.77	0.004396895
6.0	200	2010	1856	7.65	23.57	0.004361475
6.0	400	2010	1845	8.22	23.43	0.004334555
6.0	600	2010	1830	8.97	23.24	0.004299134
6.0	800	2010	1820	9.44	23.12	0.004276937
6.0	1000	2010	1718	14.55	21.81	0.004035604
6.0	50	4083	3843	5.87	24.41	0.004515209
6.0	100	4083	3751	8.13	23.82	0.004406801
6.0	150	4083	3707	9.20	23.54	0.004355476
6.0	200	4083	3636	10.96	23.09	0.004271053
6.0	400	4083	3582	12.28	22.74	0.004207735
6.0	600	4083	3516	13.89	22.33	0.004130507
6.0	800	4083	3555	12.94	22.57	0.004176076
6.0	1000	4083	3464	15.17	21.99	0.004069108
6.0	50	6147	5600	8.90	23.71	0.004385920
6.0	100	6147	5543	9.82	23.47	0.004341628
6.0	150	6147	5227	14.97	22.13	0.004093686
6.0	200	6147	5120	16.70	21.68	0.004010397

Flow rate, m ³ /h	Concentration, ppm	Pressure drop, kg/(ms ²)			After		
		Before	After	%DR	Wall shear stress, τ_w (kg/(ms ²))	Fanning friction factor, C_f	
					$\tau_w = D\Delta P/4L$	$C_f = 2\tau_w / \rho v^2$	
6.0	400	6147	5010	18.50	21.21	0.003923738	
6.0	600	6147	4992	18.79	21.13	0.003909776	
6.0	800	6147	5215	15.16	22.08	0.004084539	
6.0	1000	6147	5089	17.21	21.54	0.003985843	
6.0	50	7651	6754	11.73	21.44	0.003967087	
6.0	100	7651	6483	15.27	20.58	0.003807990	
6.0	150	7651	6301	17.65	20.00	0.003701027	
6.0	200	7651	5623	26.51	17.85	0.003302835	
6.0	400	7651	5585	27.00	17.73	0.003280813	
6.0	600	7651	5539	27.61	17.58	0.003253398	
6.0	800	7651	5516	27.90	17.51	0.003240364	
6.0	1000	7651	5390	29.55	17.11	0.003166209	
5.5	50	1685	1602	4.95	20.34	0.004478469	
5.5	100	1685	1587	5.80	20.16	0.004438419	
5.5	150	1685	1582	6.11	20.09	0.004423813	
5.5	200	1685	1562	7.32	19.83	0.004366801	
5.5	400	1685	1553	7.85	19.72	0.004341829	
5.5	600	1685	1547	8.21	19.64	0.004324867	
5.5	800	1685	1538	8.70	19.54	0.004301780	
5.5	1000	1685	1515	10.10	19.24	0.004235816	
5.5	50	2964	2798	5.60	17.77	0.003911990	

Flow rate, m ³ /h	Concentration, ppm	Pressure drop, kg/(ms ²)			After	
		Before	After	%DR	Wall shear stress, τ_w (kg/(ms ²))	Fanning friction factor, C_f
					$\tau_w = D\Delta P/4L$	$C_f = 2\tau_w / \rho v^2$
5.5	100	2964	2733	7.79	17.36	0.003821235
5.5	150	2964	2730	7.91	17.33	0.003816262
5.5	200	2964	2704	8.78	17.17	0.003780209
5.5	400	2964	2688	9.32	17.07	0.003757831
5.5	600	2964	2674	9.78	16.98	0.003738768
5.5	800	2964	2669	9.94	16.95	0.003732138
5.5	1000	2964	2569	13.31	16.32	0.003592483
5.5	50	4513	4161	7.79	17.62	0.003878820
5.5	100	4513	4087	9.44	17.30	0.003809412
5.5	150	4513	4052	10.21	17.15	0.003777022
5.5	200	4513	3933	12.85	16.65	0.003665971
5.5	400	4513	3909	13.39	16.55	0.003643255
5.5	600	4513	3897	13.65	16.50	0.003632319
5.5	800	4513	3891	13.78	16.47	0.003626850
5.5	1000	4513	3886	13.90	16.45	0.003621802
5.5	50	6487	5829	10.15	18.51	0.004074549
5.5	100	6487	5694	12.22	18.08	0.003980677
5.5	150	6487	5539	14.61	17.59	0.003872295
5.5	200	6487	5266	18.82	16.72	0.003681378
5.5	400	6487	5247	19.12	16.66	0.003667774
5.5	600	6487	5114	21.17	16.24	0.003574810
5.5	800	6487	5088	21.56	16.16	0.003557124

Flow rate, m ³ /h	Concentration, ppm	Pressure drop, kg/(ms ²)			After	
		Before	After	%DR	Wall shear stress, τ_w (kg/(ms ²))	Fanning friction factor, C_f
					$\tau_w = D\Delta P/4L$	$C_f = 2\tau_w / \rho v^2$
5.5	1000	6487	5181	20.14	16.45	0.003621519
5.0	50	1255	1194	4.90	15.16	0.004038193
5.0	100	1255	1188	5.31	15.09	0.004020784
5.0	150	1255	1182	5.80	15.01	0.003999977
5.0	200	1255	1170	6.74	14.86	0.003960062
5.0	400	1255	1166	7.11	14.81	0.003944351
5.0	600	1255	1158	7.75	14.70	0.003917175
5.0	800	1255	1151	8.32	14.61	0.003892971
5.0	1000	1255	1145	8.76	14.54	0.003874288
5.0	50	2439	2311	5.24	14.68	0.003909937
5.0	100	2439	2292	6.01	14.56	0.003878165
5.0	150	2439	2282	6.42	14.49	0.003861248
5.0	200	2439	2243	8.03	14.24	0.003794817
5.0	400	2439	2221	8.94	14.10	0.003757269
5.0	600	2439	2212	9.30	14.05	0.003742415
5.0	800	2439	2207	9.51	14.01	0.003733750
5.0	1000	2439	2109	13.52	13.39	0.003568292
5.0	50	4001	3719	7.04	15.75	0.004194752
5.0	100	4001	3641	9.00	15.41	0.004106308
5.0	150	4001	3607	9.84	15.27	0.004068404
5.0	200	4001	3517	12.10	14.89	0.003966423

Flow rate, m ³ /h	Concentration, ppm	Pressure drop, kg/(ms ²)			After		
		Before	After	%DR	Wall shear stress, τ_w (kg/(ms ²))	Fanning friction factor, C_f	
					$\tau_w = D\Delta P/4L$	$C_f = 2\tau_w / \rho v^2$	
5.0	400	4001	3492	12.73	14.78	0.003937995	
5.0	600	4001	3476	13.11	14.72	0.003920848	
5.0	800	4001	3494	12.67	14.79	0.003940702	
5.0	1000	4001	3393	15.20	14.36	0.003826538	
5.0	50	5763	5341	7.33	16.96	0.004517422	
5.0	100	5763	5241	9.06	16.64	0.004433089	
5.0	150	5763	5069	12.04	16.09	0.004287822	
5.0	200	5763	4997	13.29	15.87	0.004226888	
5.0	400	5763	4982	13.56	15.82	0.004213726	
5.0	600	5763	4922	14.60	15.63	0.004163028	
5.0	800	5763	4892	15.11	15.53	0.004138167	
5.0	1000	5763	4855	15.76	15.41	0.004106481	

Table 4.25: Friction factor in pipe with ID 0.0127m while testing red gypsum in water

Flow rate, m ³ /h	Concentration, ppm	Pressure drop, kg/(ms ²)			After	
		Before	After	%DR	Wall shear stress, τ_w (kg/(ms ²))	Fanning friction factor, C_f
					$\tau_w = D\Delta P/4L$	$C_f = 2\tau_w / \rho v^2$
2.4	50	10961	10418	4.95	66.16	0.004781154
2.4	100	10961	10335	5.71	65.63	0.004742925
2.4	150	10961	10302	6.01	65.42	0.004727834
2.4	200	10961	10216	6.80	64.87	0.004688096
2.4	400	10961	10173	7.19	64.60	0.004668479
2.4	600	10961	10151	7.39	64.46	0.004658418
2.4	800	10961	10102	7.84	64.15	0.004635783
2.4	1000	10961	9514	13.20	60.41	0.004366167
2.4	50	20507	16668	18.72	52.92	0.003824602
2.4	100	20507	15245	25.66	48.40	0.003498043
2.4	150	20507	14113	31.18	44.81	0.003238301
2.4	200	20507	13520	34.07	42.93	0.003102313
2.4	400	20507	13490	34.22	42.83	0.003095255
2.4	600	20507	13356	34.87	42.41	0.003064669
2.4	800	20507	13321	35.04	42.30	0.003056670
2.4	1000	20507	13204	35.61	41.92	0.003029849
2.4	50	28123	22780	19.00	48.22	0.003484623
2.4	100	28123	20611	26.71	43.63	0.003152939
2.4	150	28123	19191	31.76	40.62	0.002935688
2.4	200	28123	18359	34.72	38.86	0.002808348

Flow rate, m ³ /h	Concentration, ppm	Pressure drop, kg/(ms ²)			After	
		Before	After	%DR	Wall shear stress, τ_w (kg/(ms ²))	Fanning friction factor, C_f
					$\tau_w = D\Delta P/4L$	$C_f = 2\tau_w / \rho v^2$
2.4	400	28123	18300	34.93	38.73	0.002799314
2.4	600	28123	18137	35.51	38.39	0.002774362
2.4	800	28123	17436	38.00	36.91	0.002667243
2.4	1000	28123	17388	38.17	36.81	0.002659929
2.4	50	37466	30119	19.61	47.81	0.003455491
2.4	100	37466	26710	28.71	42.40	0.003064336
2.4	150	37466	24604	34.33	39.06	0.002822765
2.4	200	37466	22412	40.18	35.58	0.002571308
2.4	400	37466	22393	40.23	35.55	0.002569159
2.4	600	37466	22277	40.54	35.37	0.002555834
2.4	800	37466	22154	40.87	35.17	0.002541649
2.4	1000	37466	22292	40.50	35.39	0.002557553
2.2	50	9847	9416	4.38	59.79	0.005142333
2.2	100	9847	9333	5.22	59.26	0.005097159
2.2	150	9847	9270	5.86	58.86	0.005062741
2.2	200	9847	9239	6.17	58.67	0.005046069
2.2	400	9847	9200	6.57	58.42	0.005024558
2.2	600	9847	9179	6.78	58.29	0.005013264
2.2	800	9847	9158	7.00	58.15	0.005001433
2.2	1000	9847	8670	11.95	55.06	0.004735227
2.2	50	17588	14580	17.10	46.29	0.003981517

Flow rate, m ³ /h	Concentration, ppm	Pressure drop, kg/(ms ²)			After	
		Before	After	%DR	Wall shear stress, τ_w (kg/(ms ²))	Fanning friction factor, C_f
					$\tau_w = D\Delta P/4L$	$C_f = 2\tau_w / \rho v^2$
2.2	100	17588	13557	22.92	43.04	0.003701994
2.2	150	17588	12700	27.79	40.32	0.003468098
2.2	200	17588	11817	32.81	37.52	0.003226998
2.2	400	17588	11766	33.10	37.36	0.003213070
2.2	600	17588	11663	33.69	37.03	0.003184733
2.2	800	17588	11608	34.00	36.86	0.003169844
2.2	1000	17588	12276	30.20	38.98	0.003352351
2.2	50	23009	18909	17.82	40.02	0.003442312
2.2	100	23009	17540	23.77	37.13	0.003193081
2.2	150	23009	16327	29.04	34.56	0.002972334
2.2	200	23009	15163	34.10	32.09	0.002760384
2.2	400	23009	15071	34.50	31.90	0.002743629
2.2	600	23009	14970	34.94	31.69	0.002725198
2.2	800	23009	14625	36.44	30.96	0.002662367
2.2	1000	23009	14839	35.51	31.41	0.002701322
2.2	50	30203	24483	18.94	38.87	0.003342753
2.2	100	30203	22598	25.18	35.87	0.003085427
2.2	150	30203	21067	30.25	33.44	0.002876351
2.2	200	30203	19188	36.47	30.46	0.002619850
2.2	400	30203	19064	36.88	30.26	0.002602943
2.2	600	30203	22018	27.10	34.95	0.003006250
2.2	800	30203	18995	37.11	30.15	0.002593458

Flow rate, m ³ /h	Concentration, ppm	Pressure drop, kg/(ms ²)			After	
		Before	After	%DR	Wall shear stress, τ_w (kg/(ms ²))	Fanning friction factor, C_f
					$\tau_w = D\Delta P/4L$	$C_f = 2\tau_w / \rho v^2$
2.2	1000	30203	18714	38.04	29.71	0.002555107
2.0	50	7125	6856	3.77	43.54	0.004530940
2.0	100	7125	6839	4.01	43.43	0.004519639
2.0	150	7125	6801	4.55	43.19	0.004494214
2.0	200	7125	6797	4.61	43.16	0.004491389
2.0	400	7125	6696	6.02	42.52	0.004424999
2.0	600	7125	6665	6.45	42.33	0.004404753
2.0	800	7125	6642	6.78	42.18	0.004389215
2.0	1000	7125	6323	11.26	40.15	0.004178277
2.0	50	15857	14542	8.29	46.17	0.004805080
2.0	100	15857	14398	9.20	45.71	0.004757401
2.0	150	15857	14311	9.75	45.44	0.004728585
2.0	200	15857	14027	11.54	44.54	0.004634799
2.0	400	15857	13574	14.40	43.10	0.004484951
2.0	600	15857	13497	14.88	42.85	0.004459802
2.0	800	15857	13172	16.93	41.82	0.004352394
2.0	1000	15857	12923	18.50	41.03	0.004270134
2.0	50	20707	17829	13.90	37.74	0.003927281
2.0	100	20707	17719	14.43	37.51	0.003903106
2.0	150	20707	17044	17.69	36.08	0.003754408
2.0	200	20707	16669	19.50	35.28	0.003671848

Flow rate, m ³ /h	Concentration, ppm	Pressure drop, kg/(ms ²)			After	
		Before	After	%DR	Wall shear stress, τ_w (kg/(ms ²))	Fanning friction factor, C_f
					$\tau_w = D\Delta P/4L$	$C_f = 2\tau_w / \rho v^2$
2.0	400	20707	16402	20.79	34.72	0.003613007
2.0	600	20707	16321	21.18	34.55	0.003595218
2.0	800	20707	16243	21.56	34.38	0.003577885
2.0	1000	20707	16359	21.00	34.63	0.003603429
2.0	50	28674	23450	18.22	37.23	0.003874078
2.0	100	28674	21815	23.92	34.63	0.003604057
2.0	150	28674	21359	25.51	33.91	0.003528736
2.0	200	28674	20439	28.72	32.45	0.003376672
2.0	400	28674	20353	29.02	32.31	0.003362461
2.0	600	28674	20267	29.32	32.17	0.003348249
2.0	800	28674	19071	33.49	30.28	0.003150708
2.0	1000	28674	18807	34.41	29.86	0.003107126
1.8	50	5639	5490	2.64	34.86	0.004479098
1.8	100	5639	5470	3.00	34.73	0.004462536
1.8	150	5639	5443	3.47	34.57	0.004440913
1.8	200	5639	5413	4.00	34.38	0.004416530
1.8	400	5639	5319	5.67	33.78	0.004339701
1.8	600	5639	5310	5.83	33.72	0.004332340
1.8	800	5639	5302	5.97	33.67	0.004325900
1.8	1000	5639	5098	9.59	32.37	0.004159360
1.8	50	13672	12930	5.43	41.05	0.005274282

Flow rate, m ³ /h	Concentration, ppm	Pressure drop, kg/(ms ²)			After	
		Before	After	%DR	Wall shear stress, τ_w (kg/(ms ²))	Fanning friction factor, C_f
					$\tau_w = D\Delta P/4L$	$C_f = 2\tau_w / \rho v^2$
1.8	100	13672	12897	5.67	40.95	0.005260897
1.8	150	13672	12854	5.98	40.81	0.005243608
1.8	200	13672	12822	6.22	40.71	0.005230223
1.8	400	13672	12749	6.75	40.48	0.005200664
1.8	600	13672	12828	6.17	40.73	0.005233011
1.8	800	13672	12763	6.65	40.52	0.005206241
1.8	1000	13672	12312	9.95	39.09	0.005022196
1.8	50	16833	15634	7.12	33.09	0.004251776
1.8	100	16833	15513	7.84	32.84	0.004218816
1.8	150	16833	15300	9.11	32.38	0.004160680
1.8	200	16833	15148	10.01	32.06	0.004119480
1.8	400	16833	15246	9.43	32.27	0.004146031
1.8	600	16833	15059	10.54	31.87	0.004095218
1.8	800	16833	14899	11.49	31.54	0.004051730
1.8	1000	16833	14140	16.00	29.93	0.003845275
1.8	50	22195	18466	16.80	29.32	0.003766399
1.8	100	22195	18273	17.67	29.01	0.003727015
1.8	150	22195	16997	23.42	26.98	0.003466717
1.8	200	22195	16582	25.29	26.32	0.003382064
1.8	400	22195	17046	23.20	27.06	0.003476676
1.8	600	22195	16475	25.77	26.15	0.003360335
1.8	800	22195	16424	26.00	26.07	0.003349923

Flow rate, m ³ /h	Concentration, ppm	Pressure drop, kg/(ms ²)			After	
		Before	After	%DR	Wall shear stress, τ_w (kg/(ms ²))	Fanning friction factor, C_f
					$\tau_w = D\Delta P/4L$	$C_f = 2\tau_w / \rho v^2$
1.8	1000	22195	16269	26.70	25.83	0.003318234
1.6	50	5018	4910	2.16	31.18	0.005069441
1.6	100	5018	4882	2.72	31.00	0.005040425
1.6	150	5018	4866	3.02	30.90	0.005024881
1.6	200	5018	4842	3.50	30.75	0.005000010
1.6	400	5018	4789	4.56	30.41	0.004945088
1.6	600	5018	4781	4.73	30.36	0.004936280
1.6	800	5018	4771	4.92	30.30	0.004926435
1.6	1000	5018	4560	9.12	28.96	0.004708818
1.6	50	10856	10514	3.15	33.38	0.005428157
1.6	100	10856	10493	3.34	33.32	0.005417508
1.6	150	10856	10436	3.87	33.13	0.005387803
1.6	200	10856	10421	4.01	33.09	0.005379957
1.6	400	10856	10301	5.11	32.71	0.005318305
1.6	600	10856	10245	5.63	32.53	0.005289160
1.6	800	10856	10207	5.98	32.41	0.005269544
1.6	1000	10856	9885	8.94	31.39	0.005103645
1.6	50	14555	13861	4.77	29.34	0.004770651
1.6	100	14555	13830	4.98	29.27	0.004760131
1.6	150	14555	13803	5.17	29.22	0.004750613
1.6	200	14555	13391	8.00	28.34	0.004608841

Flow rate, m ³ /h	Concentration, ppm	Pressure drop, kg/(ms ²)			After	
		Before	After	%DR	Wall shear stress, τ_w (kg/(ms ²))	Fanning friction factor, C_f
					$\tau_w = D\Delta P/4L$	$C_f = 2\tau_w / \rho v^2$
1.6	400	14555	13372	8.13	28.30	0.004602328
1.6	600	14555	13281	8.75	28.11	0.004571269
1.6	800	14555	13126	9.82	27.78	0.004517666
1.6	1000	14555	12773	12.24	27.04	0.004396434
1.6	50	19047	16449	13.64	26.11	0.004246119
1.6	100	19047	15799	17.05	25.08	0.004078457
1.6	150	19047	15354	19.39	24.37	0.003963405
1.6	200	19047	14906	21.74	23.66	0.003847861
1.6	400	19047	14826	22.16	23.54	0.003827211
1.6	600	19047	14704	22.80	23.34	0.003795743
1.6	800	19047	14601	23.34	23.18	0.003769193
1.6	1000	19047	14447	24.15	22.93	0.003729367
1.4	50	4730	4662	1.43	29.61	0.006287858
1.4	100	4730	4631	2.10	29.40	0.006245118
1.4	150	4730	4607	2.61	29.25	0.006212585
1.4	200	4730	4589	2.99	29.14	0.006188344
1.4	400	4730	4541	4.00	28.83	0.006123916
1.4	600	4730	4578	3.22	29.07	0.006173673
1.4	800	4730	4536	4.10	28.80	0.006117537
1.4	1000	4730	4383	7.34	27.83	0.005910855
1.4	50	8226	7996	2.79	25.39	0.005392206

Flow rate, m ³ /h	Concentration, ppm	Pressure drop, kg/(ms ²)			After	
		Before	After	%DR	Wall shear stress, τ_w (kg/(ms ²))	Fanning friction factor, C_f
					$\tau_w = D\Delta P/4L$	$C_f = 2\tau_w / \rho v^2$
1.4	100	8226	7985	2.93	25.35	0.005384440
1.4	150	8226	7951	3.34	25.25	0.005361698
1.4	200	8226	7924	3.67	25.16	0.005343393
1.4	400	8226	7843	4.65	24.90	0.005289033
1.4	600	8226	7831	4.80	24.86	0.005280712
1.4	800	8226	7815	5.00	24.81	0.005269618
1.4	1000	8226	7555	8.16	23.99	0.005094334
1.4	50	12177	11769	3.35	24.91	0.005290756
1.4	100	12177	11684	4.05	24.73	0.005252437
1.4	150	12177	11580	4.90	24.51	0.005205907
1.4	200	12177	11351	6.78	24.03	0.005102993
1.4	400	12177	11348	6.81	24.02	0.005101351
1.4	600	12177	11286	7.32	23.89	0.005073433
1.4	800	12177	11232	7.76	23.77	0.005049347
1.4	1000	12177	10939	10.17	23.15	0.004917420
1.4	50	15693	14332	8.67	22.75	0.004832327
1.4	100	15693	14150	9.83	22.46	0.004770950
1.4	150	15693	13611	13.27	21.61	0.004588938
1.4	200	15693	13090	16.59	20.78	0.004413274
1.4	400	15693	13060	16.78	20.73	0.004403221
1.4	600	15693	13035	16.94	20.69	0.004394756
1.4	800	15693	12937	17.56	20.54	0.004361951

Flow rate, m ³ /h	Concentration, ppm	Pressure drop, kg/(ms ²)			After	
		Before	After	%DR	Wall shear stress, τ_w (kg/(ms ²))	Fanning friction factor, C_f
					$\tau_w = D\Delta P/4L$	$C_f = 2\tau_w / \rho v^2$
1.4	1000	15693	12867	18.01	20.43	0.004338141
1.2	50	3006	2974	1.05	18.89	0.005460032
1.2	100	3006	2962	1.46	18.81	0.005437408
1.2	150	3006	2937	2.30	18.65	0.005391057
1.2	200	3006	2929	2.57	18.60	0.005376159
1.2	400	3006	2913	3.11	18.49	0.005346362
1.2	600	3006	2899	3.57	18.41	0.005320979
1.2	800	3006	2889	3.89	18.35	0.005303322
1.2	1000	3006	2872	4.45	18.24	0.005272421
1.2	50	5641	5545	1.70	17.61	0.005089440
1.2	100	5641	5526	2.03	17.55	0.005072355
1.2	150	5641	5499	2.51	17.46	0.005047503
1.2	200	5641	5477	2.90	17.39	0.005027311
1.2	400	5641	5430	3.74	17.24	0.004983820
1.2	600	5641	5413	4.05	17.18	0.004967770
1.2	800	5641	5387	4.50	17.10	0.004944472
1.2	1000	5641	5241	7.09	16.64	0.004810375
1.2	50	8739	8475	3.02	17.94	0.005185768
1.2	100	8739	8438	3.45	17.86	0.005162775
1.2	150	8739	8340	4.57	17.65	0.005102885
1.2	200	8739	8206	6.10	17.37	0.005021072

Flow rate, m ³ /h	Concentration, ppm	Pressure drop, kg/(ms ²)			After	
		Before	After	%DR	Wall shear stress, τ_w (kg/(ms ²))	Fanning friction factor, C_f
					$\tau_w = D\Delta P/4L$	$C_f = 2\tau_w / \rho v^2$
1.2	400	8739	8283	5.22	17.53	0.005068128
1.2	600	8739	8133	6.93	17.22	0.004976690
1.2	800	8739	8109	7.21	17.16	0.004961718
1.2	1000	8739	7952	9.00	16.83	0.004866002
1.2	50	12667	12131	4.23	19.26	0.005567160
1.2	100	12667	11849	6.46	18.81	0.005437529
1.2	150	12667	11513	9.11	18.28	0.005283483
1.2	200	12667	11051	12.76	17.54	0.005071306
1.2	400	12667	11614	8.31	18.44	0.005329987
1.2	600	12667	11037	12.87	17.52	0.005064912
1.2	800	12667	11018	13.02	17.49	0.005056192
1.2	1000	12667	11106	12.32	17.63	0.005096884

APPENDIX D3
FRICITION FACTOR IN PIPE WHILE TESTING MUCILAGE IN DIESEL

Table 4.26: Friction factor in pipe with ID 0.0381m while testing mucilage in diesel

Flow rate, m ³ /h	Concentration, ppm	Pressure drop, kg/(ms ²)			After	
		Before	After	%DR	Wall shear stress, τ_w (kg/(ms ²))	Fanning friction factor, C_f
					$\tau_w = D\Delta P/4L$	$C_f = 2\tau_w / \rho v^2$
10.5	50	625	551	11.88	10.49	0.003837063
10.5	100	625	538	13.90	10.25	0.003749105
10.5	150	625	531	15.07	10.11	0.003698159
10.5	200	625	523	16.39	9.95	0.003640682
10.5	400	625	519	16.90	9.89	0.003618474
10.5	600	625	499	20.14	9.51	0.003477393
10.5	800	625	484	22.52	9.22	0.003373759
10.5	1000	625	506	19.00	9.64	0.003527033
10.5	50	1272	1106	13.08	10.53	0.003851424
10.5	100	1272	1081	15.00	10.30	0.003766348
10.5	150	1272	1032	18.83	9.83	0.003596641
10.5	200	1272	1006	20.90	9.58	0.003504920
10.5	400	1272	995	21.78	9.48	0.003465927
10.5	600	1272	839	34.03	7.99	0.002923129
10.5	800	1272	803	36.91	7.64	0.002795517
10.5	1000	1272	699	45.03	6.66	0.002435720
10.5	50	1969	1615	18.00	10.25	0.003749581
10.5	100	1969	1558	20.88	9.89	0.003617889

Flow rate, m ³ /h	Concentration, ppm	Pressure drop, kg/(ms ²)			After	
		Before	After	%DR	Wall shear stress, τ_w (kg/(ms ²))	Fanning friction factor, C_f
					$\tau_w = D\Delta P/4L$	$C_f = 2\tau_w / \rho v^2$
10.5	150	1969	1510	23.33	9.59	0.003505858
10.5	200	1969	1495	24.09	9.49	0.003471106
10.5	400	1969	1448	26.44	9.20	0.003363649
10.5	600	1969	1256	36.22	7.97	0.002916443
10.5	800	1969	1045	46.92	6.64	0.002427168
10.5	1000	1969	1063	46.00	6.75	0.002469236
10.5	50	2786	2127	23.67	10.13	0.003703913
10.5	100	2786	2090	25.00	9.95	0.003639375
10.5	150	2786	2045	26.61	9.74	0.003561250
10.5	200	2786	2027	27.26	9.65	0.003529709
10.5	400	2786	1953	29.91	9.30	0.003401117
10.5	600	2786	1506	45.95	7.17	0.002622776
10.5	800	2786	1440	48.31	6.86	0.002508257
10.5	1000	2786	1578	43.37	7.51	0.002747971
10.0	50	573	516	10.00	9.82	0.003961140
10.0	100	573	510	11.04	9.71	0.003915367
10.0	150	573	498	13.04	9.49	0.003827341
10.0	200	573	493	14.00	9.39	0.003785089
10.0	400	573	484	15.60	9.21	0.003714669
10.0	600	573	470	18.00	8.95	0.003609039
10.0	800	573	456	20.34	8.70	0.003506049

Flow rate, m ³ /h	Concentration, ppm	Pressure drop, kg/(ms ²)			After	
		Before	After	%DR	Wall shear stress, τ_w (kg/(ms ²))	Fanning friction factor, C_f
					$\tau_w = D\Delta P/4L$	$C_f = 2\tau_w / \rho v^2$
10.0	1000	573	469	18.12	8.94	0.003603757
10.0	50	1154	1017	11.86	9.69	0.003906357
10.0	100	1154	1005	12.87	9.58	0.003861594
10.0	150	1154	981	14.97	9.35	0.003768522
10.0	200	1154	969	16.04	9.23	0.003721100
10.0	400	1154	935	18.97	8.91	0.003591242
10.0	600	1154	915	20.69	8.72	0.003515012
10.0	800	1154	717	37.88	6.83	0.002753153
10.0	1000	1154	635	44.98	6.05	0.002438481
10.0	50	1810	1520	16.03	9.65	0.003891388
10.0	100	1810	1504	16.89	9.55	0.003851533
10.0	150	1810	1480	18.22	9.40	0.003789898
10.0	200	1810	1464	19.10	9.30	0.003749116
10.0	400	1810	1411	22.05	8.96	0.003612405
10.0	600	1810	1161	35.84	7.37	0.002973341
10.0	800	1810	1021	43.60	6.48	0.002613722
10.0	1000	1810	1006	44.41	6.39	0.002576185
10.0	50	2418	1951	19.33	9.29	0.003745686
10.0	100	2418	1894	21.66	9.02	0.003637499
10.0	150	2418	1862	22.98	8.87	0.003576209
10.0	200	2418	1858	23.15	8.85	0.003568315
10.0	400	2418	1761	27.18	8.39	0.003381194

Flow rate, m ³ /h	Concentration, ppm	Pressure drop, kg/(ms ²)			After	
		Before	After	%DR	Wall shear stress, τ_w (kg/(ms ²))	Fanning friction factor, C_f
					$\tau_w = D\Delta P/4L$	$C_f = 2\tau_w / \rho v^2$
10.0	600	2418	1456	39.78	6.93	0.002796148
10.0	800	2418	1313	45.68	6.26	0.002522198
10.0	1000	2418	1451	40.00	6.91	0.002785933
9.5	50	526	488	7.16	9.30	0.004156203
9.5	100	526	478	9.22	9.10	0.004063982
9.5	150	526	472	10.31	8.99	0.004015185
9.5	200	526	464	11.78	8.84	0.003949377
9.5	400	526	458	12.99	8.72	0.003895209
9.5	600	526	443	15.76	8.44	0.003771203
9.5	800	526	392	25.44	7.47	0.003337855
9.5	1000	526	395	25.00	7.52	0.003357553
9.5	50	1093	973	11.00	9.27	0.004139577
9.5	100	1093	959	12.26	9.13	0.004080972
9.5	150	1093	941	13.88	8.97	0.004005623
9.5	200	1093	938	14.15	8.94	0.003993064
9.5	400	1093	915	16.32	8.71	0.003892133
9.5	600	1093	787	28.04	7.49	0.003347011
9.5	800	1093	650	40.56	6.19	0.002764680
9.5	1000	1093	621	43.18	5.92	0.002642818
9.5	50	1647	1408	14.51	8.94	0.003994510
9.5	100	1647	1382	16.10	8.77	0.003920217
9.5	150	1647	1366	17.05	8.68	0.003875829

Flow rate, m ³ /h	Concentration, ppm	Pressure drop, kg/(ms ²)			After	
		Before	After	%DR	Wall shear stress, τ_w (kg/(ms ²))	Fanning friction factor, C_f
					$\tau_w = D\Delta P/4L$	$C_f = 2\tau_w / \rho v^2$
9.5	200	1647	1335	18.96	8.48	0.003786584
9.5	400	1647	1299	21.10	8.25	0.003686593
9.5	600	1647	1153	30.00	7.32	0.003270742
9.5	800	1647	856	48.05	5.43	0.002427357
9.5	1000	1647	904	45.11	5.74	0.002564729
9.5	50	2209	1820	17.60	8.67	0.003872922
9.5	100	2209	1762	20.23	8.39	0.003749308
9.5	150	2209	1708	22.70	8.13	0.003633215
9.5	200	2209	1694	23.31	8.07	0.003604544
9.5	400	2209	1652	25.22	7.87	0.003514771
9.5	600	2209	1357	38.57	6.46	0.002887301
9.5	800	2209	919	58.40	4.38	0.001955262
9.5	1000	2209	1144	48.22	5.45	0.002433737
9.0	50	482	459	4.85	8.74	0.004349045
9.0	100	482	453	6.05	8.63	0.004294196
9.0	150	482	442	8.20	8.43	0.004195925
9.0	200	482	434	10.04	8.26	0.004111824
9.0	400	482	428	11.27	8.15	0.004055604
9.0	600	482	413	14.38	7.86	0.003913455
9.0	800	482	407	15.48	7.76	0.003863177
9.0	1000	482	410	15.04	7.80	0.003883288

Flow rate, m ³ /h	Concentration, ppm	Pressure drop, kg/(ms ²)			After	
		Before	After	%DR	Wall shear stress, τ_w (kg/(ms ²))	Fanning friction factor, C_f
					$\tau_w = D\Delta P/4L$	$C_f = 2\tau_w / \rho v^2$
9.0	50	986	880	10.75	8.38	0.004172470
9.0	100	986	873	11.43	8.32	0.004140679
9.0	150	986	858	13.00	8.17	0.004067281
9.0	200	986	854	13.43	8.13	0.004047179
9.0	400	986	852	13.59	8.12	0.004039699
9.0	600	986	752	23.77	7.16	0.003563780
9.0	800	986	669	32.15	6.37	0.003172012
9.0	1000	986	690	30.01	6.57	0.003272058
9.0	50	1485	1282	13.70	8.14	0.004050923
9.0	100	1485	1277	14.00	8.11	0.004036841
9.0	150	1485	1257	15.34	7.98	0.003973942
9.0	200	1485	1231	17.08	7.82	0.003892266
9.0	400	1485	1199	19.27	7.61	0.003789467
9.0	600	1485	1068	28.10	6.78	0.003374987
9.0	800	1485	936	37.00	5.94	0.002957221
9.0	1000	1485	908	38.85	5.77	0.002870382
9.0	50	2003	1682	16.05	8.01	0.003986389
9.0	100	2003	1661	17.05	7.91	0.003938904
9.0	150	2003	1605	19.88	7.64	0.003804520
9.0	200	2003	1581	21.05	7.53	0.003748963
9.0	400	2003	1525	23.87	7.26	0.003615054
9.0	600	2003	1344	32.90	6.40	0.003186262

Flow rate, m ³ /h	Concentration, ppm	Pressure drop, kg/(ms ²)			After	
		Before	After	%DR	Wall shear stress, τ_w (kg/(ms ²))	Fanning friction factor, C_f
					$\tau_w = \Delta P / 4L$	$C_f = 2\tau_w / \rho v^2$
9.0	800	2003	1171	41.55	5.58	0.002775515
9.0	1000	2003	1221	39.04	5.82	0.002894703
8.5	50	450	432	4.00	8.23	0.004592709
8.5	100	450	430	4.53	8.18	0.004567354
8.5	150	450	423	6.00	8.06	0.004497028
8.5	200	450	415	7.80	7.90	0.004410914
8.5	400	450	414	8.01	7.89	0.004400868
8.5	600	450	405	10.11	7.71	0.004300402
8.5	800	450	387	14.10	7.36	0.004109518
8.5	1000	450	387	13.90	7.38	0.004119086
8.5	50	901	826	8.31	7.87	0.004391390
8.5	100	901	803	10.90	7.65	0.004267344
8.5	150	901	800	11.17	7.62	0.004254413
8.5	200	901	784	13.04	7.46	0.004164852
8.5	400	901	764	15.16	7.28	0.004063317
8.5	600	901	722	19.89	6.88	0.003836778
8.5	800	901	622	30.97	5.92	0.003306114
8.5	1000	901	658	27.00	6.26	0.003496253
8.5	50	1380	1223	11.36	7.77	0.004334837
8.5	100	1380	1205	12.70	7.65	0.004269306
8.5	150	1380	1201	13.00	7.62	0.004254635

Flow rate, m ³ /h	Concentration, ppm	Pressure drop, kg/(ms ²)			After	
		Before	After	%DR	Wall shear stress, τ_w (kg/(ms ²))	Fanning friction factor, C_f
					$\tau_w = \Delta P / 4L$	$C_f = 2\tau_w / \rho v^2$
8.5	200	1380	1164	15.66	7.39	0.004124550
8.5	400	1380	1144	17.12	7.26	0.004053151
8.5	600	1380	1001	27.45	6.36	0.003547974
8.5	800	1380	926	32.90	5.88	0.003281448
8.5	1000	1380	938	32.00	5.96	0.003325462
8.5	50	1880	1600	14.88	7.62	0.004253189
8.5	100	1880	1585	15.70	7.55	0.004212216
8.5	150	1880	1559	17.06	7.43	0.004144261
8.5	200	1880	1506	19.88	7.17	0.004003354
8.5	400	1880	1472	21.69	7.01	0.003912914
8.5	600	1880	1335	29.00	6.36	0.003547655
8.5	800	1880	1219	35.14	5.81	0.003240858
8.5	1000	1880	1256	33.17	5.98	0.003339293
8.0	50	399	386	3.37	7.34	0.004627303
8.0	100	399	383	4.00	7.30	0.004597134
8.0	150	399	380	4.66	7.25	0.004565529
8.0	200	399	379	4.92	7.23	0.004553079
8.0	400	399	374	6.30	7.12	0.004486995
8.0	600	399	351	12.07	6.68	0.004210688
8.0	800	399	348	12.69	6.64	0.004180998
8.0	1000	399	351	12.00	6.69	0.004214040

Flow rate, m ³ /h	Concentration, ppm	Pressure drop, kg/(ms ²)			After	
		Before	After	%DR	Wall shear stress, τ_w (kg/(ms ²))	Fanning friction factor, C_f
					$\tau_w = D\Delta P/4L$	$C_f = 2\tau_w / \rho v^2$
8.0	50	802	746	7.04	7.10	0.004473872
8.0	100	802	737	8.07	7.02	0.004424301
8.0	150	802	719	10.40	6.84	0.004312166
8.0	200	802	699	12.87	6.66	0.004193293
8.0	400	802	698	13.01	6.65	0.004186555
8.0	600	802	670	16.47	6.38	0.004020036
8.0	800	802	573	28.58	5.46	0.003437220
8.0	1000	802	593	26.12	5.64	0.003555612
8.0	50	1230	1119	9.00	7.11	0.004477837
8.0	100	1230	1101	10.50	6.99	0.004404027
8.0	150	1230	1079	12.30	6.85	0.004315454
8.0	200	1230	1058	14.00	6.72	0.004231802
8.0	400	1230	1034	15.93	6.57	0.004136833
8.0	600	1230	939	23.69	5.96	0.003754987
8.0	800	1230	838	31.84	5.32	0.003353949
8.0	1000	1230	882	28.31	5.60	0.003527650
8.0	50	1692	1455	14.00	6.93	0.004365982
8.0	100	1692	1439	14.98	6.85	0.004316230
8.0	150	1692	1420	16.10	6.76	0.004259370
8.0	200	1692	1405	16.97	6.69	0.004215203
8.0	400	1692	1344	20.55	6.40	0.004033456
8.0	600	1692	1186	29.88	5.65	0.003559798

Flow rate, m ³ /h	Concentration, ppm	Pressure drop, kg/(ms ²)			After	
		Before	After	%DR	Wall shear stress, τ_w (kg/(ms ²))	Fanning friction factor, C_f
					$\tau_w = D\Delta P/4L$	$C_f = 2\tau_w / \rho v^2$
8.0	800	1692	1138	32.76	5.42	0.003413588
8.0	1000	1692	1184	30.03	5.64	0.003552183
7.5	50	371	361	2.78	6.87	0.004925270
7.5	100	371	360	3.03	6.85	0.004912605
7.5	150	371	359	3.10	6.85	0.004909059
7.5	200	371	355	4.33	6.76	0.004846745
7.5	400	371	352	5.00	6.71	0.004812802
7.5	600	371	350	5.55	6.68	0.004784939
7.5	800	371	344	7.32	6.55	0.004695269
7.5	1000	371	345	7.11	6.57	0.004705908
7.5	50	743	708	4.66	6.75	0.004836537
7.5	100	743	701	5.61	6.68	0.004788344
7.5	150	743	698	6.02	6.65	0.004767545
7.5	200	743	684	8.00	6.51	0.004667101
7.5	400	743	670	9.89	6.38	0.004571222
7.5	600	743	615	17.18	5.86	0.004201405
7.5	800	743	556	25.11	5.30	0.003799121
7.5	1000	743	577	22.40	5.49	0.003936598
7.5	50	1120	1051	6.14	6.68	0.004784955
7.5	100	1120	1037	7.41	6.59	0.004720211
7.5	150	1120	1033	7.75	6.56	0.004702877

Flow rate, m ³ /h	Concentration, ppm	Pressure drop, kg/(ms ²)			After	
		Before	After	%DR	Wall shear stress, τ_w (kg/(ms ²))	Fanning friction factor, C_f
					$\tau_w = D\Delta P/4L$	$C_f = 2\tau_w / \rho v^2$
7.5	200	1120	1003	10.43	6.37	0.004566252
7.5	400	1120	977	12.74	6.21	0.004448489
7.5	600	1120	897	19.90	5.70	0.004083474
7.5	800	1120	820	26.79	5.21	0.003732224
7.5	1000	1120	851	24.00	5.41	0.003874457
7.5	50	1508	1314	12.87	6.26	0.004485487
7.5	100	1508	1295	14.12	6.17	0.004421136
7.5	150	1508	1281	15.04	6.10	0.004373774
7.5	200	1508	1259	16.50	6.00	0.004298613
7.5	400	1508	1231	18.38	5.86	0.004201830
7.5	600	1508	1129	25.14	5.38	0.003853822
7.5	800	1508	1074	28.79	5.11	0.003665919
7.5	1000	1508	1132	24.94	5.39	0.003864118

Table 4.27: Friction factor in pipe with ID 0.0254m while testing mucilage in diesel

Flow rate, m ³ /h	Concentration, ppm	Pressure drop, kg/(ms ²)			After	
		Before	After	%DR	Wall shear stress, τ_w (kg/(ms ²))	Fanning friction factor, C_f
					$\tau_w = D\Delta P/4L$	$C_f = 2\tau_w / \rho v^2$
8.0	50	2862	2604	9.03	33.07	0.004114856
8.0	100	2862	2550	10.90	32.39	0.004030270
8.0	150	2862	2512	12.23	31.90	0.003970110
8.0	200	2862	2441	14.70	31.00	0.003858384
8.0	400	2862	2416	15.57	30.69	0.003819031
8.0	600	2862	2401	16.10	30.50	0.003795058
8.0	800	2862	2317	19.05	29.42	0.003661620
8.0	1000	2862	2347	18.00	29.80	0.003709115
8.0	50	5811	5056	13.00	32.10	0.003995093
8.0	100	5811	4937	15.04	31.35	0.003901415
8.0	150	5811	4881	16.00	31.00	0.003857331
8.0	200	5811	4755	18.17	30.20	0.003757684
8.0	400	5811	4638	20.19	29.45	0.003664924
8.0	600	5811	3902	32.85	24.78	0.003083569
8.0	800	5811	3726	35.88	23.66	0.002944430
8.0	1000	5811	3860	33.58	24.51	0.003050047
8.0	50	8810	7481	15.09	31.67	0.003940944
8.0	100	8810	7224	18.00	30.58	0.003805882
8.0	150	8810	7013	20.40	29.69	0.003694490
8.0	200	8810	6796	22.86	28.77	0.003580314

Flow rate, m ³ /h	Concentration, ppm	Pressure drop, kg/(ms ²)			After	
		Before	After	%DR	Wall shear stress, τ_w (kg/(ms ²))	Fanning friction factor, C_f
					$\tau_w = \Delta P / 4L$	$C_f = 2\tau_w / \rho v^2$
8.0	400	8810	6690	24.06	28.32	0.003524618
8.0	600	8810	5724	35.03	24.23	0.003015465
8.0	800	8810	4827	45.21	20.43	0.002542979
8.0	1000	8810	5286	40.00	22.38	0.002784791
8.0	50	11789	9431	20.00	29.94	0.003726437
8.0	100	11789	9161	22.29	29.09	0.003619767
8.0	150	11789	8947	24.11	28.41	0.003534991
8.0	200	11789	8766	25.64	27.83	0.003463723
8.0	400	11789	8534	27.61	27.10	0.003371959
8.0	600	11789	6504	44.83	20.65	0.002569844
8.0	800	11789	6314	46.44	20.05	0.002494849
8.0	1000	11789	6861	41.80	21.78	0.002710983
7.5	50	2533	2315	8.61	29.40	0.004162729
7.5	100	2533	2304	9.04	29.26	0.004143142
7.5	150	2533	2250	11.16	28.58	0.004046578
7.5	200	2533	2204	13.00	27.99	0.003962768
7.5	400	2533	2179	13.98	27.67	0.003918130
7.5	600	2533	2149	15.17	27.29	0.003863927
7.5	800	2533	2063	18.56	26.20	0.003709515
7.5	1000	2533	2085	17.68	26.48	0.003749599
7.5	50	5197	4583	11.81	29.10	0.004120845

Flow rate, m ³ /h	Concentration, ppm	Pressure drop, kg/(ms ²)			After	
		Before	After	%DR	Wall shear stress, τ_w (kg/(ms ²))	Fanning friction factor, C_f
					$\tau_w = \Delta P / 4L$	$C_f = 2\tau_w / \rho v^2$
7.5	100	5197	4486	13.69	28.48	0.004032999
7.5	150	5197	4414	15.06	28.03	0.003968983
7.5	200	5197	4312	17.03	27.38	0.003876931
7.5	400	5197	4232	18.56	26.88	0.003805439
7.5	600	5197	3608	30.57	22.91	0.003244248
7.5	800	5197	3361	35.32	21.35	0.003022296
7.5	1000	5197	3552	31.65	22.56	0.003193783
7.5	50	7951	6917	13.00	29.28	0.004146331
7.5	100	7951	6758	15.01	28.61	0.004050537
7.5	150	7951	6510	18.12	27.56	0.003902317
7.5	200	7951	6440	19.00	27.26	0.003860377
7.5	400	7951	6288	20.92	26.62	0.003768872
7.5	600	7951	5283	33.55	22.37	0.003166939
7.5	800	7951	4532	43.00	19.19	0.002716562
7.5	1000	7951	4918	38.14	20.82	0.002948184
7.5	50	10626	8599	19.08	27.30	0.003865538
7.5	100	10626	8409	20.86	26.70	0.003780507
7.5	150	10626	8235	22.50	26.15	0.003702165
7.5	200	10626	8143	23.37	25.85	0.003660605
7.5	400	10626	7877	25.87	25.01	0.003541180
7.5	600	10626	6380	39.96	20.26	0.002868103
7.5	800	10626	5972	43.80	18.96	0.002684667

Flow rate, m ³ /h	Concentration, ppm	Pressure drop, kg/(ms ²)			After	
		Before	After	%DR	Wall shear stress, τ_w (kg/(ms ²))	Fanning friction factor, C_f
					$\tau_w = D\Delta P/4L$	$C_f = 2\tau_w / \rho v^2$
7.5	1000	10626	6335	40.38	20.11	0.002848040
7.0	50	2184	2038	6.70	25.88	0.004206346
7.0	100	2184	1992	8.77	25.30	0.004113022
7.0	150	2184	1987	9.03	25.23	0.004101300
7.0	200	2184	1965	10.04	24.95	0.004055765
7.0	400	2184	1937	11.32	24.60	0.003998057
7.0	600	2184	1886	13.66	23.95	0.003892560
7.0	800	2184	1832	16.10	23.27	0.003782555
7.0	1000	2184	1835	16.00	23.30	0.003787064
7.0	50	4513	4069	9.83	25.84	0.004200182
7.0	100	4513	3926	13.00	24.93	0.004052521
7.0	150	4513	3909	13.39	24.82	0.004034354
7.0	200	4513	3809	15.60	24.19	0.003931411
7.0	400	4513	3716	17.67	23.59	0.003834989
7.0	600	4513	3299	26.91	20.95	0.003404583
7.0	800	4513	2993	33.69	19.00	0.003088766
7.0	1000	4513	3159	30.00	20.06	0.003260649
7.0	50	6830	6030	11.72	25.52	0.004148895
7.0	100	6830	5833	14.60	24.69	0.004013544
7.0	150	6830	5726	16.16	24.24	0.003940228
7.0	200	6830	5648	17.30	23.91	0.003886652

Flow rate, m ³ /h	Concentration, ppm	Pressure drop, kg/(ms ²)			After	
		Before	After	%DR	Wall shear stress, τ_w (kg/(ms ²))	Fanning friction factor, C_f
					$\tau_w = \Delta P / 4L$	$C_f = 2\tau_w / \rho v^2$
7.0	400	6830	5469	19.93	23.15	0.003763050
7.0	600	6830	4769	30.18	20.19	0.003281330
7.0	800	6830	4153	39.19	17.58	0.002857887
7.0	1000	6830	4440	34.99	18.80	0.003055275
7.0	50	9116	7516	17.55	23.86	0.003878874
7.0	100	9116	7347	19.40	23.33	0.003791840
7.0	150	9116	7233	20.66	22.96	0.003732563
7.0	200	9116	7187	21.16	22.82	0.003709041
7.0	400	9116	6957	23.68	22.09	0.003590487
7.0	600	9116	5780	36.59	18.35	0.002983134
7.0	800	9116	5398	40.78	17.14	0.002786015
7.0	1000	9116	5824	36.11	18.49	0.003005716
6.5	50	1982	1892	4.55	24.03	0.004529180
6.5	100	1982	1862	6.05	23.65	0.004458004
6.5	150	1982	1827	7.80	23.21	0.004374965
6.5	200	1982	1808	8.76	22.97	0.004329412
6.5	400	1982	1786	9.91	22.68	0.004274844
6.5	600	1982	1728	12.83	21.94	0.004136288
6.5	800	1982	1690	14.75	21.46	0.004045182
6.5	1000	1982	1704	14.05	21.63	0.004078398
6.5	50	3997	3657	8.51	23.22	0.004377416

Flow rate, m ³ /h	Concentration, ppm	Pressure drop, kg/(ms ²)			After	
		Before	After	%DR	Wall shear stress, τ_w (kg/(ms ²))	Fanning friction factor, C_f
					$\tau_w = \Delta P / 4L$	$C_f = 2\tau_w / \rho v^2$
6.5	100	3997	3594	10.09	22.82	0.004301820
6.5	150	3997	3517	12.00	22.34	0.004210434
6.5	200	3997	3444	13.83	21.87	0.004122876
6.5	400	3997	3425	14.31	21.75	0.004099910
6.5	600	3997	3094	22.58	19.65	0.003704225
6.5	800	3997	2754	31.09	17.49	0.003297057
6.5	1000	3997	2807	29.76	17.83	0.003360692
6.5	50	6035	5489	9.04	23.24	0.004380730
6.5	100	6035	5354	11.29	22.66	0.004272368
6.5	150	6035	5188	14.03	21.96	0.004140407
6.5	200	6035	5099	15.51	21.59	0.004069128
6.5	400	6035	4989	17.33	21.12	0.003981475
6.5	600	6035	4410	26.93	18.67	0.003519129
6.5	800	6035	3798	37.07	16.08	0.003030776
6.5	1000	6035	3952	34.52	16.73	0.003153586
6.5	50	8084	6801	15.87	21.59	0.004070589
6.5	100	8084	6707	17.03	21.30	0.004014463
6.5	150	8084	6470	19.97	20.54	0.003872212
6.5	200	8084	6465	20.03	20.53	0.003869309
6.5	400	8084	6307	21.98	20.03	0.003774960
6.5	600	8084	5472	32.31	17.37	0.003275148
6.5	800	8084	4924	39.09	15.63	0.002947101

Flow rate, m ³ /h	Concentration, ppm	Pressure drop, kg/(ms ²)			After	
		Before	After	%DR	Wall shear stress, τ_w (kg/(ms ²))	Fanning friction factor, C_f
					$\tau_w = D\Delta P/4L$	$C_f = 2\tau_w / \rho v^2$
6.5	1000	8084	5251	35.04	16.67	0.003143058
6.0	50	1704	1643	3.60	20.86	0.004615416
6.0	100	1704	1636	4.00	20.78	0.004596265
6.0	150	1704	1618	5.02	20.55	0.004547430
6.0	200	1704	1593	6.50	20.23	0.004476571
6.0	400	1704	1581	7.22	20.08	0.004442099
6.0	600	1704	1512	11.27	19.20	0.004248194
6.0	800	1704	1483	12.96	18.84	0.004167280
6.0	1000	1704	1500	12.00	19.04	0.004213243
6.0	50	3467	3232	6.79	20.52	0.004539945
6.0	100	3467	3185	8.12	20.23	0.004475165
6.0	150	3467	3119	10.05	19.80	0.004381162
6.0	200	3467	3042	12.26	19.32	0.004273520
6.0	400	3467	2993	13.66	19.01	0.004205331
6.0	600	3467	2799	19.26	17.78	0.003932573
6.0	800	3467	2408	30.54	15.29	0.003383163
6.0	1000	3467	2460	29.04	15.62	0.003456223
6.0	50	5211	4805	7.80	20.34	0.004499818
6.0	100	5211	4719	9.45	19.98	0.004419290
6.0	150	5211	4494	13.76	19.02	0.004208941
6.0	200	5211	4476	14.11	18.95	0.004191859

Flow rate, m ³ /h	Concentration, ppm	Pressure drop, kg/(ms ²)			After	
		Before	After	%DR	Wall shear stress, τ_w (kg/(ms ²))	Fanning friction factor, C_f
					$\tau_w = D\Delta P/4L$	$C_f = 2\tau_w / \rho v^2$
6.0	400	5211	4401	15.54	18.63	0.004122068
6.0	600	5211	3948	24.24	16.71	0.003697465
6.0	800	5211	3518	32.48	14.89	0.003295312
6.0	1000	5211	3643	30.09	15.42	0.003411956
6.0	50	6971	5918	15.10	18.79	0.004157259
6.0	100	6971	5812	16.62	18.45	0.004082829
6.0	150	6971	5714	18.03	18.14	0.004013787
6.0	200	6971	5582	19.92	17.72	0.003921240
6.0	400	6971	5507	21.00	17.49	0.003868356
6.0	600	6971	4907	29.61	15.58	0.003446754
6.0	800	6971	4617	33.77	14.66	0.003243053
6.0	1000	6971	4819	30.87	15.30	0.003385056
5.5	50	1389	1357	2.33	17.23	0.004536332
5.5	100	1389	1341	3.42	17.04	0.004485706
5.5	150	1389	1327	4.49	16.85	0.004436009
5.5	200	1389	1319	5.01	16.76	0.004411858
5.5	400	1389	1304	6.09	16.57	0.004361697
5.5	600	1389	1237	10.92	15.71	0.004137365
5.5	800	1389	1223	11.94	15.53	0.004089991
5.5	1000	1389	1250	10.03	15.87	0.004178701
5.5	50	2781	2614	6.00	16.60	0.004370592

Flow rate, m ³ /h	Concentration, ppm	Pressure drop, kg/(ms ²)			After	
		Before	After	%DR	Wall shear stress, τ_w (kg/(ms ²))	Fanning friction factor, C_f
					$\tau_w = D\Delta P/4L$	$C_f = 2\tau_w / \rho v^2$
5.5	100	2781	2593	6.77	16.46	0.004334790
5.5	150	2781	2561	7.90	16.26	0.004282250
5.5	200	2781	2502	10.03	15.89	0.004183214
5.5	400	2781	2453	11.78	15.58	0.004101847
5.5	600	2781	2299	17.34	14.60	0.003843331
5.5	800	2781	2055	26.09	13.05	0.003436494
5.5	1000	2781	2072	25.50	13.16	0.003463926
5.5	50	4385	4098	6.54	17.35	0.004567888
5.5	100	4385	4050	7.64	17.14	0.004514126
5.5	150	4385	3821	12.87	16.17	0.004258508
5.5	200	4385	3813	13.04	16.14	0.004250199
5.5	400	4385	3756	14.34	15.90	0.004186661
5.5	600	4385	3399	22.48	14.39	0.003788816
5.5	800	4385	3106	29.17	13.15	0.003461840
5.5	1000	4385	3076	29.86	13.02	0.003428116
5.5	50	5880	5101	13.24	16.20	0.004264600
5.5	100	5880	5054	14.05	16.05	0.004224785
5.5	150	5880	4939	16.00	15.68	0.004128935
5.5	200	5880	4914	16.43	15.60	0.004107798
5.5	400	5880	4768	18.91	15.14	0.003985896
5.5	600	5880	4258	27.58	13.52	0.003559731
5.5	800	5880	4078	30.65	12.95	0.003408829

Flow rate, m ³ /h	Concentration, ppm	Pressure drop, kg/(ms ²)			After	
		Before	After	%DR	Wall shear stress, τ_w (kg/(ms ²))	Fanning friction factor, C_f
					$\tau_w = D\Delta P/4L$	$C_f = 2\tau_w / \rho v^2$
5.5	1000	5880	4116	30.00	13.07	0.003440779
5.0	50	1208	1184	1.99	15.04	0.004790315
5.0	100	1208	1175	2.76	14.92	0.004752681
5.0	150	1208	1171	3.10	14.87	0.004736063
5.0	200	1208	1167	3.38	14.82	0.004722378
5.0	400	1208	1152	4.66	14.63	0.004659817
5.0	600	1208	1148	4.98	14.58	0.004644176
5.0	800	1208	1118	7.42	14.20	0.004524919
5.0	1000	1208	1123	7.00	14.27	0.004545447
5.0	50	2450	2349	4.11	14.92	0.004752653
5.0	100	2450	2303	6.00	14.62	0.004658978
5.0	150	2450	2270	7.33	14.42	0.004593059
5.0	200	2450	2253	8.04	14.31	0.004557869
5.0	400	2450	2226	9.13	14.14	0.004503844
5.0	600	2450	2060	15.90	13.08	0.004168299
5.0	800	2450	1865	23.86	11.85	0.003773772
5.0	1000	2450	1911	22.00	12.13	0.003865961
5.0	50	3744	3521	5.96	14.90	0.004748473
5.0	100	3744	3482	7.00	14.74	0.004695959
5.0	150	3744	3332	11.00	14.11	0.004493982
5.0	200	3744	3270	12.67	13.84	0.004409657

Flow rate, m ³ /h	Concentration, ppm	Pressure drop, kg/(ms ²)			After	
		Before	After	%DR	Wall shear stress, τ_w (kg/(ms ²))	Fanning friction factor, C_f
					$\tau_w = D\Delta P/4L$	$C_f = 2\tau_w / \rho v^2$
5.0	400	3744	3221	13.98	13.63	0.004343509
5.0	600	3744	3024	19.23	12.80	0.004078415
5.0	800	3744	2772	25.97	11.73	0.003738084
5.0	1000	3744	2887	22.89	12.22	0.003893606
5.0	50	5028	4495	10.60	14.27	0.004546734
5.0	100	5028	4411	12.27	14.01	0.004461801
5.0	150	5028	4342	13.65	13.78	0.004391616
5.0	200	5028	4249	15.50	13.49	0.004297528
5.0	400	5028	4129	17.88	13.11	0.004176485
5.0	600	5028	3804	24.35	12.08	0.003847432
5.0	800	5028	3605	28.30	11.45	0.003646542
5.0	1000	5028	3771	25.00	11.97	0.003814374

Table 4.28: Friction factor in pipe with ID 0.0127m while testing mucilage in diesel

Flow rate, m ³ /h	Concentration, ppm	Pressure drop, kg/(ms ²)			After	
		Before	After	%DR	Wall shear stress, τ_w (kg/(ms ²))	Fanning friction factor, C_f
					$\tau_w = D\Delta P/4L$	$C_f = 2\tau_w / \rho v^2$
2.4	50	9201	8833	4.00	56.09	0.004847307
2.4	100	9201	8450	8.16	53.66	0.004637257
2.4	150	9201	8304	9.75	52.73	0.004556974
2.4	200	9201	8152	11.40	51.77	0.004473661
2.4	400	9201	8026	12.77	50.97	0.004404486
2.4	600	9201	7823	14.98	49.67	0.004292897
2.4	800	9201	7507	18.41	47.67	0.004119706
2.4	1000	9201	7815	15.06	49.63	0.004288857
2.4	50	18546	16678	10.07	52.95	0.004576349
2.4	100	18546	16456	11.27	52.25	0.004515284
2.4	150	18546	15909	14.22	50.51	0.004365164
2.4	200	18546	15579	16.00	49.46	0.004274584
2.4	400	18546	15187	18.11	48.22	0.004167210
2.4	600	18546	14575	21.41	46.28	0.003999280
2.4	800	18546	13767	25.77	43.71	0.003777409
2.4	1000	18546	14651	21.00	46.52	0.004020144
2.4	50	27849	24599	11.67	52.07	0.004499776
2.4	100	27849	24368	12.50	51.58	0.004457493
2.4	150	27849	22931	17.66	48.54	0.004194629
2.4	200	27849	22279	20.00	47.16	0.004075422

Flow rate, m ³ /h	Concentration, ppm	Pressure drop, kg/(ms ²)			After	
		Before	After	%DR	Wall shear stress, τ_w (kg/(ms ²))	Fanning friction factor, C_f
					$\tau_w = \Delta P / 4L$	$C_f = 2\tau_w / \rho v^2$
2.4	400	27849	22070	20.75	46.72	0.004037215
2.4	600	27849	20377	26.83	43.13	0.003727483
2.4	800	27849	19478	30.06	41.23	0.003562938
2.4	1000	27849	20146	27.66	42.64	0.003685201
2.4	50	37163	31711	14.67	50.34	0.004350577
2.4	100	37163	30845	17.00	48.97	0.004231781
2.4	150	37163	29983	19.32	47.60	0.004113495
2.4	200	37163	29021	21.91	46.07	0.003981443
2.4	400	37163	28311	23.82	44.94	0.003884061
2.4	600	37163	26780	27.94	42.51	0.003674001
2.4	800	37163	25029	32.65	39.73	0.003433861
2.4	1000	37163	26014	30.00	41.30	0.003568972
2.2	50	7932	7512	5.30	47.70	0.004905735
2.2	100	7932	7360	7.21	46.74	0.004806792
2.2	150	7932	7282	8.20	46.24	0.004755507
2.2	200	7932	7139	10.00	45.33	0.004662261
2.2	400	7932	7020	11.50	44.58	0.004584557
2.2	600	7932	6797	14.31	43.16	0.004438991
2.2	800	7932	6629	16.43	42.09	0.004329169
2.2	1000	7932	6871	13.37	43.63	0.004487686
2.2	50	14668	13348	9.00	42.38	0.004358667

Flow rate, m ³ /h	Concentration, ppm	Pressure drop, kg/(ms ²)			After	
		Before	After	%DR	Wall shear stress, τ_w (kg/(ms ²))	Fanning friction factor, C_f
					$\tau_w = \Delta P / 4L$	$C_f = 2\tau_w / \rho v^2$
2.2	100	14668	13143	10.40	41.73	0.004291611
2.2	150	14668	12805	12.70	40.66	0.004181447
2.2	200	14668	12603	14.08	40.01	0.004115348
2.2	400	14668	12326	15.97	39.13	0.004024822
2.2	600	14668	11818	19.43	37.52	0.003859097
2.2	800	14668	11088	24.41	35.20	0.003620568
2.2	1000	14668	11896	18.90	37.77	0.003884483
2.2	50	23054	20513	11.02	43.42	0.004465693
2.2	100	23054	19944	13.49	42.21	0.004341729
2.2	150	23054	19435	15.70	41.14	0.004230815
2.2	200	23054	18983	17.66	40.18	0.004132447
2.2	400	23054	18780	18.54	39.75	0.004088282
2.2	600	23054	17281	25.04	36.58	0.003762063
2.2	800	23054	17293	24.99	36.60	0.003764572
2.2	1000	23054	17521	24.00	37.09	0.003814258
2.2	50	30792	26789	13.00	42.53	0.004373897
2.2	100	30792	26112	15.20	41.45	0.004263293
2.2	150	30792	25351	17.67	40.24	0.004139114
2.2	200	30792	25323	17.76	40.20	0.004134590
2.2	400	30792	25246	18.01	40.08	0.004122021
2.2	600	30792	22746	26.13	36.11	0.003713791
2.2	800	30792	21296	30.84	33.81	0.003476997

Flow rate, m ³ /h	Concentration, ppm	Pressure drop, kg/(ms ²)			After	
		Before	After	%DR	Wall shear stress, τ_w (kg/(ms ²))	Fanning friction factor, C_f
					$\tau_w = D\Delta P/4L$	$C_f = 2\tau_w / \rho v^2$
2.2	1000	30792	22749	26.12	36.11	0.003714293
2.0	50	6634	6385	3.76	40.54	0.005045310
2.0	100	6634	6289	5.20	39.94	0.004969819
2.0	150	6634	6197	6.58	39.35	0.004897474
2.0	200	6634	6029	9.12	38.28	0.004764316
2.0	400	6634	5967	10.06	37.89	0.004715037
2.0	600	6634	5768	13.05	36.63	0.004558289
2.0	800	6634	5949	10.33	37.77	0.004700883
2.0	1000	6634	5868	11.55	37.26	0.004636925
2.0	50	13324	12311	7.60	39.09	0.004864446
2.0	100	13324	12146	8.84	38.56	0.004799166
2.0	150	13324	12125	9.00	38.50	0.004790742
2.0	200	13324	11689	12.27	37.11	0.004618591
2.0	400	13324	11341	14.88	36.01	0.004481187
2.0	600	13324	10968	17.68	34.82	0.004333779
2.0	800	13324	10658	20.01	33.84	0.004211115
2.0	1000	13324	11120	16.54	35.31	0.004393795
2.0	50	19657	17888	9.00	37.86	0.004711879
2.0	100	19657	17581	10.56	37.21	0.004631104
2.0	150	19657	17045	13.29	36.08	0.004489748
2.0	200	19657	16620	15.45	35.18	0.004377905

Flow rate, m ³ /h	Concentration, ppm	Pressure drop, kg/(ms ²)			After	
		Before	After	%DR	Wall shear stress, τ_w (kg/(ms ²))	Fanning friction factor, C_f
					$\tau_w = D\Delta P/4L$	$C_f = 2\tau_w / \rho v^2$
2.0	400	19657	16439	16.37	34.80	0.004330269
2.0	600	19657	15500	21.15	32.81	0.004082766
2.0	800	19657	13235	32.67	28.01	0.003486273
2.0	1000	19657	15266	22.34	32.31	0.004021149
2.0	50	26511	23534	11.23	37.36	0.004649317
2.0	100	26511	22964	13.38	36.46	0.004536711
2.0	150	26511	22089	16.68	35.07	0.004363874
2.0	200	26511	21694	18.17	34.44	0.004285835
2.0	400	26511	21381	19.35	33.94	0.004224033
2.0	600	26511	20488	22.72	32.52	0.004047529
2.0	800	26511	16652	37.19	26.43	0.003289665
2.0	1000	26511	21233	19.91	33.71	0.004194703
1.8	50	5379	5213	3.08	33.10	0.005086121
1.8	100	5379	5164	4.00	32.79	0.005037842
1.8	150	5379	5108	5.04	32.44	0.004983265
1.8	200	5379	4998	7.09	31.73	0.004875686
1.8	400	5379	4923	8.48	31.26	0.004802743
1.8	600	5379	4767	11.38	30.27	0.004650558
1.8	800	5379	4680	12.99	29.72	0.004566069
1.8	1000	5379	4836	10.09	30.71	0.004718254
1.8	50	10945	10228	6.55	32.47	0.004989268

Flow rate, m ³ /h	Concentration, ppm	Pressure drop, kg/(ms ²)			After	
		Before	After	%DR	Wall shear stress, τ_w (kg/(ms ²))	Fanning friction factor, C_f
					$\tau_w = D\Delta P/4L$	$C_f = 2\tau_w / \rho v^2$
1.8	100	10945	10167	7.11	32.28	0.004959370
1.8	150	10945	10044	8.23	31.89	0.004899573
1.8	200	10945	9851	10.00	31.28	0.004805074
1.8	400	10945	9736	11.05	30.91	0.004749014
1.8	600	10945	9523	12.99	30.24	0.004645438
1.8	800	10945	8933	18.38	28.36	0.004357668
1.8	1000	10945	9744	10.97	30.94	0.004753286
1.8	50	16374	15197	7.19	32.17	0.004941970
1.8	100	16374	14948	8.71	31.64	0.004861032
1.8	150	16374	14527	11.28	30.75	0.004724184
1.8	200	16374	14362	12.29	30.40	0.004670404
1.8	400	16374	14105	13.86	29.85	0.004586804
1.8	600	16374	13409	18.11	28.38	0.004360499
1.8	800	16374	12929	21.04	27.37	0.004204481
1.8	1000	16374	13343	18.51	28.24	0.004339199
1.8	50	21067	18855	10.50	29.93	0.004598726
1.8	100	21067	18695	11.26	29.68	0.004559675
1.8	150	21067	18118	14.00	28.76	0.004418887
1.8	200	21067	17479	17.03	27.75	0.004263199
1.8	400	21067	17359	17.60	27.56	0.004233911
1.8	600	21067	16919	19.69	26.86	0.004126521
1.8	800	21067	16253	22.85	25.80	0.003964153

Flow rate, m ³ /h	Concentration, ppm	Pressure drop, kg/(ms ²)			After	
		Before	After	%DR	Wall shear stress, τ_w (kg/(ms ²))	Fanning friction factor, C_f
					$\tau_w = D\Delta P/4L$	$C_f = 2\tau_w / \rho v^2$
1.8	1000	21067	16854	20.00	26.76	0.004110593
1.6	50	4153	4069	2.03	25.84	0.005023794
1.6	100	4153	4038	2.78	25.64	0.004985335
1.6	150	4153	3987	4.00	25.32	0.004922775
1.6	200	4153	3928	5.41	24.94	0.004850472
1.6	400	4153	3862	7.01	24.52	0.004768425
1.6	600	4153	3776	9.07	23.98	0.004662791
1.6	800	4153	3678	11.43	23.36	0.004541773
1.6	1000	4153	3789	8.76	24.06	0.004678687
1.6	50	8501	8084	4.90	25.67	0.004991112
1.6	100	8501	7997	5.93	25.39	0.004937055
1.6	150	8501	7948	6.51	25.23	0.004906615
1.6	200	8501	7752	8.81	24.61	0.004785905
1.6	400	8501	7709	9.32	24.48	0.004759138
1.6	600	8501	7494	11.85	23.79	0.004626357
1.6	800	8501	7161	15.76	22.74	0.004421149
1.6	1000	8501	7646	10.06	24.28	0.004720301
1.6	50	12449	11640	6.50	24.64	0.004790729
1.6	100	12449	11566	7.09	24.48	0.004760499
1.6	150	12449	11464	7.91	24.27	0.004718484
1.6	200	12449	11222	9.86	23.75	0.004618570

Flow rate, m ³ /h	Concentration, ppm	Pressure drop, kg/(ms ²)			After	
		Before	After	%DR	Wall shear stress, τ_w (kg/(ms ²))	Fanning friction factor, C_f
					$\tau_w = \Delta P / 4L$	$C_f = 2\tau_w / \rho v^2$
1.6	400	12449	11066	11.11	23.42	0.004554523
1.6	600	12449	10498	15.67	22.22	0.004320879
1.6	800	12449	10155	18.43	21.49	0.004179463
1.6	1000	12449	10457	16.00	22.13	0.004303971
1.6	50	16674	15117	9.34	24.00	0.004666296
1.6	100	16674	14973	10.20	23.77	0.004622032
1.6	150	16674	14765	11.45	23.44	0.004557694
1.6	200	16674	14340	14.00	22.76	0.004426445
1.6	400	16674	14008	15.99	22.24	0.004324019
1.6	600	16674	13573	18.60	21.55	0.004189682
1.6	800	16674	13356	19.90	21.20	0.004122770
1.6	1000	16674	13828	17.07	21.95	0.004268431
1.4	50	3374	3314	1.77	21.05	0.005345027
1.4	100	3374	3303	2.10	20.97	0.005327071
1.4	150	3374	3277	2.88	20.81	0.005284628
1.4	200	3374	3237	4.07	20.55	0.005219876
1.4	400	3374	3206	4.99	20.36	0.005169816
1.4	600	3374	3152	6.57	20.02	0.005083843
1.4	800	3374	3104	8.00	19.71	0.005006032
1.4	1000	3374	3167	6.13	20.11	0.005107785
1.4	50	6287	6029	4.11	19.14	0.004861245

Flow rate, m ³ /h	Concentration, ppm	Pressure drop, kg/(ms ²)			After	
		Before	After	%DR	Wall shear stress, τ_w (kg/(ms ²))	Fanning friction factor, C_f
					$\tau_w = D\Delta P/4L$	$C_f = 2\tau_w / \rho v^2$
1.4	100	6287	5966	5.10	18.94	0.004811056
1.4	150	6287	5910	6.00	18.76	0.004765429
1.4	200	6287	5897	6.21	18.72	0.004754783
1.4	400	6287	5836	7.17	18.53	0.004706115
1.4	600	6287	5694	9.44	18.08	0.004591035
1.4	800	6287	5429	13.64	17.24	0.004378111
1.4	1000	6287	5734	8.79	18.21	0.004623987
1.4	50	9622	9101	5.41	19.26	0.004892716
1.4	100	9622	8948	7.00	18.94	0.004810473
1.4	150	9622	8891	7.60	18.82	0.004779437
1.4	200	9622	8784	8.71	18.59	0.004722022
1.4	400	9622	8725	9.32	18.47	0.004690469
1.4	600	9622	8294	13.80	17.56	0.004458739
1.4	800	9622	8110	15.71	17.17	0.004359943
1.4	1000	9622	8313	13.60	17.60	0.004469084
1.4	50	13778	12786	7.20	20.30	0.005155074
1.4	100	13778	12571	8.76	19.96	0.005068415
1.4	150	13778	12355	10.33	19.61	0.004981201
1.4	200	13778	12002	12.89	19.05	0.004838992
1.4	400	13778	11900	13.63	18.89	0.004797885
1.4	600	13778	11596	15.84	18.41	0.004675118
1.4	800	13778	11343	17.67	18.01	0.004573461

Flow rate, m ³ /h	Concentration, ppm	Pressure drop, kg/(ms ²)			After	
		Before	After	%DR	Wall shear stress, τ_w (kg/(ms ²))	Fanning friction factor, C_f
					$\tau_w = \Delta P / 4L$	$C_f = 2\tau_w / \rho v^2$
1.4	1000	13778	11780	14.50	18.70	0.004749556
1.2	50	2650	2616	1.29	16.61	0.005741975
1.2	100	2650	2606	1.67	16.55	0.005719870
1.2	150	2650	2600	1.90	16.51	0.005706491
1.2	200	2650	2576	2.80	16.36	0.005654138
1.2	400	2650	2544	4.00	16.15	0.005584334
1.2	600	2650	2541	4.11	16.14	0.005577935
1.2	800	2650	2498	5.72	15.86	0.005484281
1.2	1000	2650	2538	4.21	16.12	0.005572118
1.2	50	5525	5337	3.40	16.95	0.005857789
1.2	100	5525	5302	4.03	16.83	0.005819586
1.2	150	5525	5261	4.78	16.70	0.005774106
1.2	200	5525	5246	5.05	16.66	0.005757733
1.2	400	5525	5175	6.34	16.43	0.005679508
1.2	600	5525	5117	7.39	16.25	0.005615836
1.2	800	5525	4970	10.05	15.78	0.005454535
1.2	1000	5525	5077	8.11	16.12	0.005572176
1.2	50	7931	7532	5.03	15.94	0.005511216
1.2	100	7931	7457	5.98	15.78	0.005456086
1.2	150	7931	7486	5.61	15.85	0.005477558
1.2	200	7931	7463	5.90	15.80	0.005460729

Flow rate, m ³ /h	Concentration, ppm	Pressure drop, kg/(ms ²)			After	
		Before	After	%DR	Wall shear stress, τ_w (kg/(ms ²))	Fanning friction factor, C_f
					$\tau_w = D\Delta P/4L$	$C_f = 2\tau_w / \rho v^2$
1.2	400	7931	7315	7.77	15.48	0.005352211
1.2	600	7931	7102	10.45	15.03	0.005196687
1.2	800	7931	6978	12.01	14.77	0.005106159
1.2	1000	7931	7155	9.78	15.15	0.005235568
1.2	50	10934	10176	6.93	16.15	0.005584484
1.2	100	10934	10169	7.00	16.14	0.005580284
1.2	150	10934	10071	7.89	15.99	0.005526881
1.2	200	10934	9975	8.77	15.84	0.005474079
1.2	400	10934	9782	10.54	15.53	0.005367873
1.2	600	10934	9587	12.32	15.22	0.005261068
1.2	800	10934	9258	15.33	14.70	0.005080459
1.2	1000	10934	9574	12.44	15.20	0.005253867

APPENDIX D4
FRICITION FACTOR IN PIPE WHILE TESTING RED GYPSUM IN DIESEL

Table 4.29: Friction factor in pipe with ID 0.0381m while testing red gypsum in diesel

Flow rate, m ³ /h	Concentration, ppm	Pressure drop, kg/(ms ²)			After	
		Before	After	%DR	Wall shear stress, τ_w (kg/(ms ²))	Fanning friction factor, C_f
					$\tau_w = D\Delta P/4L$	$C_f = 2\tau_w / \rho v^2$
10.5	50	625	521	16.61	9.93	0.003631102
10.5	100	625	500	20.05	9.52	0.003481312
10.5	150	625	479	23.40	9.12	0.003335441
10.5	200	625	356	43.10	6.77	0.002477632
10.5	400	625	445	28.77	8.48	0.003101612
10.5	600	625	353	43.48	6.73	0.002461085
10.5	800	625	324	48.11	6.18	0.002259478
10.5	1000	625	350	44.05	6.66	0.002436265
10.5	50	1272	941	26.03	8.96	0.003277609
10.5	100	1272	776	39.00	7.39	0.002702909
10.5	150	1272	691	45.70	6.58	0.002406032
10.5	200	1272	554	56.44	5.28	0.001930143
10.5	400	1272	850	33.14	8.10	0.002962565
10.5	600	1272	548	56.92	5.22	0.001908874
10.5	800	1272	512	59.71	4.88	0.001785249
10.5	1000	1272	649	49.00	6.18	0.002259809
10.5	50	1969	1426	27.56	9.06	0.003312435
10.5	100	1969	1168	40.68	7.42	0.002712502

Flow rate, m ³ /h	Concentration, ppm	Pressure drop, kg/(ms ²)			After	
		Before	After	%DR	Wall shear stress, τ_w (kg/(ms ²))	Fanning friction factor, C_f
					$\tau_w = D\Delta P/4L$	$C_f = 2\tau_w / \rho v^2$
10.5	150	1969	989	49.76	6.28	0.002297304
10.5	200	1969	816	58.55	5.18	0.001895368
10.5	400	1969	813	58.71	5.16	0.001888051
10.5	600	1969	807	59.00	5.13	0.001874791
10.5	800	1969	788	59.99	5.00	0.001829521
10.5	1000	1969	782	60.30	4.96	0.001815346
10.5	50	2786	1977	29.03	9.42	0.003443819
10.5	100	2786	1557	44.12	7.41	0.002711577
10.5	150	2786	1329	52.31	6.33	0.002314157
10.5	200	2786	1158	58.44	5.51	0.002016699
10.5	400	2786	1141	59.06	5.43	0.001986614
10.5	600	2786	1123	59.68	5.35	0.001956528
10.5	800	2786	1059	62.00	5.04	0.001843950
10.5	1000	2786	1062	61.87	5.06	0.001850258
10.0	50	573	489	14.64	9.32	0.003756921
10.0	100	573	466	18.76	8.87	0.003575589
10.0	150	573	464	19.05	8.84	0.003562825
10.0	200	573	378	33.98	7.21	0.002905716
10.0	400	573	378	34.10	7.19	0.002900435
10.0	600	573	372	35.00	7.10	0.002860823
10.0	800	573	369	35.66	7.02	0.002831775

Flow rate, m ³ /h	Concentration, ppm	Pressure drop, kg/(ms ²)			After	
		Before	After	%DR	Wall shear stress, τ_w (kg/(ms ²))	Fanning friction factor, C_f
					$\tau_w = D\Delta P/4L$	$C_f = 2\tau_w / \rho v^2$
10.0	1000	573	331	42.31	6.30	0.002539091
10.0	50	1154	935	19.00	8.90	0.003589913
10.0	100	1154	881	23.65	8.39	0.003383825
10.0	150	1154	807	30.05	7.69	0.003100178
10.0	200	1154	736	36.23	7.01	0.002826281
10.0	400	1154	739	36.00	7.03	0.002836474
10.0	600	1154	729	36.87	6.94	0.002797916
10.0	800	1154	687	40.51	6.54	0.002636591
10.0	1000	1154	618	46.42	5.89	0.002374661
10.0	50	1810	1455	19.60	9.24	0.003725945
10.0	100	1810	1360	24.85	8.64	0.003482646
10.0	150	1810	1246	31.18	7.91	0.003189298
10.0	200	1810	1209	33.21	7.68	0.003095222
10.0	400	1810	809	55.32	5.14	0.002070587
10.0	600	1810	785	56.63	4.98	0.002009878
10.0	800	1810	1050	42.00	6.67	0.002687871
10.0	1000	1810	936	48.31	5.94	0.002395449
10.0	50	2418	1936	19.92	9.22	0.003718291
10.0	100	2418	1798	25.65	8.56	0.003452235
10.0	150	2418	1589	34.27	7.57	0.003051989
10.0	200	2418	1494	38.23	7.11	0.002868118
10.0	400	2418	1108	54.18	5.28	0.002127524

Flow rate, m ³ /h	Concentration, ppm	Pressure drop, kg/(ms ²)			After	
		Before	After	%DR	Wall shear stress, τ_w (kg/(ms ²))	Fanning friction factor, C_f
					$\tau_w = D\Delta P/4L$	$C_f = 2\tau_w / \rho v^2$
10.0	600	2418	1063	56.04	5.06	0.002041160
10.0	800	2418	1366	43.51	6.51	0.002622956
10.0	1000	2418	1229	49.18	5.85	0.002359685
9.5	50	526	459	12.78	8.74	0.003904610
9.5	100	526	443	15.71	8.45	0.003773442
9.5	150	526	441	16.09	8.41	0.003756430
9.5	200	526	399	24.22	7.59	0.003392471
9.5	400	526	357	32.12	6.80	0.003038809
9.5	600	526	391	25.76	7.44	0.003323530
9.5	800	526	389	26.08	7.41	0.003309204
9.5	1000	526	383	27.11	7.30	0.003263094
9.5	50	1093	909	16.80	8.66	0.003869807
9.5	100	1093	888	18.78	8.46	0.003777713
9.5	150	1093	818	25.14	7.79	0.003481896
9.5	200	1093	793	27.46	7.55	0.003373988
9.5	400	1093	726	33.57	6.92	0.003089799
9.5	600	1093	732	33.05	6.97	0.003113985
9.5	800	1093	774	29.14	7.38	0.003295848
9.5	1000	1093	712	34.90	6.78	0.003027938
9.5	50	1647	1367	16.99	8.68	0.003878632
9.5	100	1647	1325	19.56	8.41	0.003758549

Flow rate, m ³ /h	Concentration, ppm	Pressure drop, kg/(ms ²)			After	
		Before	After	%DR	Wall shear stress, τ_w (kg/(ms ²))	Fanning friction factor, C_f
					$\tau_w = D\Delta P/4L$	$C_f = 2\tau_w / \rho v^2$
9.5	150	1647	1189	27.80	7.55	0.003373536
9.5	200	1647	1148	30.31	7.29	0.003256257
9.5	400	1647	808	50.93	5.13	0.002292790
9.5	600	1647	1073	34.88	6.81	0.003042724
9.5	800	1647	1155	29.87	7.33	0.003276816
9.5	1000	1647	979	40.55	6.22	0.002777794
9.5	50	2209	1832	17.08	8.72	0.003897363
9.5	100	2209	1728	21.78	8.23	0.003676456
9.5	150	2209	1590	28.00	7.57	0.003384107
9.5	200	2209	1580	28.46	7.53	0.003362486
9.5	400	2209	1081	51.07	5.15	0.002299783
9.5	600	2209	1030	53.37	4.91	0.002191679
9.5	800	2209	1565	29.14	7.45	0.003330525
9.5	1000	2209	1193	46.00	5.68	0.002538080
9.0	50	482	430	10.86	8.18	0.004074344
9.0	100	482	423	12.33	8.05	0.004007154
9.0	150	482	408	15.44	7.76	0.003865005
9.0	200	482	385	20.08	7.34	0.003652923
9.0	400	482	368	23.66	7.01	0.003489291
9.0	600	482	371	23.10	7.06	0.003514887
9.0	800	482	373	22.67	7.10	0.003534541

Flow rate, m ³ /h	Concentration, ppm	Pressure drop, kg/(ms ²)			After	
		Before	After	%DR	Wall shear stress, τ_w (kg/(ms ²))	Fanning friction factor, C_f
					$\tau_w = D\Delta P/4L$	$C_f = 2\tau_w / \rho v^2$
9.0	1000	482	363	24.76	6.91	0.003439013
9.0	50	986	847	14.09	8.07	0.004016323
9.0	100	986	813	17.55	7.74	0.003854567
9.0	150	986	788	20.12	7.50	0.003734419
9.0	200	986	759	22.98	7.23	0.003600713
9.0	400	986	701	28.91	6.68	0.003323483
9.0	600	986	751	23.87	7.15	0.003559105
9.0	800	986	741	24.80	7.06	0.003515627
9.0	1000	986	728	26.13	6.94	0.003453449
9.0	50	1485	1257	15.32	7.99	0.003974881
9.0	100	1485	1204	18.94	7.64	0.003804958
9.0	150	1485	1103	25.71	7.01	0.003487174
9.0	200	1485	1068	28.11	6.78	0.003374518
9.0	400	1485	786	47.06	4.99	0.002485004
9.0	600	1485	764	48.53	4.85	0.002416003
9.0	800	1485	1101	25.87	6.99	0.003479663
9.0	1000	1485	983	33.80	6.24	0.003107429
9.0	50	2003	1676	16.33	7.98	0.003973093
9.0	100	2003	1621	19.05	7.72	0.003843933
9.0	150	2003	1460	27.11	6.95	0.003461202
9.0	200	2003	1511	24.56	7.20	0.003582289
9.0	400	2003	1011	49.55	4.81	0.002395632

Flow rate, m ³ /h	Concentration, ppm	Pressure drop, kg/(ms ²)			After	
		Before	After	%DR	Wall shear stress, τ_w (kg/(ms ²))	Fanning friction factor, C_f
					$\tau_w = D\Delta P/4L$	$C_f = 2\tau_w / \rho v^2$
9.0	600	2003	958	52.18	4.56	0.002270746
9.0	800	2003	1466	26.80	6.98	0.003475922
9.0	1000	2003	1200	40.09	5.71	0.002844843
8.5	50	450	408	9.40	7.77	0.004334369
8.5	100	450	405	9.90	7.72	0.004310449
8.5	150	450	390	13.35	7.43	0.004145398
8.5	200	450	371	17.65	7.06	0.003939683
8.5	400	450	352	21.78	6.71	0.003742101
8.5	600	450	373	17.04	7.11	0.003968866
8.5	800	450	365	18.89	6.95	0.003880361
8.5	1000	450	360	20.07	6.85	0.003823909
8.5	50	901	782	13.21	7.45	0.004156710
8.5	100	901	762	15.45	7.26	0.004049427
8.5	150	901	731	18.91	6.96	0.003883714
8.5	200	901	728	19.18	6.94	0.003870783
8.5	400	901	684	24.13	6.51	0.003633708
8.5	600	901	670	25.60	6.39	0.003563304
8.5	800	901	714	20.77	6.80	0.003794632
8.5	1000	901	678	24.70	6.46	0.003606409
8.5	50	1380	1186	14.03	7.53	0.004204264
8.5	100	1380	1149	16.77	7.29	0.004070267

Flow rate, m ³ /h	Concentration, ppm	Pressure drop, kg/(ms ²)			After	
		Before	After	%DR	Wall shear stress, τ_w (kg/(ms ²))	Fanning friction factor, C_f
					$\tau_w = D\Delta P/4L$	$C_f = 2\tau_w / \rho v^2$
8.5	150	1380	1049	23.99	6.66	0.003717181
8.5	200	1380	1042	24.46	6.62	0.003694197
8.5	400	1380	762	44.80	4.84	0.002699492
8.5	600	1380	742	46.22	4.71	0.002630049
8.5	800	1380	1056	23.46	6.71	0.003743100
8.5	1000	1380	963	30.19	6.12	0.003413978
8.5	50	1880	1610	14.36	7.67	0.004279172
8.5	100	1880	1558	17.15	7.42	0.004139764
8.5	150	1880	1500	20.19	7.15	0.003987864
8.5	200	1880	1467	21.98	6.99	0.003898423
8.5	400	1880	1009	46.31	4.81	0.002682727
8.5	600	1880	993	47.16	4.73	0.002640255
8.5	800	1880	1445	23.14	6.88	0.003840462
8.5	1000	1880	1192	36.60	5.68	0.003167906
8.0	50	399	367	7.95	7.00	0.004407981
8.0	100	399	367	8.01	6.99	0.004405108
8.0	150	399	350	12.23	6.67	0.004203026
8.0	200	399	344	13.77	6.55	0.004129280
8.0	400	399	320	19.74	6.10	0.003843396
8.0	600	399	346	13.20	6.60	0.004156576
8.0	800	399	342	14.19	6.52	0.004109168

Flow rate, m ³ /h	Concentration, ppm	Pressure drop, kg/(ms ²)			After	
		Before	After	%DR	Wall shear stress, τ_w (kg/(ms ²))	Fanning friction factor, C_f
					$\tau_w = D\Delta P/4L$	$C_f = 2\tau_w / \rho v^2$
8.0	1000	399	340	14.87	6.47	0.004076605
8.0	50	802	723	9.87	6.89	0.004337673
8.0	100	802	713	11.07	6.79	0.004279921
8.0	150	802	685	14.55	6.53	0.004112439
8.0	200	802	673	16.10	6.41	0.004037843
8.0	400	802	622	22.50	5.92	0.003729831
8.0	600	802	609	24.05	5.80	0.003655234
8.0	800	802	667	16.82	6.35	0.004003191
8.0	1000	802	657	18.06	6.26	0.003943514
8.0	50	1230	1098	10.71	6.97	0.004393693
8.0	100	1230	1086	11.70	6.90	0.004344979
8.0	150	1230	1024	16.77	6.50	0.004095499
8.0	200	1230	987	19.75	6.27	0.003948862
8.0	400	1230	791	35.72	5.02	0.003163026
8.0	600	1230	737	40.05	4.68	0.002949960
8.0	800	1230	1009	17.99	6.41	0.004035466
8.0	1000	1230	889	27.75	5.64	0.003555206
8.0	50	1692	1505	11.07	7.17	0.004514729
8.0	100	1692	1461	13.66	6.96	0.004383242
8.0	150	1692	1404	17.04	6.69	0.004211649
8.0	200	1692	1406	16.91	6.70	0.004218249
8.0	400	1692	1005	40.58	4.79	0.003016589

Flow rate, m ³ /h	Concentration, ppm	Pressure drop, kg/(ms ²)			After	
		Before	After	%DR	Wall shear stress, τ_w (kg/(ms ²))	Fanning friction factor, C_f
					$\tau_w = D\Delta P/4L$	$C_f = 2\tau_w / \rho v^2$
8.0	600	1692	922	45.53	4.39	0.002765291
8.0	800	1692	1387	18.02	6.61	0.004161897
8.0	1000	1692	1130	33.20	5.38	0.003391251
7.5	50	371	348	6.19	6.63	0.004752516
7.5	100	371	346	6.82	6.59	0.004720599
7.5	150	371	337	9.06	6.43	0.004607118
7.5	200	371	334	10.10	6.35	0.004554431
7.5	400	371	306	17.45	5.83	0.004182072
7.5	600	371	312	16.03	5.93	0.004254011
7.5	800	371	324	12.70	6.17	0.004422712
7.5	1000	371	322	13.08	6.14	0.004403461
7.5	50	743	676	9.01	6.44	0.004615864
7.5	100	743	668	10.03	6.37	0.004564120
7.5	150	743	652	12.27	6.21	0.004450486
7.5	200	743	628	15.51	5.98	0.004286123
7.5	400	743	602	19.02	5.73	0.004108063
7.5	600	743	567	23.67	5.40	0.003872172
7.5	800	743	623	16.11	5.94	0.004255686
7.5	1000	743	603	18.79	5.75	0.004119731
7.5	50	1120	1007	10.05	6.40	0.004585624
7.5	100	1120	998	10.89	6.34	0.004542801

Flow rate, m ³ /h	Concentration, ppm	Pressure drop, kg/(ms ²)			After	
		Before	After	%DR	Wall shear stress, τ_w (kg/(ms ²))	Fanning friction factor, C_f
					$\tau_w = D\Delta P/4L$	$C_f = 2\tau_w / \rho v^2$
7.5	150	1120	983	12.26	6.24	0.004472959
7.5	200	1120	920	17.88	5.84	0.004186453
7.5	400	1120	783	30.10	4.97	0.003563481
7.5	600	1120	713	36.30	4.53	0.003247407
7.5	800	1120	929	17.02	5.90	0.004230296
7.5	1000	1120	834	25.52	5.30	0.003796968
7.5	50	1508	1351	10.39	6.44	0.004613158
7.5	100	1508	1343	10.91	6.40	0.004586388
7.5	150	1508	1309	13.21	6.23	0.004467983
7.5	200	1508	1267	15.95	6.04	0.004326927
7.5	400	1508	946	37.27	4.51	0.003229365
7.5	600	1508	893	40.80	4.25	0.003047639
7.5	800	1508	1262	16.29	6.01	0.004309424
7.5	1000	1508	1055	30.04	5.02	0.003601568

Table 4.30: Friction factor in pipe with ID 0.0254m while testing red gypsum in diesel

Flow rate, m ³ /h	Concentration, ppm	Pressure drop, kg/(ms ²)			After	
		Before	After	%DR	Wall shear stress, τ_w (kg/(ms ²))	Fanning friction factor, C_f
					$\tau_w = D\Delta P/4L$	$C_f = 2\tau_w / \rho v^2$
8.0	50	2862	2463	13.93	31.28	0.003893213
8.0	100	2862	2337	18.33	29.68	0.003694188
8.0	150	2862	2261	21.00	28.71	0.003573415
8.0	200	2862	1983	30.71	25.19	0.003134202
8.0	400	2862	1975	31.00	25.08	0.003121084
8.0	600	2862	1916	33.07	24.33	0.003027452
8.0	800	2862	1862	34.94	23.65	0.002942866
8.0	1000	2862	1895	33.79	24.07	0.002994884
8.0	50	5811	4901	15.66	31.12	0.003872944
8.0	100	5811	4251	26.84	27.00	0.003359552
8.0	150	5811	3898	32.92	24.75	0.003080355
8.0	200	5811	3437	40.85	21.83	0.002716204
8.0	400	5811	3351	42.33	21.28	0.002648242
8.0	600	5811	3306	43.10	21.00	0.002612883
8.0	800	5811	3262	43.87	20.71	0.002577524
8.0	1000	5811	3267	43.78	20.75	0.002581657
8.0	50	8810	7108	19.32	30.09	0.003744616
8.0	100	8810	6272	28.81	26.55	0.003304155
8.0	150	8810	5293	39.92	22.41	0.002788505
8.0	200	8810	5052	42.66	21.39	0.002661332

Flow rate, m ³ /h	Concentration, ppm	Pressure drop, kg/(ms ²)			After	
		Before	After	%DR	Wall shear stress, τ_w (kg/(ms ²))	Fanning friction factor, C_f
					$\tau_w = D\Delta P/4L$	$C_f = 2\tau_w / \rho v^2$
8.0	400	8810	4973	43.55	21.05	0.002620025
8.0	600	8810	4876	44.65	20.64	0.002568970
8.0	800	8810	4831	45.17	20.45	0.002544835
8.0	1000	8810	4816	45.33	20.39	0.002537409
8.0	50	11789	8971	23.90	28.48	0.003544773
8.0	100	11789	7984	32.28	25.35	0.003154429
8.0	150	11789	6861	41.80	21.78	0.002710983
8.0	200	11789	6562	44.34	20.83	0.002592668
8.0	400	11789	6476	45.07	20.56	0.002558665
8.0	600	11789	6095	48.30	19.35	0.002408210
8.0	800	11789	5792	50.87	18.39	0.002288498
8.0	1000	11789	6037	48.79	19.17	0.002385385
7.5	50	2533	2209	12.80	28.05	0.003971878
7.5	100	2533	2120	16.30	26.93	0.003812456
7.5	150	2533	2074	18.11	26.34	0.003730012
7.5	200	2533	1910	24.60	24.26	0.003434399
7.5	400	2533	1883	25.67	23.91	0.003385662
7.5	600	2533	1874	26.00	23.81	0.003370630
7.5	800	2533	1810	28.55	22.98	0.003254480
7.5	1000	2533	1824	28.00	23.16	0.003279532
7.5	50	5197	4459	14.21	28.31	0.004008701

Flow rate, m ³ /h	Concentration, ppm	Pressure drop, kg/(ms ²)			After	
		Before	After	%DR	Wall shear stress, τ_w (kg/(ms ²))	Fanning friction factor, C_f
					$\tau_w = D\Delta P/4L$	$C_f = 2\tau_w / \rho v^2$
7.5	100	5197	4204	19.11	26.69	0.003779739
7.5	150	5197	3440	33.80	21.85	0.003093321
7.5	200	5197	3333	35.87	21.16	0.002996596
7.5	400	5197	3114	40.09	19.77	0.002799408
7.5	600	5197	3026	41.78	19.21	0.002720440
7.5	800	5197	3289	36.71	20.89	0.002957345
7.5	1000	5197	3004	42.19	19.08	0.002701282
7.5	50	7951	6676	16.04	28.26	0.004001448
7.5	100	7951	6230	21.65	26.37	0.003734081
7.5	150	7951	5243	34.06	22.19	0.003142633
7.5	200	7951	5547	30.23	23.48	0.003325167
7.5	400	7951	4677	41.18	19.80	0.002803301
7.5	600	7951	4636	41.69	19.63	0.002778995
7.5	800	7951	4799	39.64	20.32	0.002876696
7.5	1000	7951	6532	42.19	27.65	0.003915185
7.5	50	10626	8225	17.85	26.11	0.003697388
7.5	100	10626	6910	22.60	21.94	0.003106475
7.5	150	10626	6589	34.97	20.92	0.002962210
7.5	200	10626	6058	37.99	19.23	0.002723360
7.5	400	10626	5937	42.99	18.85	0.002668903
7.5	600	10626	6353	44.13	20.17	0.002856160
7.5	800	10626	5830	40.21	18.51	0.002621133

Flow rate, m ³ /h	Concentration, ppm	Pressure drop, kg/(ms ²)			After	
		Before	After	%DR	Wall shear stress, τ_w (kg/(ms ²))	Fanning friction factor, C_f
					$\tau_w = D\Delta P/4L$	$C_f = 2\tau_w / \rho v^2$
7.5	1000	10626	10626	45.13	33.74	0.004776987
7.0	50	2184	1918	12.16	24.36	0.003960186
7.0	100	2184	1864	14.67	23.67	0.003847025
7.0	150	2184	1812	17.05	23.01	0.003739725
7.0	200	2184	1776	18.66	22.56	0.003667140
7.0	400	2184	1745	20.09	22.16	0.003602670
7.0	600	2184	1704	22.00	21.63	0.003516559
7.0	800	2184	1743	20.18	22.14	0.003598612
7.0	1000	2184	1700	22.17	21.59	0.003508895
7.0	50	4513	3887	13.87	24.68	0.004011996
7.0	100	4513	3705	17.90	23.53	0.003824275
7.0	150	4513	3653	19.06	23.20	0.003770242
7.0	200	4513	3529	21.80	22.41	0.003642611
7.0	400	4513	2853	36.78	18.12	0.002944832
7.0	600	4513	2793	38.11	17.74	0.002882880
7.0	800	4513	3448	23.59	21.90	0.003559231
7.0	1000	4513	2693	40.33	17.10	0.002779470
7.0	50	6830	5866	14.12	24.83	0.004036102
7.0	100	6830	5538	18.92	23.44	0.003810517
7.0	150	6830	5411	20.78	22.91	0.003723102
7.0	200	6830	5250	23.14	22.22	0.003612189

Flow rate, m ³ /h	Concentration, ppm	Pressure drop, kg/(ms ²)			After	
		Before	After	%DR	Wall shear stress, τ_w (kg/(ms ²))	Fanning friction factor, C_f
					$\tau_w = D\Delta P/4L$	$C_f = 2\tau_w / \rho v^2$
7.0	400	6830	4255	37.70	18.01	0.002927913
7.0	600	6830	4078	40.30	17.26	0.002805721
7.0	800	6830	5002	26.77	21.17	0.003441590
7.0	1000	6830	4037	40.89	17.09	0.002777993
7.0	50	9116	7602	16.61	24.14	0.003923096
7.0	100	9116	7291	20.02	23.15	0.003762672
7.0	150	9116	7006	23.15	22.24	0.003615421
7.0	200	9116	6772	25.71	21.50	0.003494985
7.0	400	9116	5424	40.50	17.22	0.002799187
7.0	600	9116	5371	41.08	17.05	0.002771901
7.0	800	9116	6555	28.09	20.81	0.003383018
7.0	1000	9116	5308	41.77	16.85	0.002739440
6.5	50	1982	1782	10.11	22.63	0.004265354
6.5	100	1982	1726	12.94	21.91	0.004131068
6.5	150	1982	1669	15.77	21.20	0.003996782
6.5	200	1982	1668	15.83	21.19	0.003993935
6.5	400	1982	1630	17.74	20.71	0.003903304
6.5	600	1982	1645	17.00	20.89	0.003938418
6.5	800	1982	1627	17.90	20.67	0.003895712
6.5	1000	1982	1632	17.68	20.72	0.003906151
6.5	50	3997	3555	11.06	22.57	0.004255409

Flow rate, m ³ /h	Concentration, ppm	Pressure drop, kg/(ms ²)			After	
		Before	After	%DR	Wall shear stress, τ_w (kg/(ms ²))	Fanning friction factor, C_f
					$\tau_w = D\Delta P/4L$	$C_f = 2\tau_w / \rho v^2$
6.5	100	3997	3425	14.30	21.75	0.004100389
6.5	150	3997	3316	17.03	21.06	0.003969769
6.5	200	3997	3245	18.81	20.61	0.003884604
6.5	400	3997	3154	21.08	20.03	0.003775994
6.5	600	3997	2797	30.02	17.76	0.003348252
6.5	800	3997	3171	20.66	20.14	0.003796089
6.5	1000	3997	2514	37.10	15.96	0.003009503
6.5	50	6035	5223	13.45	22.11	0.004168340
6.5	100	6035	5027	16.71	21.28	0.004011335
6.5	150	6035	4940	18.15	20.91	0.003941983
6.5	200	6035	4782	20.76	20.24	0.003816283
6.5	400	6035	4594	23.88	19.45	0.003666020
6.5	600	6035	4049	32.91	17.14	0.003231126
6.5	800	6035	4698	22.16	19.89	0.003748857
6.5	1000	6035	3745	37.95	15.85	0.002988394
6.5	50	8084	6871	15.00	21.82	0.004112683
6.5	100	8084	6632	17.96	21.06	0.003969465
6.5	150	8084	6463	20.05	20.52	0.003868342
6.5	200	8084	6236	22.86	19.80	0.003732381
6.5	400	8084	5807	28.17	18.44	0.003475459
6.5	600	8084	5401	33.19	17.15	0.003232569
6.5	800	8084	6081	24.78	19.31	0.003639483

Flow rate, m ³ /h	Concentration, ppm	Pressure drop, kg/(ms ²)			After	
		Before	After	%DR	Wall shear stress, τ_w (kg/(ms ²))	Fanning friction factor, C_f
					$\tau_w = D\Delta P/4L$	$C_f = 2\tau_w / \rho v^2$
6.5	1000	8084	4862	39.86	15.44	0.002909844
6.0	50	1704	1568	7.98	19.91	0.004405712
6.0	100	1704	1551	9.00	19.69	0.004356876
6.0	150	1704	1496	12.20	19.00	0.004203668
6.0	200	1704	1476	13.37	18.75	0.004147651
6.0	400	1704	1446	15.17	18.36	0.004061471
6.0	600	1704	1445	15.21	18.35	0.004059555
6.0	800	1704	1439	15.56	18.27	0.004042798
6.0	1000	1704	1422	16.54	18.06	0.003995878
6.0	50	3467	3129	9.75	19.87	0.004395774
6.0	100	3467	3078	11.21	19.55	0.004324662
6.0	150	3467	3003	13.37	19.07	0.004219456
6.0	200	3467	2943	15.12	18.69	0.004134219
6.0	400	3467	2833	18.30	17.99	0.003979332
6.0	600	3467	2474	28.65	15.71	0.003475218
6.0	800	3467	2862	17.45	18.17	0.004020732
6.0	1000	3467	2421	30.17	15.37	0.003401184
6.0	50	5211	4596	11.80	19.46	0.004304599
6.0	100	5211	4522	13.22	19.14	0.004235295
6.0	150	5211	4352	16.48	18.42	0.004076191
6.0	200	5211	4244	18.55	17.97	0.003975165

Flow rate, m ³ /h	Concentration, ppm	Pressure drop, kg/(ms ²)			After	
		Before	After	%DR	Wall shear stress, τ_w (kg/(ms ²))	Fanning friction factor, C_f
					$\tau_w = D\Delta P/4L$	$C_f = 2\tau_w / \rho v^2$
6.0	400	5211	4091	21.50	17.32	0.003831190
6.0	600	5211	3639	30.17	15.40	0.003408051
6.0	800	5211	4127	20.80	17.47	0.003865354
6.0	1000	5211	3485	33.12	14.75	0.003264077
6.0	50	6971	6043	13.31	19.19	0.004244909
6.0	100	6971	5890	15.51	18.70	0.004137182
6.0	150	6971	5716	18.00	18.15	0.004015256
6.0	200	6971	5534	20.61	17.57	0.003887453
6.0	400	6971	5207	25.30	16.53	0.003657800
6.0	600	6971	4824	30.80	15.32	0.003388484
6.0	800	6971	5437	22.01	17.26	0.003818900
6.0	1000	6971	4407	36.78	13.99	0.003095664
5.5	50	1389	1291	7.02	16.40	0.004318502
5.5	100	1389	1279	7.92	16.24	0.004276701
5.5	150	1389	1253	9.81	15.91	0.004188919
5.5	200	1389	1275	8.19	16.20	0.004264161
5.5	400	1389	1261	9.23	16.01	0.004215858
5.5	600	1389	1250	10.04	15.87	0.004178237
5.5	800	1389	1233	11.23	15.66	0.004122967
5.5	1000	1389	1203	13.39	15.28	0.004022645
5.5	50	2781	2553	8.19	16.21	0.004268766

Flow rate, m ³ /h	Concentration, ppm	Pressure drop, kg/(ms ²)			After	
		Before	After	%DR	Wall shear stress, τ_w (kg/(ms ²))	Fanning friction factor, C_f
					$\tau_w = D\Delta P/4L$	$C_f = 2\tau_w / \rho v^2$
5.5	100	2781	2528	9.09	16.05	0.004226920
5.5	150	2781	2503	10.00	15.89	0.004184609
5.5	200	2781	2501	10.08	15.88	0.004180889
5.5	400	2781	2408	13.40	15.29	0.004026524
5.5	600	2781	2206	20.66	14.01	0.003688965
5.5	800	2781	2415	13.17	15.33	0.004037218
5.5	1000	2781	2036	26.80	12.93	0.003403482
5.5	50	4385	3991	8.99	16.89	0.004448144
5.5	100	4385	3933	10.31	16.65	0.004383628
5.5	150	4385	3850	12.19	16.30	0.004291743
5.5	200	4385	3784	13.71	16.02	0.004217452
5.5	400	4385	3722	15.11	15.76	0.004149027
5.5	600	4385	3220	26.57	13.63	0.003588916
5.5	800	4385	3657	16.61	15.48	0.004075714
5.5	1000	4385	3065	30.10	12.98	0.003416386
5.5	50	5880	5300	9.87	16.83	0.004430248
5.5	100	5880	5183	11.86	16.45	0.004332432
5.5	150	5880	5174	12.01	16.43	0.004325059
5.5	200	5880	5024	14.56	15.95	0.004199716
5.5	400	5880	4286	27.11	13.61	0.003582834
5.5	600	5880	4175	29.00	13.25	0.003489933
5.5	800	5880	4840	17.69	15.37	0.004045864

Flow rate, m ³ /h	Concentration, ppm	Pressure drop, kg/(ms ²)			After	
		Before	After	%DR	Wall shear stress, τ_w (kg/(ms ²))	Fanning friction factor, C_f
					$\tau_w = D\Delta P/4L$	$C_f = 2\tau_w / \rho v^2$
5.5	1000	5880	3846	34.60	12.21	0.003214670
5.0	50	1208	1136	5.93	14.43	0.004597744
5.0	100	1208	1134	6.14	14.40	0.004587480
5.0	150	1208	1110	8.09	14.10	0.004492173
5.0	200	1208	1123	7.07	14.26	0.004542026
5.0	400	1208	1111	8.00	14.11	0.004496572
5.0	600	1208	1097	9.18	13.93	0.004438898
5.0	800	1208	1077	10.88	13.67	0.004355809
5.0	1000	1208	1062	12.08	13.49	0.004297158
5.0	50	2450	2270	7.33	14.42	0.004593059
5.0	100	2450	2239	8.62	14.22	0.004529122
5.0	150	2450	2235	8.78	14.19	0.004521191
5.0	200	2450	2222	9.30	14.11	0.004495418
5.0	400	2450	2193	10.50	13.92	0.004435942
5.0	600	2450	2023	17.41	12.85	0.004093458
5.0	800	2450	2164	11.67	13.74	0.004377953
5.0	1000	2450	1958	20.09	12.43	0.003960627
5.0	50	3744	3441	8.10	14.57	0.004640415
5.0	100	3744	3406	9.04	14.42	0.004592951
5.0	150	3744	3374	9.88	14.28	0.004550536
5.0	200	3744	3284	12.29	13.90	0.004428845

Flow rate, m ³ /h	Concentration, ppm	Pressure drop, kg/(ms ²)			After	
		Before	After	%DR	Wall shear stress, τ_w (kg/(ms ²))	Fanning friction factor, C_f
					$\tau_w = D\Delta P/4L$	$C_f = 2\tau_w / \rho v^2$
5.0	400	3744	3228	13.79	13.66	0.004353103
5.0	600	3744	2879	23.10	12.19	0.003883002
5.0	800	3744	3186	14.90	13.49	0.004297055
5.0	1000	3744	2740	26.81	11.60	0.003695669
5.0	50	5028	4571	9.09	14.51	0.004623530
5.0	100	5028	4530	9.90	14.38	0.004582335
5.0	150	5028	4344	13.60	13.79	0.004394159
5.0	200	5028	4324	14.00	13.73	0.004373816
5.0	400	5028	3977	20.91	12.63	0.004022385
5.0	600	5028	3765	25.12	11.95	0.003808271
5.0	800	5028	4268	15.11	13.55	0.004317363
5.0	1000	5028	3520	30.00	11.17	0.003560082

Table 4.31: Friction factor in pipe with ID 0.0127m while testing red gypsum in diesel

Flow rate, m ³ /h	Concentration, ppm	Pressure drop, kg/(ms ²)			After	
		Before	After	%DR	Wall shear stress, τ_w (kg/(ms ²))	Fanning friction factor, C_f
				$\tau_w = D\Delta P/4L$	$C_f = 2\tau_w / \rho v^2$	
2.4	50	9201	8020	12.84	50.92	0.004400951
2.4	100	9201	7749	15.78	49.21	0.004252502
2.4	150	9201	7675	16.59	48.73	0.004211603
2.4	200	9201	6851	25.54	43.50	0.003759693
2.4	400	9201	6812	25.96	43.26	0.003738486
2.4	600	9201	6698	27.20	42.53	0.003675875
2.4	800	9201	6384	30.62	40.54	0.003503189
2.4	1000	9201	6517	29.17	41.38	0.003576404
2.4	50	18546	15874	14.41	50.40	0.004355496
2.4	100	18546	14792	20.24	46.97	0.004058819
2.4	150	18546	14549	21.55	46.19	0.003992156
2.4	200	18546	12407	33.10	39.39	0.003404401
2.4	400	18546	12231	34.05	38.83	0.003356057
2.4	600	18546	11869	36.00	37.69	0.003256826
2.4	800	18546	11562	37.66	36.71	0.003172352
2.4	1000	18546	11508	37.95	36.54	0.003157594
2.4	50	27849	22962	17.55	48.60	0.004200232
2.4	100	27849	21291	23.55	45.07	0.003894576
2.4	150	27849	20942	24.80	44.33	0.003830897
2.4	200	27849	17698	36.45	37.46	0.003237414

Flow rate, m ³ /h	Concentration, ppm	Pressure drop, kg/(ms ²)			After	
		Before	After	%DR	Wall shear stress, τ_w (kg/(ms ²))	Fanning friction factor, C_f
					$\tau_w = D\Delta P/4L$	$C_f = 2\tau_w / \rho v^2$
2.4	400	27849	17333	37.76	36.69	0.003170679
2.4	600	27849	16980	39.03	35.94	0.003105981
2.4	800	27849	16537	40.62	35.00	0.003024982
2.4	1000	27849	16746	39.87	35.44	0.003063189
2.4	50	37163	29857	19.66	47.40	0.004096160
2.4	100	37163	26085	29.81	41.41	0.003578659
2.4	150	37163	26007	30.02	41.29	0.003567952
2.4	200	37163	22480	39.51	35.69	0.003084101
2.4	400	37163	22276	40.06	35.36	0.003056059
2.4	600	37163	21740	41.50	34.51	0.002982641
2.4	800	37163	21123	43.16	33.53	0.002898005
2.4	1000	37163	20848	43.90	33.10	0.002860276
2.2	50	7932	7003	11.71	44.47	0.004573679
2.2	100	7932	6777	14.56	43.03	0.004426040
2.2	150	7932	6733	15.11	42.76	0.004397549
2.2	200	7932	6336	20.12	40.23	0.004138016
2.2	400	7932	6173	22.17	39.20	0.004031820
2.2	600	7932	6120	22.85	38.86	0.003996594
2.2	800	7932	6005	24.30	38.13	0.003921480
2.2	1000	7932	6028	24.01	38.27	0.003936503
2.2	50	14668	12639	13.83	40.13	0.004127323

Flow rate, m ³ /h	Concentration, ppm	Pressure drop, kg/(ms ²)			After	
		Before	After	%DR	Wall shear stress, τ_w (kg/(ms ²))	Fanning friction factor, C_f
					$\tau_w = D\Delta P/4L$	$C_f = 2\tau_w / \rho v^2$
2.2	100	14668	12063	17.76	38.30	0.003939086
2.2	150	14668	11734	20.00	37.26	0.003831795
2.2	200	14668	10750	26.71	34.13	0.003510404
2.2	400	14668	10561	28.00	33.53	0.003448616
2.2	600	14668	10426	28.92	33.10	0.003404550
2.2	800	14668	10260	30.05	32.58	0.003350426
2.2	1000	14668	9901	32.50	31.44	0.003233077
2.2	50	23054	19557	15.17	41.40	0.004257414
2.2	100	23054	18457	19.94	39.07	0.004018019
2.2	150	23054	17941	22.18	37.97	0.003905599
2.2	200	23054	16500	28.43	34.92	0.003591927
2.2	400	23054	16129	30.04	34.14	0.003511125
2.2	600	23054	15421	33.11	32.64	0.003357049
2.2	800	23054	15121	34.41	32.01	0.003291805
2.2	1000	23054	14678	36.33	31.07	0.003195445
2.2	50	30792	25551	17.02	40.56	0.004171793
2.2	100	30792	24326	21.00	38.62	0.003971700
2.2	150	30792	22746	26.13	36.11	0.003713791
2.2	200	30792	20686	32.82	32.84	0.003377453
2.2	400	30792	19470	36.77	30.91	0.003178868
2.2	600	30792	19393	37.02	30.79	0.003166299
2.2	800	30792	19168	37.75	30.43	0.003129599

Flow rate, m ³ /h	Concentration, ppm	Pressure drop, kg/(ms ²)			After	
		Before	After	%DR	Wall shear stress, τ_w (kg/(ms ²))	Fanning friction factor, C_f
					$\tau_w = \Delta P / 4L$	$C_f = 2\tau_w / \rho v^2$
2.2	1000	30792	18466	40.03	29.31	0.003014973
2.0	50	6634	5933	10.57	37.67	0.004688301
2.0	100	6634	5820	12.27	36.96	0.004599180
2.0	150	6634	5681	14.36	36.08	0.004489613
2.0	200	6634	5604	15.53	35.58	0.004428277
2.0	400	6634	5530	16.64	35.12	0.004370086
2.0	600	6634	5507	16.99	34.97	0.004351737
2.0	800	6634	5504	17.04	34.95	0.004349116
2.0	1000	6634	5411	18.44	34.36	0.004275722
2.0	50	13324	11689	12.27	37.11	0.004618591
2.0	100	13324	11301	15.18	35.88	0.004465393
2.0	150	13324	10948	17.83	34.76	0.004325882
2.0	200	13324	10748	19.33	34.13	0.004246914
2.0	400	13324	10389	22.03	32.98	0.004104771
2.0	600	13324	10298	22.71	32.70	0.004068972
2.0	800	13324	10423	21.77	33.09	0.004118459
2.0	1000	13324	9900	25.70	31.43	0.003911562
2.0	50	19657	17023	13.40	36.03	0.004484052
2.0	100	19657	16339	16.88	34.58	0.004303862
2.0	150	19657	15889	19.17	33.63	0.004185288
2.0	200	19657	15350	21.91	32.49	0.004043414

Flow rate, m ³ /h	Concentration, ppm	Pressure drop, kg/(ms ²)			After	
		Before	After	%DR	Wall shear stress, τ_w (kg/(ms ²))	Fanning friction factor, C_f
					$\tau_w = D\Delta P/4L$	$C_f = 2\tau_w / \rho v^2$
2.0	400	19657	14517	26.15	30.73	0.003823871
2.0	600	19657	13742	30.09	29.09	0.003619862
2.0	800	19657	15067	23.35	31.89	0.003968852
2.0	1000	19657	12836	34.70	27.17	0.003381162
2.0	50	26511	22399	15.51	35.56	0.004425152
2.0	100	26511	21535	18.77	34.19	0.004254410
2.0	150	26511	20042	24.40	31.82	0.003959540
2.0	200	26511	20151	23.99	31.99	0.003981013
2.0	400	26511	18547	30.04	29.44	0.003664145
2.0	600	26511	17762	33.00	28.20	0.003509116
2.0	800	26511	19777	25.40	31.40	0.003907165
2.0	1000	26511	16766	36.76	26.62	0.003312186
1.8	50	5379	4865	9.55	30.89	0.004746592
1.8	100	5379	4788	10.98	30.41	0.004671549
1.8	150	5379	4734	12.00	30.06	0.004618022
1.8	200	5379	4720	12.26	29.97	0.004604378
1.8	400	5379	4644	13.66	29.49	0.004530909
1.8	600	5379	4623	14.05	29.36	0.004510443
1.8	800	5379	4538	15.63	28.82	0.004427528
1.8	1000	5379	4501	16.32	28.58	0.004391319
1.8	50	10945	9774	10.70	31.03	0.004767701

Flow rate, m ³ /h	Concentration, ppm	Pressure drop, kg/(ms ²)			After	
		Before	After	%DR	Wall shear stress, τ_w (kg/(ms ²))	Fanning friction factor, C_f
					$\tau_w = D\Delta P/4L$	$C_f = 2\tau_w / \rho v^2$
1.8	100	10945	9553	12.72	30.33	0.004659854
1.8	150	10945	9395	14.16	29.83	0.004582972
1.8	200	10945	9117	16.70	28.95	0.004447363
1.8	400	10945	9080	17.04	28.83	0.004429210
1.8	600	10945	8029	26.64	25.49	0.003916669
1.8	800	10945	8877	18.89	28.19	0.004330439
1.8	1000	10945	8298	24.18	26.35	0.004048008
1.8	50	16374	14434	11.85	30.55	0.004693833
1.8	100	16374	13957	14.76	29.54	0.004538880
1.8	150	16374	13666	16.54	28.93	0.004444098
1.8	200	16374	13530	17.37	28.64	0.004399902
1.8	400	16374	12985	20.70	27.48	0.004222586
1.8	600	16374	11653	28.83	24.67	0.003789678
1.8	800	16374	13040	20.36	27.60	0.004240690
1.8	1000	16374	11460	30.01	24.26	0.003726845
1.8	50	21067	18025	14.44	28.61	0.004396279
1.8	100	21067	17663	16.16	28.04	0.004307901
1.8	150	21067	16948	19.55	26.91	0.004133715
1.8	200	21067	16782	20.34	26.64	0.004093123
1.8	400	21067	15242	27.65	24.20	0.003717517
1.8	600	21067	14713	30.16	23.36	0.003588547
1.8	800	21067	16603	21.19	26.36	0.004049448

Flow rate, m ³ /h	Concentration, ppm	Pressure drop, kg/(ms ²)			After	
		Before	After	%DR	Wall shear stress, τ_w (kg/(ms ²))	Fanning friction factor, C_f
					$\tau_w = D\Delta P/4L$	$C_f = 2\tau_w / \rho v^2$
1.8	1000	21067	14079	33.17	22.35	0.003433886
1.6	50	4153	3846	7.39	24.42	0.004748939
1.6	100	4153	3813	8.19	24.21	0.004707916
1.6	150	4153	3725	10.31	23.65	0.004599205
1.6	200	4153	3733	10.11	23.71	0.004609461
1.6	400	4153	3695	11.03	23.46	0.004562284
1.6	600	4153	3655	12.00	23.21	0.004512544
1.6	800	4153	3627	12.67	23.03	0.004478187
1.6	1000	4153	3570	14.05	22.67	0.004407422
1.6	50	8501	7737	8.99	24.56	0.004776458
1.6	100	8501	7643	10.09	24.27	0.004718727
1.6	150	8501	7562	11.05	24.01	0.004668343
1.6	200	8501	7330	13.78	23.27	0.004525065
1.6	400	8501	7216	15.12	22.91	0.004454738
1.6	600	8501	7226	15.00	22.94	0.004461036
1.6	800	8501	7183	15.50	22.81	0.004434795
1.6	1000	8501	6860	19.30	21.78	0.004235360
1.6	50	12449	11202	10.02	23.71	0.004610372
1.6	100	12449	10933	12.18	23.14	0.004499699
1.6	150	12449	10595	14.89	22.43	0.004360845
1.6	200	12449	10460	15.98	22.14	0.004304995

Flow rate, m ³ /h	Concentration, ppm	Pressure drop, kg/(ms ²)			After	
		Before	After	%DR	Wall shear stress, τ_w (kg/(ms ²))	Fanning friction factor, C_f
					$\tau_w = D\Delta P/4L$	$C_f = 2\tau_w / \rho v^2$
1.6	400	12449	10239	17.75	21.67	0.004214305
1.6	600	12449	9954	20.04	21.07	0.004096970
1.6	800	12449	10295	17.30	21.79	0.004237362
1.6	1000	12449	9565	23.17	20.24	0.003936596
1.6	50	16674	14625	12.29	23.22	0.004514459
1.6	100	16674	14233	14.64	22.59	0.004393504
1.6	150	16674	13673	18.00	21.71	0.004220564
1.6	200	16674	13738	17.61	21.81	0.004240637
1.6	400	16674	12786	23.32	20.30	0.003946742
1.6	600	16674	12020	27.91	19.08	0.003710493
1.6	800	16674	13334	20.03	21.17	0.004116079
1.6	1000	16674	11520	30.91	18.29	0.003556082
1.4	50	3374	3144	6.82	19.96	0.005070240
1.4	100	3374	3135	7.07	19.91	0.005056636
1.4	150	3374	3036	10.02	19.28	0.004896117
1.4	200	3374	3113	7.75	19.76	0.005019635
1.4	400	3374	3104	8.00	19.71	0.005006032
1.4	600	3374	3073	8.93	19.51	0.004955427
1.4	800	3374	3059	9.34	19.42	0.004933118
1.4	1000	3374	3033	10.11	19.26	0.004891220
1.4	50	6287	5784	8.00	18.36	0.004664037

Flow rate, m ³ /h	Concentration, ppm	Pressure drop, kg/(ms ²)			After	
		Before	After	%DR	Wall shear stress, τ_w (kg/(ms ²))	Fanning friction factor, C_f
					$\tau_w = D\Delta P/4L$	$C_f = 2\tau_w / \rho v^2$
1.4	100	6287	5729	8.88	18.19	0.004619425
1.4	150	6287	5616	10.68	17.83	0.004528172
1.4	200	6287	4363	30.60	13.85	0.003518306
1.4	400	6287	5279	16.03	16.76	0.004256948
1.4	600	6287	5226	16.87	16.59	0.004214363
1.4	800	6287	5590	11.09	17.75	0.004507386
1.4	1000	6287	5153	18.04	16.36	0.004155049
1.4	50	9622	8802	8.52	18.63	0.004731850
1.4	100	9622	8657	10.03	18.32	0.004653744
1.4	150	9622	8467	12.00	17.92	0.004551845
1.4	200	9622	8459	12.09	17.90	0.004547190
1.4	400	9622	7984	17.02	16.90	0.004292183
1.4	600	9622	7742	19.54	16.39	0.004161835
1.4	800	9622	8329	13.44	17.63	0.004477360
1.4	1000	9622	7591	21.11	16.07	0.004080626
1.4	50	13778	12532	9.04	19.90	0.005052861
1.4	100	13778	12271	10.94	19.48	0.004947315
1.4	150	13778	11696	15.11	18.57	0.004715670
1.4	200	13778	9197	33.25	14.60	0.003707987
1.4	400	13778	10938	20.61	17.36	0.004410143
1.4	600	13778	10726	22.15	17.03	0.004324596
1.4	800	13778	11182	18.84	17.75	0.004508467

Flow rate, m ³ /h	Concentration, ppm	Pressure drop, kg/(ms ²)			After	
		Before	After	%DR	Wall shear stress, τ_w (kg/(ms ²))	Fanning friction factor, C_f
					$\tau_w = D\Delta P/4L$	$C_f = 2\tau_w / \rho v^2$
1.4	1000	13778	10196	26.00	16.19	0.004110727
1.2	50	2650	2514	5.13	15.96	0.005518602
1.2	100	2650	2500	5.67	15.87	0.005487190
1.2	150	2650	2494	5.90	15.83	0.005473811
1.2	200	2650	2487	6.16	15.79	0.005458687
1.2	400	2650	2459	7.21	15.61	0.005397608
1.2	600	2650	2445	7.73	15.53	0.005367359
1.2	800	2650	2440	7.91	15.50	0.005356889
1.2	1000	2650	2437	8.04	15.47	0.005349327
1.2	50	5525	5143	6.91	16.33	0.005644943
1.2	100	5525	5093	7.81	16.17	0.005590368
1.2	150	5525	5022	9.10	15.95	0.005512143
1.2	200	5525	5027	9.02	15.96	0.005516994
1.2	400	5525	4906	11.20	15.58	0.005384799
1.2	600	5525	4804	13.05	15.25	0.005272616
1.2	800	5525	4937	10.65	15.67	0.005418151
1.2	1000	5525	4635	16.10	14.72	0.005087665
1.2	50	7931	7314	7.78	15.48	0.005351630
1.2	100	7931	7228	8.87	15.30	0.005288376
1.2	150	7931	7125	10.16	15.08	0.005213516
1.2	200	7931	7088	10.63	15.00	0.005186241

Flow rate, m ³ /h	Concentration, ppm	Pressure drop, kg/(ms ²)			After	
		Before	After	%DR	Wall shear stress, τ_w (kg/(ms ²))	Fanning friction factor, C_f
					$\tau_w = D\Delta P/4L$	$C_f = 2\tau_w / \rho v^2$
1.2	400	7931	6870	13.38	14.54	0.005026656
1.2	600	7931	6654	16.10	14.08	0.004868811
1.2	800	7931	6965	12.18	14.74	0.005096293
1.2	1000	7931	6438	18.82	13.63	0.004710967
1.2	50	10934	9985	8.68	15.85	0.005479479
1.2	100	10934	9930	9.18	15.76	0.005449477
1.2	150	10934	9472	13.37	15.04	0.005198065
1.2	200	10934	9592	12.27	15.23	0.005264068
1.2	400	10934	9173	16.11	14.56	0.005033656
1.2	600	10934	8933	18.30	14.18	0.004902250
1.2	800	10934	9481	13.29	15.05	0.005202865
1.2	1000	10934	8619	21.17	13.68	0.004730041

UMP

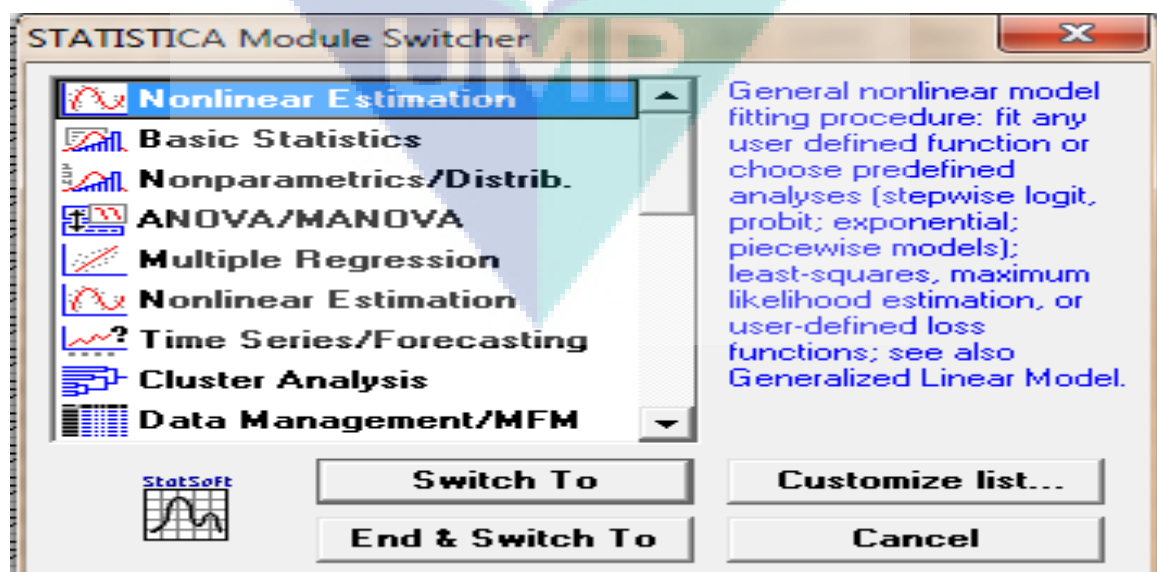
APPENDIX E

STEPS FOR STATISTICAL CORRELATION ESTIMATION

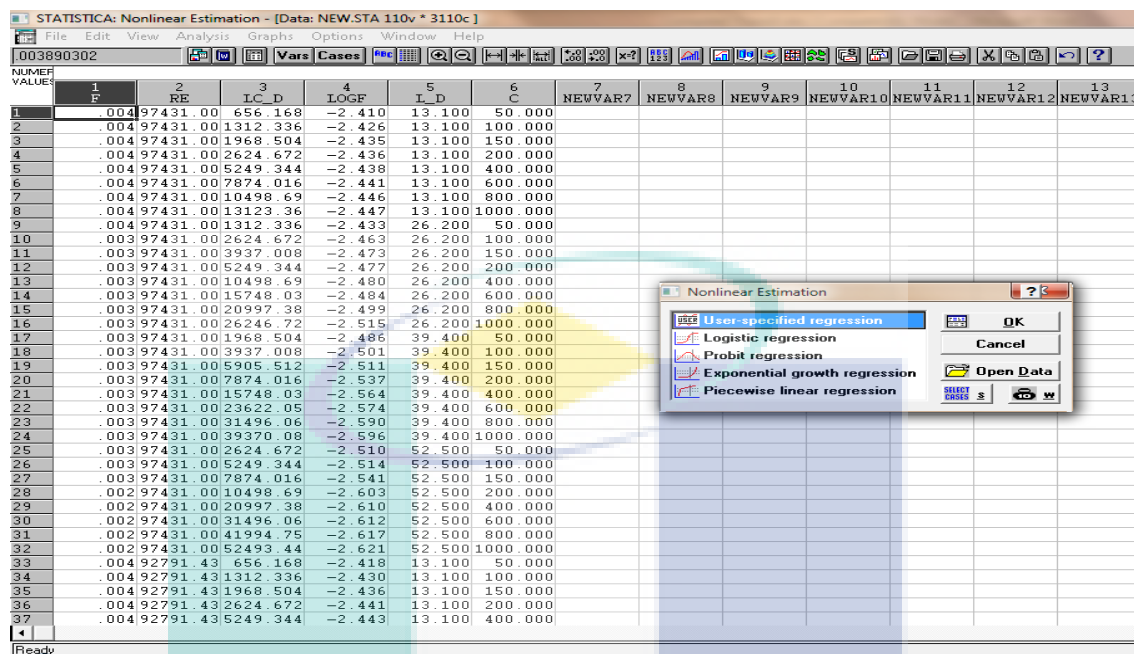
Step 1: Estimation initiated by inserting in the values of the variables investigated, i.e. friction factor, Re, C and L/D.

NUMER VALUE	1	2	3	4	5	6	7	8	9	10	11	12	13	14	15	16	17	18	19	20
	RE	IC_D	LOGE	IC_D	C	NEUVAR7	NEUVAR8	NEUVAR9	NEUVAR10	NEUVAR11	NEUVAR12	NEUVAR13	NEUVAR14	NEUVAR15	NEUVAR16	NEUVAR17	NEUVAR18	NEUVAR19	NEUVAR20	
1	0.04	97431.00	656.169	-2.410	13.100	50.000														
2	0.04	97431.00	1312.336	-2.426	13.100	100.000														
3	0.04	97431.00	1968.504	-2.435	13.100	150.000														
4	0.04	97431.00	2624.672	-2.436	13.100	200.000														
5	0.04	97431.00	5249.344	-2.438	13.100	400.000														
6	0.04	97431.00	7874.016	-2.441	13.100	600.000														
7	0.04	97431.00	10498.69	-2.446	13.100	800.000														
8	0.04	97431.00	13123.36	-2.447	13.100	1000.000														
9	0.04	97431.00	1312.336	-2.433	26.200	50.000														
10	0.03	97431.00	2624.672	-2.463	26.200	100.000														
11	0.03	97431.00	3937.008	-2.473	26.200	150.000														
12	0.03	97431.00	5249.344	-2.477	26.200	200.000														
13	0.03	97431.00	10498.69	-2.480	26.200	400.000														
14	0.03	97431.00	15748.03	-2.484	26.200	600.000														
15	0.03	97431.00	20997.38	-2.499	26.200	800.000														
16	0.03	97431.00	26246.72	-2.515	26.200	1000.000														
17	0.03	97431.00	1968.504	-2.486	39.400	50.000														
18	0.03	97431.00	3937.008	-2.501	39.400	100.000														
19	0.03	97431.00	5905.512	-2.511	39.400	150.000														
20	0.03	97431.00	7874.016	-2.537	39.400	200.000														
21	0.03	97431.00	15748.03	-2.564	39.400	400.000														
22	0.03	97431.00	23622.05	-2.574	39.400	600.000														
23	0.03	97431.00	31496.06	-2.590	39.400	800.000														
24	0.03	97431.00	39370.08	-2.596	39.400	1000.000														
25	0.03	97431.00	2624.672	-2.510	52.500	50.000														
26	0.03	97431.00	5249.344	-2.514	52.500	100.000														
27	0.03	97431.00	7874.016	-2.541	52.500	150.000														
28	0.02	97431.00	10498.69	-2.603	52.500	200.000														
29	0.02	97431.00	20997.38	-2.610	52.500	400.000														
30	0.02	97431.00	31496.06	-2.612	52.500	600.000														
31	0.02	97431.00	41994.75	-2.617	52.500	800.000														
32	0.02	97431.00	52493.44	-2.621	52.500	1000.000														
33	0.04	92791.43	656.169	-2.418	13.100	50.000														
34	0.04	92791.43	1312.336	-2.430	13.100	100.000														
35	0.04	92791.43	1968.504	-2.436	13.100	150.000														
36	0.04	92791.43	2624.672	-2.441	13.100	200.000														
37	0.04	92791.43	5249.344	-2.443	13.100	400.000														

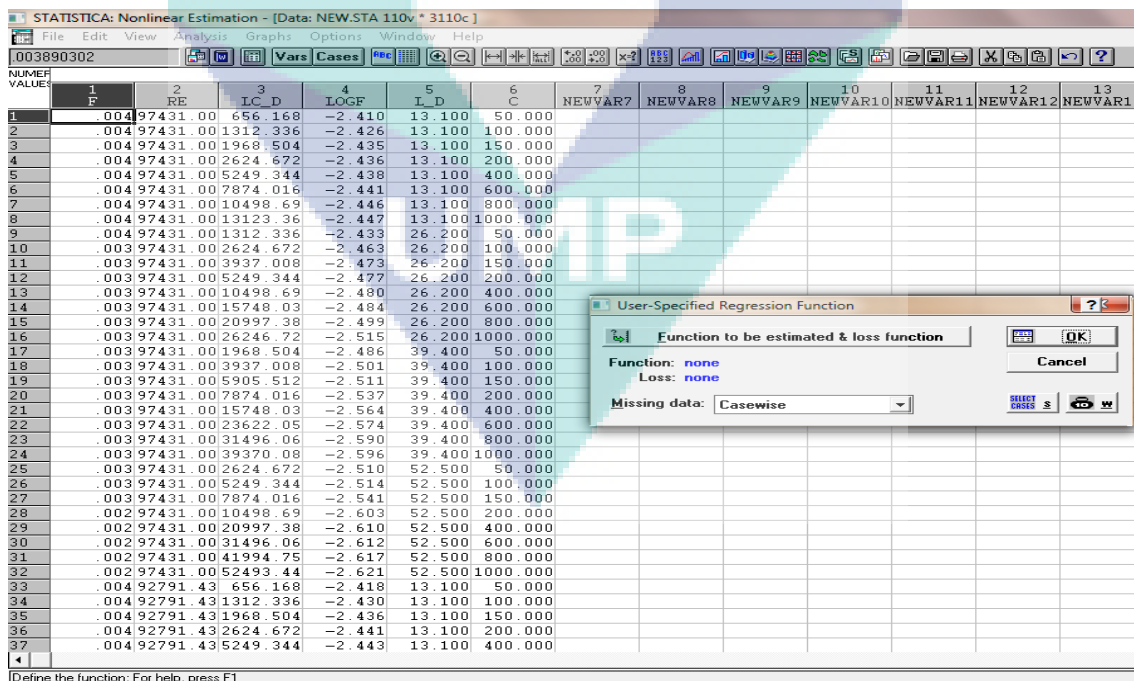
Step 2: The nonlinear estimation mode selected.



Step 3: User specified regression mode selected.



Step 4: Regression function specified.



Step 5: Equation derived from the dimensional analysis ($f = [(k/\log f) + s] \times [(L \times C/D) \times \text{Re}]^b$) is typed.

STATISTICA: Nonlinear Estimation - [Data: NEW_STA 110v * 3110c]

003890302

Estimated function and loss function

Estimated function:
 $f = a \cdot \left(\frac{k}{v_4} + s \right) \cdot \left(v_5 \cdot v_6 \cdot v_2 \right)^b$

Loss function:
 $L = [\text{OBS} - \text{PRED}]^2$

Estimated function: 'estimated var' = expression; e.g. v2=constant+param*v3
 Loss function: L = expression; e.g. L=[obs-pred]**2
 Valid operators: + * / < > <= >= <= ()
 Reference variables by number or name; e.g.: v3=b1*v4 or COST=b1*SIZE
 All unrecognized names are parameters; e.g.: v3=const+param*v4
 Use standard or scientific notation; e.g.: v3=b1**y/3e-2
 Constants: Pi=3.14... Euler=2.71... e.g.: v3=b*Euler*v3
 Functions: abs arcsin cos exp log log2 log10 sign sin sinh sqrt tan
 Logical operations: true=1, false=0; e.g.: v2=b1*v3*(v1<0)+b2*v3*(v1=0)
 In loss function: PRED = predicted value, OBS = observed value
 Default loss function is 'Least Squares,' that is: L=[OBS-PRED]**2
 Example 1: Failure=exp[b0+b1*Stlength] L=v5*[OBS-PRED]**2
 Example 2: v4=exp(a+b1*v4)/(1+exp(a+b1*v4)) L=Weight*abs(OBS-PRED)

Step 6: Iteration analysis initiated.

STATISTICA: Nonlinear Estimation - [Data: NEW_STA 110v * 3110c]

003890302

Model Estimation

Model is: $f = a \cdot \left(\frac{k}{v_4} + s \right) \cdot \left(v_5 \cdot v_6 \cdot v_2 \right)^b$
 Number of parameters to be estimated: 4
 Loss function: (OBS-PRED)**2

Parameter Estimation

Iteration	Loss	Parameters
* 26	.000011	.3399441 -1.14963 -.05036 -.00061
* 27	.000011	.3399870 -1.15026 -.05058 -.00085
* 28	.000011	.3399193 -1.15035 -.05062 -.00088
* 29	.000011	.3398377 -1.15027 -.05059 -.00083
* 30	.000011	.339768 -1.15025 -.05059 -.00079
* 31	.000011	.3397977 -1.15027 -.05059 -.00081
* 32	.000011	.3397977 -1.15027 -.05059 -.00081

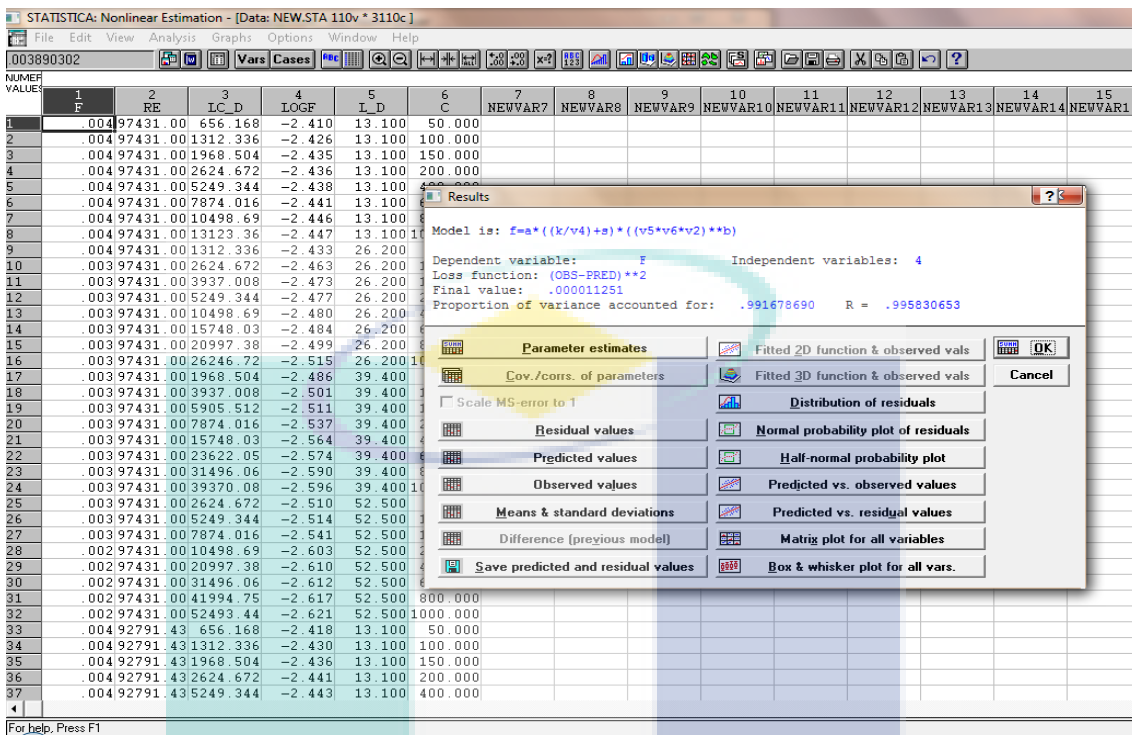
Parameter estimation process converged

Convergence criterion: .0001

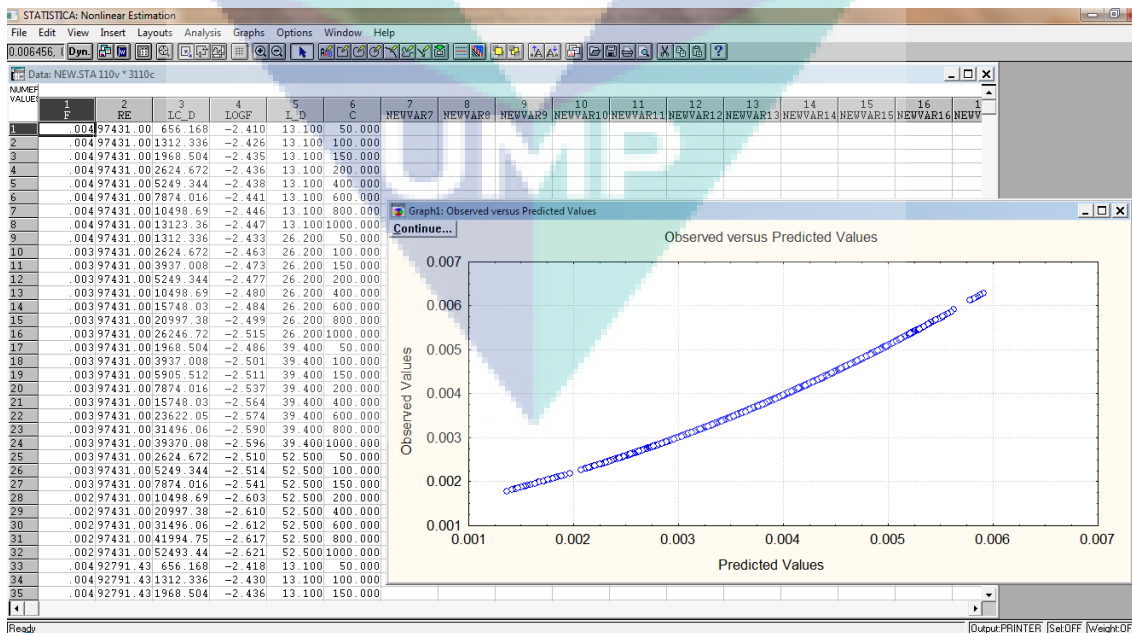
Start values: .1 for all parameters
 Initial step size: .50 for all parameters

Matrix plot for all variables
 Box & whisker plot for all vars.

Step 7: Iteration ended. All the statistical parameters appeared.



Step 8: Observed versus predicted values shown.



APPENDIX F
LIST OF PUBLICATIONS

1. Nithiya Arumugam and Hayder A. Abdul Bari. 2010. Comparative study between high and low concentration of natural additives on drag reduction in pipelines carrying water. *4th International Conference on Postgraduate Education, 26-28 November.*
2. Nithiya Arumugam, Hayder A. Abdul Bari and Arun Gupta. 2011. Drag reduction efficiency of solid particles in pipelines of two phase flow. *2011 International Conference on Computer and Communication Devices, 1-3 April. 2: 319-322.*
3. Siti Nuraffini bt. Kamarulizam, Hayder A. Abdul Bari and Nithiya Arumugam. 2011. Studying the potential of slag waste particle as suspended solid drag reducing agent. *2011 International Conference on Computer and Communication Devices, 1-3 April. 2: 323-327.*
4. Nithiya Arumugam, Hayder A. Abdul Bari and Arun Gupta. 2011. Improving the flow of petroleum product using grafted natural additive. *Book of Abstract, 5th International Congress of Chemistry and Environment, 27-29 May. p. 112.*
5. Nithiya Arumugam and Hayder A. Abdul Bari. 2010. Testing the drag reduction performance of a new drag reduction agent using closed loop liquid circulation system. *3rd RC-NRM Regional Conference Interdisciplinary on Natural Resources and Materials Engineering, 25-26 October. p. 373-379.*
6. Nithiya Arumugam, Hayder A. Abdul Bari and Arun Gupta. 2011. Effect of titanium dioxide manufacturing waste on drag reduction in pipelines carrying gas-oil. *International Conference of Chemical Engineering and Industrial Biotechnology in conjunction with 25th Symposium of Malaysian Chemical Engineers, 28 November – 1 December. p. 17.*
7. Patent Application: 2011001490, A novel plant-derived polymer drag reducing agent and a method for preparing same.
8. IN PRESS: CICEQ, The Drag Reducing Ability of Grafted Mucilage From Hibiscus Leaves for Pipelines Carrying Gas-Oil.
9. AWARDS: Gold Medal in CITREX2011 UMP and Bronze Medal in PECIPTA2011.